

60

SONAR BEAMFORMING BASED UPON
MONAURAL LOCALISATION
TECHNIQUES

BY

PETER ALAN TOLLMAN

SUBMITTED IN FULFILMENT OF THE
REQUIREMENTS FOR THE DEGREE OF
DOCTOR OF PHILOSOPHY

UNIVERSITY OF CAPE TOWN
MARCH 1987

The University of Cape Town has been given
the right to reproduce this thesis in whole
or in part. Copyright is held by the author.

The copyright of this thesis vests in the author. No quotation from it or information derived from it is to be published without full acknowledgement of the source. The thesis is to be used for private study or non-commercial research purposes only.

Published by the University of Cape Town (UCT) in terms of the non-exclusive license granted to UCT by the author.

ABSTRACT

Sonar beamforming is usually accomplished using a multi-element transducer array. To obtain high resolution, such a system is costly and complex. In contrast, many mammals are capable of good angular resolution using only a single active element surrounded by an irregular reflector - the ear. A study of monaural localisation was therefore undertaken, with a view to the development of a novel beamforming system which uses only a single active element. Computer simulations have shown that the direction of a source can be determined by cross-correlating the output signal spectrum with the known spectral responses of the receiving system for all angles.

The technique developed emulates one possible mechanism of monaural localisation. This has been demonstrated using a mannikin human head. An experimental underwater active sonar system was also constructed. The results obtained from this system verified those obtained in computer simulations: angular resolution is similar to that of a conventional array of comparable dimensions; however, detection performance is somewhat inferior. Owing to the substantial practical advantages of a sonar system which achieves multiple beams using only a single active element, the proposed technique is suggested as a possible alternative to certain sonar applications.

DECLARATION

I declare that this dissertation is my original work. No part of it has been previously submitted to any University.

signature removed

P. A. Tollman

March 1987

ACKNOWLEDGEMENTS

Professor P. N. Denbigh, my supervisor, consistently provided invaluable encouragement, guidance and inspiration.

My wife, Linda, assisted with many of the diagrams.

CONTENTS

	<u>Page</u>
1.0 INTRODUCTION	1-1
2.0 CONVENTIONAL ARRAY THEORY	2-1
3.0 ANIMAL SONAR SYSTEMS	3-1
3.1 The sonar equipment	3-3
3.2 Angle estimation	3-20
3.3 Theories of angle estimation	3-31
3.4 Range accuracy and range determination	3-42
3.5 Sensitivity of echolocation	3-48
3.6 Target classification and recognition	3-50
3.7 Resistance to interference	3-55
3.8 On the development of a sonar system based upon monaural echolocation	3-58
4.0 COMPUTER SIMULATIONS OF BEAMFORMING BASED UPON MONAURAL ECHOLOCATION	4-1
4.1 Beamforming by the solution of simultaneous equations	4-3
4.2 Beamforming by the deconvolution processing of received sounds	4-12
4.3 Beamforming by the cross-correlation analysis of received spectra	4-20
4.4 Simultaneous angle and range determination based upon monaural echolocation techniques	4-35
4.5 An evaluation of sonar beamforming by the cross-correlation analysis of received spectra	4-42
5.0 THE LOCALISATION OF SOUNDS BY A MANNIKIN HUMAN HEAD	5-1
5.1 The localisation of impulsive sounds	5-3
5.2 The localisation of longer sounds	5-13

	<u>Page</u>
6.0 THE DESIGN AND CONSTRUCTION OF AN EXPERIMENTAL ACTIVE SONAR	6-1
6.1 System design	6-2
6.2 Experimental method	6-5
6.3 Results	6-7
6.4 Discussion	6-10
7.0 CONCLUSION	7-1
8.0 REFERENCES	8-1
APPENDIX A: Computer programs used in beam-forming simulations	A-1
APPENDIX B: Computer programs used in the localisation of sounds by a mannikin human head	B-1
APPENDIX C: Transducer equivalent circuit and receiver design	C-1
APPENDIX D: Computer programs used by the active sonar	D-1
APPENDIX E: Published papers	E-1

1.0 INTRODUCTION

It has long been common knowledge that mammals can localise sounds. Consequently, it is somewhat surprising that the initial discovery that bats orientate themselves through the reception of ultrasonic echoes met with a large degree of disbelief. When, in 1794, Lazzaro Spallanzini had amassed sufficient evidence to postulate that bats orientate using ultrasonic emissions, his view was derided by the leading scientists of the day:

"Since bats see with their ears do they hear with their eyes?"

mocked Montagu in 1809 (Griffen, 1950).

It took some 150 years before Donald Griffen, then a postgraduate student at Harvard University, proved beyond doubt that bats spatially orientate primarily through the use of a highly developed sonar capability. At first bats were thought to be the only animals which use echolocation for spatial orientation. However, in 1953 sonic localisation was discovered in the Guacharos (oil-birds) of South America, and later in swiftlets. A more sensational subsequent discovery occurred in 1956 when McBride observed the use of highly evolved echolocation in cetaceans - the dolphins and whales. Experimental evidence of this was obtained later through the efforts of many investigators, amongst whom Kellogg features prominently (Airapet'yants and Konstantinov, 1973).

The inspiration for many technological developments has been the slowly evolved specialisations of living organisms. Thus man's attempt to imitate the birds has led to the advent of powered flight; man's attempt to imitate the fishes has led to the development of submarines. In the case of sonar, the opposite has occurred: the sonar systems of echolocating animals have come to be understood largely by comparison with technologically developed systems. Consequently, animal

sonar bears little similarity to its man-made counterpart. Although many mechanisms of animal sonar remain poorly understood, recent research has revealed that some mammals possess a sophisticated sonar capability which in many respects outclasses the most advanced technological systems.

The goal of this work has been to use the inspiration provided by animal echolocation to design and develop a novel sonar system. Since monaural localisation cues are a vital constituent of spatial hearing, it was decided to base the sonar upon monaural echolocation techniques. This is due to the great practical advantages of simplicity and low cost which would be associated with a beamforming system which uses only a single active output surrounded by an irregular passive reflector - analogous to the ear.

A detailed study of animal sonar systems revealed that the direction dependent spectrum modifications which the pinna imposes on incident wavefronts is the main monaural cue to localisation. A number of possible methods of using these spectrum modifications to locate targets were devised and evaluated in computer simulations. The most successful of these - beamforming by the cross-correlation analysis of received spectra - was evaluated as a model of human monaural localisation: a mannikin human head was required to locate a number of different sounds. Methods of circumventing the fundamental difficulty of locating unknown spectra were proposed and tested. Finally, the technique was used in the construction of an experimental underwater active sonar system. Results obtained indicate that, in certain applications, the system could be a viable and attractive alternative to conventional sonar.

2.0 CONVENTIONAL ARRAY THEORY

Before describing the novel beamforming techniques which have been developed, it is useful to briefly review the angular localisation capabilities of conventional sonar systems.

Most beamforming systems locate targets by sequentially scanning a narrow beam. Perhaps the least sophisticated of these is the mechanically scanned radar antenna. However, mechanical scanning below the sea surface is seldom feasible: the low propagation velocity of sound limits scan speed while mechanical rotation in an under-sea environment is usually impractical. Instead, transducer arrays are used in which either a narrow beam is electronically steered or multiple preformed beams are interrogated.

The angular resolution of a beamforming system is defined as the minimum angular separation at which two targets are distinguishable. Lord Rayleigh (1879) formulated a concept of resolution which to a first approximation can be paraphrased: for two equal point targets the angular resolution is one beamwidth.

The half-power beamwidth of a transducer array is in inverse proportion to array length:

$$\theta = K(\lambda/D) \quad (2.1)$$

where: θ is the angle bounded by the half-power points
 λ is the wavelength of radiation
 D is the array length
 K is constant depending on array illumination.

For uniform array illumination K is 0,89. However, the dynamic range is limited by the presence of sidelobes, the levels of which decay with distance from the main beam. The first sidelobe level is -13,2dB. By a judicious choice of aperture illumination, it is possible to increase dynamic

range at the expense of beamwidth; or to decrease the beamwidth while reducing the dynamic range. One discrete illumination function, known as Dolph-Chebyscheff shading, gives the narrowest main lobe for a given maximum sidelobe level (Urick, 1983). This is achieved by having all sidelobes at equal levels. More extreme forms of aperture shading have been shown to give super-directivity: narrow beams are obtained using small arrays by reversing the polarity of adjacent elements. However, this procedure reduces the antenna efficiency to impractical levels. Consequently, in the vast majority of applications, the aperture illumination is chosen to obtain a K of around unity: angular resolution is then simply the array length measured in wavelengths.

While the Rayleigh criterion is a useful practical estimate of resolution, it is not a natural physical limitation. Theoretical analysis has shown that in the absence of noise and with sufficient a priori information, two targets which are infinitesimally close can still be separated, since the image of two targets will always differ from that of one (Hausz, 1964). Therefore, the interaction of system and background noise, together with aperture size, imposes a more fundamental limit than the Rayleigh criterion on the minimum angle at which a given probability of separation is achieved. However, the severe practical constraints of such a super-resolution system have limited its applicability: to achieve substantially better resolution than that predicted by the Rayleigh criterion requires an extremely high signal-to-noise ratio. Consequently, the major achievement of super-resolution has been to demonstrate the possibility of exceeding the Rayleigh criterion.

A two-dimensional passive sonar system can be configured using just two spatially separated transducers: the time difference of arrival of incident signals indicates target bearing. This time difference is determined by cross-correlating the transducer outputs; it is the displacement of

the correlogram peak from zero time. If they are uncorrelated, multiple sources can be resolved provided the correlogram peaks are separated such that they are distinct. This separation corresponds to the width of the correlogram peak at the -3dB level, which is the inverse of signal bandwidth. In turn, angular resolution is inversely proportional to the product of signal bandwidth and transducer separation.

$$d\theta = \frac{c}{\ell B \cos\theta} \quad (2.2)$$

where: $d\theta$ is the angular resolution
 c is the speed of sound
 B is the signal bandwidth
 ℓ is the transducer separation
 θ is the angle between the source and boresight.

Angular accuracy - the precision with which the bearing of a single target can be determined - is often confused with resolution. The two are quite different: under noise-free conditions a system with coarse angular resolution can locate targets infinitely accurately by interpolating to the centre of the beam. One realisation of this principle is the split-beam system: interpolation between two or more broad beams accurately locates a target. Owing to the coarse angular resolution of such a system, successful operation is limited to environments in which only a single target is present in each range bin. Therefore, its usefulness can be increased by using a wide bandwidth to ensure a narrow range resolution.

The beamforming techniques developed in this thesis are conceptually different from those described above: multiple beams are achieved using only a single active element and without scanning a narrow beam. Rather, the use of broadband signals allows angular localisation through the examination of direction dependent spectral features of target returns. It will be seen that good angular resolution and accuracy can be obtained.

3.0 ANIMAL SONAR SYSTEMS

Since the intention has been to develop beamforming techniques based upon animal echolocation, the sonar systems of three species of mammal are reviewed. They are: cetaceans (which comprise the dolphins and whales), bats and humans. Cetaceans and bats are the mammals which rely most heavily on their echolocating abilities: cetaceans often have to navigate in water through which light does not penetrate, and most species of bat are blind. Therefore, visual orientation in these animals is limited. Instead, they have evolved sophisticated active sonar systems. Owing to the high rate of attenuation of sound at frequencies employed by these mammals, the range of echolocation is limited. In bats, it has been estimated to be approximately 2 to 3 metres (Fenton, 1980; Griffen, 1958), while the range of echolocation in dolphins is between 75 and 110 metres (Murchison, 1980; Snyder, 1980). However, in terms of angular resolution, range resolution, sensitivity, target recognition and resistance to interference, the sonar capabilities of these animals frequently surpass those of man-made beamforming systems.

Although the blind are known to echolocate actively (by listening to the echoes of a tapped stick or to echoes of their footsteps), most humans locate targets only in the passive listening mode. Since sight is the primary mechanism of spatial localisation in humans, they have not exploited their sonar capabilities to the full. Nevertheless, human spatial hearing has been shown to rely on sophisticated mechanisms, many of which have not been satisfactorily explained. An example is the ability to focus on a single conversation amidst a din of voices - the so-called "cocktail party effect". Notwithstanding, since it is far easier to obtain experimental feedback from humans than from other mammals, investigations of human spatial hearing have often provided better insight into the mechanisms of animal sonar

than have similar experiments performed on bats or cetaceans.

This review contains somewhat more than the necessary background to the work undertaken. Because research into animal sonar draws from numerous disciplines, many discoveries have not been contextualised within the framework of communications engineering. Consequently, an attempt has been made to discuss animal echolocation from within this perspective. The first subsection of this chapter describes the equipment which these animals use in beamforming; both the sonar transmissions and the receivers are conceptually different from those of conventional systems. Thereafter, the major performance parameters of animal sonar - angle estimation and target ranging - are described and evaluated. In addition, the more plausible theories of target localisation are appraised. The following three subsections cover some of the sonar skills of these mammals, and indicate the sophistication of their echolocation systems. The final subsection summarises those aspects of animal sonar systems which have inspired the beamforming techniques described in this document.

3.1 The sonar equipment

3.1.1 The transmit signals of cetaceans

Although the echolocation signals of these animals vary with species, the sonar transmissions of most smaller cetaceans have a common character: short, wideband clicks, with maximum energy occurring between 15 and 30kHz (Watkins, 1980). However, significant pulse energy is also found at frequencies below 500Hz.

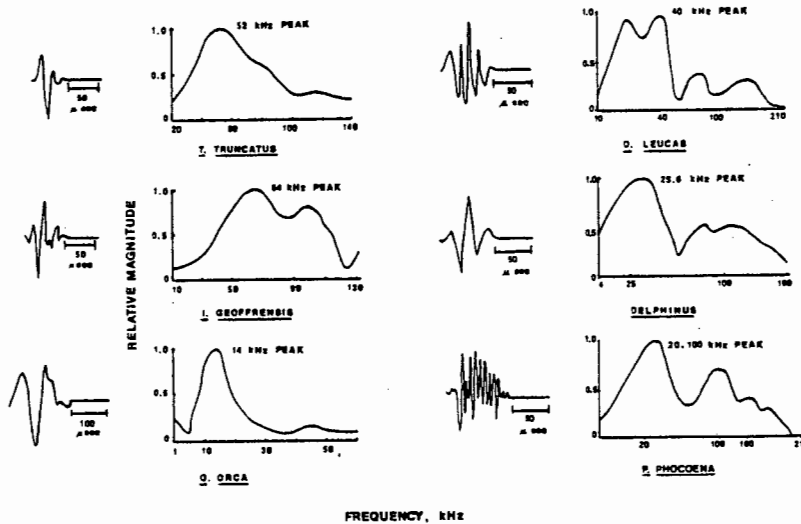


Figure 3.1 - Typical cetacean echolocation clicks (Wood and Evans, 1980).

A detailed study of the echolocation signals of the Atlantic bottlenosed dolphin, *Tursiops truncatus*, has revealed strongly directional beampatterns; average half-power beamwidths of 11,7 degrees in the vertical plane and 10,7 degrees in the horizontal plane were obtained. Beamwidth decreases with increasing frequency (Au, 1980).

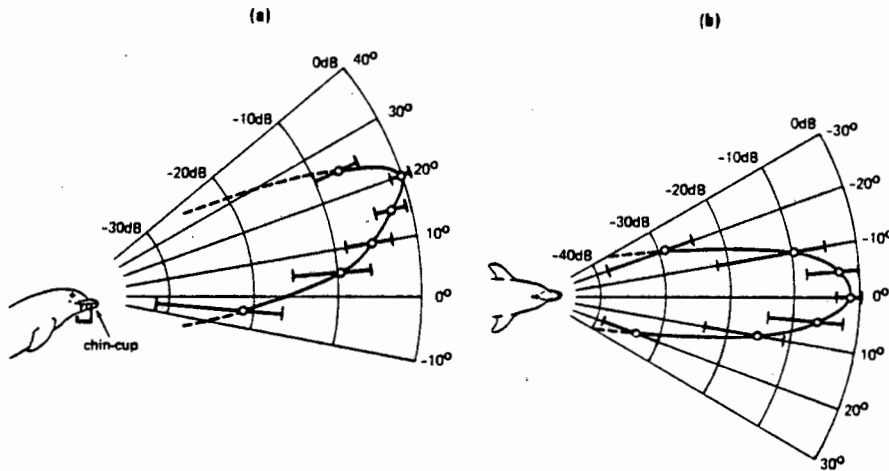


Figure 3.2 - Composite broadband beampatterns of Tursiops
 (a) in the vertical plane
 (b) in the horizontal plane (Au, 1980).

Source levels of the orientation clicks of these animals are adaptive; varying as a function of ocean condition, ambient noise, target range and target cross-section. The maximum recorded source level at a distance of one metre from the mouth of Tursiops was 227,6dB, while the average for these animals is somewhat lower at around 170dB (re 1 micro-Pa) (Au, 1980).

Acoustic data obtained from a variety of cetaceans is tabulated below (Evans, 1980).

Table 3.1 - Acoustic Data on Cetaceans

SPECIES	PULSE FREQUENCY RANGE	SOUND PRESSURE AT 1 METRE (rel- 1 micro- Pa)	PULSE DURA- TION (milli- seconds)	HORIZONTAL BEAMWIDTH (-6dB pressure)
Phocoena phocoena	40Hz-10kHz	125-130dB	0,5-1,5	-
Phocoena dalli	40Hz-12kHz	-	0,5-1,5	-
Ornicus orca	100Hz-30kHz	178dB	0,5-1,5	40 deg.
Physter catadon	40Hz-15kHz	185dB	0,75-5	-
Inia geoffren- sis	100Hz-150kHz	166dB	0,1-0,15	-
Platanis- ta gangetica	100Hz-150kHz	140dB	0,075-0,5	20 deg.
Tursiops truncatus	100Hz-100kHz	170dB	0,05-0,25	30 deg.
Globice- phala scammoni	100Hz-100kHz	180dB	0,25-2	-
Steno bredanen- sis	100Hz-200kHz	-	0,05-0,25	24 deg.
Delphinus delphus	100Hz-150kHz	140dB	0,05-0,25	-

3.1.2 The transmit signals of bats

Bats divide into two categories according to the nature of their sonar cries: those which emit short frequency modulated pulses, and those which employ long constant frequency pulses.

Between these two extremes, there exist a number of bats which combine both forms of orientation pulses. Further, recent research has revealed that certain bats vary their pulse structure to suit particular echolocation requirements. Thus, constant frequency components have been observed to be tacked onto what are usually frequency modulated sweeps; while in the laboratory, widely varying pulse structures have been induced by exposing the bats to diverse conditions (Simmons, Lavender and Lavender, 1974; Pye, 1980).

3.1.2.1 Frequency modulated pulses

Frequency modulated pulses are best suited to insectivorous bats that hunt in open spaces. Pulse lengths vary from 1ms to 4ms. Frequency descends linearly with time within each pulse over approximately an octave, with peak amplitude occurring at mid-pulse (Airapet'yants and Konstantinov, 1973). At rest, the pulse repetition frequency is 10 to 15 pulses per second. However, during the interception of prey, negotiation of an obstacle or landing, pulse repetition frequency increases to between 100 and 200 pulses per second, while pulse duration reduces to about 0,25ms. Centre frequency decreases along with pulse width (Pye, 1980).

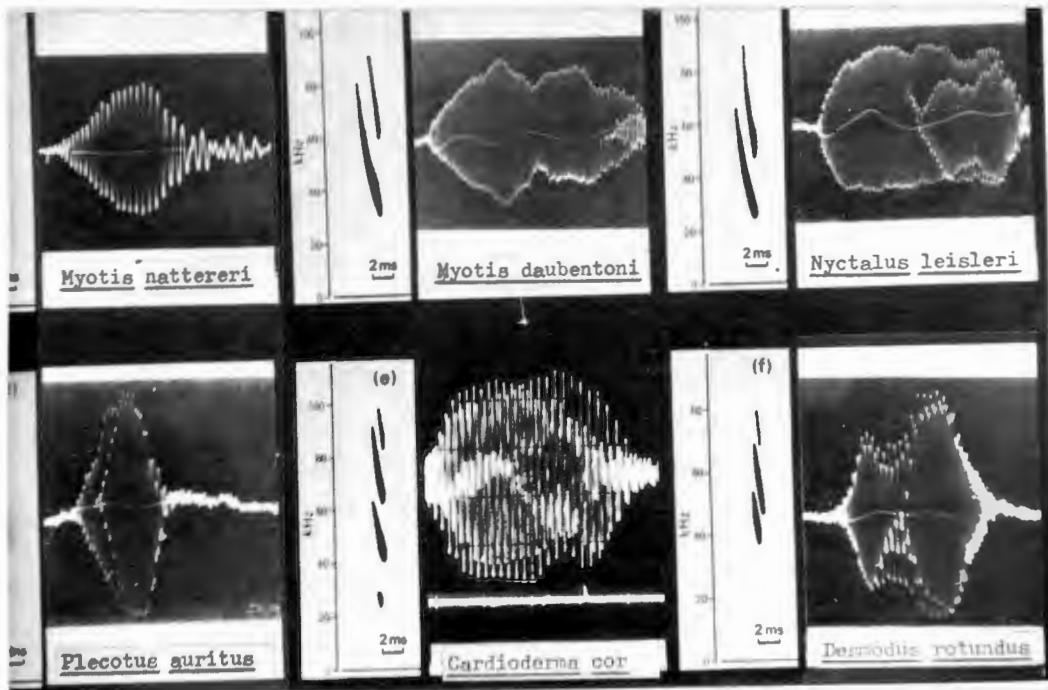


Figure 3.3 - Orientation cries of some fm bats (Pye, 1980)

The beamwidths of fm bats are broad, and display little variation with frequency: the species *Eptesicus fuscus* and *Pteronotus parnelli rubiginosus* have a measured horizontal half-power beamwidth of 23 degrees at 30kHz, while a typical sonar cry of the bat *Myotis grisens* has an azimuth half-power beamwidth of 34 degrees at a frequency of 55kHz, a beamwidth of 38 degrees at 75kHz, and a beamwidth of 30 degrees at a frequency of 95kHz. In the vertical plane, the half power beamwidth of *Myotis* is 68 degrees, 40 degrees and 30 degrees respectively at frequencies of 55kHz, 75kHz and 95kHz (Shimozawa et al, 1974).

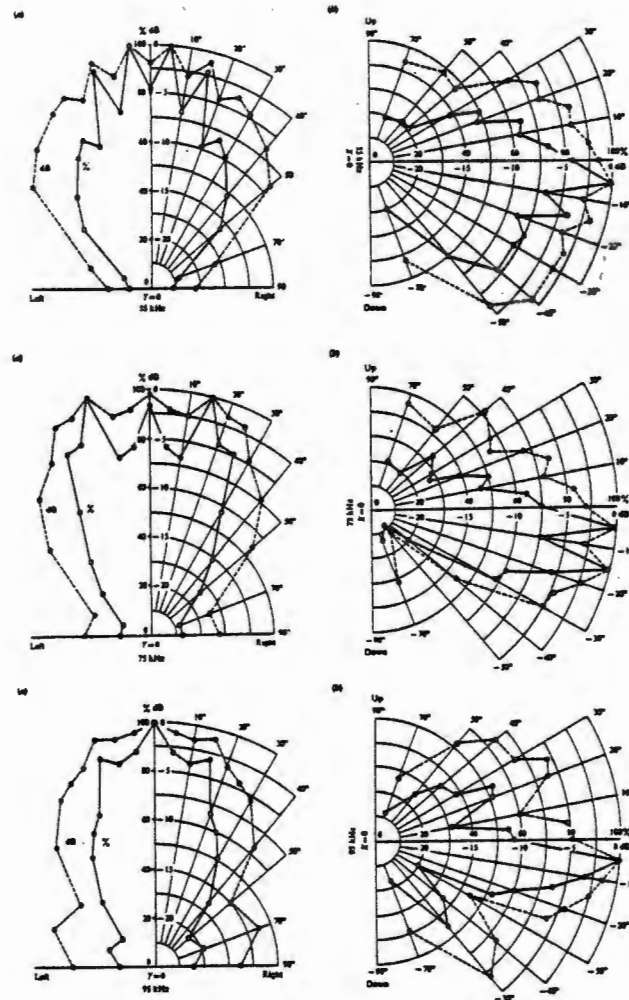


Figure 3.4 - Vertical and horizontal sound pressure fields in the bat *Myotis grisescens*. Solid line: percentage of maximum. Dashed line: decibels.
 (a) horizontal plane
 (b) vertical plane (Shimozawa et al, 1974).

Peak source levels are lower than those of cetaceans. However, the far longer pulse lengths ensure a high pulse energy, a more relevant index of range capability. A maximum pressure of 145dB (re 1 micro-Pa) has been measured 5 to 10 cm from the mouth of *Myotis lucifugus*, while pulse pressures of 136dB are typical. Higher pressures have been obtained from four tropical species of the family Vespertilionidae - source levels of between 160dB and 166dB were recorded (Airapet'yants and Konstantinov, 1973). A survey of some location signal parameters is reproduced below.

Table 3.2. - Location signal parameters of fm bats
(Airapet'yants and Konstantinov, 1973)

SPECIES	PULSE DURATION (ms)	FREQUENCY SWEEP (kHz)	ACOUSTIC PRESSURE (dB re 1 Pa)
<i>Myotis lucifugus</i>	2,3	78-39	136(10)
<i>Myotis macrotarsis</i>	2,3-3,7	43/59-23,5/33	160-164(15)
<i>Myotis oxygna- thus</i>	0,8-4,2	120/80-35/15	137(15)
<i>Iniopteris schreibersii escholtzii</i>	1,5-3,7	104/67-52/35	164-166(15)
<i>Miniopteris tristis</i>	2,9-6,5	58/37,5-31/30	160-165(15)
<i>Pipistrellus ceylonicus</i>	1,7-3,3	42/31-26/24	130-133(15)
<i>Pipistrellus coramandra</i>	0,8-3,6	76/67-29/26	136-143(10-15)
<i>Eptesicus fuscus</i>	2,7	50-25	-
<i>Plecotus rafinesquii</i>	1,7	39-27	98(20)
<i>Tadaridia tragota</i>	3,1-8,1	32/22-14/11	137-144(5)

Note: The figures in parenthesis indicate distance (cm) from the bats' mouths.

3.1.2.2 Constant frequency pulses

Constant frequency bats often have a similar ecology to fm bats: largely insectivorous. However, they generally hunt in the vicinity of dense foliage.

Although pure cf signals have been observed in certain cf species, the constant frequency portion of the pulse is often preceded by a short upward sweep and almost always terminated with a downward sweep. At rest, their sonar cries are commonly over 70 ms, while the frequency of the constant frequency portion is 80 to 100kHz. In order to maintain a uniform echo frequency during flight, the transmit frequency is reduced to compensate for doppler shifts. Pulse repetition rate is around 4 pulses per second, increasing to between 5 and 6 pulses per second for an animal in flight.

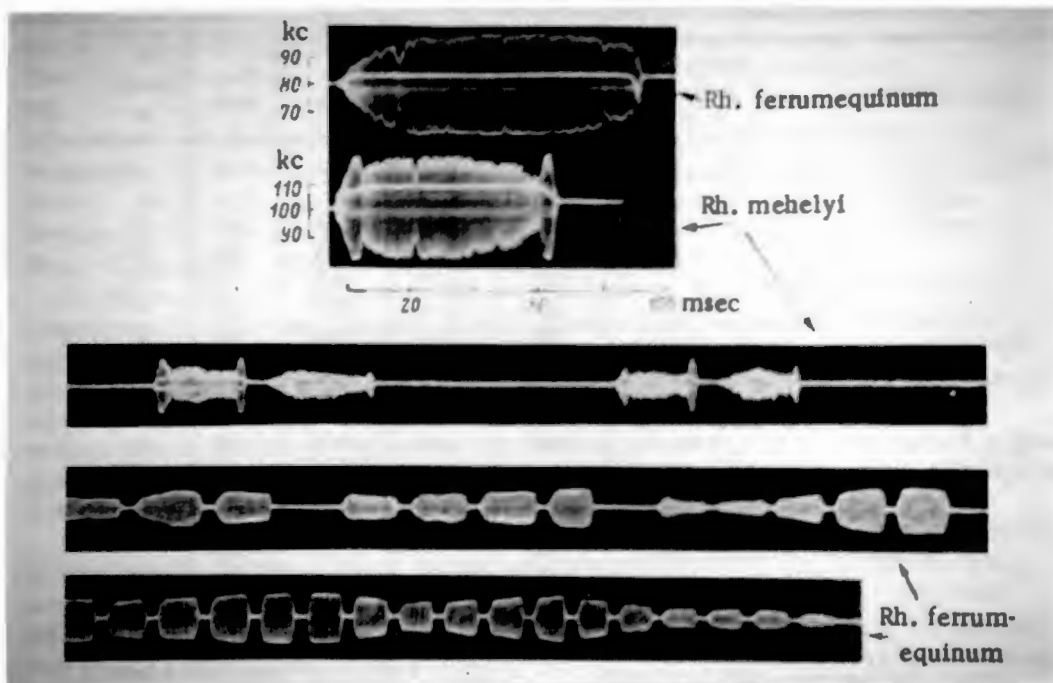


Figure 3.5 - Orientation pulses of two species of cf bat (Airapet'yants and Konstantinov, 1973).

The radiation patterns of cf bats are relatively narrow: half power beamwidths of 20 degrees in both azimuth and elevation have been measured in the species *Rhinolophus ferrumequinum* and *Rhinolophus eurayle*. Pulse pressures of

149dB and 146dB (re 1 micro-Pa) respectively were recorded 10 cm from their mouths (Schinzler, 1968). Since signal duration in cf bats is 20 to 30 times that of fm bats, pulse energy is significantly greater.

When cf bats detect an obstacle, their pulse structure alters: length and interpulse period decrease concurrently, while pulse repetition rate increases. This results in signals comprising between two and twenty short pulses. Some parameters of the orientation signals of three species of cf bat are summarised below:

Table 3.3. Location signal parameters of 3 species of the family Rhinolophus (Airapet'yants and Konstantinov, 1973)

SPECIES	NO. OF PULSES IN A SERIES	SERIES DURATION (ms)	PULSE DURATION (ms)	PULSE REPETITION RATE (1/s)
Rhinolo- phus ferrume- quinum	single pulses	-	50,6	9
	2	75,2	34,5	16
	3	94,9	27,9	19
	4	112,5	24,3	22
	5	138,5	23,7	25
	6	156,3	22,3	27
	7	174,5	21,5	29
	8	192,0	20,5	33
Rhinolo- phus mehelyi	single pulses	-	36,2	9
	2	66,6	29,1	14
	3	88,5	24,1	18
	4	91,9	21,8	24
	7	184,4	21,2	27
Rhinolo- phus hipposi- deros	single pulses	-	33,4	9
	2	55,1	24,5	20
	3	69,7	19,3	26
	4	102,1	20,2	27

3.1.2 The receiving structures

The receiving structures of land based mammals comprise the externally visible structures of their ears, called pinnae or auricles. These structures have been shown to be indispensable to successful echolocation: it is held that the direction dependent spectrum modification which the various facets of the pinna imposes on target echoes is perhaps the most significant indication of target position (Griffen, 1958; Batteau, 1966; Shaw, 1975; Blauert, 1983).

A secondary function of the pinna is to increase the sensitivity of hearing to sounds coming from certain directions.

While the pinnae of land based mammals are entirely absent in cetaceans, structures exist in these animals which fulfil a similar function.

3.1.2.1 The receiving structures of cetaceans

The ears of land mammals are inappropriate for acoustic reception below the sea surface. Consequently, the hearing structures of cetaceans have been substantially reorganised.

In the place of pinnae, there exist small apertures on the sides of the head. It has been suggested that these apertures, of 1,5 to 2mm diameter, together with a fibro-elastic conus and the muscles and cartilages surrounding it, are homologous to the pinnae of land mammals. In addition, it is thought that the lower jaw acts as a waveguide, transmitting sound to the cochlea (Bullock et al, cited in Airapet'yants and Konstantinov, 1973).

Unfortunately, very little is known about the hearing of these graceful animals. However, evidence points to the existence of acoustically independent transmission channels

to the two cochleae. These serve as linear filters, the transfer functions of which are direction dependent.

Interestingly, the reason for the dearth of data on cetacean hearing is that, unlike other mammals, those of the sea breathe voluntarily. Therefore any attempt to anaesthetise a cetacean for purposes of experimentation results in asphyxiation.

3.1.2.2 The pinnae of bats

Most bats possess outsize pinnae, the size, shape and structure of which varies with species. A narrow spear or club shaped dermal outgrowth, the tragus, is usually found rising from the base of the pinna, positioned such that it intercepts incident acoustic waves. Because it blocks the direct sound path, the tragus serves to increase the effect of the spectrum modification imposed on target echoes.



Figure 3.6 - The external ears of a few bats (Pye, 1980).

While most cf bats scan their pinnae in synchronism with vocalisation, fm bats maintain their pinnae in a fixed orientation which, if altered even slightly, prevents successful echolocation. To demonstrate this phenomenon, the pinnae of the bat *Plecotus* were bent inwards, and their minor edges glued together. This procedure caused the obstacle avoidance score to fall from 97% to 62%. On allowing the ears to return to their normal position, the obstacle avoidance score immediately returned to 90% (Griffen, 1958). This is evidence that the direction dependent spectrum modification which the pinna imposes on received sounds is crucial to spatial hearing: alteration of the characteristic spectrum modification yields disastrous results.

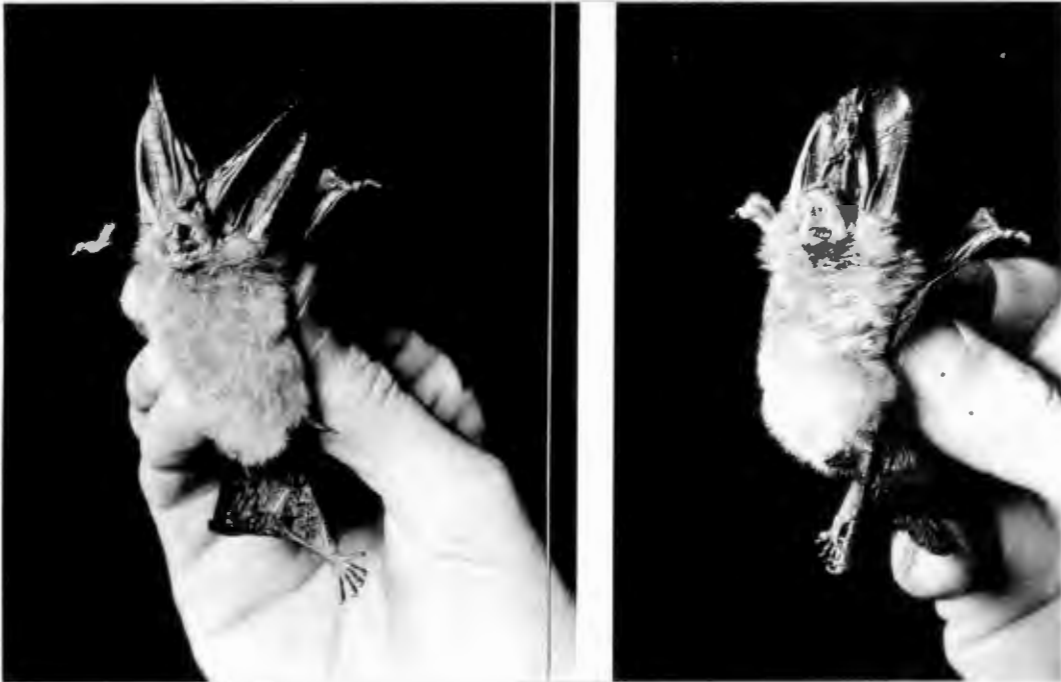


Figure 3.7 - The pinnae of *Plecotus* were joined (Griffen, 1958).

The pinna dimensions of insectivorous bats range from 20 to 40mm. Since the upper frequency limit of transmission is of the order of 100kHz, the receiving aperture is between 6 and 12 wavelengths across.

3.1.2.3 The pinnae of humans

As early as 1901 Angel and Fite recognised that the human pinna acts as a linear filter, the transfer function of which varies according to the direction of sound incidence.

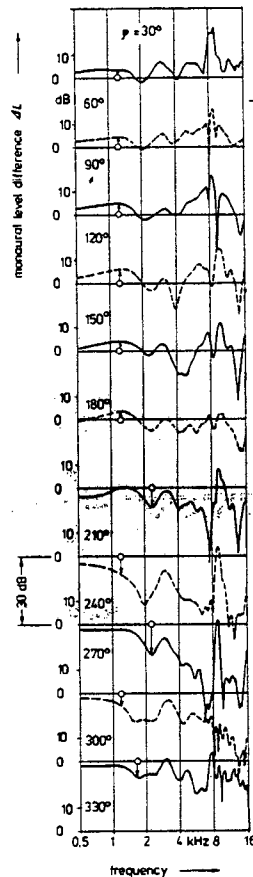


Figure 3.8 - Some averaged horizontal plane pinna transfer functions (Blauert, 1983).

Gardner and Gardner (1973) confirmed the importance of the pinna in human sound localisation by increasingly occluding the pinna cavities of a number of subjects. As the spectrum modification imposed on received sounds was progressively altered, the ability to localise sounds in the median plane decreased dramatically.

The limit of human hearing is somewhat below 20kHz. Since the human ear is about 50mm across, pinna width is at most 3 wavelengths at the highest frequency of audition.

3.1.3 Hearing and spectral sensitivity

The inner ears of mammals perform a spectral analysis of auditory stimuli before passing the information on to the

brain.

An acoustic pressure wave striking the ear drum releases a travelling wave along the basilar membrane. For the present purpose, the basilar membrane can be likened to a bank of contiguous mechanical bandpass filters. Because the membrane's width decreases from base to apex while its thickness increases, descending resonant frequencies occur along its length. These are usually of equal fractional bandwidth.

The basilar membrane is covered with hair cells, which respond to the wave amplitudes through the cochlea. Spiral ganglion cells convert this mechanical resonance into an electrical potential which is transmitted to the brain. Since the ratio of ganglion cells to hair cells is an indication of aural sensitivity, it is interesting to note that of all the mammals, dolphins possess the highest ratio, followed closely by bats. The ratio of ganglion cells to hair cells in the bat *Myotis lucifugus*, for example, is 15:1.

Recordings of the cochlear responses of fm bats to stepped series of tone bursts indicate a response which corresponds to banks of constant Q filters, the fractional bandwidths of which range from 5 to 15 at the -10dB level (Suga, 1965; Grinell, 1972; Suga and Schlegel, 1972; Suga and O'Neill, 1978; Neuweiler, 1980; Neuweiler, 1980b, Neuweiler, Bruns and Schuller, 1980).

Although these results provide a rough guide to frequency selectivity, they are probably overly simplistic. Pollack (1980) has found an:

"exceptionally high degree of frequency selectivity which only becomes apparent when the stimuli are fm bursts."

The varying basilar membrane responses to different stimuli suggest that the frequency responses of the cochleae of

mammals are rather more complicated than are simple time-invariant bandpass filters.

While frequency resolution is determined by the selectivity of hair cells, the prowess with which small shifts in frequency can be discriminated is a function of the sensitivity of the bat brain. No reference to the frequency discrimination acuity of these mammals was found in the literature reviewed.

It is noteworthy that the uniform pattern of logarithmic frequency representation found along the basilar membranes of other mammals is not apparent in the cf bats: the thickness and width of their basilar membranes are regionally differentiated. For example, in the bat *Rhinolophus ferrumequinum*, the frequency band from 82kHz to 86kHz is represented on the basilar membrane in a greatly expanded fashion. The tuning curves of this region have fractional bandwidths at the -10dB level of up to 500 (Neuweiler, Bruns and Schuller, 1980). Virtually all orientation sounds are received within this expanded region of the basilar membrane as a consequence of the doppler shift compensation practised by cf bats (refer section 3.1.2.2).

The frequency discrimination capabilities of cetaceans and humans are measured in relative discrimination limens: the ratio of just noticeable frequency difference to centre frequency. For the bottlenose dolphin, *Tursiops truncatus*, relative discrimination limens of 0,2% to 0,4% have been measured at frequencies between 2kHz and 53kHz, while at all other frequencies between 1kHz and 140kHz, discrimination limens of 0,4% to 0,87% were obtained. The harbour porpoise, *Phocoena phocoena*, obtained relative discrimination limens of 0,1% to 0,29% in the frequency band 3kHz to 225kHz.

In addition, *Tursiops* was able to discriminate intensity differences of as little as 1dB, and to distinguish between signal durations of 300ms and 324ms (Popper, 1980).

Humans display a similar amplitude and frequency selectivity to cetaceans. Van Békésy (1960) measured relative discrimination limens of 0,3% in humans for 800Hz pulses of duration 140 to 150 seconds.

3.2 Angle estimation

One of the most fascinating aspect of animal sonar is the ability to determine the direction of incident sound fields. Of particular significance to the current research is the contribution of monaural localisation cues to angle estimation.

Two separate concepts define angular localisation: angular accuracy and angular resolution. Angular accuracy refers to the precision with which the direction of a single target can be estimated. Resolution has a more stringent requirement: it refers to the minimum angular separation at which two simultaneously presented targets are distinguishable. The difference between these two parameters is often overlooked, resulting in incorrect conclusions. Therefore, an effort has been made to distinguish between instances in which angular accuracy has been measured, and those in which angular resolution has been determined.

Unfortunately, it is not possible to isolate the monaural localisation abilities of cetaceans, while in bats only sketchy evidence has been accumulated of the importance of monaural cues to orientation. In contrast, the well researched field of human monaural localisation provides important insight into this aspect of mammalian spatial hearing.

Since it is not possible to investigate monaural localisation in isolation, a review of the full angular localisation abilities of these mammals follows.

3.2.1 Angle estimation in cetaceans

Angular accuracy in cetaceans has been investigated in the passive listening mode.

A number of dolphins were required to determine which of two medially placed transducers was radiating a sound field. It was found that the minimum angular separation at which this can be achieved varies widely according to the nature of the signal. For pure tone emissions between 2kHz and 6kHz, the harbour porpoise, *Phocoena phocoena* was able to discriminate angles of between 3 and 4 degrees. The bottlenose dolphin, *Tursiops truncatus* could discern angles of between 2 and 3 degrees for tones in the range 20 to 90kHz. However, when the transducers were excited with broadband pulses centred at 64,4kHz, *Tursiops* was able to discern angles to an accuracy of 0,7 to 0,8 degrees (Popper, 1981).

Since the orientation clicks of these animals are broadband, the true angular accuracy of cetacean sonar systems should at least match the 0,8 degrees measured for *Tursiops*.

Popper claims that angular resolution, and not accuracy, was determined in these experiments. He claims:

"The minimum auditory angle (MAA) between two spatially separated underwater speakers resolvable by the dolphin ranged from 2 to 3 degrees for pure tones from 20 to 90 kHz."

At no stage did the two transducers radiate sound fields simultaneously. Therefore, the procedure employed by the dolphins in separating the transducers was to sequentially estimate the bearing of each as it radiated a sound field. Then a decision was reached on their relative positions. This tests the precision with which targets can be passively located, but does not test the ability to resolve two simultaneously presented targets. No test of the true angular resolution capability of cetaceans was found in the literature reviewed.

3.2.2 Angle estimation in bats

The active mode angular accuracy of two fm bats, *Eptesicus fuscus* and *Phyllostomus hastus*, was examined by training the bats to discriminate the horizontal angle between a spherical target offered at 0 degrees and a fixed target at 19 degrees, from the angle between the target at 0 degrees and an adjustable target offered at angles which varied between -37 and 0 degrees. The sphere separation was always maintained greater than 14mm, the largest wavelength in the orientation cries of these animals (Peff and Simmons, 1972).

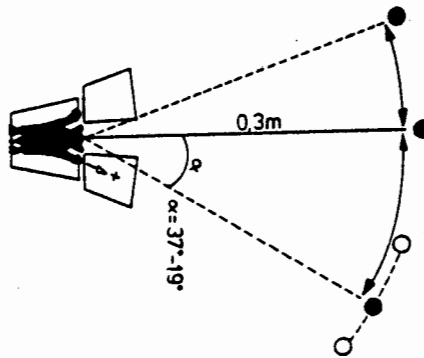


Figure 3.9 - Peff and Simmons' experimental configuration.

The horizontal angular accuracy of *Eptesicus* was subsequently re-examined by training the bat to discriminate between two simultaneously presented pairs of vertical brass rods; the one pair fixed such that their angular separation was 6,5 degrees, while the angle between the second pair of rods was varied. A fourfold improvement in acuity over the previous experiment was demonstrated (Simmons et. al., 1982).

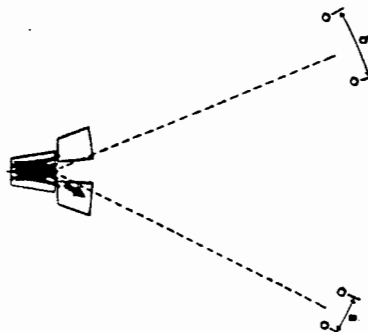


Figure 3.10 - Simmons' experimental configuration.

The horizontal angular accuracy of *Rhinolophus ferrumequinus*, a cf bat, was tested by training the animal to discriminate a pair of rods 0,4 degrees apart from a pair of similar rods of varying separation (Schinzler and Henson, 1980).

The results of the above investigations have been tabulated using an arbitrary 75% correct response threshold.

Table 3.4. Horizontal angular discrimination thresholds of three species of bat.

SPECIES	DISCRIMINATION THRESHOLD	AUTHOR
<i>Phyllostomus hastus</i>	4 - 6	Peff and Simmons (1972)
<i>Eptesicus fuscus</i>	6 - 8	Peff and Simmons (1972)
<i>Eptesicus fuscus</i>	1,5	Simmons (1982)
<i>Rhinolophus ferrumequinum</i>	4,5	Airapet'yants and Konstantinov (1974)

The vertical angular acuity of *Eptesicus* was determined by training the bats to discriminate between two simultaneously presented pairs of horizontal brass rods; the lower pair separated by 6,5 degrees while the angle between the upper pair was varied. The 75% correct response threshold occurred at angles of 3 to 3,5 degrees; somewhat inferior to that obtained in the horizontal plane.

Angular accuracy in the passive listening mode has been measured by training an fm bat, *Myotis* sp., and a cf bat, *Rhinolophus ferrumequinum*, to discriminate which of two loudspeakers, situated 2,7m away, and positioned at varying horizontal angles relative to one another, was transmitting 5ms constant frequency pulses. The 75% threshold of correct responses was reached at an angle of 5 degrees for *Myotis* and

at an angle of 4 degrees for *Rhinolophus* (Konstantinov et al, 1973). *Rhinolophus* could also discriminate an angle of 4 degrees when the loudspeakers were separated in the vertical plane (Golinsky and Konstantinov, cited in Schinzler and Henson, 1980).

Although it has been claimed that the above experiments measured angular resolution, a review of the experimental procedures clearly reveals that accuracy was measured: the precision with which the bearing of a target could be estimated was determined in each instance. Therefore, a comparison of these results with the angular resolution capabilities of comparable man-made beamforming systems is meaningless.

No reference to the angular resolution or multiple target capability of these mammals has been found. However, their behaviour pattern indicates the likelihood that a multiple target capability exists: they are exceptionally gregarious and are able to navigate with ease through dense clutter. A study of their angular resolution capabilities could be an important contribution to current knowledge of animal sonar.

Tests of the ability of echolocating bats to locate targets using only a single ear have produced conflicting results. Griffen showed that monaural earplugs drastically reduce the obstacle avoidance capability of *Myotis lucifugus*, an fm bat, while Mohres demonstrated that obstacle avoidance in the cf bat, *Rhinolophus ferrumequinum*, is not significantly altered by plugging one ear (cited in Griffen, 1958). However, in a subsequent investigation, the obstacle avoidance score of *Rhinolophus* reduced from 90% to 60% when a monaural earplug, having a measured attenuation of 15 to 20dB, was inserted (Fleiger and Schinzler, 1972).

In order to reduce the sensitivity of one ear more effectively without causing undue discomfort, a large part of the tympanium of one ear of two fm bats, *Plecotus* and *Myotis*

lucifugus, was removed. Post-operative experiments on Plecotus indicated a substantial deterioration in both the accuracy and sensitivity of echolocation: the normal obstacle avoidance performance of 75,5% dropped to 29%. However, the post-operative obstacle avoidance performance of Myotis was only marginally affected: the measured pre-operational obstacle avoidance performance of 81% dropped to 80%. (Airapet'yants and Konstantinov, 1973).

The major difference between the experimental procedures described above is the degree to which the ear was occluded. An attenuation of 15 to 20dB, for example, would serve to unbalance binaural hearing rather than force an animal to echolocate monaurally. For this reason, the results of experiments in which one ear was surgically deafened are considered most reliable.

The ability of bats to echolocate monaurally varies. However, that certain species can spatially orientate using only a single ear is proof enough of the relevance of monaural localisation cues to auditory spatial perception.

3.2.3 Angle estimation in humans

Owing to the ease with which feedback can be obtained from human subjects, direct tests of their localisation acuity have been performed. Blauert (1983) has differentiated two abilities: "Localisation" - the accuracy with which the location of an auditory event can be determined; and "Localisation blur" - the smallest change in the position of a sound source which produces a just noticeable change in position of the auditory event. He claims that localisation blur is a measure of angular resolution:

"In the majority of relevant works, the localisation blur for changes in the azimuth of the sound source near the forward direction is consequently taken to represent the maximum spatial resolution of the auditory system."

However, localisation blur measures the ability to recognise a change in position of a single sound source. This depends on the acuity with which the position of the source can be judged, and has no bearing on the just noticeable separation of two simultaneously presented sources. A more precise representation of localisation blur is: a measure of the relative angular accuracy of localisation. Thus, what is determined is not the absolute precision with which a source can be located, but the acuity with which a positional change relative to a fixed reference can be determined.

Not all sounds can be localised: the apparent direction of narrowband signals, for example, is often markedly different from the direction of sound incidence. However, this anomaly disappears when the signal duration is sufficient to allow exploratory head movements.

To test the localisation of broadband signals, two large scale experiments of the ability to displace a loudspeaker, radiating 100ms white noise pulses forward, to the left, to the right and behind were performed. To determine the localisation blur of similar pulses, the subjects were required to align a movable loudspeaker with a fixed position reference, each alternately radiating white noise pulses (Blauert, 1983).

In both experiments, the most accurate spatial hearing was obtained in the forward direction.

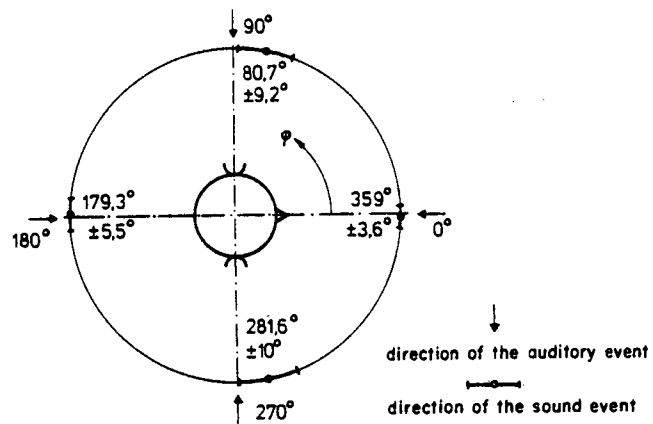


Figure 3.11 - Localisation and localisation blur using white noise pulses.

A survey of measurements of the localisation blur of a variety of sounds in the forward direction is reproduced below.

Table 3.5. Localisation blur for horizontal displacement of the sound source from the forward direction (Blauert, 1983).

REFERENCE	TYPE OF SIGNAL	LOCALISATION BLUR (Degrees)
Klemm (1920)	Impulses (clicks)	0.75-2
King and Laird (1930)	Impulse (click) train	1.6
Stevens and Newman (1936)	Sinusoids	4.4
Schmidt et al. (1953)	Sinusoids	>1
Sandel et al. (1955)	Sinusoids	1.1-1.4
Mills (1958)	Sinusoids	1.0-3.1
Stiller (1960)	Narrow-band noise, cos tone bursts	1.4-2.8
Boerger (1965a)	Gaussian tone bursts	0.8-3.3
Gardner (1968a)	Speech	0.9
Perrott (1969)	Tone bursts with differing onset and decay times and frequencies	1.8-11.8
Blauert (1970b)	Speech	1.5
Haustein and Schirmer (1970)	Broadband noise	3.2

The ability of humans to localise sounds monaurally has long been recognised; Angle and Fite (1901) demonstrated that localisation by persons totally deaf in one ear is commonplace. Batteau (1967) constructed a series of histograms which give an indication of the comparative localisation abilities of monaural and binaural hearing.

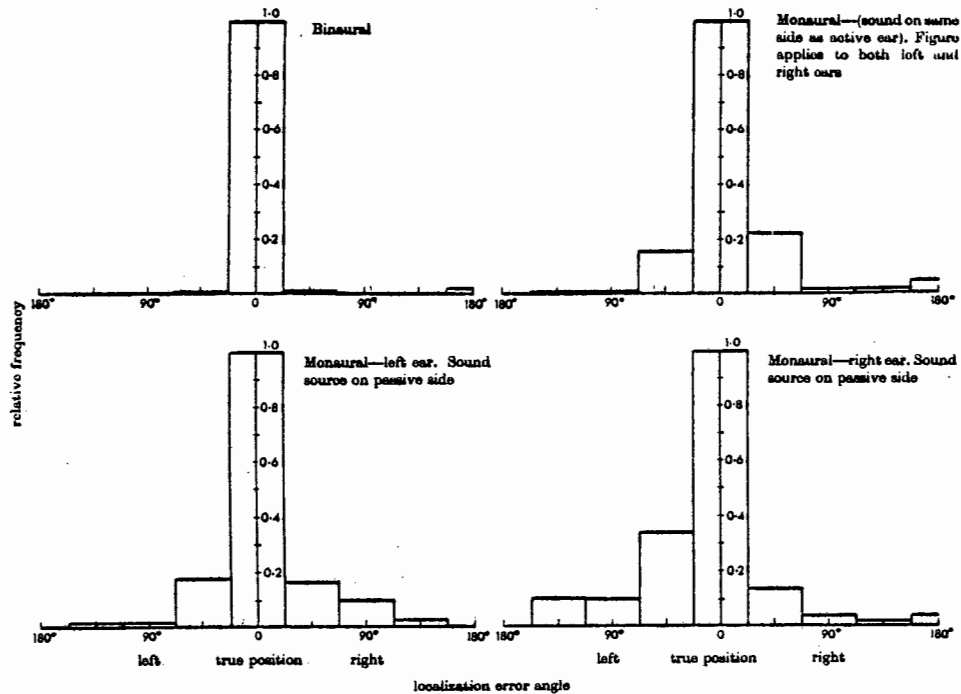


Figure 3.12 - Comparative localisation abilities of monaural and binaural hearing.

Localisation and localisation blur in 32 subjects totally deaf in one ear has been determined using white-noise pulses of 100 ms duration (Blauert, 1983).

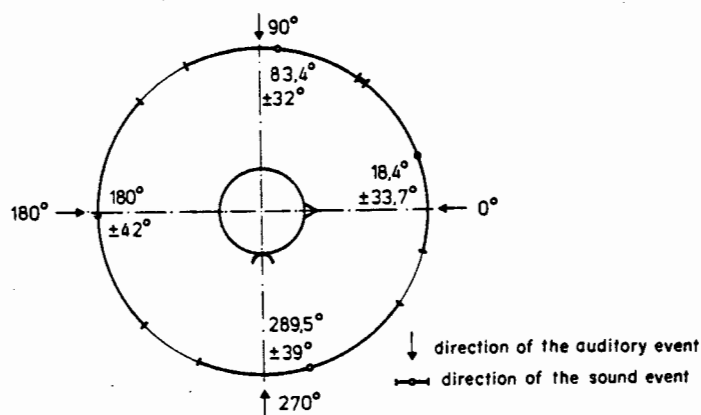


Figure 3.13 - Localisation of white-noise by subjects totally deaf in the left ear.

Pure monaural localisation is not restricted to the hearing impaired - persons with normal hearing frequently use only monaural cues to locate sounds (Blauert, 1969). The most

obvious instance of this is median plane localisation: the signals at both ears are identical, consequently interaural signal differences are of no avail.

For narrowband sounds (less than 0,7 octave) in the median plane, the direction of the auditory event depends not on elevation, but solely on frequency. The ability to localise broadband signals in the median plane varies as a function of sound spectrum (Blauert, 1969). For example, for sounds in the forward direction, the localisation blur for continuous speech by an unfamiliar person is roughly 17 degrees, around 9 degrees for continuous speech by a familiar person and approximately 4 degrees for white noise (Blauert, 1983).

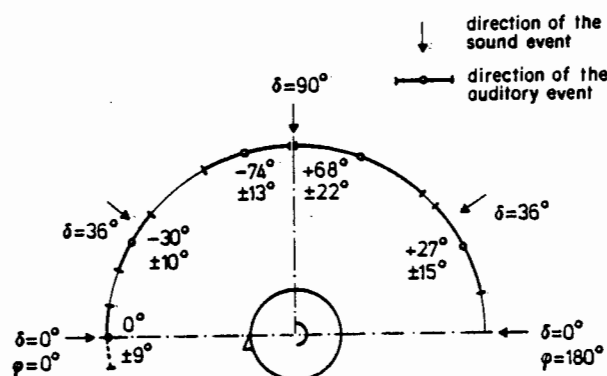


Figure 3.14 - Localisation and localisation blur of continuous speech by an unfamiliar person.

No reference to the true angular resolution capability of humans was found in the literature reviewed. However, well known human auditory phenomena such as the "cocktail-party effect" suggest that a multiple target capability probably exists. The extent to which this capability is aided by spectral differences between sources is not known. Consequently, it is difficult to postulate the extent of the human multiple target capability. The lack of data on angular resolution precludes a comparison with conventional beamforming.

3.3 Theories of angle estimation

The success of animal sonar can be attributed to the many different localisation cues which are employed in concert. These cues can be divided into two classes: binaural cues, which derive from interaural signal differences; and monaural cues, which are obtained from the interaction of an incident sound field with a single ear.

It is often held that sounds are located using binaural cues alone. However, the relationship between: the angle of incidence of sounds and differences between attributes at the two ears, cannot be described unambiguously if the ears are assumed to be simple omnidirectional receivers. Rather, there are so-called "cones of confusion", comprising geometric loci in space, at any point along which a sound source will produce identical interaural signal differences. One of these loci is the median plane, while another is illustrated below. Since it is common knowledge that sounds can be uniquely located, monaural cues must contribute to localisation.

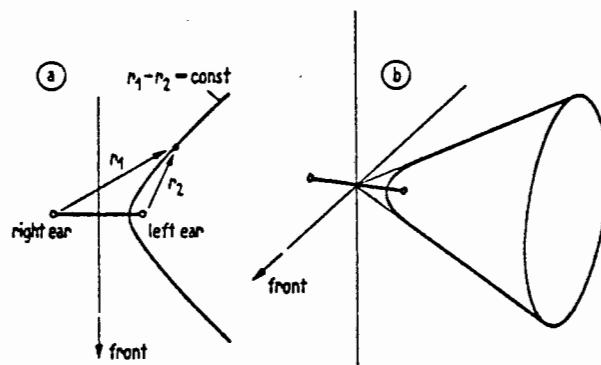


Figure 3.15 - One of the "cones of confusion"
 (a) in the plane
 (b) in space (Blauert, 1967).

Many proposed techniques of angle estimation can only localise signals under single target conditions. Since it has been observed that animals often orientate in complex multiple target situations, a number of suggested methods of localisation have limited applicability.

Binaural and monaural localisation cues will be reviewed in turn.

3.3.1 Binaural localisation cues

3.3.1.1 Interaural phase comparison

The relative interaural phase due to different path lengths to the ears is a function of angle of incidence. Therefore, it could serve as a cue to localisation.

To avoid phase ambiguities, the frequency should be low enough such that the interaural distance is less than a single wavelength - approximately 1,5kHz in man. Since humans are phase sensitive up to this frequency, it is plausible that they use interaural phase differences to aid in the localisation of sounds (Grinell, 1963). However, many possible source locations can cause an identical interaural phase difference, due to the "cones of confusion" described in section 3.3. Furthermore, if more than a single incident sound is simultaneously received, it will not be possible to separate out the individual interaural phase differences. Consequently, the technique is only useful under single target conditions.

The sonar cries of most bats contain wavelengths which are far smaller than their pinna separation. In addition, it is thought that they are phase insensitive at the high frequencies which constitute their sonar cries. Grinell (1963) writes:

"One to one volleying of auditory cells to every cycle of a sound probably fails above 2 to 5kHz, even in the bat".

For this reason, the interaural phase comparison of sonar echoes is not a useful localisation cue to bats.

The literature reviewed contains no reference to the ability of cetaceans to measure phase; however, it is probable that they have a similar phase resolution to bats and humans. Their range of sensitivity would therefore be well below the frequency band present in their sonar clicks. Consequently, target localisation based upon interaural phase differences is not considered a significant directional cue in these animals.

3.3.1.2 Interaural arrival time comparison

Target bearing can be expressed as a function of the interaural arrival time difference:

$$\theta = \arcsin(Tc/d) \quad (3.1)$$

where: T is the interaural arrival time difference.
 d is the pinna separation.
 c is the speed of sound.

This expression is differentiated to obtain angular accuracy:

$$\frac{d\theta}{dT} = \frac{1}{(1-(Tc/d)^2)^{3/2}} \cdot \frac{c}{d} \quad (3.2)$$

However, since:

$$T = (d/c)\sin\theta, \quad (3.3)$$

the angular accuracy $d\theta$ is:

$$d\theta = \frac{cdT}{d\cos\theta} \quad (3.4)$$

where: dT is the just detectable arrival time difference.

The just detectable arrival time difference in humans is approximately 9 microseconds, while a minimum value of 5 microseconds has been observed. Since the interaural distance in humans is roughly 200 mm, an angular accuracy of 0,9 degrees is predicted using a just detectable arrival time difference of 9 microseconds.

It is postulated that the just detectable arrival time difference in bats and cetaceans is similar to that of humans (Shimozawa et al, 1974). The pinna separation of echolocating bats is between 15mm and 20mm. If their just detectable interaural time difference is assumed to be no better than 5 microseconds, then their angular accuracy will only be 5 to 6,5 degrees. The cetacean head is at least 300mm across. Assuming a just noticeable interaural arrival time difference of 5 microseconds, an angular accuracy of 0,3 degrees is obtained.

This theoretical analysis predicts a best case angular accuracy which is well in excess of the measured localisation abilities of humans and cetaceans; while for bats, the predicted angular accuracy is slightly poorer than their demonstrated angular acuity. Therefore, a comparison of interaural arrival time differences could be a useful localisation cue for humans and cetaceans, but is probably less relevant to bats.

A limitation of this technique of localisation is that a whole locus of possible source positions can result in a single interaural time difference. These loci are the "cones of confusion" described in section 3.3. A further drawback is that the technique is ambiguous if more than one target echo is simultaneously received, since it will not be possible to separate out more than a single arrival time difference.

3.3.1.3 Interaural frequency differences

Since the sonar echoes of fm bats are chirps, a comparison of the instantaneous frequency difference present at the two ears could be used to determine target position (Kay, 1962).

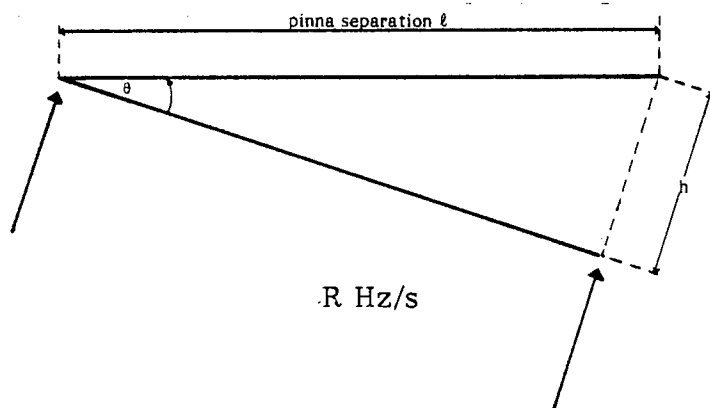


Figure 3.16 - A chirp received at the two pinnae.

The frequency difference f present at the two ears owing to a chirp sweeping at a rate R Hz/s is:

$$f = (R\ell/c)\sin\theta \quad (3.5)$$

where: ℓ is the pinna separation.
 θ is the target bearing.
 c is the speed of sound.

Therefore bearing can be determined as:

$$\theta = \arcsin(cf/R\ell) \quad (3.6)$$

Angular accuracy is obtained by differentiating this expression with respect to frequency:

$$\frac{d\theta}{df} = \frac{1}{(1-(cf/R\ell)^2)^{1/2}} \cdot \frac{c}{R\ell} \quad (3.7)$$

Combining equations (3.5) and (3.7):

$$\frac{d\theta}{df} = \frac{1}{(1-\sin^2\theta)^{\frac{1}{2}}} \cdot \frac{c}{R\ell} \quad (3.8)$$

Hence angular accuracy is:

$$d\theta = \frac{cdf}{R\ell \cos\theta} \quad (3.9)$$

A typical fm bat has a pinna separation of 20mm and a sonar cry which sweeps at a rate of 50kHz/ms (Grinell, 1963). Consequently, to obtain an accuracy of 5 degrees at an angle of 45 degrees, such a bat would only be required to discriminate a frequency difference of 180Hz; many orders of magnitude within the capabilities of these animals.

The limitations of most binaural localisation techniques apply here: "cones of confusion" exist for every interaural frequency difference. In addition, if multiple target echoes are simultaneously received, it will not be possible to distinguish the respective interaural frequency differences. Therefore, the technique will only function successfully under single target conditions.

3.3.1.4 Doppler shifts as a cue to localisation

Doppler shifts in the echoes of the orientation cries of cf bats could be used in the initial determination of target bearing: while objects in the forward direction return echoes of maximum doppler shift, targets off the direct flight line return echoes at lower frequencies (Grinell and Schinzler, 1977).

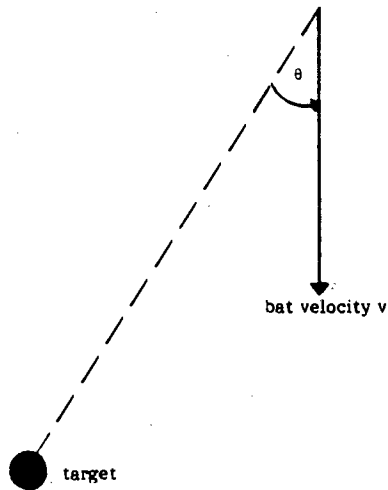


Figure 3.17 - Doppler shifts as a cue to localisation.

The doppler shift for a broadside target is:

$$\delta f = 2vf/c \quad (3.10)$$

where: δf is the shift in frequency.
 v is the bat velocity.
 f is the transmit pulse frequency.
 c is the speed of sound.

Since the axial target velocity is $v \sin \theta$, target bearing is determined by:

$$\theta = \arcsin \frac{c(\delta f)}{2vf} \quad (3.11)$$

Angular accuracy is obtained by differentiating this expression:

$$\frac{d\theta}{d(\delta f)} = \frac{1}{1 - (c(\delta f)/2vf)} \cdot \frac{c}{2vf} \quad (3.12)$$

However, since:

$$\delta f = \frac{2vf}{c} \cdot \sin \theta, \quad (3.13)$$

Angular accuracy is:

$$d\theta = \frac{cd(\delta f)}{2vf} \quad (3.14)$$

A typical cf bat might fly at 5 metres per second, transmitting a pulse of around 80 kHz. To obtain an accuracy of 5 degrees at an angle of 45 degrees, a frequency shift of 145Hz must be detected; well within its capability.

A moving target would result in a false estimate of target bearing. However, since all targets travel very much slower than bats, their velocity would only cause a marginal inaccuracy.

A limitation of this technique is that a "cone of confusion" exists for each possible doppler shift. However, unlike most other binaural localisation techniques, localisation using doppler shifts can locate more than a single target. The reason is that the presence of multiple targets will result in a number of doppler shifted frequencies. Each of these can be individually recognised provided the individual doppler shifts are separated by at least the minimum resolvable frequency separation.

3.3.1.5 Interaural comparison of echo frequency components

The irregular pinna structure of mammals modifies the spectrum of received sounds uniquely for every possible incident angle. Dividing the sound spectrum received at one pinna by that received at the other results in a set of binaural ratios; unique for incident direction and independent of the spectral shading of any particular sound.

These ratios have been widely proposed as a powerful localisation cue to those echolocating animals which receive broadband signals: the fm bats, cetaceans and humans

(Grinell, 1963; Grinell and Grinell, 1965; Grinell, 1973; Shimozawa et al, 1974; Neuweiler, 1980a; Schinzler and Henson, 1980; Musicant and Butler, 1985). The strength of this technique is that it eliminates the "cones of confusion" which prevent all previously described techniques from uniquely locating targets. However, because the calculation of binaural ratios is a non-linear procedure, superposition does not apply. Therefore, it is difficult to locate multiple targets using the interaural comparison of echo frequency components.

Consider the example of two simultaneously received signals, A and B. These will result in the spectra $A_1(f)$ and $B_1(f)$ at one pinna, and $A_2(f)$ and $B_2(f)$ at the other. The resulting binaural spectral ratios will be:

$$\frac{A_1(f)+B_1(f)}{A_2(f)+B_2(f)} = \frac{A_1(f)}{A_2(f)} + \frac{B_1(f)}{B_2(f)} + \frac{A_1(f)B_2(f)^2 - A_2(f)B_1(f)^2}{A_2(f)^2 B_2(f) + A_2(f)B_2(f)^2} \quad (3.15)$$

The terms $A_1(f)/A_2(f)$ and $B_1(f)/B_2(f)$ correspond to the binaural ratios of each of the incident sounds. However, the cross-product term will confuse the received ratios.

Consequently, in any one range cell, only a single incident sound field can be located. Since a multiple target capability is an important feature of animal sonar, the importance of this method of localisation has probably been overemphasised.

3.3.1.6 Interaural comparison of cf echo components

This technique is analogous to the interaural comparison of echo frequency components; however, it is applicable to cf bats.

By scanning their pinnae in synchronism with each sonar return, and sampling the binaural ratios at intervals along

the scan, a unique set of ratios can be obtained for each possible incident angle (Schinzler and Henson, 1980).

The interaural comparison of cf echo components has similar limitations to the interaural comparison of echo frequency components. While unambiguous source localisation can be performed under single target conditions, non-linearities present in the processing render it unsuitable for the localisation of a number of simultaneously incident sounds.

3.3.2 Monaural localisation cues

The inability of binaural localisation to fully explain the angle estimation capabilities of animal sonar systems, and the demonstrated ability of humans and some bats to locate targets monaurally, verifies the importance of these cues to localisation.

The essential cue for monaural localisation is the direction dependent linear filtering which the pinna performs on incident sounds. The spectrum modification caused by this filtering can be used to determine incident direction: animals have learned to associate different spectral features with different directions.

A major advantage of monaural localisation is that multiple simultaneously incident sounds can be localised, since the pinna filtering is a linear procedure. This multiple target capability is fully explored in section 4.3.

The major difficulty in monaural localisation lies in differentiating between the pinna spectrum modification and the raw spectrum of received sounds. The problem is most severe when localisation is performed in the passive mode, since the animal has no prior knowledge of the incident spectrum. When cetaceans and bats echolocate in the active mode, the echo spectrum is a replica of the transmitted

spectrum, modified by interaction with the target. Computer simulations described in section 4.3 have shown that even when this modification is substantial, recognition of the pinna spectrum modification is still possible.

Humans echolocating passively have no prior knowledge whatsoever of the spectrum of incident sounds. As a result, certain sounds are localised erroneously, while for others, the perceived source location is a function of the sound spectrum rather than of incident angle (Blauert, 1983). However, techniques have been developed which enable certain classes of signal, including many naturally occurring sounds, to be located in the passive mode. These are described in chapter 5.

Monaural localisation cues fulfil an important role in animal echolocation, and constitute the major field of interest of the current research. A number of possible techniques of beamforming based upon monaural echolocation have been modelled and evaluated. They are fully documented in chapters 4 through 6.

3.4 Range accuracy and range resolution

The accuracy of range determination and range resolution are differentiated in the same manner as are angular accuracy and resolution. The accuracy of range determination refers to the precision with which the range of a single target can be estimated, while range resolution describes the minimum discernable range separation between two identical targets present in the same angular cell.

Researchers of animal sonar have often equated these two concepts. Consequently, mistaken conclusions have sometimes been drawn about the range determination capabilities of echolocating animals.

3.4.1 Range accuracy and range resolution in cetaceans

To investigate the accuracy of range determination in the bottlenose dolphin, *Tursiops truncatus*, two identical polyurethane spheres, 7,6cm in diameter, were suspended 0,4 metres below the water surface. Target distance was adjusted until the smallest perceivable range difference had been determined by the descending method of limits (Murchison, 1980).

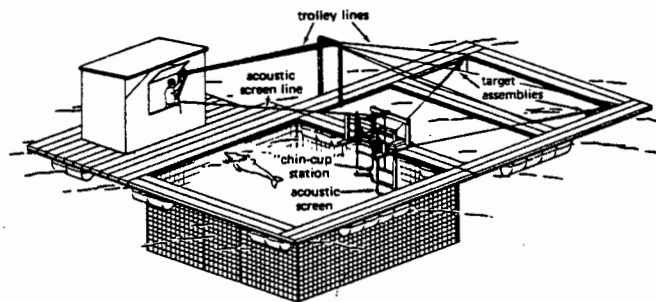


Figure 3.18 - Range determination in the bottlenose dolphin.

Murchison claims to have measured range resolution. However, the targets spanned a sector of 40 degrees. Since the half-power beamwidth of Tursiops is little over 10 degrees, the animal would have scanned the spheres sequentially, estimated each target distance, and then assessed which was closer. Consequently, the investigation did not measure the minimum discernable range distance between two simultaneously presented targets, but measured the accuracy with which the range of each could be determined.

The experiment was conducted at absolute target ranges of 1 metre, 3 metres and 7 metres; the respective 75% correct response thresholds occurred at range differences of 9mm, 15mm and 28mm.

The measured accuracy of range determination fell off linearly with absolute range; a plausible result since the error in estimating the two-way propagation time is a function of absolute time, a parameter which varied from 1,3ms to 9,3ms.

3.4.2 Range accuracy and range resolution in bats

The accuracy with which four species of bat can measure range was tested by training them to fly from a perch to the closer of two identical platforms, situated 40 degrees apart. In the back of each platform was mounted a triangular target.

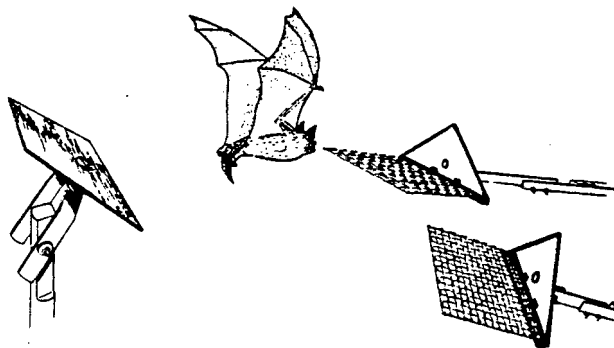


Figure 3.19 - Range determination in bats (Simmons, 1973).

Two of the species participated in a second experiment, in which the targets were replaced by target simulators - two electrostatic transducers. The sonar cries were received on two microphones. These were positioned in line with the simulated targets, 7cm distant. Between each microphone and transducer was inserted a variable delay line, enabling the "target distance" to be altered at will. Therefore, this experiment ensured that no cue other than a difference in the two-way propagation times was employed in the range determination procedure.

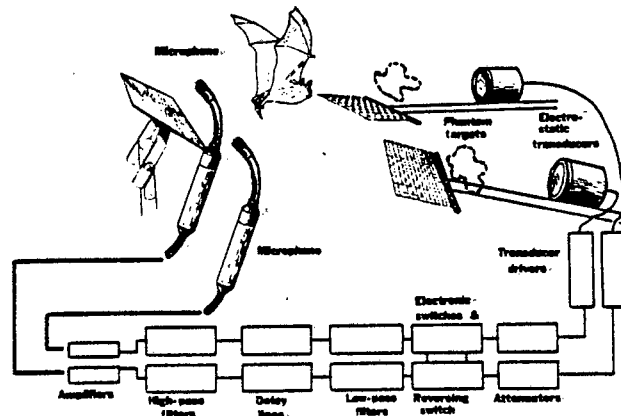


Figure 3.20 - The two-channel target simulator.

For those bats that participated in both experiments, the measured just noticeable range difference coincided in each case. Therefore, it can be concluded that the two experiments were equivalent.

In all four species, the accuracy of range determination was independent of absolute range investigated (20cm to 60cm). The differences in target distance at the 75%^{*} correct response threshold of each species, together with their measured pulse bandwidths, are tabulated below:

Table 3.6. Range determination thresholds in four species of bat. The echolocating pulse bandwidth is also given (Simmons, 1973; Simmons, Howell and Suga 1975).

SPECIES	DISCRIMINATION THRESHOLD	PULSE BANDWIDTH
<i>Eptesicus fuscus</i> (fm)	13mm	23kHz
<i>Phyllostomus hastatus</i> (fm)	12mm	35kHz
<i>Pteronotus suapurensis</i> (cf)	15mm	22.5kHz
<i>Rhinolophus ferrumequinum</i> (cf)	25mm	15kHz

In each instance, the just noticeable target difference closely matches the range resolution which would be predicted were the bats to perform target ranging by a biological equivalent of cross-correlation detection. Taking the results of these experiments as a measure of range resolution, Simmons (1973) has analysed this relationship in detail, concluding that echolocating bats resolve range by an equivalent procedure to matched filtering.

However, the experiments measured the accuracy of range determination rather than range resolution. The target separation was 40 degrees, very much coarser than the angular resolution capability of these animals. Therefore, to determine the closer target, the bats scanned from one to the other, indicating that target ranges were being estimated successively. Consequently, the just noticeable range difference in this instance is a function of the accuracy with which the range of each target was estimated, rather than of resolution.

One possible method of determining range resolution would be to feed two separate delay lines with the output of a single microphone. This would simulate targets differing in range

alone. Simmons attempted just such an experiment:

"... the bat would not easily accept the simultaneous operation of the two channels driven from one microphone ... This version of the target simulator destroyed any information that the bat could derive by aiming the sounds first at one simulated target and then at the other ..."

Thus, the assertion that accuracy rather than resolution was measured, is confirmed. The quotation also evinces that the range resolution of bat sonar is rather disappointing. Perhaps their sophisticated target recognition and angular resolution capabilities reduce the range resolution requirement.

Contrary to the cetacean experiment, range determination remained constant as a function of absolute range. It is possible that the smaller range of absolute two way propagation times, 1ms to 3,5ms, accounts for this; an investigation of range determination at greater absolute distances is required to verify this assertion.

3.4.3 Range determination in humans

Although passive beamforming systems do not generally perform target ranging, certain range dependent attributes of incident sounds afford humans a partial range determination capability.

If a sound source is in the nearfield, then the curvature of incident wavefronts can no longer be neglected.

Consequently, the spectrum modification imposed will be a function of both bearing and range. The approximate limit of the nearfield is determined by the expression $(2d^2/\lambda)$ (Skolnik, 1981); where d is the diameter of the head in the sagittal plane (approximately 200mm) and λ is the signal wavelength (17mm at the highest audible frequency).

The expression yields a nearfield region of 4,7 metres at 20kHz. However, since the extent of the nearfield decreases proportionately with frequency, it can be expected that the region in which the pinna transfer function varies significantly with range is somewhat smaller; in practice it extends to around 3 metres (Blauert, 1983).

Between approximately 3 and 15 metres, the only angle dependent attribute is attenuation due to spherical spreading. In this region subjects have been observed to estimate distance by assessing the probable source power; unusual sounds sometimes result in erroneous target ranging.

At greater distances the shorter wavelength constituents of a sound are increasingly attenuated: this attribute is used to identify distant sources (Blauert, 1983).

3.5 Sensitivity of echolocation

The ability of echolocating bats to avoid copper wires of varying diameters stretched across a room has been determined for the fm bats: *Myotis lucifugus*, *Myotis oxygnathus* and *Plecotus auritus*; and for the cf bat: *Rhinolophus mehelyi* (Griffen, 1958, Airapet'yants and Konstantinov, 1973).

A monotonic decrease in obstacle avoidance for diminishing wire diameters was observed: the sensitivity threshold for the fm bats was around 0,12mm, while *Rhinolophus* even negotiated 0,08mm wires with a high percentage avoidance. The results of these experiments are tabulated below:

Table 3.7. Avoidance of wires of varying diameters.

DIAMETER OF WIRES (mm)	SPECIES			
	MYOTIS LUCIFUGUS	MYOTIS OXYGNATHUS	PLECOTUS AURITIS	RHINOLOPHUS MEHELYI
4,8	85%			
1,21	85%			
1,12		85,2%	91,5%	91,6%
0,68	77%			
0,55		79,8%	86,3%	91,4%
0,35	72%	70,9%	72,5%	
0,26	52%			
0,20		67,3%	72%	82,4%
0,12	39%	53,9%	60,6%	82,2%
0,08		48,5%		76,8%
0,07	36%			

The sensitivity of echolocation in the harbour porpoise, *Phocoena phocoena* has been tested in a similar fashion (Nachtigall, 1980). The animal was observed to consistently avoid iron, copper and steel wires 0,5mm in diameter, but frequently collided with 0,2mm wires. More detailed results are tabulated below:

Table 3.8. Sensitivity of echolocation in the harbour porpoise.

TARGET	WIRE DIAMETERS (cm)	PERCENTAGE CORRECT RESPONSES
Iron, copper and steel wires	0,35	98,9
	0,15	98,9
	0,075	94,7
	0,05	90,9
	0,035	78,9
	0,02	46

Unfortunately, no measurement of the backscattered echo strength was taken during these experiments. Consequently, it is not possible to obtain a quantitative measure of the sensitivity of echolocation. However, it was established that bats can consistently avoid wires of diameter $1/30$ of the shortest wavelength present in their sonar cries, and that the harbour porpoise can avoid wires $1/60$ of the wavelength of its highest click frequency. This demonstrates at least that these mammals are able to detect extremely weak target echoes.

3.6 Target classification and recognition

Humans echolocate passively, identifying active targets on the basis of attributes of the received sound. Their pattern recognition ability is exceptional: their ability to recognise speech is a feat which no machine has yet managed to emulate.

However, the pattern recognition and classification abilities of the cetaceans and bats are more analogous to those of conventional beamforming. These animals are able to recognise and classify targets by analysing the target modification of their sonar cries.

3.6.1 Target classification and recognition in cetaceans

The ability of cetaceans to discriminate between objects differing only in size has been determined on a number of occasions. Unfortunately, experimental procedures and training methods differed between investigations, consequently a direct comparison is not wholly valid (Nachtigall, 1980). A review of some of the findings is tabulated below:

Table 3.9. Acuity of Cetacean object size perception.

TARGET	DIAMETERS DISCRIMINATED (cm)	% CORRECT RESPONSE	SPECIES	AUTHOR
Solid spheres (steel- nickel)	6,35:5,72 :5,40 :5,08 :4,76	77 90 93 98	Tursiops truncatus	Turner and Norris (1967)
Solid cylinders length =7,78 cm (chloro- prene)	1,64:2,07 :2,62 :3,28 :4,16 :5,20	85 94 89 96 90	Tursiops truncatus	Evans (1973)
Solid cylinders length =7,78 cm (chloro- prene)	1,64:2,07 :2,62 :3,28 :4,16 :5,20	70 77 89 90 90	Inia geo- frensis	Evans (1973)
Circular discs (neo- prene backed with Alu- minium)	15,2:25,0 :20,0 :18,0 :17,2 :16,1 :15,7 :15,2	98,3 98,5 97 94,1 74,8 57,5 50,7	Tursiops truncatis	Barta and Evans
Circular discs (copper: thick- ness discrimi- nated) D=20cm	0,22:0,16 :0,27 :0,33 :0,64	50 60 75 90	Tursoips truncatis	Barta and Evans

The results of two investigations of the ability of the bottlenose dolphin, *Tursiops truncatus*, to discriminate targets by shape are tabulated below (Nachtigall, 1980):

Table 3.10 Target shape discrimination by the dolphin *Tursiops truncatus* (Nachtigall, 1980; Nachtigall, Murchison and Au, 1980)

TARGET		TARGET SIZE		%CORRECT RESPONSES
POSITIVE	NEGATIVE	POSITIVE	NEGATIVE	
Circular discs	flat squares	182 cm	428 cm 269 cm 182 cm 87 cm	100 98,6 93,1 100
Circular discs	flat triangles	182 cm	346 cm 187 cm 48 cm	97,9 92,3 100
Circular discs	circular discs	182 cm	182 cm	49,6
Solid cylinders (up-right)	solid cubes (flat face forward)	4x4x4 cm	4x4x4 cm	75
			5x5x5 cm	94
			6x6x6 cm	91
		5x5x5 cm	4x4x4 cm	87
			5x5x5 cm	87
			6x6x6 cm	98
		6x6x6 cm	4x4x4 cm	91
			5x5x5 cm	94
			6x6x6 cm	96

A more quantitative analysis is required to obtain a measure of the target recognition capabilities of these animals. However, what has been determined thus far is that the ability to recognise and classify targets is integral to cetacean sonar.

3.6.2 Target classification and recognition in bats

The acuity with which the fm bat, *Eptesicus fuscus*, can distinguish differences of size in similarly shaped objects was determined by training the bats to fly to the larger of two simultaneously presented isosceles triangles.

The 75% correct response threshold occurred for the discrimination of a triangle of base 10cm and height 5cm from one of base 9cm and height 4,5cm. This represents a difference in area of 20% and corresponds to an echo intensity difference of between 1,5 and 3dB (Simmons, 1968).

The just noticeable diameter difference between cylinders was determined for two fm bats: *Noctilio leporinus* and *Myotis oxygnathus*; and a cf bat: *Rhinolophus ferrumequinum*. The 75% correct response threshold in *Noctilio* occurred at an echo intensity difference of 1dB; *Myotis* required an echo intensity difference of 2dB; while *Rhinolophus* could only discriminate between two cylinders when their echo intensity difference was between 4 and 5dB (Schinzler and Henson, 1980).

A shape discrimination test, in which the fm bat *Myotis oxygnathus* and the cf bat *Rhinolophus ferrumequinum* were trained to differentiate between a circle, a triangle and a square, all of area 156 square centimetres, resulted in a correct response score of between 86,6% and 92,3% for the fm bat, while *Rhinolophus* scored between 70% and 85% correct responses (Airapet'yants and Konstantinov, 1973).

It has also been observed that the fm bat, *Eptesicus fuscus*, can discriminate differences of less than a millimeter in the depth of small holes drilled into the face of planar targets; *Eptesicus serotinus* can distinguish between similar targets covered in the one instance with glass, and in the other with velvet; while both the fm bat, *Myotis oxygnathus*, and the cf bat, *Rhinolophus ferrumequinum*, can discriminate an aluminium

plate from similar plates constructed of plexiglass and plywood, but not from similar plates constructed of iron and brass (Schinzler and Henson, 1980; Simmons, Howell and Suga, 1975).

The ability to distinguish fluttering targets enables bats to ignore unwanted clutter while locating and pursuing prospective prey. Both fm and cf bats have consistently been observed to avoid motionless targets, among which were freshly killed insects, and pursue fluttering targets (including in one instance a stationary mechanical insect with flapping wings). It has been found that the cf bat, *Rhinolophus*, requires only 0,3mm oscillation amplitude of a target flapping at 40Hz to recognise a fluttering target (Airapet'yants and Konstantinov, 1973; Novick, 1973; Goldman and Henson, 1977; Schinzler and Henson, 1980).

While a proper evaluation of the target recognition skills of echolocating bats requires a more systematic treatment, it has been demonstrated that bat sonar includes a sophisticated target classification ability. The superior target classification ability of fm bats to that of cf bats is no doubt due to the wider bandwidth of their sonar cries.

3.7 Resistance to interference

It is self-evident that echolocating animals need to be able to spatially orientate in the vicinity of clutter, reverberation and other echolocating animals: the apparent effortlessness with which bats echolocate through highly reverberant caves in the company of hundreds of other echolocating bats is particularly impressive.

The ability of the bottlenose dolphin, *Tursiops truncatis*, to determine the presence of a 7,5cm diameter steel water-filled sphere of target strength -32dB in the presence of high intensity white noise has been investigated. The sphere was positioned at a distance of 16,5m, while five levels of white noise: 67dB/Hz, 72dB/Hz, 77dB/Hz, 82dB/Hz and 87dB/Hz (re 1 micro-Pa) were beamed at the animals. Since the bandwidth of the sonar clicks of *Tursiops* is approximately 100kHz, noise levels in this range varied between 72dB and 92dB. The chance threshold of 50% correct responses was reached at a noise level of between 87 and 92dB, while the 75% correct response threshold was reached at a noise level of 75dB (Penner and Kadane, 1980). The source level of transmission was approximately 170dB.

It is possible to determine the received signal-to-noise ratio by calculating the received echo strength: a transmit level of 170dB corresponds to a pressure of 316,23 Pa. Intensity is related to pressure according to the expression:

$$I = p^2/Z \quad (3.16)$$

where: Z is the characteristic impedance of water ($\rho_0 c$)
 $= 1,54E6$ Rayls.

Hence the transmitted intensity is:

$$I = (316,23)^2 / (1,54E6) = 0,065 \text{ W/m}^2 \quad (3.17)$$

The target strength is -32dB or $1/1585$, while the intensity loss due to spherical spreading is $1/R$ or $1/(7,41E4)$.

Therefore the echo intensity will be:

$$0,065 \times (1/1585) \times (1/7,41E4) = 0,55E-9 \text{ W/m}^2 \quad (3.18)$$

This intensity corresponds to an acoustic pressure of 0,029 Pa or 89,3dB (re 1 micro-Pa).

Consequently, the signal-to-noise ratio at the chance threshold was 0dB, while the signal-to-noise ratio at the 75% correct response threshold was 14dB. Unfortunately, insufficient information was presented about both the experiment and the cetacean transmissions to allow a meaningful comparison with the performance of an equivalent conventional active sonar system. To achieve this, data regarding the noise distribution, the transmit pulse length and the number of pulses used would be required. Therefore, it is not possible to comment on the relative detection performance of Tursiops.

The fm bat, *Plecotus auritus*, was forced to negotiate vertically strung wires of diameter 1,07mm, in the presence of white noise bandlimited between 20 and 120kHz. When the bats reached a distance of 50cm from the wires, their pulse repetition rate was observed to increase suddenly. If this response is taken as an indication of the distance at which the bats first detected the obstacles, then the wires were detected when the signal-to-noise ratio was -5dB. The bats detected wires more than 80% of the time with a false alarm rate of 0,01% (Griffen, 1958). As is the case with the cetacean experiment, insufficient information prevents a comparative evaluation between the detection performance of *Plecotus* and that of an equivalent conventional sonar system.

To quantify the effect of interfering noise on human sound localisation is a more complicated matter. Since humans echolocate passively, the ability to localise in the presence of noise is a function of the nature of the incident sound. One direct attempt measured the localisation blur of sinusoidal test signals in the forward direction in the presence of a homogeneous mix of sounds of automotive traffic. It was found that localisation blur was not adversely affected, provided the test signal was 10 to 15dB above the masked threshold (Blauert, 1983).

One method of improving echolocation in the presence of noise would be to invoke filters of high sensitivity, which narrowly bandlimit the received signal, and thereby increase the signal-to-noise ratio. Certain bats have been observed to increase their hearing sensitivity at coded frequencies, and to sharpen their cochlear tuning curves when subjected to wideband noise; while evidence has been found of up to forty critical wavebands in the dolphin *Tursiops truncatus*, each of which is narrower than the wavebands found in other mammals (Grinell, 1963; Popper, 1980).

The flexibility of the orientation signals of echolocating animals is a further aid in combating noise interference, since they are able to adapt their sonar transmissions to occupy spectral regions of least noise.

Another technique employed in resisting interference is to utilise the directional sensitivity of the pinnae. For example, when the bat *Plecotus* was forced to fly through a bank of wires in the presence of noise, it flew obliquely from side to side, constantly maintaining one pinna in the direction of minimum noise (Grinell, 1963). Finally, binaural interaction has been shown to play an important role in resisting interference. Provided that the interaural phase relationships between the signal and the noise differ, then a significant advantage is obtained in overcoming the masking effects of noise (Blauert, 1983).

3.8 On the development of a sonar system based upon monaural echolocation

The remarkable sonar skills of echolocating animals suggest the possibility that a novel sonar based upon their echolocation capability could fulfil certain requirements currently served by conventional sonar systems. The significance of such a development is that the mechanisms of animal sonar are so profoundly different from those of conventional beamforming.

Conventional beamforming systems locate targets by forming multiple beams or by sequentially scanning a single narrow beam. In sonar this involves using a transducer array of many separate elements, and entails pre-processing the output of each element before it enters a beamformer. To achieve N angular resolution cells, there must be N transducer elements and an N element beamformer. Despite the current advanced state of digital technology, such a system is complex and costly if N is large.

Animal sonar provides an attractive alternative. Mammals generally use only two receivers, each surrounded by an irregular reflector. Furthermore, experiments into monaural localisation have shown that successful localisation can be obtained using only one of these receivers. Thus multiple beams are achieved using a single active element and without resorting to mechanical scanning.

While conventional beamforming is founded on essentially narrowband techniques (the only uses of a wide bandwidth in active systems being to improve range resolution and to steer the beam in a frequency scanned array), monaural echolocation has been shown to rely on a wide bandwidth: the spectrum modification caused by the interaction of broadband incident signals with the pinna has been demonstrated to be the essential localisation cue. Therefore, by exploiting a wide bandwidth, a simple, low-cost and yet effective beamforming

system can be constructed from a single receiver and a fixed passive reflector. (An exception are the cf bats. They echolocate using narrowband transmissions by scanning their pinnae in synchronism with vocalisation - a less attractive model on which to base the development of a sonar system.)

A number of possible methods of monaural beamforming have been evaluated in computer simulations. In addition to angular resolution, the range resolution of a sonar based upon monaural echolocation has also been examined. The most successful of these computer models was implemented in an experimental active underwater sonar system which was constructed and tested in the underwater tank facility of the Central Acoustics Laboratory at the University of Cape Town. Since the technique is proposed as a possible mechanism of monaural localisation, the ability of a mannikin human head to localise a variety of sounds in the median plane was also investigated. The results obtained can be compared directly with the measured localisation ability of human subjects.

4.0 COMPUTER SIMULATIONS OF BEAMFORMING BASED UPON MONAURAL ECHOLOCATION

A number of possible techniques of monaural localisation have been evaluated in computer simulations. The main aim was to develop a beamforming system which uses only a single hydrophone surrounded by an irregular reflecting structure. Since this is similar to a single ear, it was also considered useful to evaluate the techniques developed as possible models of monaural localisation.

A beamforming system based upon monaural echolocation should incorporate analogous structures to those used by animals: the pinna, which modifies the spectrum of incoming sounds; the eardrum, which is sensitive to incident pressure; the basilar membrane, which analyses received spectra; and the brain, which analyses the cochlear output in order to locate sources. The analogous structures which were simulated are: a transducer surrounded by an irregular reflector; a bank of contiguous bandpass filters; and the digital signal processing techniques devised to locate targets. These processing techniques comprise the nub of this research project: to develop a method of using received spectra to determine incident angle.

Of the many potential techniques of localisation investigated, three will be described. They have been named: beamforming by the solution of simultaneous equations, beamforming by the deconvolution processing of received sounds, and beamforming by the cross-correlation analysis of received spectra.

Simulations of the first two techniques indicate that they are capable of determining target direction. However, it was found that the cross-correlation analysis of received spectra is the most successful of these models. It is suggested that this is a beamforming technique which could have certain important advantages over the conventional phased array.

Although all of these techniques can locate sounds in three dimensions, they have only been evaluated in the azimuth plane.

4.1 Beamforming by the solution of simultaneous equations

This method of beamforming locates incident sounds by measuring the power outputs of a bank of contiguous bandpass filters. These are used as the right-hand vector of a system of linear equations. The coefficient matrix consists of stored spectral responses to white noise, predetermined in each angular cell along the sector of scan. The solution vector, obtained by reducing this linear system, indicates target direction.

4.1.1 Description of technique

To predetermine the characteristic spectrum modifications which a receiver imposes on incident sounds, the frequency response to a white noise source is recorded at angular increments along the sector of scan. This is achieved by measuring the power outputs of a bank of contiguous bandpass filters. The result of one such calibration is shown below.

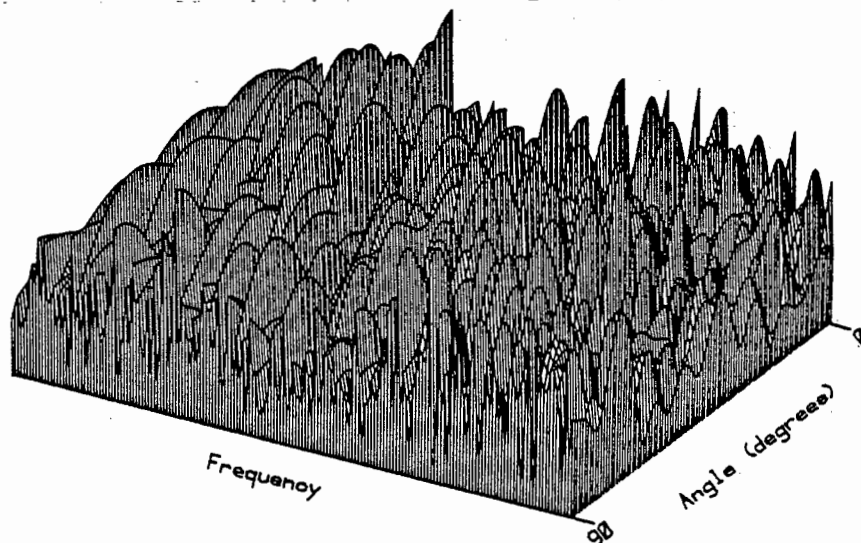


Figure 4.1 - The spectrum responses of a receiver taken at 181 angles between 0 and 90 degrees. The receiver was 10,5 wavelengths across at the highest frequency of calibration.

The grid values obtained from such a calibration constitute the coefficient matrix of a linear system: the coefficients of successive rows are the recorded filter power outputs measured at successive angular increments. Since a unique solution requires that the number of rows does not exceed the number of columns, the number of angular increments should be no greater than the number of bandpass filters. The coefficient matrix therefore takes the form:

$$\begin{bmatrix} a_{11} & . & . & . & a_{1n} \\ . & & & & . \\ . & & & & . \\ . & & & & . \\ a_{n1} & . & . & . & a_{nn} \end{bmatrix} \quad (4.1)$$

where: a_{ij} is the predetermined power output of the i th filter, for a sound incident at angular increment j .

To locate incident signals, the following linear system is solved by Gauss-Jordan Reduction (Sokolnikoff and Redheffer, 1958):

$$\begin{bmatrix} a_{11} & . & . & . & a_{1n} \\ . & & & & . \\ . & & & & . \\ . & & & & . \\ a_{n1} & . & . & . & a_{nn} \end{bmatrix} \begin{bmatrix} I_1 \\ . \\ . \\ . \\ I_n \end{bmatrix} = \begin{bmatrix} P_1 \\ . \\ . \\ . \\ P_n \end{bmatrix} \quad (4.2)$$

where: P_i is the power output of filter i in response to the incident signal.

The solution vector $(I_1 \dots I_n)$ determines the contribution of each angular cell to the incident spectrum. It also indicates target strength.

4.1.2 Approximate solutions and matrix conditioning

If the right-hand vector of a linear system is an exact linear combination of rows of the coefficient matrix, then any number of concurrently received targets can be unambiguously localised, provided they are spaced more than a single angular increment. However, interpolation between the angles of predetermined spectra, spectral shading of targets, and system noise, will always ensure that only an approximate right-hand vector will be obtained. The severity with which this affects the solution vector is determined by the "conditioning" of the coefficient matrix.

If two or more rows of a coefficient matrix are nearly linearly related, then the matrix determinant will be small. Consequently, a minor perturbation of the right-hand vector will be greatly magnified in the solution vector. Such a matrix is termed nearly-singular, or ill-conditioned. Conversely, in a well-conditioned matrix, a minor perturbation of the right-hand vector results in moderate errors in the solution.

The requirement of well-conditioning determines the minimum angular increment at which the receiver can be calibrated: if the increment is too small, then the similarity between adjacent rows of the coefficient matrix will result in ill-conditioning. Conversely, the increment between spectra should not be so large that excessive errors of interpolation are introduced due to targets at intermediate angles.

While it is not possible to determine the conditioning of a matrix precisely, a rough measure is obtained by computing the condition number (Steinberg, 1974):

$$\text{cond}(A) = \|A\| \cdot \|A^{-1}\| \quad (4.3)$$

where: $\|A\|$ is the norm of the coefficient matrix
 $\|A^{-1}\|$ is the norm of the inverse coefficient matrix.

Either the matrix row sum norm or the matrix column sum norm may be used. A small condition number indicates a well-conditioned linear system.

4.1.3 Computer simulations

The irregular reflector and receiver were replaced by a two dimensional array of randomly spaced isotropic elements, the outputs of which were summed vectorially. The resulting interference effect is an approximation of that which might be obtained from a single receiver surrounded by an irregular reflector.

The first computer simulation uses a receiver containing 50 point sources, irregularly spaced within an equilateral triangle of side-length 50mm. The responses of the receiver to a uniform incident spectrum were determined at 19 frequency points, linearly spaced between 25kHz and 115 kHz. Since an undersea environment was selected, the speed of sound was set at 1500 metres per second. The receiver was therefore 3,8 wavelengths across at a frequency of 115kHz. The dimensions chosen are similar to those of a small cetacean.

The spectral responses of the receiver were predetermined at 19 five degree increments across a 90 degree sector. The row sum norm condition number of 50, and the column sum norm condition number of 283, both indicate that the linear system is well-conditioned.

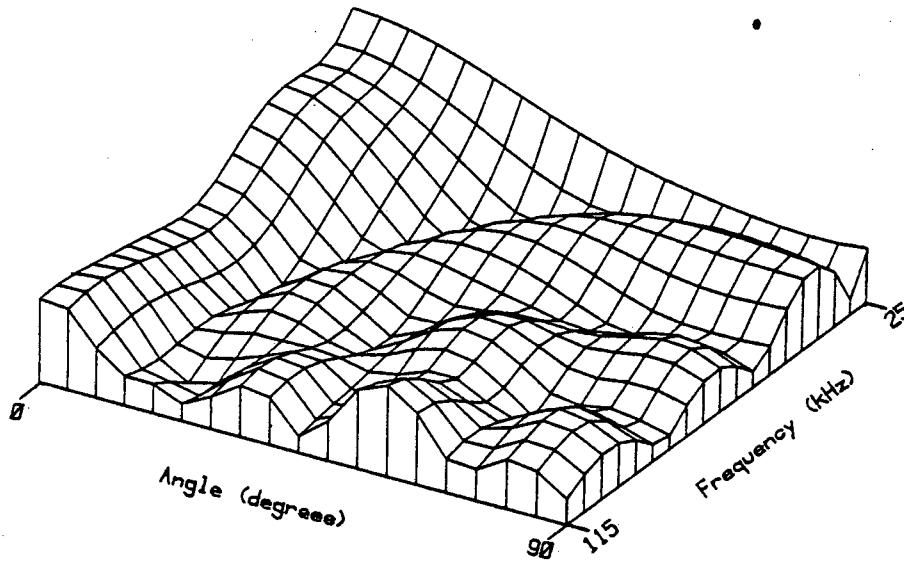


Figure 4.2 - Spectral responses of a simulated receiver which is 3,8 wavelengths across at the highest frequency of operation.

Figure 4.3(a) is the solution vector obtained when two signals of equal strength were simultaneously incident; while figure 4.3(b) is the result when three sounds were concurrently received.

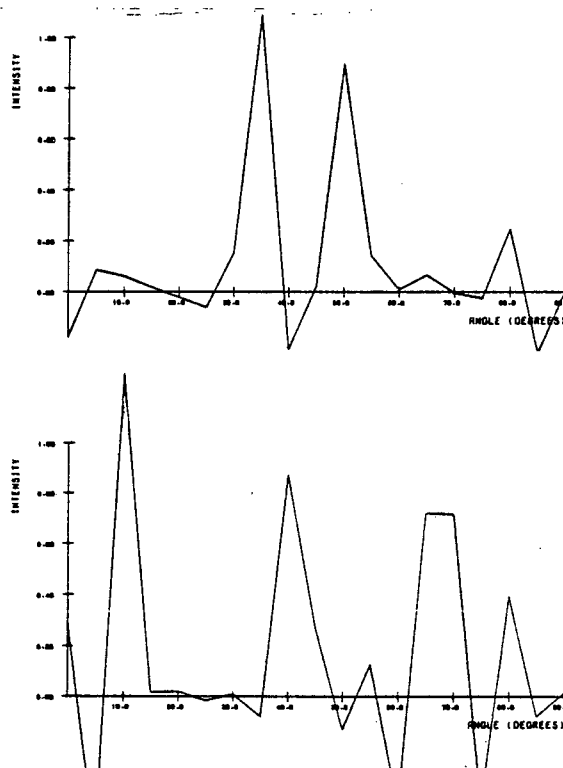


Figure 4.3 - The localisation of multiple targets
 (a) Targets at 33 and 52 degrees
 (b) Targets at 10, 33 and 52 degrees.

A second simulation was performed, in which the receiver comprised 200 point sources, randomly located within a square of side length 18mm; roughly the dimension of a bat's pinna. Since sonar beamforming in air was being simulated, the speed of sound was set at 344 metres per second. The receiver was therefore 5,2 wavelengths across at a maximum frequency of 100kHz. The simulation of an irregular reflector and receiver was made more realistic by passing the output of each element through a random time delay prior to summation. This procedure takes account of the effect of propagation delays from the facets of the reflector to the single collection point.

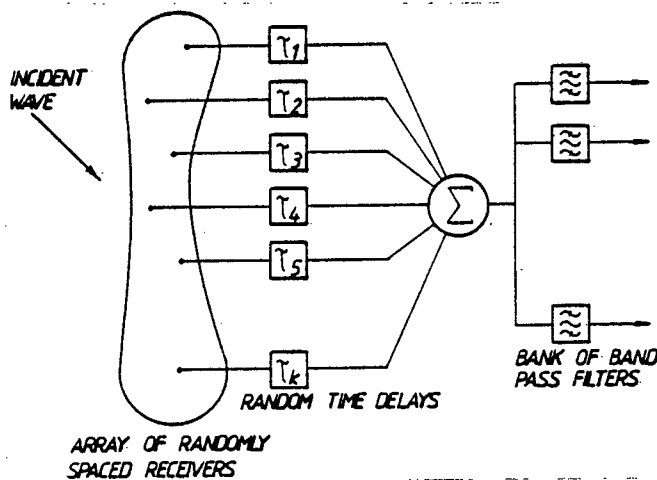


Figure 4.4 - The simulated receiving system

The response of the receiver to a uniform incident spectrum was predetermined at 32 frequency points, logarithmically spaced between 25kHz and 100kHz. As a result, the 90 degree sector of scan was divided into thirty-two angular cells, each of width 2,8 degrees.

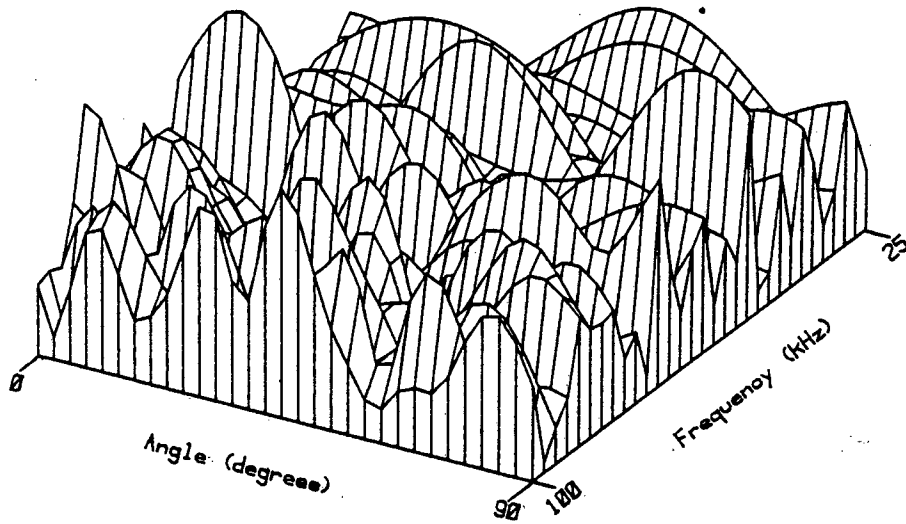


Figure 4.5 - Spectral responses of a simulated receiver which is 5,8 wavelengths across at the highest frequency of operation.

The condition number obtained using the row sum norm (8), and the column sum norm condition number (757) indicate a well-conditioned linear system.

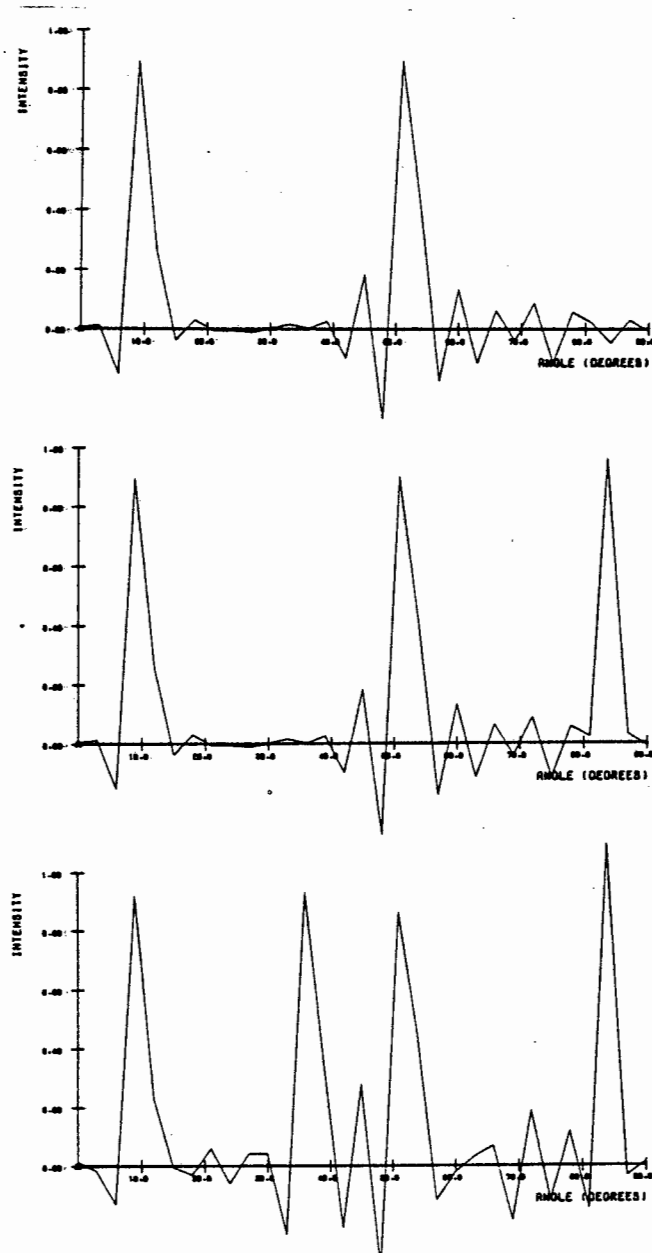


Figure 4.6 - The localisation of multiple targets
 (a) Targets at 10 and 52 degrees
 (b) Targets at 10, 52 and 84 degrees
 (c) Targets at 10, 33, 52 and 84 degrees.

4.1.3 Discussion

Computer simulations of this technique have demonstrated a well-developed multiple target capability and exceptionally good angular resolution. The resolution of a single angular cell - 5,2 and 3,8 degrees in each of the two simulations - compares favourably with the resolution expected from a similarly dimensioned conventional array - 15 and 11 degrees respectively.

However, the simulations investigated the somewhat idealised conditions of a fully determined target echo spectrum and zero noise. If the target echo spectrum is unknown (as is often the case during animal echolocation), and if significant noise is introduced, then the resulting perturbations in the right-hand vector will produce a highly unstable solution vector - simulations in which ambient noise was introduced failed to give a meaningful indication of target bearing.

Consequently, it appears unlikely that a useful beamforming system could be designed to locate targets by reducing a system of linear equations. Instead, alternative beamforming techniques were investigated.

4.2 Beamforming by the deconvolution processing of received sounds

A fundamental difficulty of beamforming based upon monaural echolocation lies in the localisation of unknown spectra: if the incident spectrum is not known, then it is problematic to differentiate the spectrum modification due to the irregular reflector from the spectrum of the incident sound. This problem is particularly acute in the case of a system designed to operate in the passive listening mode, since no control whatsoever is exerted over the nature of incident sounds. The investigation of beamforming by the solution of simultaneous equations highlighted this difficulty, since signals could only be successfully located when the incident spectrum was fully determined. Therefore, an effort was made to devise a beamforming technique which would not require prior knowledge of incident spectra: the result is a technique of beamforming by the deconvolution processing of received sounds.

To differentiate the pinna spectrum modification of a sound from its incident spectrum, a characteristic unique to either the incident signal or the spectrum modification has to be identified. One attribute specific to many naturally occurring sounds is the occurrence of sharp rise-times; a feature which could not be due to a reflector since its effect would be to time-smear incident wavefronts. Beamforming by the deconvolution processing of received sounds is a procedure which attempts to exploit this characteristic.

A technique which attempts to recognise sharp rise-times requires knowledge of both the spectral amplitude responses and the spectral phase responses of received signals. Consequently, a time domain representation was selected: both of these responses are incorporated into a single plot.

4.2.1 Description of technique

In the time domain, a receiver can be characterised by a set of direction dependent impulse responses. Consider the case of a receiver output being passed through a set of filters, the transfer functions of which are the inverse of the receiver's impulse responses. The output of that inverse filter corresponding to the incident direction will replicate the original signal. However, the effect of all the other inverse filters will only be to convolve the original signal even further.

The deconvolved signal can be differentiated from the others provided some unique characteristic can be attributed to the incident spectrum, which is no longer evident once the signal has interacted with the passive reflecting structure. If the original sound contains steep wavefronts, then these could serve as one such characteristic: at the outputs of all filters other than that of the deconvolved signal any steep wavefronts will have been smeared.

A method of approximating the inverse filter has been developed by considering its requirements in the frequency domain. These comprise the insertion of an amplitude and phase modification at each frequency. This can be accomplished by altering the amplitude and phase responses of a bank of ideal and contiguous filters, each with a constant amplitude response and a linear phase response. Computer simulations have confirmed that an approximate deconvolution of incident signals does occur when this procedure is implemented.

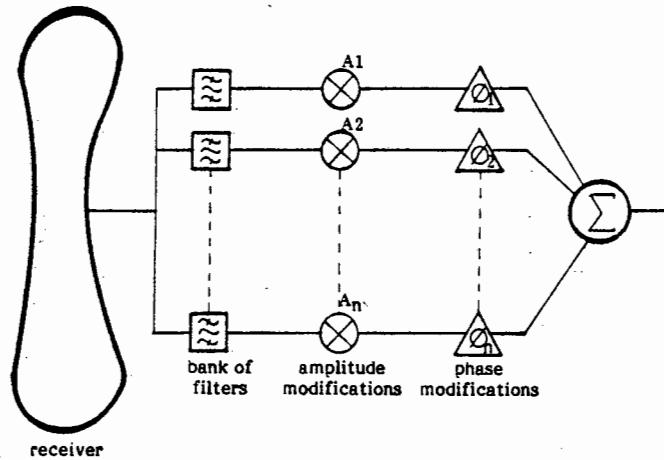


Figure 4.7 - A receiver with one "inverse filter".

4.2.3 Computer simulations

The irregular reflector and receiver were simulated using a number of line reflectors, the lengths and orientations of which were randomly assigned. Echoes off these reflectors were passed through random time delays prior to summation at a single collection point.

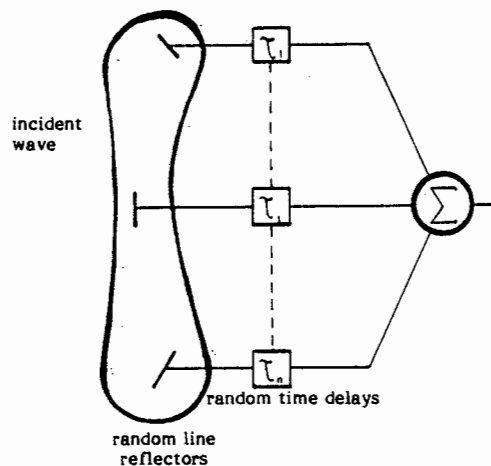


Figure 4.8 - The simulated receiving system.

Some impulse responses of such a receiver, 50mm in dimension, are illustrated in figure 4.9. Since the simulation was performed in air, the speed of sound was set at 344 metres per second. The receiver output was bandlimited to 20kHz; the receiver is 2,9 wavelengths across at this frequency.

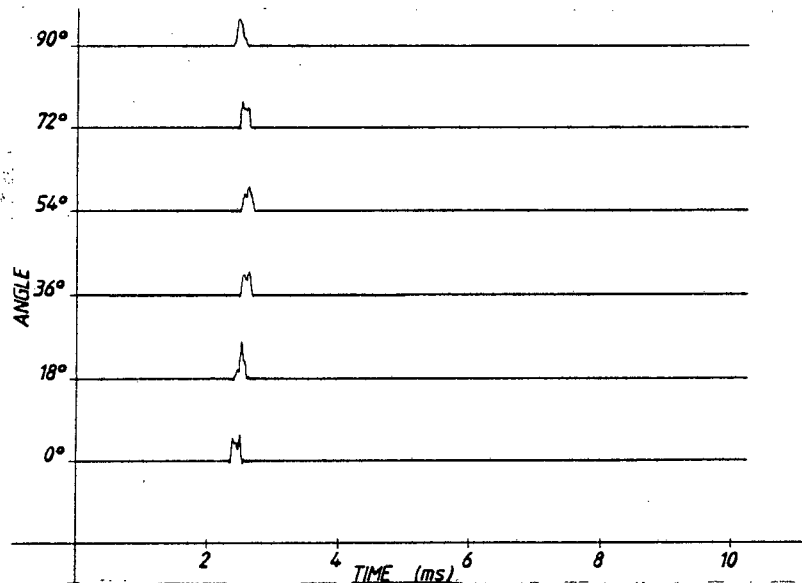


Figure 4.9 - Six impulse responses of a simulated receiver.

The bank of ideal and contiguous filters was simulated by programming the finite impulse responses of a series of filters, each having a rectangular passband and a linear phase response. The amplitude and phase alterations required to approximate the inverse filter were obtained by recording the spectrum modifications imposed by the reflector on an impulse received from each angle of interest. Amplitude and phase modifications were then programmed such that the relationships which existed between spectral points prior to reception would be restored. These relationships are simply that all spectral points should have constant amplitude and be in phase.

Figure 4.10 illustrates that six "inverse filters" were able to approximately deconvolve the six impulse responses illustrated in figure 4.9.

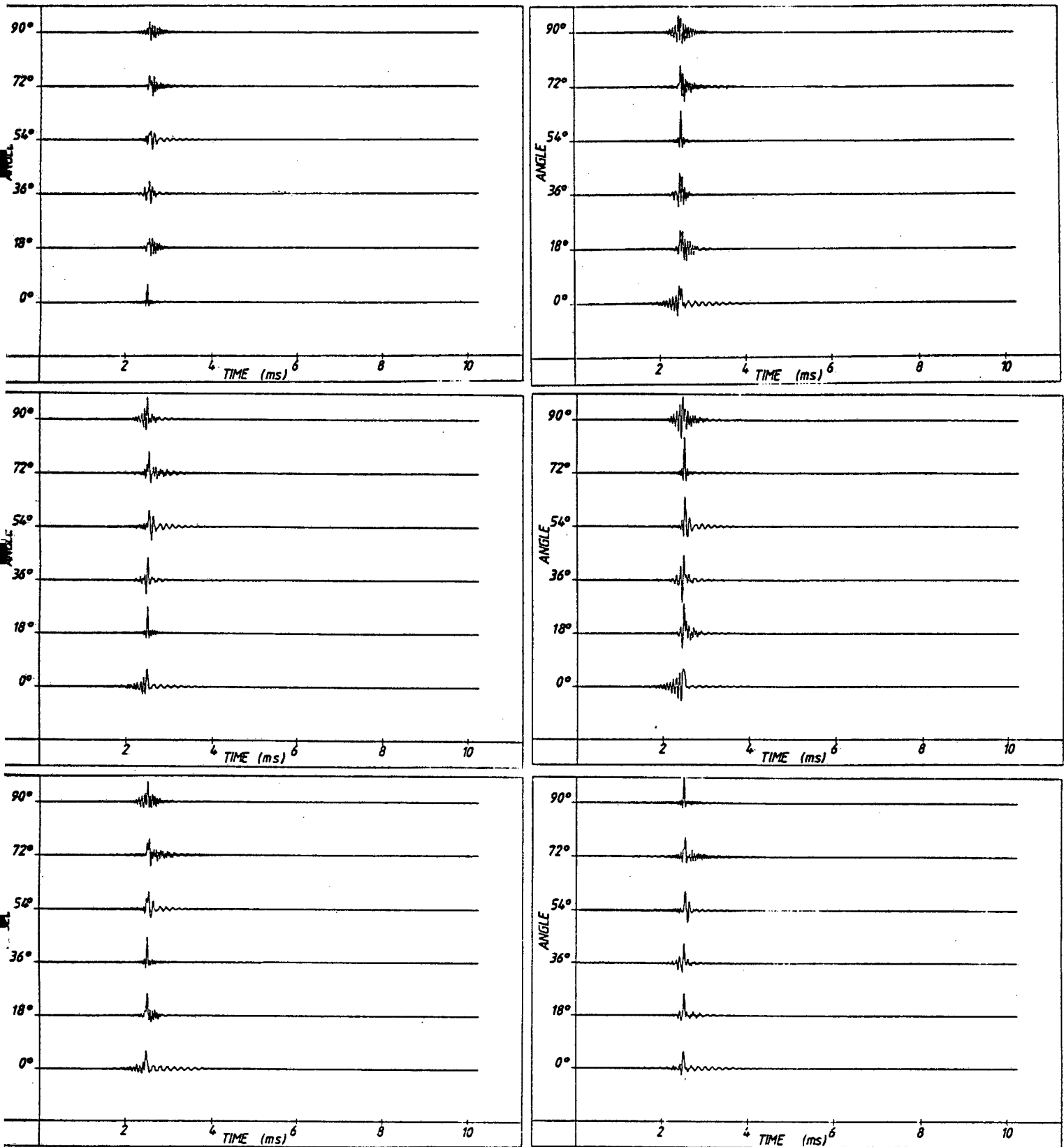


Figure 4.9 - The deconvolution of six impulses.

Figure 4.11 illustrates the localisation of a pulse incident at 36 degrees. Inspection of the leading and lagging pulse edges reveals that the pulse was deconvolved by only the 36 degree inverse filter. It is therefore possible to deduce its bearing.

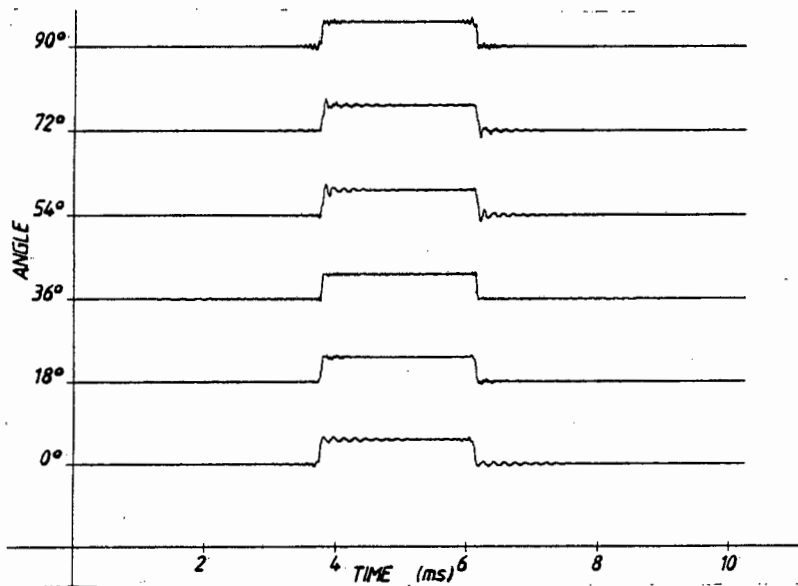


Figure 4.11 - The deconvolution of a pulse incident at 36 degrees.

An example of the application of this technique to a typical naturally occurring sound is presented in figure 4.12. The steep onset of the deconvolved time waveform is not apparent in the waveform which has interacted with a receiver and an incorrect inverse filter. Therefore, inspection of these two plots for the occurrence of a steep onset reveals that the waveform illustrated in figure 4.12(b) is the one which has been deconvolved. Consequently the source location is in the direction of that inverse filter.

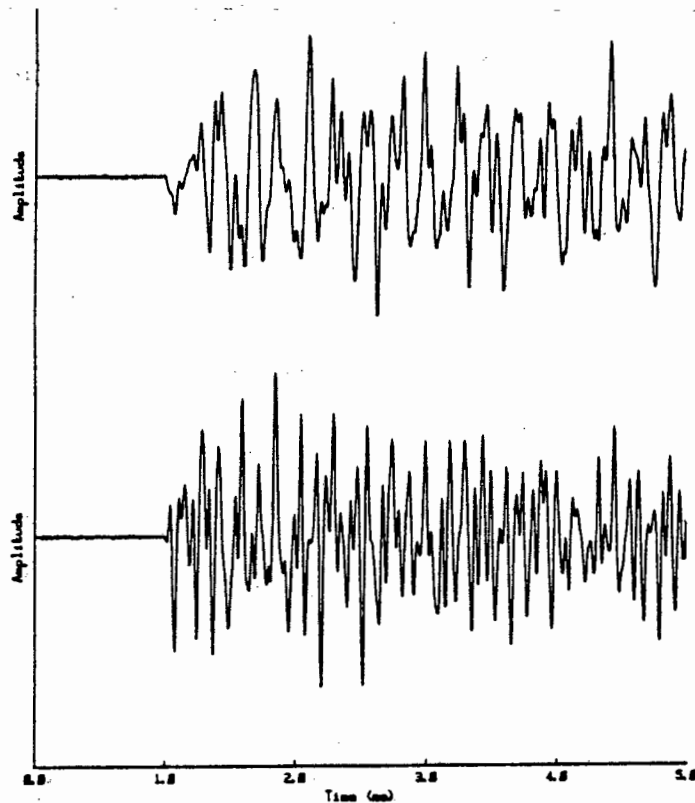


Figure 4.12 - An arbitrary received waveform.
 (a) not deconvolved.
 (b) deconvolved.

4.2.4 Discussion

Simulations indicate that a small receiving structure - in this instance the approximate size of a human pinna - can be used to locate certain commonly occurring sounds of unknown spectrum. (The localisation of known spectra is, of course, trivial.)

However, to unscramble the constituents of simultaneously incident multiple sources could prove insurmountable, since it would be very difficult to differentiate a correctly deconvolved signal when it is superimposed on a different incorrectly deconvolved signal. Even under single target conditions, it might be difficult to locate certain signals if they do not contain sharp rise-times or steep wavefronts.

Consequently, a third beamforming technique was investigated. This time, an attempt was made to be able to locate multiple targets and sources of unknown spectrum. An additional requirement was to be able to locate targets in noisy environments.

4.3 Beamforming by the cross-correlation analysis of received spectra

If the spectrum of an incident wavefront is directly compared with each of a series of stored power spectra which have been predetermined at all possible angles of incidence, then the closest match will indicate target bearing. This proposal forms the basis of beamforming by the cross-correlation analysis of received spectra.

If more than a single incident source is simultaneously received, then the resulting received spectrum will bear a resemblance to more than one pre-determined spectrum. Consequently, more than a single target can be localised. In addition, if the sound source has an unknown and non-uniform spectrum, or if the incident wavefront is contaminated by noise, localisation might still be possible. This would result from the spectrum modification due to the receiver being so characteristic of a particular angle that some degree of correlation with the stored spectrum corresponding to the angle of incidence will still exist.

4.3.1 Description of technique

To match an incident spectrum against one that has been predetermined, the correlation-coefficient between the two is calculated (Keeping, 1962):

$$r = \frac{\sum x_i y_i - n \bar{x} \bar{y}}{((\sum x_i^2 - n \bar{x}^2)(\sum y_i^2 - n \bar{y}^2))^{\frac{1}{2}}} \quad (4.4)$$

where : r is the correlation-coefficient.
 n is the number of frequency samples.
 x_i are the spectral samples of the incident signal.
 y_i are the predetermined spectral samples.

A correlation-coefficient of 1 indicates perfect matching, a correlation-coefficient of -1 indicates perfect anti-phase, and zero correlation represents total dissimilarity.

However, the correlation-coefficient usually lies between these extremes. In such instances, an estimate of the confidence with which the hypothesis of zero correlation can be rejected from bivariate normal populations can be obtained using the following expression (Miller and Freund, 1965):

$$z = \frac{(n-3)^{\frac{1}{2}} \cdot \ln(1+r)}{2 \cdot \ln(1-r)} \quad (4.5)$$

where : z is the variable in the normal distribution function. The confidence is the normal distribution corresponding to this variable, usually obtained from a table of the normal distribution function.
 n is the number of independent frequency samples.
 r is the correlation coefficient.

Since histogram plots of sample magnitude spectra have shown that these are indeed approximately normal about the mean, this expression can be used to evaluate the significance of coefficients obtained by cross-correlating spectra.

Since the confidence with which the hypothesis of zero correlation can be rejected is related to the number of independent frequency samples, it is useful to estimate this number for a given receiver design. The number of time samples required to sample the band-limited impulse response of a receiver at the Nyquist rate is the product of twice the highest frequency component present and the impulse response length. If the magnitude response of this sampled waveform is computed using a discrete Fourier algorithm, then the number of independent frequency points obtained will be half the number of time samples used, owing to the double-sided nature of the frequency domain representation. This is the maximum number independent frequency points: half the number of time samples required to sample the impulse response at the Nyquist rate. It is possible that the number of independent frequency points is less than this amount, for example, if only a portion of the spectrum between dc and the highest frequency component is present in the incident spectrum.

This beamforming technique can locate multiple targets: the precise number depends on the relative target strengths, the number of independent frequency samples, and the permitted probabilities of detection and false alarm. For example, consider two concurrently incident signals of equal strength. If there were an infinite number of independent frequency samples, then a correlation coefficient of $1/\sqrt{2}$ would result when the received signal is correlated with the predetermined spectrum at each incident angle. However, since there are always only a finite number of independent frequency samples, an error will occur in the estimate of correlation-coefficient. The probable maximum excursion of this error can be determined from equation (4.5). Therefore, for any selected level of confidence, the maximum number of simultaneously incident signals which can be localised occurs when the minimum expected correlation-coefficient at an angle at which a target is present is equal to the limit at which the hypothesis of zero correlation can be rejected.

An extension of the technique has been developed which increases this maximum number of simultaneously incident signals. It also enables weak spectra, which might otherwise be masked by concurrently incident strong spectra, to be located. However, the technique is only applicable when the source spectrum is known. It is therefore best suited to active mode beamforming.

The crux of the procedure is that once the stronger targets have been located, knowledge of the incident spectrum allows their contribution to the composite received spectrum to be removed. When the resulting magnitude response is once again correlated with the predetermined spectra, any weaker sources are revealed. The contribution of a stronger target to an incident spectrum can be calculated in the following manner:

Suppose an incident spectrum $z(f)$ comprises a strong target $kx(f)$ - k being a scaling factor - and a number of weaker targets, all of which contribute $y(f)$:

$$z(f) = kx(f) + y(f) \quad (4.6)$$

Cross-correlating $z(f)$ with the stored spectrum which corresponds to the angle of the strong target:

$$\begin{aligned} \ell_{xz} &= \sum (x_i - \bar{x})(z_i - \bar{z}) \\ &= \sum (x_i - \bar{x})(kx_i + y_i - k\bar{x} - \bar{y}) \\ &= \sum \{x_i(kx_i + y_i) + k\bar{x}^2 + \bar{x}\bar{y} - k\bar{x}x_i - x_i\bar{y} - k\bar{x}x_i - x_i\bar{y}\} \\ &= \sum x_i(kx_i + y_i) - nk\bar{x}^2 - n\bar{x}\bar{y} \\ &= k\sum x_i^2 + \sum x_i y_i - nk\bar{x}^2 - n\bar{x}\bar{y} \end{aligned} \quad (4.7)$$

However,

$$\begin{aligned} \ell_{xy} &= \sum (x_i - \bar{x})(y_i - \bar{y}) \\ &= \sum x_i y_i + n\bar{x}\bar{y} - \sum x_i \bar{y} - \sum \bar{x} y_i \end{aligned} \quad (4.8)$$

and since : $n\bar{x}\bar{y} = \sum x_i \bar{y} = \sum \bar{x} y_i$,

$$\ell_{xy} = \sum x_i y_i - n\bar{x}\bar{y} \quad (4.9)$$

Therefore,

$$\ell_{xz} = k\sum x_i^2 - nk\bar{x}^2 + \ell_{xy} \quad (4.10)$$

However, since the spectrum $y(f)$ has no contribution from the angle of spectrum $x(f)$, $\ell_{xy} = 0$.

Hence,

$$\ell_{xz} = k \sum x_i^2 - kn\bar{x}^2 \quad (4.11)$$

or,

$$\begin{aligned} k &= \frac{\ell_{xz}}{\sum x_i^2 - n\bar{x}^2} \\ &= \frac{\sum x_i y_i - n\bar{x}\bar{y}}{\sum x_i^2 - n\bar{x}^2} \end{aligned} \quad (4.12)$$

Noting that the correlation coefficient is defined:

$$r = \frac{\sum x_i y_i - n\bar{x}\bar{y}}{((\sum x_i^2 - n\bar{x}^2)(\sum y_i^2 - n\bar{y}^2))^{\frac{1}{2}}} \quad (4.13)$$

The scaling factor k can be more conveniently computed:

$$k = r \left\{ \frac{\sum z_i^2 - n\bar{z}^2}{\sum x_i^2 - n\bar{x}^2} \right\}^{\frac{1}{2}} \quad (4.14)$$

Once this scaling factor has been determined, it is multiplied by the predetermined spectrum from the angle of the already located stronger target. The resulting product is subtracted from the original received spectrum to remove the contribution of the stronger target. Owing to errors introduced by the finite number of samples, it is not always possible to completely remove the contribution of a target on the basis of a single evaluation of this scaling factor - a few iterations are sometimes required.

4.3.2 Computer simulations

In every simulation, the irregular reflector and receiver were replaced by a two dimensional array of randomly spaced receivers. The outputs of these were passed through random time delays and then summed to obtain a single output. This is the same model which was used when simulating beamforming by the solution of simultaneous equations.

4.3.2.1 Single sound source of known spectrum

The first simulation modelled a receiver of dimension 50mm. Since the speed of sound was set at 344 metres per second, the receiver was 14,5 wavelengths at the highest frequency of 100kHz. This is roughly the head-width of a typical bat. A single sound source of uniform spectrum was introduced at an angle of 50 degrees. To simulate ambient noise, 181 weak sources, evenly distributed along the sector of scan, accompanied the wanted source. Their individual amplitudes of 0,03 relative to the source at 50 degrees resulted in a signal-to-noise ratio of -8dB.

Figure 4.13 is a plot of the correlation-coefficient between the incident spectrum and predetermined spectra from 0 to 90 degrees; first under noise-free conditions, and then with a signal-to-noise ratio of -8dB.

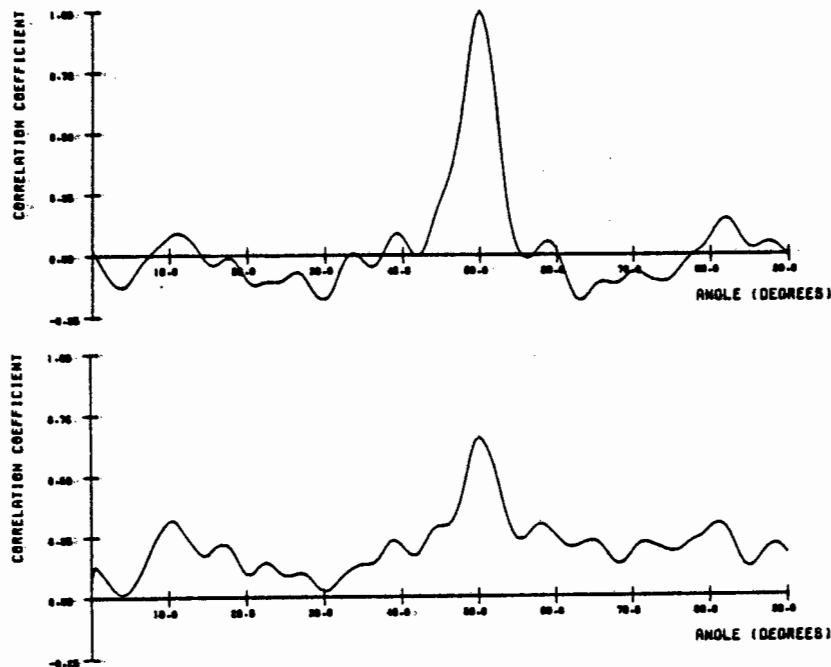


Figure 4.13 - Localisation of a source at 50 degrees.
 (a) under noise-free conditions.
 (b) with a signal-to-noise ratio of -8dB.

The arc between which the correlation-coefficient is -3dB of its maximum value is 3,8 degrees. This corresponds closely with the half-power beamwidth of a similarly dimensioned conventional beamformer.

Although not all of the 200 frequency samples used were independent, a sample size of 200 was used in equation (4.5) to test the hypothesis of zero correlation. It was found that at the 99,9% level of confidence, the hypothesis of zero correlation can be rejected only if the measured correlation coefficient is in excess of 0,22. This accounts for the noise-like background in the plots of figure 4.13.

The localisation ability of a large receiver - 50 wavelengths across at the highest frequency - was tested in a similar simulation. A single sound source was again introduced at an angle of 50 degrees. Interaction with the receiver caused the spectrum modification shown in figure 4.14(a). Figure 4.14(b) shows the received spectrum due to "ambient noise": this was simulated using 181 weak sources, evenly distributed

along the sector of scan. The signal-to-noise ratio was -15dB. Figure 4.14(c) shows the composite incident spectrum.

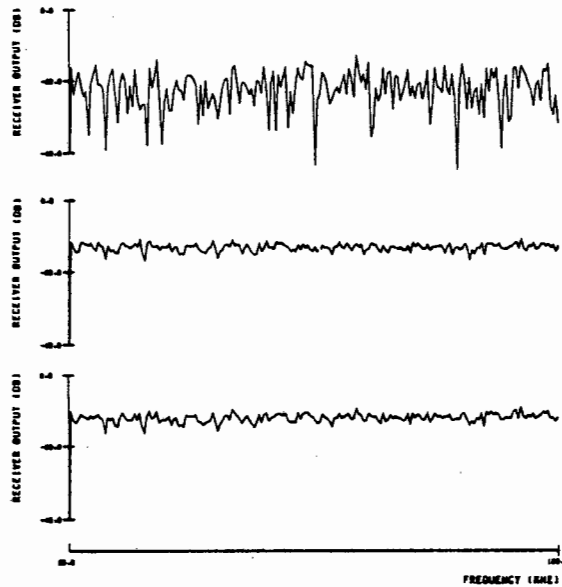


Figure 4.14.

- (a) - Received spectrum due to wanted source.
- (b) - Received spectrum due to ambient noise.
- (c) - The composite received spectrum.

Figure 4.15 is a plot of the correlation-coefficient between the incident spectrum and predetermined spectra from 0 to 90 degrees: first under noise-free conditions, and thereafter with a signal-to-noise ratio of -15dB. A comparison with figure 4.13 shows that the larger aperture gives an improved angular resolution, and enables detection at a lower signal-to-noise ratio.

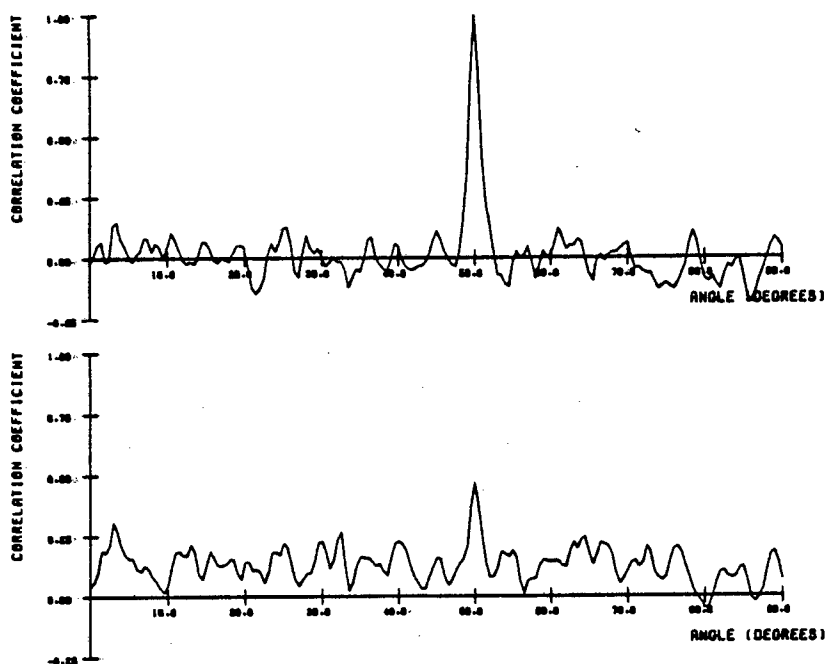


Figure 4.15 - Localisation of a source at 50 degrees.
 (a) under noise-free conditions.
 (b) with a signal-to-noise ratio of -15dB.

4.3.2.2 Single sound source of unknown spectrum

To simulate a non-uniform and unknown incident spectrum, the flat frequency response used in the previous simulation was modified to the raised cosine envelope $(1 + \cos kw)$; where k was chosen to give 10 peaks and 10 nulls between 25Hz and 100kHz. Figure 4.16 illustrates the resulting incident spectrum under noise-free conditions.

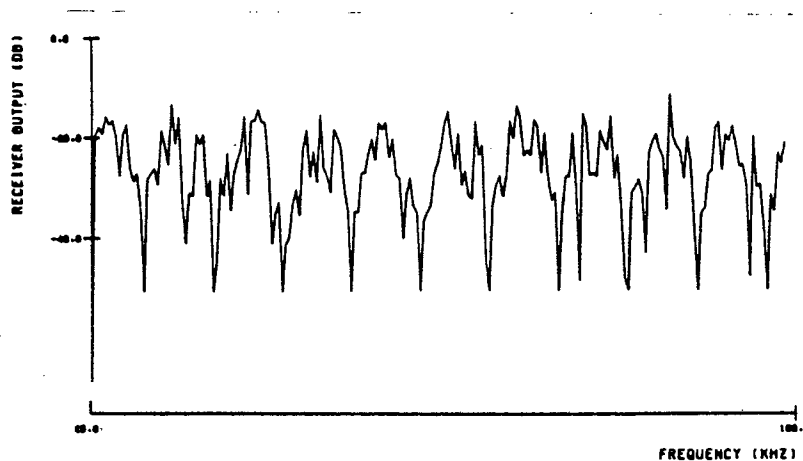


Figure 4.16 - The received modified spectrum.

Figure 4.17 is the result of correlating this spectrum with each stored spectrum in turn: first under noise free conditions and then with a signal-to-noise ratio of -12dB.

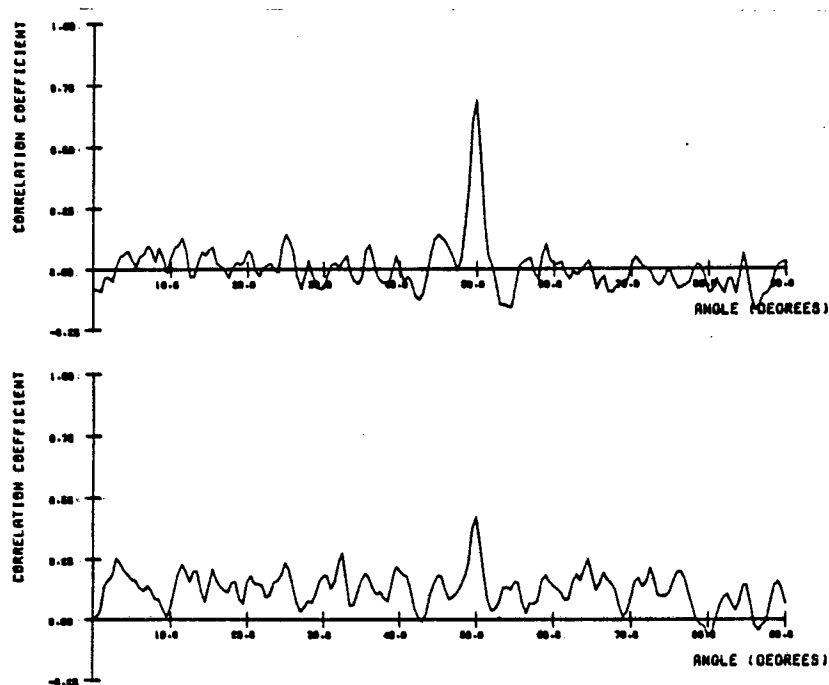


Figure 4.17 - Localisation of an unknown source at 50 degrees
 (a) under noise-free conditions.
 (b) with a signal-to-noise ratio of -12dB.

The result of this substantial spectrum modification is only a slight degradation in detection performance over the case of a uniform spectrum.

4.3.2.3 Multiple sound sources

The iterative technique developed to locate multiple sound sources of known spectrum was tested using the 14,5 wavelength receiver described in subsection 4.3.2.1. Three simultaneously incident targets were simulated; one of amplitude 1 at 10 degrees, another of amplitude 0,9 at 33 degrees, and the third of amplitude 0,05 at 52 degrees. Ambient noise was introduced into the simulation in the form of 181 weak targets distributed evenly over the sector of scan. The weak source was 26dB below the strong signal, and

6dB below the ambient noise level. Figure 4.18 shows the contribution of each constituent of the incident spectrum to the total received spectrum.

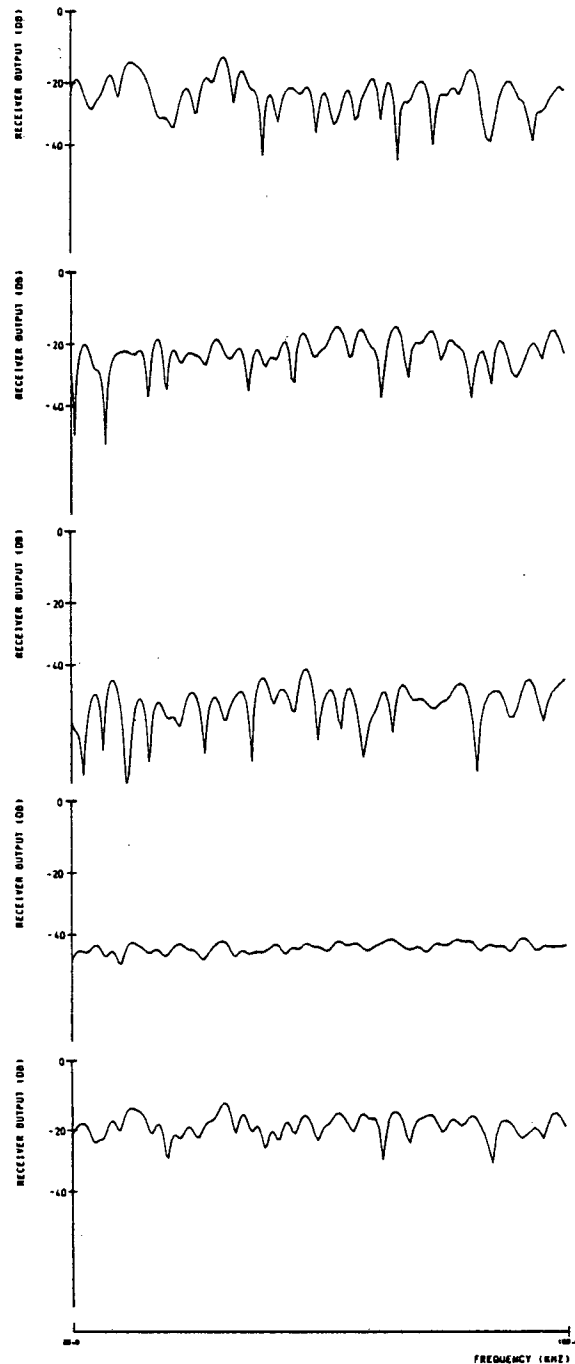


Figure 4.18.

- (a) - Received spectrum due to the target at 10 degrees.
- (b) - Received spectrum due to the target at 33 degrees.
- (c) - Received spectrum due to the target at 52 degrees.
- (d) - Received spectrum due to the ambient noise.
- (e) - Received spectrum due to the composite signal.

Figure 4.19(a) shows correlation coefficient as a function of angle when the spectrum of the received signal is correlated with stored spectra obtained at 181 angular positions. Only the target at 10 degrees is clearly present. In figure 4.19(b), the spectrum contribution due to the target at 10 degrees is removed, revealing the target at 33 degrees. When the process is repeated by removing the contribution of the target at 33 degrees, the weakest target at 52 degrees is disclosed.

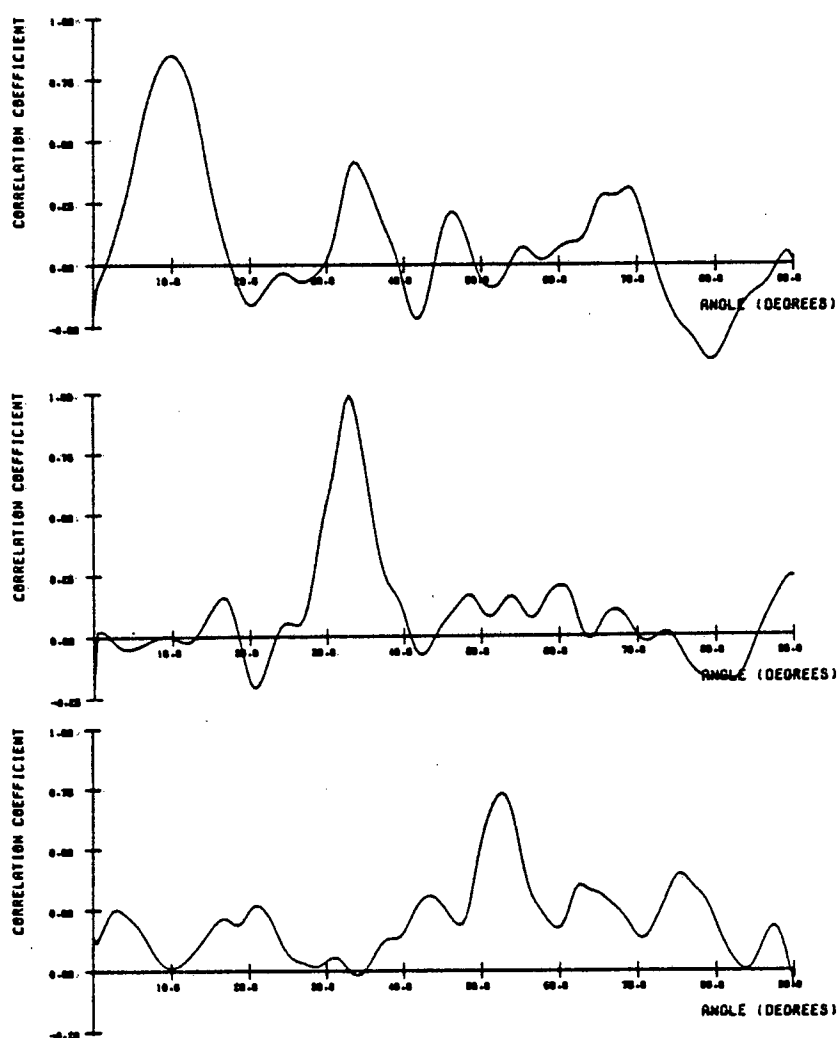


Figure 4.19 - The localisation of multiple targets.

The simulation of multiple targets was repeated using a larger receiver - 100 wavelengths across at the highest frequency. The ambient noise level was increased to obtain a weak-signal to noise ratio of -11dB. The constituent contributions to the composite received spectrum are shown in figure 4.20.

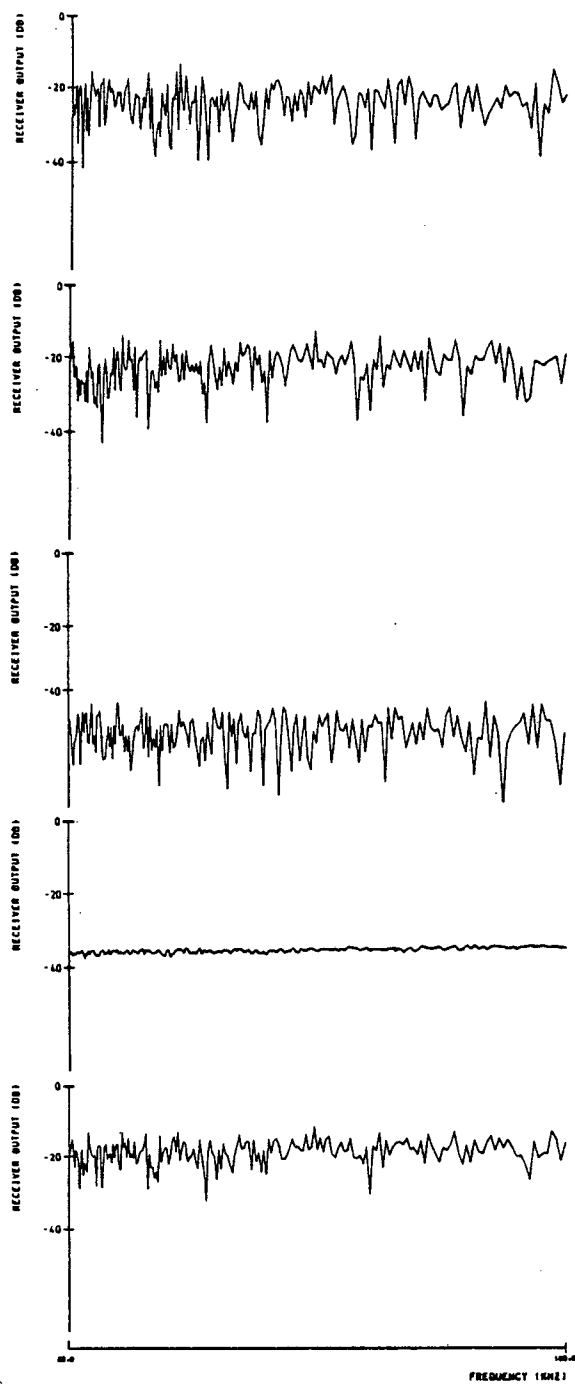


Figure 4.20.

- (a) - Received spectrum due to the target at 10 degrees.
- (b) - Received spectrum due to the target at 33 degrees.
- (c) - Received spectrum due to the target at 52 degrees.
- (d) - Received spectrum due to the ambient noise.
- (e) - Received spectrum due to the composite signal.

Figure 4.21 shows correlation coefficient as a function of angle when the incident spectrum is correlated with 181 stored spectra. Two iterations were required to remove the contributions of the stronger targets, thereby revealing the weaker target at 52 degrees.

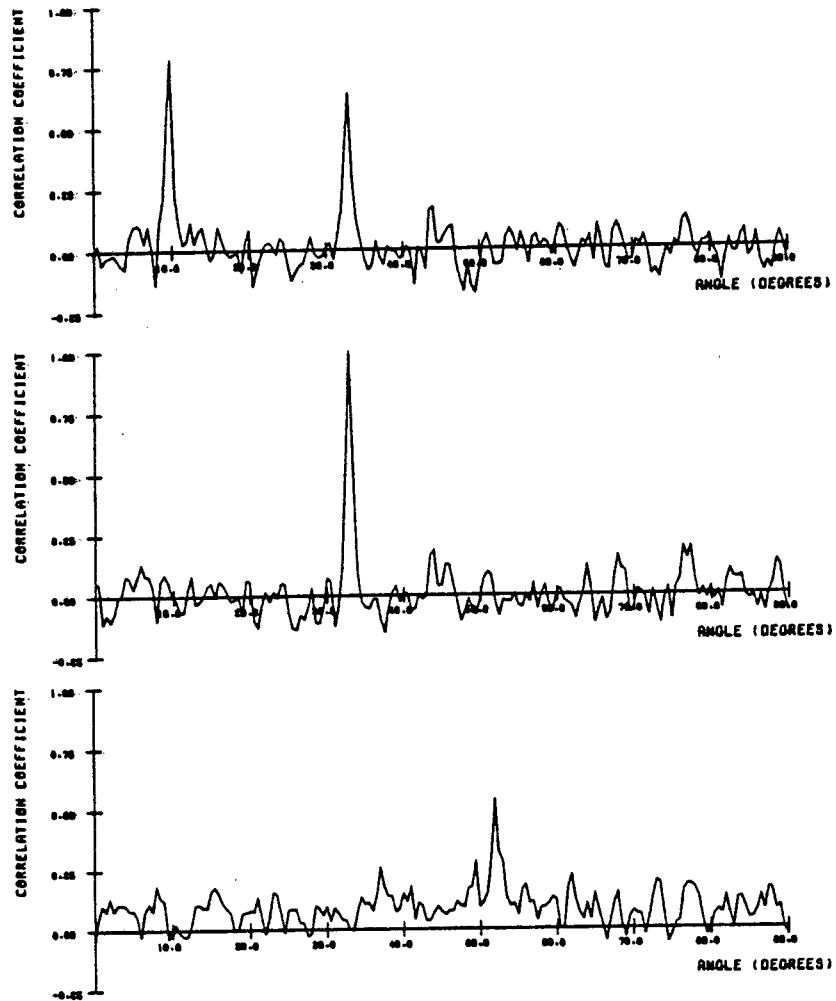


Figure 4.21 - The localisation of multiple targets.

4.3.3 Discussion

The cross-correlation analysis of received spectra is a plausible model of some aspects of monaural echolocation: multiple targets can be simultaneously located, targets can be localised against a background of ambient noise, and targets of unknown and non-uniform spectrum can be located. (However, the iterative procedure developed to detect weak signals by removing the contribution of simultaneously incident strong signals can only be employed when the incident spectra are known).

The technique could also be a viable alternative to conventional beamforming - a similar angular resolution capability has been demonstrated. However, the important practical advantage is that a very large receiving structure may be inexpensively constructed, and that only a single active receiving element is required. Indeed, in certain circumstances, an existing structure could be used: the hull of a vessel, the nose of a torpedo, a beachhead or a harbour mouth. A more detailed comparison with conventional beamforming is presented in subsection 4.5.

The cross-correlation analysis of received spectra has been evaluated as a possible model of monaural localisation. An experiment has been conducted in which the ability of a mannikin human head to locate a variety of sources was evaluated. The results obtained can be compared with the measured monaural localisation ability of human subjects. The technique was also used in the construction of an experimental active sonar system, which consists of a single hydrophone surrounded by an irregular reflecting structure. The sonar was tested in the under-water tank facility at the Central Acoustics Laboratory of the University of Cape Town. Since similar results to those presented in this subsection were obtained, it can be concluded that these simulations realistically evaluated the proposed beamforming system.

4.4 Simultaneous angle and range determination based upon monaural echolocation techniques

Echolocating animals are capable of accurate target range determination. However, it appears that their range resolution capability is significantly inferior to that of conventional beamforming systems (refer subsection 3.4). This is due to the nature of animal sonar - a biological equivalent of matched filtering is precluded.

Many of the better known active-mode alternatives to the standard phased array can unambiguously locate sources only under single target conditions; for example, the split-beam system. In these systems, a narrow range resolution capability is an important requirement: if two targets can be separated into adjacent range bins, it will be possible to locate each under single target conditions. In contrast to these single target techniques, beamforming based upon monaural echolocation can localise multiple simultaneously incident waveforms. The requirement for a narrow range resolution capability is therefore much reduced. Only in unusually highly cluttered environments, in which targets are closer in bearing than the angular resolution of the system, will a narrow range resolution be useful in separating sources. In all other circumstances an accurate range determination capability is sufficient to pin-point targets.

Conventional systems estimate range by cross-correlating received waveforms with the transmit pulse: the time resolution achieved is the reciprocal of pulse bandwidth. A beamforming system based upon monaural echolocation is not able to determine range in this fashion, since the spectrum modification due to the interaction of target echoes with an irregular reflector alters the nature of received waveforms. Consequently, they no longer replicate the transmit pulse. An alternative target ranging technique has been devised which is well suited to a beamforming system based upon the cross-correlation analysis of received spectra.

4.4.1 Description of technique

The procedure uses a spectrum analysis technique named the Fourier-t-transform (FTT); a transformation which closely emulates cochlear signal processing (Terhardt, 1985). Unlike the standard Fourier Transform, in which the integration interval is infinite, the FTT transforms a signal whose terminating instant, t , is continuously variable. Thus, the time variations of time-varying spectra be observed.

It is desirable that with the passage of time, the spectrum gradually de-emphasizes previous signal parts. Therefore, an exponential weighting modification is included in the definition of the FTT. This weighting function, of the form: $\exp(-a(t-x))$, is illustrated in figure 4.22.

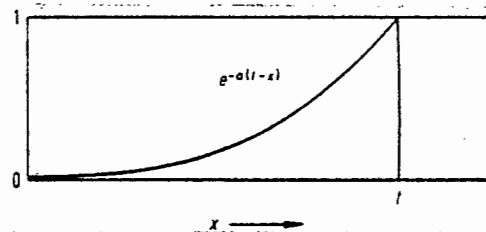


Figure 4.22 - The weighting function included in the FTT (Terhardt, 1985).

The Fourier-t-transform of causal signals is defined by:

$$P(\omega, t) = \int_0^t p(x) \exp(-a(t-x)) \exp(-j\omega x) dx \quad (4.15)$$

Since the damping factor $a(\geq 0)$ determines the effective length of the time sequence to be transformed, it also determines the time taken to achieve the steady state and governs the frequency selectivity. A reasonable approximation to the steady state is attained at about:

$$t = 1/a \quad (4.16)$$

The half-power bandwidth is given by:

$$B = a/\pi \quad (4.17)$$

Figure 4.23 shows the build-up of the FTT of a 1kHz cosine signal. A damping factor of $a=19$ was used. Consequently, the analysing bandwidth is 6Hz.

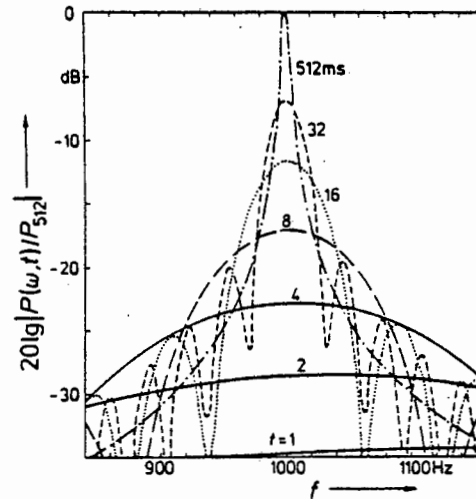


Figure 4.23 - FTT magnitude spectrum of a 1kHz cosine signal (Terhardt, 1985).

A simple and efficient digital FTT algorithm is:

$$P(\omega, t_0) = T_p(t_0)$$

$$P(\omega, t_{m+1}) = P(\omega, t_m) \exp(-aT) + T_p(t_{m+1}T) \exp(-j\omega t_{m+1}T) \quad (4.18)$$

where : T is the sampling period.
 t_i is the i th time sample.
 a is the damping factor.

A practical beamforming system based upon the cross-correlation analysis of received spectra would perform a free-running FTT on the receiver output. On reception of a target echo, the FTT output grows to resemble the stored spectrum corresponding to target bearing. Correspondingly, the correlation coefficient between these two waveforms increases to peak at the two-way propagation time. The delay of this maximum correlation peak from zero time therefore indicates target range.

The accuracy of range determination is limited only by the precision with which the two-way propagation time can be estimated. Thus, the individual ranges of multiple targets can be accurately determined, even when they occupy the same range bin, provided their angular separation is greater than the angular resolution of the beamforming system. However, when two targets occupy the same angular cell, then it is necessary to determine the minimum range separation at which they will be distinguishable - the range resolution.

The rate at which the FTT of an incident signal is refreshed is governed by the rate at which previous signal parts are diminished: as the damping factor, a , is increased, a concomitant increase in the rate of spectral fluctuation occurs. This improves the range resolution capability. However, a large damping factor also increases the effective half-power bandwidth, resulting in fewer independent frequency points. Since the level at which the hypothesis of zero correlation can be rejected is a function of the number of independent samples, a large damping factor will reduce the dynamic range capability. Consequently, a compromise between narrow range resolution and dynamic range capability has to be selected to best fulfil the requirements of a particular application.

4.4.2 Computer simulations

In each simulation, a receiver and irregular reflector were replaced by a two-dimensional array of randomly spaced receivers. The receiver outputs were passed through random time delays and then summed to obtain a single output. The receiver dimension was 1,5 metres, or 50 wavelengths across at the highest frequency of 50kHz.

Figure 4.24 contains the results of three simulations, in which the angle and range of a single target, introduced at 0 degrees, were determined. In figure 4.24(a) a damping factor of 6250 was used. This resulted in an effective time-window of approximately 160 microseconds and an effective half-power bandwidth of around 2kHz. In figure 4.24(b) the damping factor was increased to 12500, obtaining a time-window of 80 microseconds and an effective bandwidth of approximately 4kHz. In figure 4.24(c) the damping factor was again increased to 25000, resulting in an effective time-window of 40 microseconds and an effective half-power bandwidth of about 8kHz. Since the echo bandwidth was 50kHz, the numbers of independent frequency samples in each simulation were 25; 12,5 and 6,2 respectively. This implies that the hypothesis of zero correlation can only be rejected when the correlation coefficient exceeds respective values of 0,34; 0,49 and 0,73 (equation 4.5).

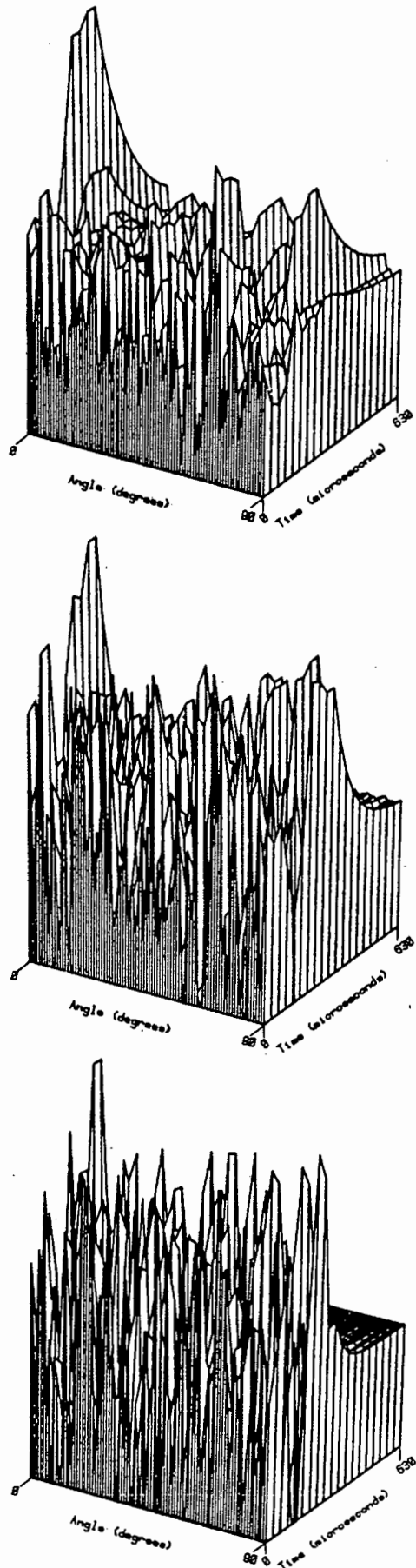


Figure 4.24 - Simultaneous angle and range determination of a target at 0 degrees.

- (a) damping factor $a = 6250$
- (b) damping factor $a = 12500$
- (c) damping factor $a = 25000$

4.4.3 Discussion

The true range resolution of a sonar based upon the cross-correlation analysis of received spectra is inferior to that of a conventional system: while the time resolution of a conventional 50kHz bandwidth system is 20 micro-seconds, the time between which the correlation coefficient is $1/2$ of its maximum is 175 microseconds, 80 microseconds, and 62 microseconds respectively in each of the three simulations. As would be expected, these range resolutions correspond closely with the effective time-window lengths used in each simulation.

However a narrow range resolution is usually not required since an accurate range determination capability is sufficient for most applications. This is achieved using a spectrum analysis technique such as the Fourier-t-transform.

4.5 An evaluation of sonar beamforming by the cross-correlation analysis of received spectra

To evaluate the usefulness of a sonar system based upon beamforming by the cross-correlation analysis of received spectra (abbreviated CCARS), its detection performance is compared with that of an equivalent conventional sonar system. Two comparisons are drawn: the first compares the performance of a CCARS sonar with that of a comparable conventional active system; while the second considers the passive case.

However, before equivalent conventional sonar designs can be considered, it is necessary to determine those parameters of a CCARS beamforming system which are required for a meaningful comparison. These are: the receiver dimensions; the probabilities of false alarm, $p(\text{FA})$, and detection, $p(\text{D})$, which result from a particular signal-to-noise ratio; the received pulse length (for an active system); the receiver response time (for a passive system); and the receiver bandwidth.

4.5.1 The detection performance of a CCARS sonar system

The detection performances of three CCARS sonar systems have been evaluated in computer simulations: using a small receiver (14.5 wavelengths across at the highest frequency) and a source of known spectrum; using a large receiver (50 wavelengths across at the highest frequency) and a source of known spectrum; and using the same large receiver, but with a source of unknown spectrum. The results of these simulations, described in section 4.3, are illustrated in figures 4.14, 4.15 and 4.17.

In each of these simulations, ambient noise was represented by introducing 181 white noise sources, evenly spaced along a 90 degree sector in the azimuth plane. Using the small receiver, a target source of known spectrum was located when the signal-to-noise ratio at the receiver input was -8dB. Using the large receiver, a source of known spectrum was located when the signal-to-noise ratio at the receiver input was -15dB; and a source of unknown spectrum was located when the signal-to-noise ratio was -12dB. Since the noise power spectrum was flat across the 75kHz receiver bandwidth, the respective signal to noise-spectral-densities in each of these simulations were: 40,8dB; 33,8dB; and 36,8dB.

An examination of the results of these simulations reveals that the limitation on detection is the noise-like background found on the plots of correlation-coefficient versus angle. This background, due to errors in the estimates of correlation-coefficient, is caused by only a finite number of frequency samples being used in the determination of the correlation-coefficients. A prediction of the probable magnitude of these errors can be used to determine the probability of detection for a given probability of false alarm. This is achieved using equation (4.5), which calculates the probability that the correlation-coefficient will remain within a given deviation of the value it would assume were an infinite number of samples to be used in its determination. The expression is reproduced below for ease of reference:

$$z = \frac{(n-3)^{\frac{1}{2}} \cdot \ln(1+r)}{2 \cdot \ln(1-r)} \quad (4.19)$$

where : z is the variable in the normal distribution function. The confidence is the normal distribution corresponding to this variable, usually obtained from a table of the normal distribution function.
 n is the number of independent frequency samples.
 r is the correlation coefficient.

Solution of this equation requires the number of independent frequency samples, n , to be known. Although 200 frequency points were used in each simulation, not all of these were independent. The number of independent samples can be estimated by solving equation (4.19) for n :

$$n = \frac{(2z \cdot (1/\ln(1+r)))^2 - 3}{1-r} \quad (4.20)$$

First, the number of independent frequency samples used by the small receiver will be estimated. Figure 4.14(a) is a plot of correlation coefficient against angle when a single source and zero noise is received. At angles at which no target is present, the maximum deviation of the correlation coefficient from zero is 0,25. As a rough estimate, it is assumed that the probability of a deviation equal to or greater than this is 0,02. Therefore, the probability that the correlation coefficient will remain within 0,25 of zero when no target is present is 0,98. Using a table of the normal distribution function, this probability is related to the variable z : if $F(z)=0,98$ then $z=2,06$ (Miller and Freund, 1965). Substituting 0,25 and 2,06 for r and z respectively in equation (4.20) yields an estimate of the number of independent frequencies samples: $n=62$.

A similar analysis can be performed for the large receiver. Figure 4.15(a) is a plot of correlation-coefficient against angle when a single target and zero noise is present. At angles at which no target is present, the maximum deviation of the correlation coefficient from zero is 0,16. Again it is assumed that the probability of a deviation equal to or greater than this is 0,02. If $r=0,16$ and $z=2,06$ are used to solve equation (4.20), an estimate of the number of independent frequency samples is obtained: $n=160$.

Having obtained estimates of the numbers of independent frequency points, the probabilities of detection for given probabilities of false alarm can be calculated. An arbitrary

$p(\text{FA})$ of 0,001 has been selected. To determine $p(\text{D})$, the required detection threshold to obtain the chosen $p(\text{FA})$ has to be calculated. First, this will be done for the simulation in which a small receiver was required to detect a target in noise.

This simulation is illustrated in figure 4.14(b). It can be observed that the average correlation-coefficient at angles at which no target was present is 0,2. This value is taken to be the mean of received correlation coefficients when the noise background is equal to that used in the simulation, and when no target is present. Equivalently, it can be thought of as the correlation-coefficient which would have been obtained were an infinite number of frequency points to have been used. In practice, this noise level could be maintained using AGC. The detection threshold must be set sufficiently far above this value such that, under the above conditions, the correlation coefficient remains below the threshold at least 0,999 of the time.

Equation (4.19) can be used to determine the probability of a correlation-coefficient remaining within a prescribed deviation above or below 0,2. However, a false alarm will occur only when a received correlation-coefficient deviates excessively above 0,2. Since the correlation-coefficient deviates equally above and below 0,2; if it is to remain below an upper limit of deviation 0,999 of the time, then it need only remain between the upper and lower limits of deviation 0,998 of the time.

A table of the normal distribution function is used to determine the value of z for a probability of 0,998: $z=2,88$. Since $n=62$, equation (4.19) can be solved for the correlation-coefficient: $r=0,35$. This determines the required level of the detection threshold to obtain a $p(\text{FA})$ of 0,001. It should be set 0,35 above 0,2: at a value of $r=0,55$.

The probability of detecting a target which is 8dB below the noise level, $p(D)$, can now be determined. In figure 4.14(b), the correlation-coefficient at the target angle is 0,75. Using this as a rough guide, a conservative estimate of the correlation-coefficient which would have been obtained, were an infinite number of frequency points used in its determination, might be 0,7. Since the detection threshold has been set to $r=0,55$, $p(D)$ is the probability that the coefficient will remain above 0,55; or, it is the probability that the correlation coefficient will not deviate by more than 0,15 below the mean of 0,7. Equation (4.19) can be solved to determine the probability that r will remain within a deviation of 0,15 above or below 0,7. Substituting values: $r=0,15$ and $n=62$, a value for the variable z is obtained: $z=1,16$. A table of the normal distribution function indicates that this corresponds to a probability of 0,88.

This signifies that the probability of the correlation-coefficient deviating by more than 0,15 above or below 0,7 is 0,12. However, detection will only fail when the deviation is more than 0,15 below 0,7. Since the number of deviations above and below 0,7 are equal, this will occur only 0,06 of the time. Therefore, the probability of detection, $p(D)$, is 0,94.

An estimate of $p(D)$ for a given $p(FA)$ can be similarly determined for the simulations in which the large receiver was used. For an arbitrarily chosen $p(FA)$ of 0,001, it has been determined that the detection threshold should be set to 0,39. For this threshold, the probability of detection, $p(D)$, is 0,89 when a target of known spectrum is 15dB below the ambient noise level; or when a target of unknown spectrum is 12dB below the ambient noise level.

Comparison with a conventional active sonar system also requires knowledge of the pulse length. From this, the receiver bandwidth can be determined. Correspondingly, comparison with a conventional passive sonar requires

knowledge of the receiver integration time. In a CCARS sonar, both of these quantities have the same value: the sum of the length of the impulse response of the receiver and the response time of the bandpass filters used to analyse received spectra.

The impulse response time of the small receiver is 0,6ms. Since there are a total of 62 independent frequency points, a bank of at least 62 contiguous bandpass filters are required to analyse incident spectra. The total bandwidth is 75kHz, therefore the bandwidth of each filter is 1,2kHz, and the corresponding response time is 0,8ms. Consequently, the total response time is 1,4ms..

The response time of the large receiver is calculated in a similar fashion. The impulse response time is 1,6ms and the filter response time is 2,1ms. Therefore, the total response time is 3,7ms.

These detection parameters are tabulated below:

Table 4.1 Detection parameters of three simulations of sonar beamforming based upon the cross-correlation analysis of received spectra.

	SMALL RECEIVER KNOWN SPECTRUM	LARGE RECEIVER KNOWN SPECTRUM	LARGE RECEIVER UNKNOWN SPECTRUM
Dimension	14,5	50	50
Bandwidth	75kHz	75kHz	75kHz
Response time	1,4ms	3,7ms	3,7ms
S/N	-8dB	-15dB	-12dB
S/Noise spectral density	40,8dB	33,8dB	36,8dB
p(D)	0,94	0,89	0,89
p(FA)	0,001	0,001	0,001

Although the estimates of $p(D)$ and $p(FA)$ might not be wholly accurate due to assumptions used in their derivation, they are considered sufficient for a meaningful evaluation. It will be seen that even relatively substantial errors in these estimates do not materially alter a comparison with conventional sonar systems.

4.5.2 The detection performance of a conventional active sonar

A comparison is drawn between the detection performance of a CCARS sonar which has been configured to operate in the active mode, and that of an equivalent hypothetical conventional active sonar. The basis chosen for comparison is the minimum signal to noise-spectral-density which will permit detection to within specified probabilities of false alarm and detection. This has already been done for the case of a CCARS sonar; in this subsection an equivalent conventional system will be described and evaluated.

The conventional active sonar to be evaluated is shown in figure 4.25. The line array is the same length as the passive reflecting structure of the system with which it is to be compared. Noise is introduced in the same manner as in the simulations evaluated in subsection 4.5.2: it is due to many weak sources evenly distributed along a 90 degree sector in the azimuth plane. To ensure a valid comparison, the range resolution is equal in the two instances. This is achieved by using a target echo of length equal to the response time of the simulated CCARS system.

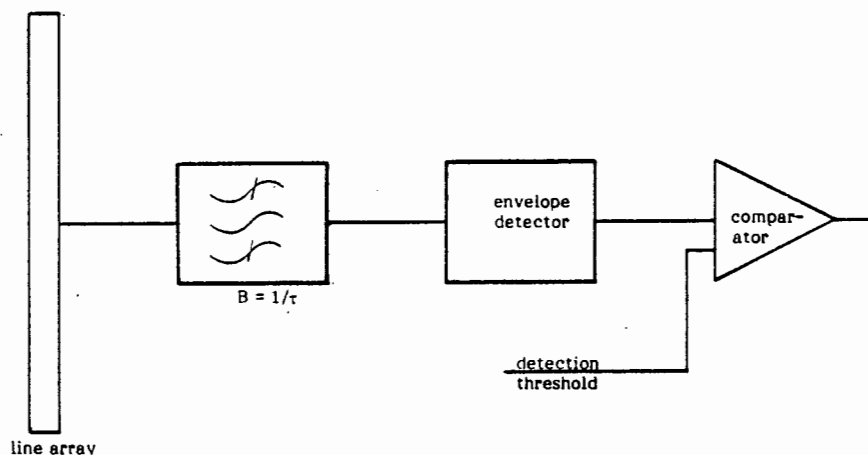


Figure 4.25 - A hypothetical active sonar system

The ambient noise is assumed to have a Gaussian distribution. Therefore, the output of the envelope detector due to noise alone will have a Rayleigh distribution. When a target echo is received, the envelope detector output will be due to signal plus noise. If the signal is sinusoidal, then this statistical distribution is called the Rice probability-density-function (Skolnik, 1981). These two distributions are shown in figure 4.26.

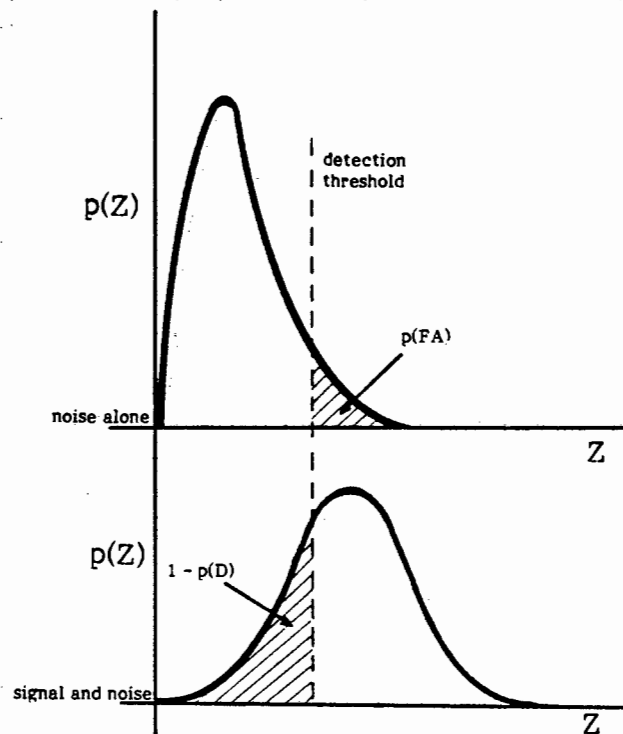


Figure 4.26 - Probability density functions due to noise alone, and signal plus noise. The probabilities of false alarm and non-detection are also shown.

A threshold detector at the output of the envelope detector is used to determine the presence of a target. Therefore, a false alarm will occur when the envelope detector output due to noise alone exceeds the detection threshold. Failure to detect the presence of a target will occur when the envelope detector output due to signal plus noise fails to exceed the detection threshold. The probabilities of these two occurrences, $p(FA)$ and $(1-p(D))$ are also shown in figure 4.26.

Families of curves have been plotted, which relate the probability of detection to the signal-to-noise ratio, with probability of false alarm as a parameter. The minimum signal-to-noise ratio required at the output of the envelope detector, which will permit detection to within a pre-selected $p(\text{FA})$ and $p(\text{D})$, can be read off the abscissa. An example of one such plot is reproduced in figure 4.27

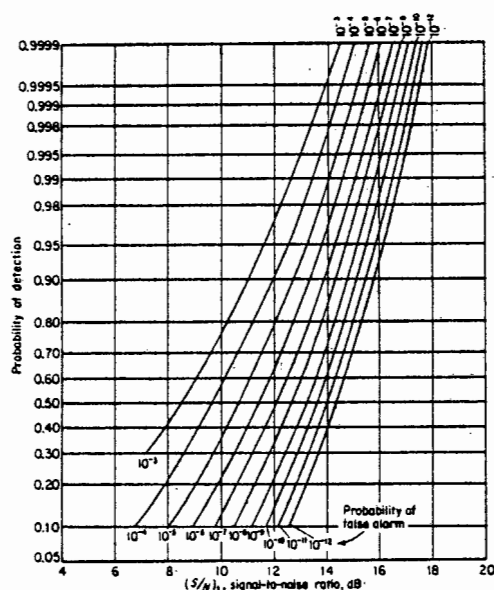


Figure 4.27 - Probability of detection for a sine wave in noise as a function of the signal-to-noise ratio and the probability of false alarm (Skolnik, 1981).

The required signal to noise-spectral-density at the output of the envelope detector is: the sum of the required signal-to-noise ratio and the receiver bandwidth (in logarithmic units). In turn, the receiver bandwidth is simply the reciprocal of the echo pulse length:

$$S/\eta = S/N + 10 \log(B) \quad (4.21)$$

$$B = 1/\tau \quad (4.22)$$

Finally the minimum signal to noise-spectral-density in the water can be determined as: the difference between the required signal to noise-spectral-density at the output of the envelope detector and the array gain (in logarithmic units). The array gain is estimated from the dimensions of the receiving array: The half-power beamwidth of an array is approximately the reciprocal of the array length measured in wavelengths. Since the noise sources are evenly distributed along a $\pi/2$ radian sector in the azimuth plane, the array gain can be approximated by:

$$AG = 10\log((\pi/2)/\text{beamwidth}) \quad (4.23)$$

Therefore, the minimum signal to noise-spectral-density in the water is:

$$(S/\eta) = -AG + (S_1/N_1) + 10\log(B) \quad (4.24)$$

where: AG is the array gain
 S_1/N_1 is the required signal-to-noise ratio at the envelope detector output
 B is the receiver bandwidth.

The performance of an active CCARS sonar can now be compared with that of a conventional system. The first simulation of the detection capability of a CCARS sonar used a small receiver and a fully determined target echo spectrum. It was found that the signal to noise-spectral-density required to obtain a $p(\text{FA})$ of 0,001 and a $p(\text{D})$ of 0,94 is 40,8dB.

The performance of an equivalent conventional active system can be considered by noting that the receiver is 14,5 wavelengths across at the maximum frequency used, and that the total response time is 1,4ms. Substituting these parameters into the above formulae, equation (4.24) can be

solved to determine the minimum signal-to-noise spectral density required by a comparable conventional active sonar:
 $(-13,6+11+28,5) = 19,9\text{dB}$.

In the simulation which uses a large receiver and a fully determined target echo, the signal to noise-spectral-density required to obtain a $p(\text{FA})$ of 0,001 and a $p(\text{D})$ of 0,89 is 33,8dB. For an echo that has been substantially modified by the target, the required signal to noise-spectral-density is 36,8dB. A comparable conventional active sonar would use a line array 50 wavelengths across, and receive an echo pulse of length 3,7ms. For this sonar, equation (4.24) is solved to determine the required signal-to-noise spectral density:
 $(-19+11+24,3) = 16,3\text{dB}$.

4.5.3 The detection performance of a conventional passive sonar system

The detection performance of a CCARS sonar configured as a passive system is compared with that of an equivalent hypothetical conventional passive sonar system. The basis for comparison is the minimum signal-to-noise ratio which will permit detection to within specified probabilities of false alarm and detection.

A hypothetical passive sonar system is shown in figure 4.28. The system uses discrete signal processing since the analysis of such a system is more straightforward. The line array in the conventional system is chosen to have the same length as the passive reflecting structure with which it is to be compared; and the gate width, T , is set equal to the total response time of the equivalent CCARS sonar. Again, ambient noise is assumed to be due to many weak white noise sources evenly distributed along a 90 degree azimuth sector. The receiver bandwidth is 75kHz. For ease of analysis, the bandwidth is chosen to extend from baseband; in practice this could be achieved by mixing down the received signal.

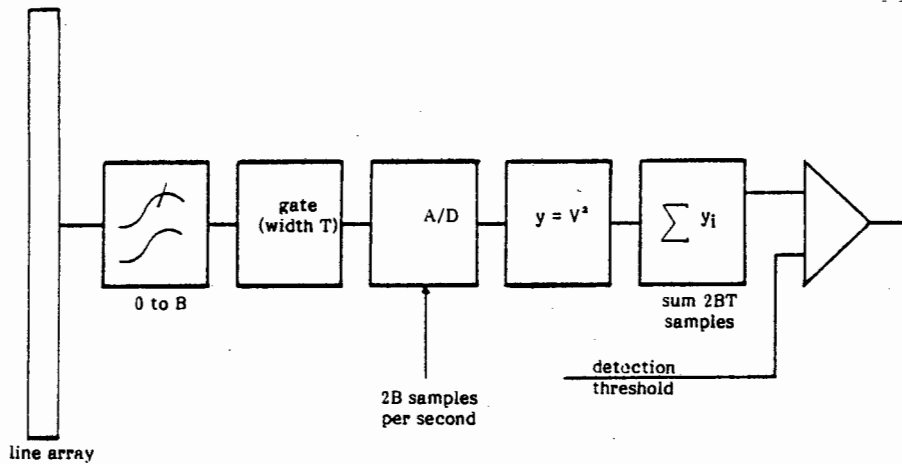


Figure 4.28 - A hypothetical passive sonar system.

If the noise power spectrum is uniform from 0 to BHz, and has a Gaussian distribution, then samples taken every $(1/2B)$ seconds are statistically independent (Denbigh, 1987). Furthermore, since $(1/2B)$ represents the Nyquist sampling rate, the entire information content of a waveform sampled at this rate is conveyed.

Since the noise has a Gaussian distribution, the voltage of each sample at the output of the analog-to-digital converter will have Gaussian statistics. Once these samples have passed through the square law device, their distribution will no longer be Gaussian. However, according to the Central Limit Theorem, if many random variables of arbitrary distribution are summed, then the probability density function of the resultant tends towards a Gaussian distribution (Schwartz, 1970). This will be the case following the summation of squared samples. The expected p.d.f.'s for noise alone and for signal plus noise are illustrated in figure 4.29. The probabilities of false alarm and of detection are also shown.

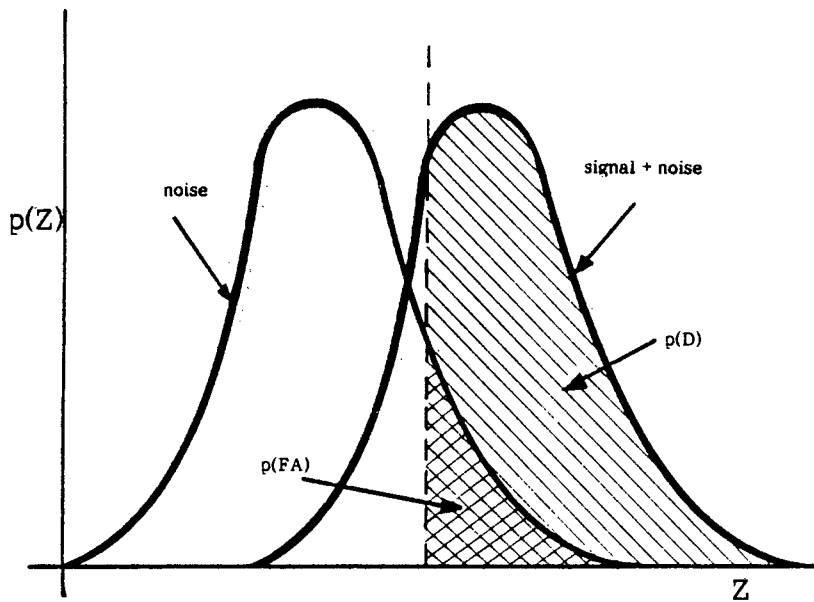


Figure 4.29 - The expected p.d.f's of noise alone, and of signal plus noise.

The summer will add $2BT$ samples. The mean values of the output of the summer for the cases of noise alone and signal plus noise can be shown to be (Denbigh, 1987; Burdic, 1984):

$$M_{S+N} = 2BT(\sigma_S^2 + \sigma_N^2) \quad (4.25)$$

$$M_N = 2BT(\sigma_N^2) \quad (4.26)$$

where: σ_N^2 is due to the noise power
 σ_S^2 is due to the signal power

If the signal strength is weak, then the variances of the two p.d.f's are similar: this is the case of interest. Therefore, both variances are assumed equal to the variance of the p.d.f. for noise alone, V (Denbigh, 1987; Burdic, 1984):

$$V_{S+N} = V_N = 4\sigma_N^2 \cdot BT \quad (4.27)$$

Now that the p.d.f's have been defined, it is possible to determine $p(D)$ for a given $p(FA)$. This is best achieved using the detection index d , where:

$$d = \frac{(M_{S+N} - M_N)^2}{V} = \frac{(2BT\sigma_S^2)^2}{4\sigma_N^2 BT} = BT(S/N)^2 \quad (4.28)$$

The detection index can be determined using curves of Receiver Operating Characteristics. An example of these is reproduced below.

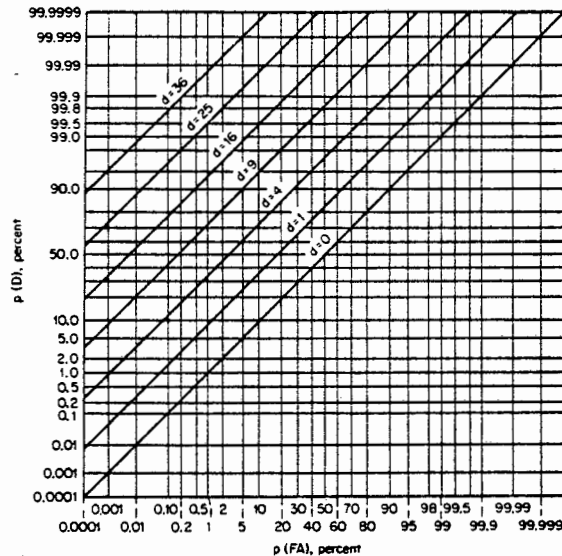


Figure 4.30 - Receiver Operating Characteristics (Urlick, 1983)

For a given $p(FA)$ and $p(D)$, the detection index, d , can be read. For this detection index, the required signal-to-noise ratio into the threshold detector is obtained by using equation (4.28) in the form:

$$S/N = 10 \log((d/BT)^2) \quad (4.29)$$

Finally, the minimum signal-to-noise ratio in the water can be determined. It is the difference between the required signal-to-noise ratio into the threshold detector and the array gain (in logarithmic units). The array gain is determined in the manner described in subsection 4.5.2.

Therefore, the minimum required signal-to-noise ratio in the water is:

$$S/N = -AG + (S/N)_T \quad (4.30)$$

where: AG is the array gain
 $(S/N)_T$ is the required signal-to-noise ratio into the threshold detector.

For the simulation in which the CCARS sonar used a small passive reflector and a source of known spectrum, the minimum signal-to-noise ratio needed to obtain a $p(D)$ of 0,94 and a $p(FA)$ of 0,001 was -8dB. The passive reflector is 14,5 wavelengths across, the receiver bandwidth is 75kHz, and the receiver response time is 1,4ms. Substituting these parameters into the above formulae, equation (4.30) can be solved to determine the minimum signal-to-noise ratio required by a comparable conventional passive sonar system. A $p(FA)$ of 0,001 and a $p(D)$ of 0,94 yields a detection index of approximately 22. Therefore, the minimum signal-to-noise ratio required at the input to the threshold detector can be obtained from equation (4.29): -6,8dB. Since the array gain is 13,6dB, the minimum required signal-to-noise ratio in the water is: 20,4dB.

For the simulation in which a large receiver detected a source of known spectrum, the signal-to-noise ratio required to obtain a $p(D)$ of 0,89 and a $P(FA)$ of 0,001 was -15dB. When the source spectrum was unknown, the required signal-to-noise ratio was found to be -12dB. A comparable conventional passive sonar uses a line array which is 50 wavelengths across, has a gate width of 3,7ms, and has a bandwidth of 75kHz. Equation (4.30) can be solved to obtain the required signal-to-noise ratio as: -24,7dB.

4.5.4 Discussion

The detection performance of a CCARS sonar system is inferior to that of a comparable conventional system. When configured as a passive sonar, a CCARS system requires a minimum signal-to-noise ratio which is 10 to 12dB higher than that required by a conventional system. This is to be expected: while the limits to detection in a conventional system are the statistical fluctuations of ocean signals and noise, the limit to detection in a CCARS system is the error in estimating the correlation-coefficient.

One method of reducing the error in the estimate of correlation-coefficient would be to use a second active element, also positioned within the passive reflector. If the two elements are sufficiently distant, then their respective errors in determining the correlation-coefficients will be independent of one another. Averaging these two sets of results will therefore reduce the error in the overall estimate of correlation-coefficient. The extent of this improvement can be determined by noting that if independent samples are added, then the variance of the resultant is the sum of the individual variances (Miller and Freund, 1965). Thus, the standard deviation of the error in estimating the correlation-coefficient will be reduced by a factor of $\sqrt{2}$. Similarly, the use of three or more elements would result in yet a further improvement. Although this procedure increases system complexity, the sonar remains very substantially less complex than a conventional beamforming system.

When configured as an active system, a CCARS sonar needs an even greater advantage. A minimum signal-to-noise ratio which is roughly 20dB higher than that required by a comparable conventional active system is needed. The reason for this is the very poor range resolution of a CCARS system: a system with a bandwidth of 75kHz has a time resolution of only 3,7ms.

These results certainly do not imply that a CCARS sonar could never be useful. Despite its inferior performance, it far more simple and inexpensive to build a large passive reflector than even a much smaller transducer array. Therefore, a sonar based upon the cross-correlation analysis of received spectra might still be the preferred solution to certain sonar applications, particularly in view of the good angular resolution which can be obtained. Indeed, for an application such as harbour protection, existing structures such as the harbour mouth could conceivably fulfil the function of a sizeable passive reflecting structure.

5.0 THE LOCALISATION OF SOUNDS BY A MANNIKIN HUMAN HEAD

The extent to which beamforming by the cross-correlation analysis of received spectra can emulate human monaural sound localisation was assessed using a mannikin human head.

The subject of the investigation is an injection moulded Sennheiser model MZK2002 artificial head. A probe microphone was inserted through a window at the rear of the head into the base of the left ear. (A Bruel and Kjaer model 4145 half-inch microphone was attached to a sawn-off 4mm probe tube - part DB0243). The artificial head was positioned on a rotatable turntable in order that its orientation could be set at any elevation in the median plan relative to a fixed position source. This projection was chosen because human median plane localisation relies solely on monaural cues, whereas azimuth plane localisation uses both monaural and binaural cues. Consequently results obtained from experiments performed in the median plane can be compared directly with the localisation performance of human subjects.

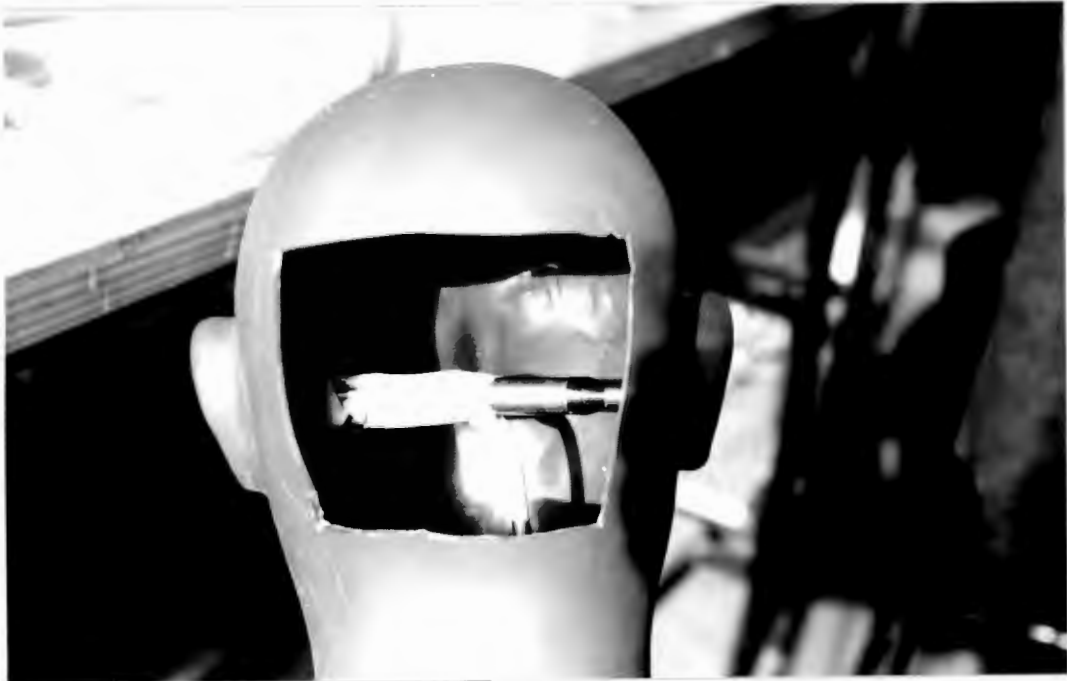


Figure 5.1 - A probe microphone was fixed inside the head.

Since humans locate sounds in the passive listening mode, one of the main difficulties lies in recognising the spectrum modification of a sound whose original spectrum is unknown. The inability of subjects to locate certain sounds in the median plane is evidence that in the general case it is not possible to achieve this (refer subsection 3.2.3 for a fuller discussion of this topic). However, most commonly occurring sounds can be located. Many of these fall into one of two categories: the first category includes sounds which are impulsive in character; for example a clap, or any other short sharp sound. The second includes those sounds which are of long duration, and whose spectra are time variant; the most common example is speech. Separate techniques have been developed for the localisation of these two categories.

5.1 The localisation of impulsive sounds

Sounds which are impulsive in the time domain are usually broadband, with minimal spectral character. Consequently, the spectrum modification which the pinna imposes will dominate the received spectrum.

The mannikin head was required to localise four different impulsive sounds: an electrical impulse driving a Philips model AD11600 tweeter; the bang of a toy cap-gun; the crack of a pulling chinese-cracker; and the click of an electric discharge gas-stove lighter.

5.1.1 Experimental method

Each source was positioned 5 metres from the mannikin head. It was ensured that the time difference of arrival between the direct path and the first echo was greater than the 2,56ms required to capture the incident sound. The received signal was bandlimited between 20Hz and 20kHz, and then captured on a Philips model PM3305 digital storage oscilloscope. The sampling rate was 50kHz, therefore 128 time samples were required. Each sound was recorded at 10 degree increments over a full 360 degree sector. Every captured waveform was downloaded via the HP-IB bus to an HP-85 microcomputer for storage on flexible disc.

To determine the magnitude responses of the pinna, and to measure the frequency response of the probe microphone, it was necessary to record a reference sound in the free field: first using the probe microphone, and second using a Bruel and Kjaer model 4145 half-inch flat response microphone. The reference sound selected was the first of the test signals - an electrical impulse applied to a Philips tweeter - since it has a relatively flat, repeatable spectrum.

$$|S(\omega)H(\omega, \theta)| = \frac{|S(\omega)H(\omega, \theta)P(\omega)|}{|P(\omega)|} \quad (5.2)$$

$$|P(\omega)| = \frac{|T(\omega)P'(\omega)|}{|T(\omega)|} \quad (5.3)$$

where: $S(\omega)$ is the source spectrum.

All software processing was programmed in Fortran on the resident Sperry 1100 Mainframe computer at the University of Cape Town. The experimental data was uploaded by means of a serial data link.

5.1.2 Results

The median plane magnitude responses of the pinna are shown in figure 5.2. The perspective has been plotted to illustrate interference nulls rather than peaks, since they are a more characteristic feature. This is consistent with measurements of the transfer functions of human pinnae.

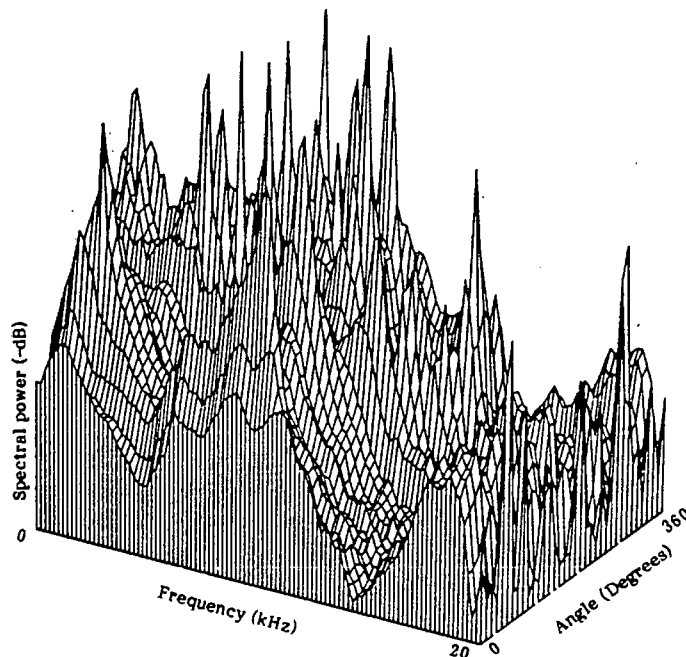


Figure 5.2 - The pinna's median plane magnitude responses (plotted such that nulls are represented by peaks).

Figure 5.3 shows sample free-field spectra of each of the four sounds used in the localisation experiment. It should be noted that, with the exception of the tweeter transmissions, the spectra showed some variation from recording to recording.

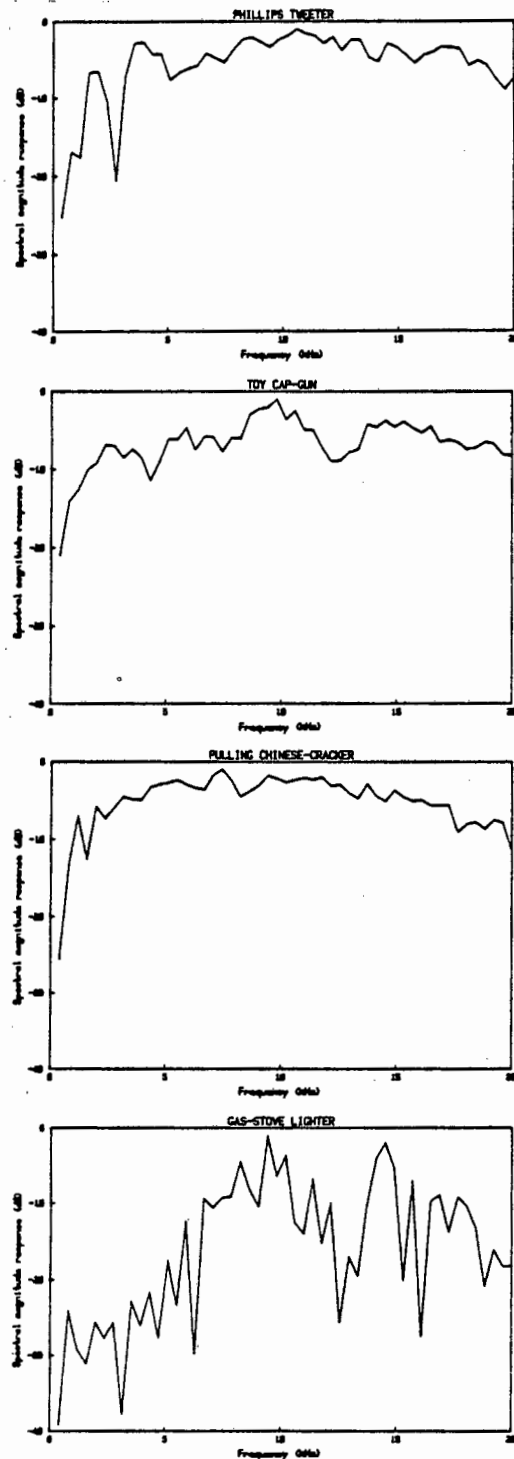


Figure 5.3 - Free-field spectra of:
 (a) The tweeter sound.
 (b) The toy cap-gun.
 (c) The chinese cracker.
 (d) The gas-stove lighter.

Figures 5.4 to 5.7 illustrate the ability of this technique to localise the four sources. Each sound has been localised at six evenly spaced median plane positions. Each plot shows correlation coefficient as a function of angle, calculated at 10 degree increments along a 360 degree sector.

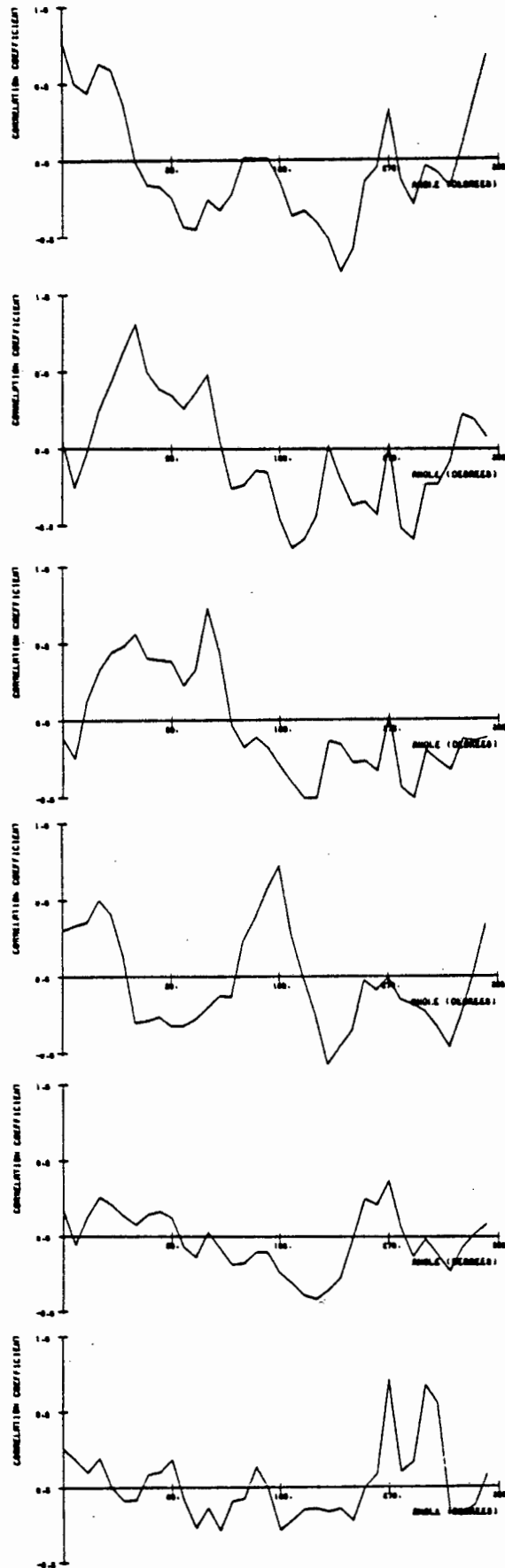


Figure 5.4 - Localisation of the electrical impulse driving the Philips tweeter. The tweeter was positioned at 0 degrees, 60 degrees, 120 degrees, 180 degrees, 240 degrees, and 300 degrees respectively.

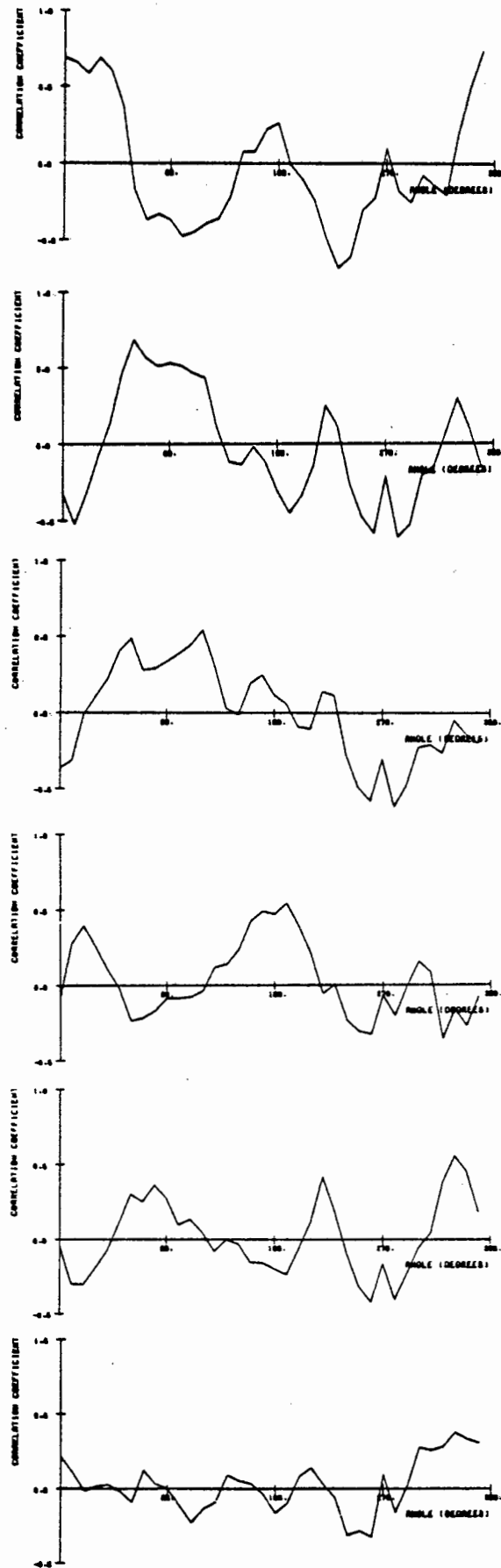


Figure 5.5 - Localisation of the toy cap-gun. The cap-gun was positioned at 0 degrees, 60 degrees, 120 degrees, 180 degrees, and 300 degrees respectively.

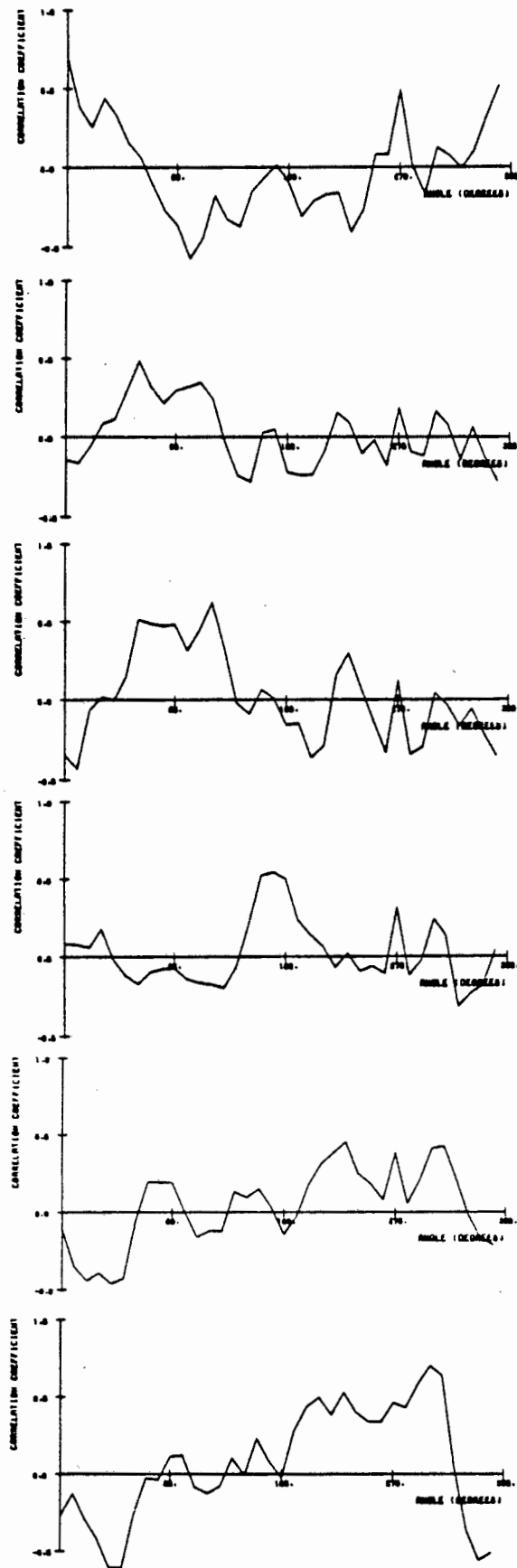


Figure 5.6 - Localisation of the pulling chinese-cracker. The pulling cracker was positioned at 0 degrees, 60 degrees, 180 degrees, 240 degrees, and 300 degrees respectively.

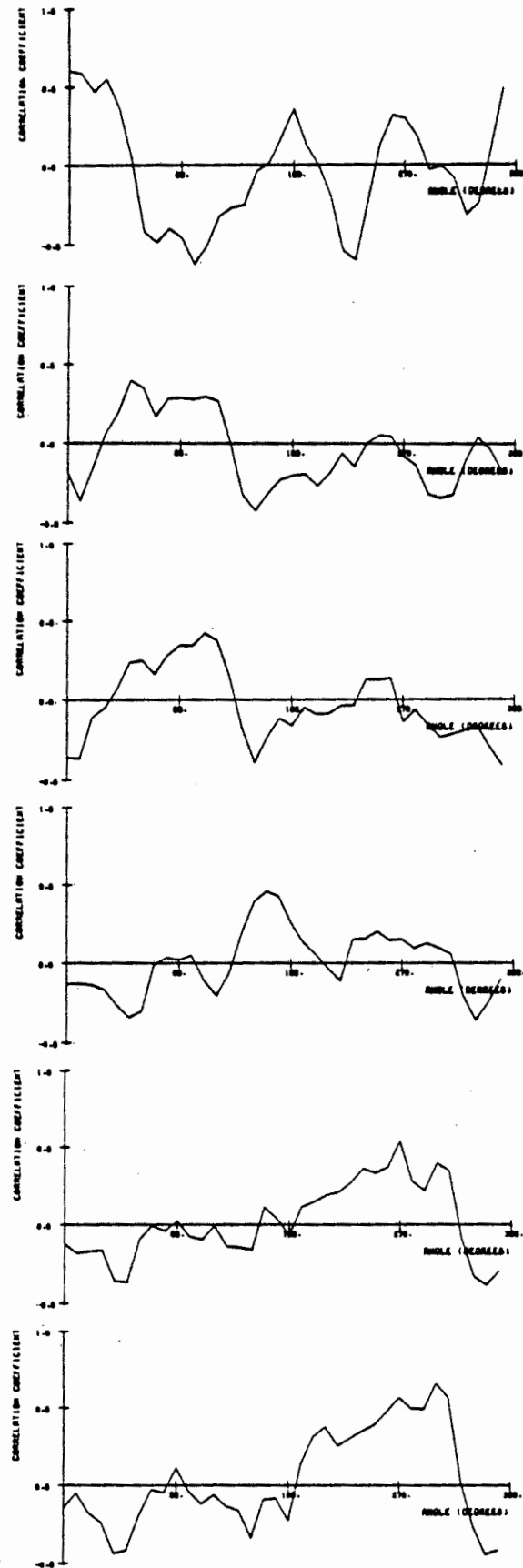


Figure 5.7 - Localisation of the electric discharge gas-stove lighter at 0 degrees, 60 degrees, 120 degrees, 180 degrees, 240 degrees, and 300 degrees respectively.

5.1.3 Discussion

The tweeter, cracker and gas-stove lighter were adequately localised at all positions investigated. The results obtained for the cap-gun were less consistent. This is due to the large spectral variations which characterised successive recordings of the source spectrum. These variations were caused by differences in the orientation of the gun: interference nulls were sometimes present due to path-length differences of sounds emanating from more than a single location on the gun. In a few instances, these prevented successful localisation.

The widths of the correlation peaks obtained are roughly equivalent to the median plane localisation blur measured in human subjects (refer subsection 3.2.3).

Consistent with the theory of this technique, the sounds best located are those whose free field spectra had the minimum feature.

5.2 The localisation of longer sounds

Although sounds of longer duration frequently exhibit highly characteristic spectral features, these features are often time-variant. In contrast, the spectrum modification imposed by the pinna is time-invariant provided the target position remains constant. Therefore, the spectrum modification imposed by the pinna can be recognised by separating those spectral features of received sounds which are time-invariant from features which vary with time. This can be achieved by using a method of frequency analysis which provides a continuously updated output; for example, the Fourier-t-transform (refer subsection 4.4).

To demonstrate the localisation of longer sounds, the following spoken passage was selected as the chosen sound:

"The creative and artistic impulse in a fragmented society often comes from the ghetto rather than from the affluent strata of society. This assertion is substantiated by the vitality of the Sophiatown Renaissance of the Fifties and the volume of black writing in South Africa today. In the last three decades a torrent of black creativity has emerged from the townships. From the early days of Sophiatown to the present there has been a distinct township culture manifested in music, in the visual arts, in drama and in literature. A culture of self-assertion, it has been both virulent and dynamic."

(Patel, 1985)

5.2.1 Experimental method

An impractically large number of samples would be required to digitize the above passage. Therefore, the proposed localisation technique was demonstrated in real time using analog equipment.

The author's rendition of the extract was recorded using a Revox high fidelity reel-to-reel tape recorder. To obtain a

more uniform spectral spread, the output of the Bruel and Kjaer model 4145 half-inch microphone was modified by a bank of variable-gain third-octave filters prior to recording. The required modification was achieved by emphasizing the high frequency spectral components.

The recorded passage was played-back using a Philips model AD11600 tweeter, which was positioned a distance of 2 metres from the mannikin head. The head was mounted such that the tweeter output would be received in the median plane. The response of the probe microphone, mounted in the moulded base of the left ear, was fed to a Spectral Dynamics model SD301C real time analyser. This device has a frequency selectivity of 60Hz. Since a new spectrum is generated every 50 milliseconds, one reading of the passage comprises approximately 512 spectra. These spectra were photographically recorded using a Honeywell model 1856A fiberoptic cathode ray oscillograph. The resulting images are a good representation of what would be obtained were the Fourier-t-transform to be applied directly.

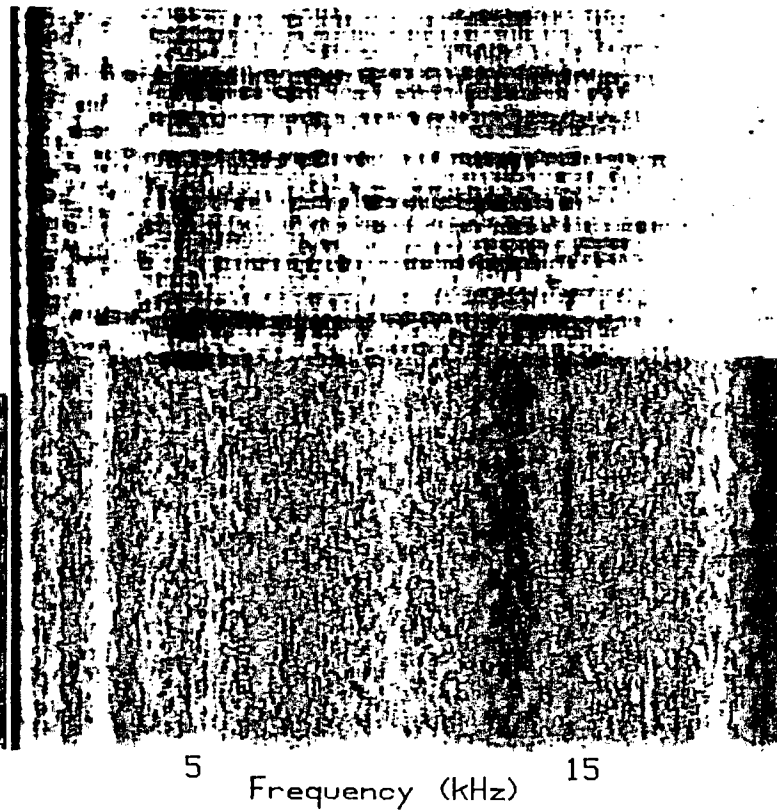
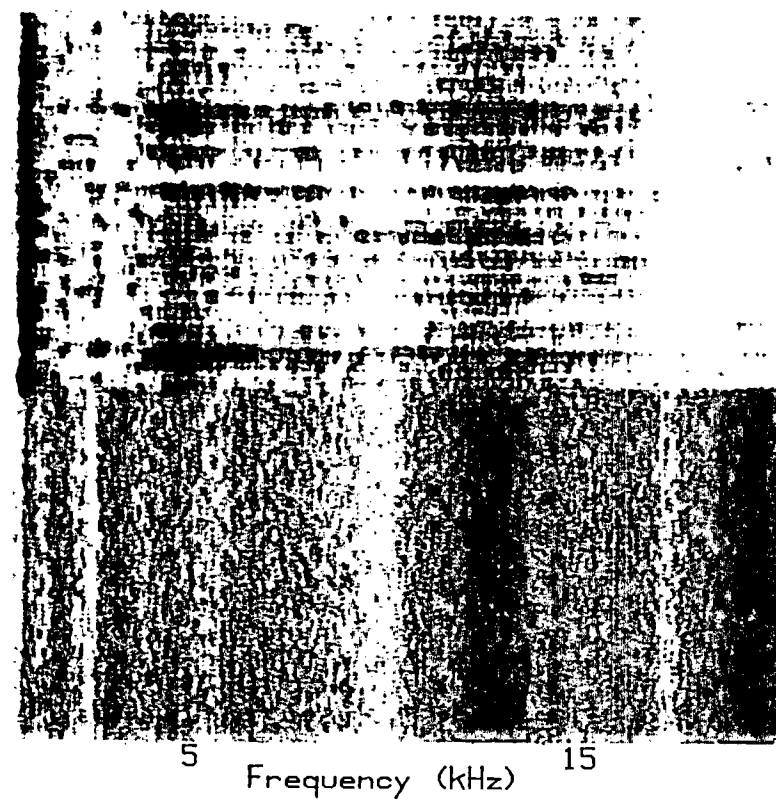
To supplement these visual recordings with a more quantitative analysis, each ensemble of spectra was averaged using the Model SD302C ensemble-averaging feature of the real time analyser. This arithmetic procedure is somewhat analogous to the visual integration which occurs when the photographic records are viewed: common features are reinforced, while time fluctuations are de-emphasized. The averaged spectra were digitised using the Philips storage oscilloscope, and then downloaded to an HP-85 microcomputer. To assess localisation, each averaged spectrum was cross-correlated with stored pinna magnitude responses to white noise, predetermined at each angular increment.

5.2.2 Results

Figure 5.8 shows the photographic oscillograph records taken at 10 degree increments over a 360 degree sector. Each contains the pinna response to the passage of speech. For comparison, the pinna magnitude response to white noise is also provided.

10 DEGREES

20 DEGREES



30 DEGREES

40 DEGREES

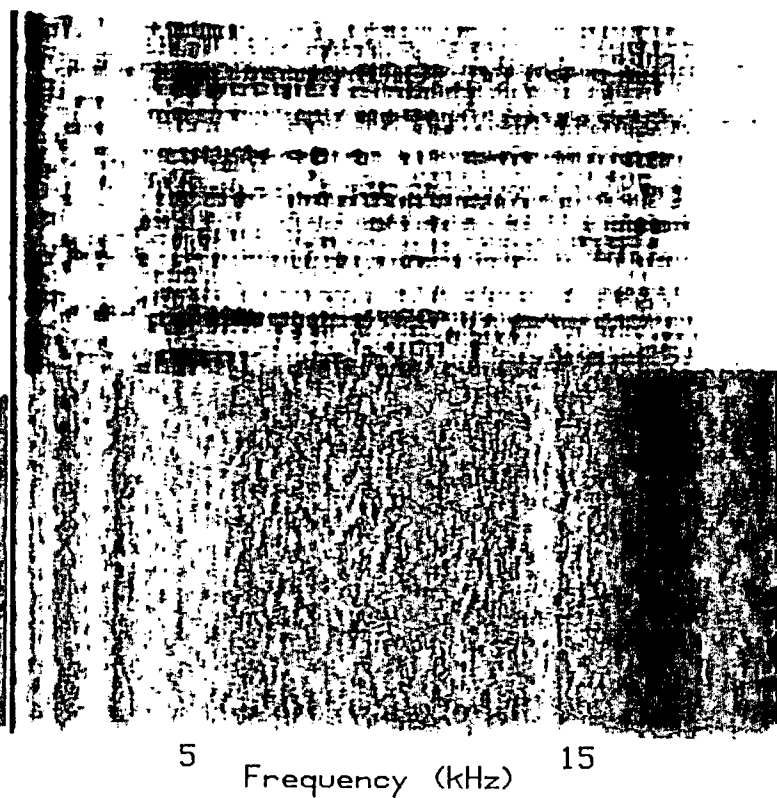
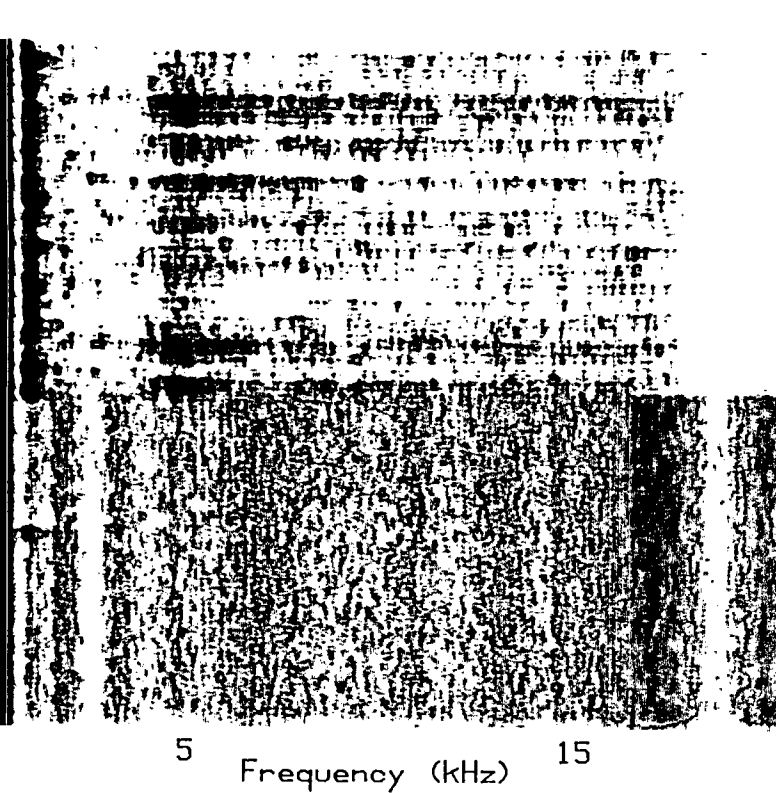
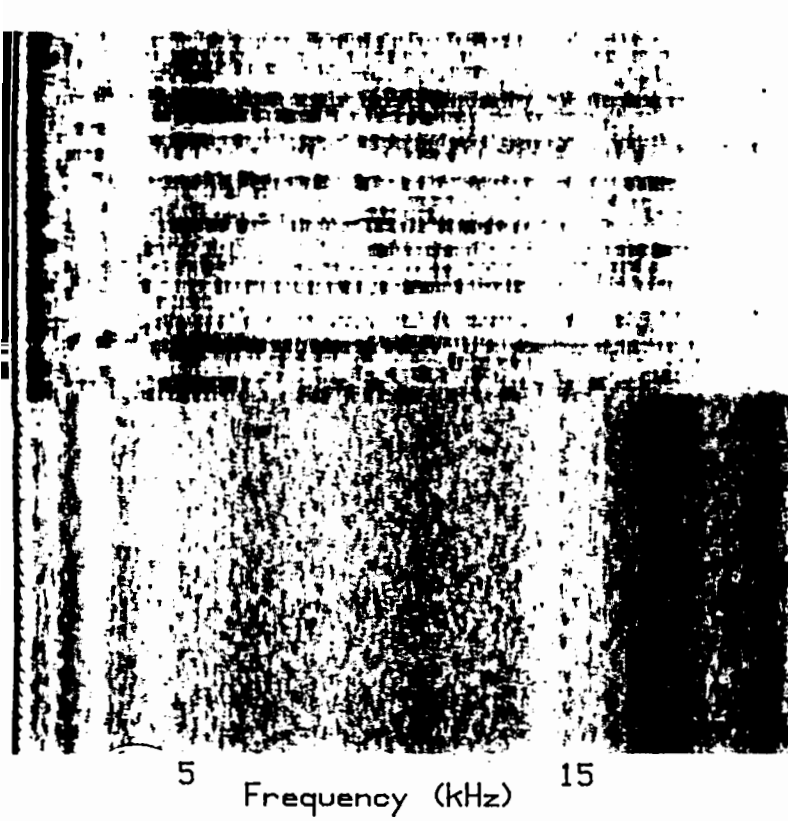
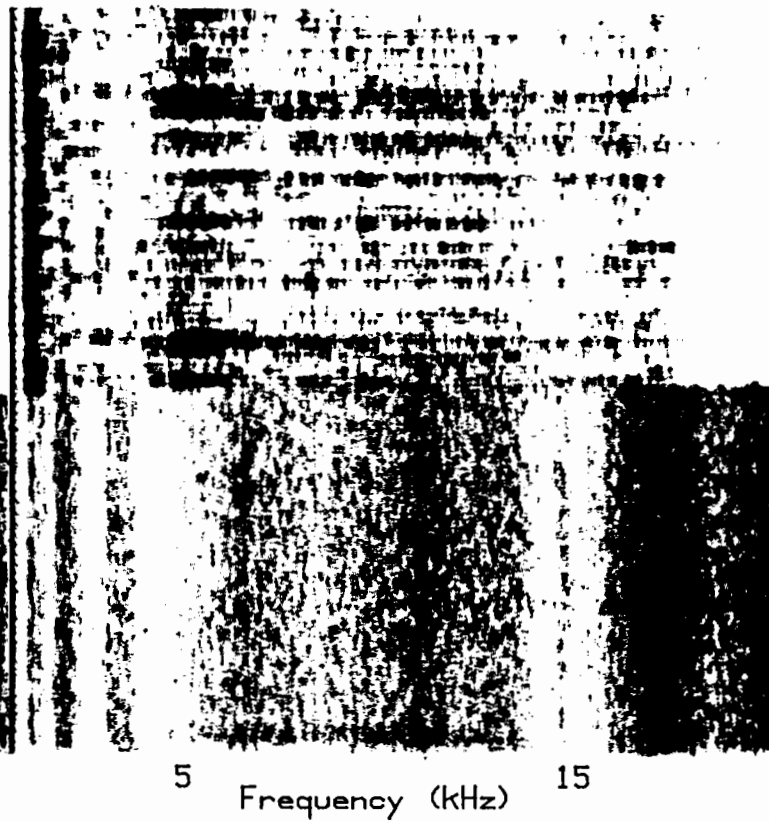


Figure 5.8 - The oscillograph recordings of the pinna magnitude response to white noise and to a passage of speech.

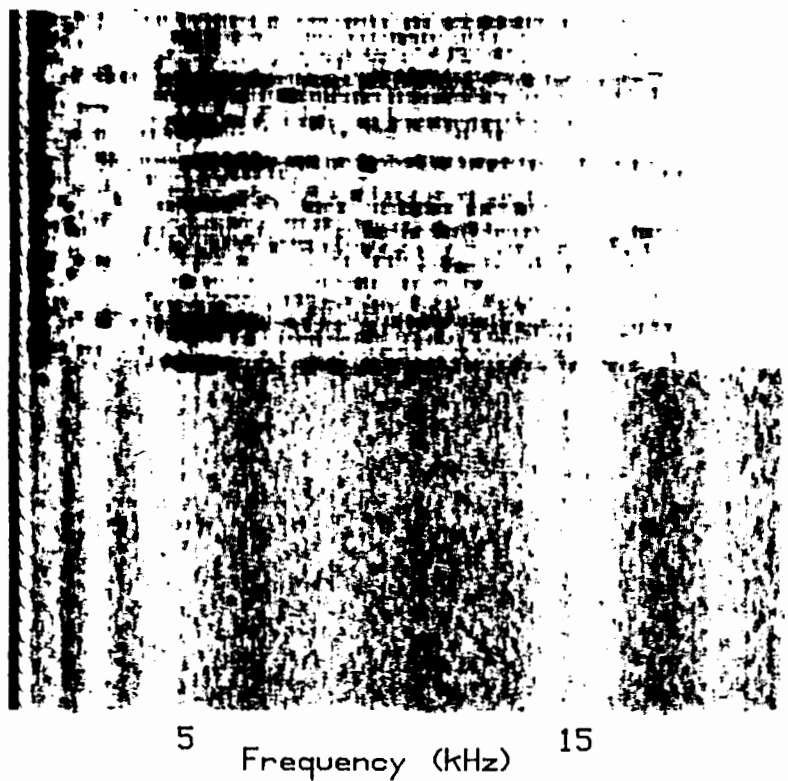
50 DEGREES



60 DEGREES



70 DEGREES



80 DEGREES

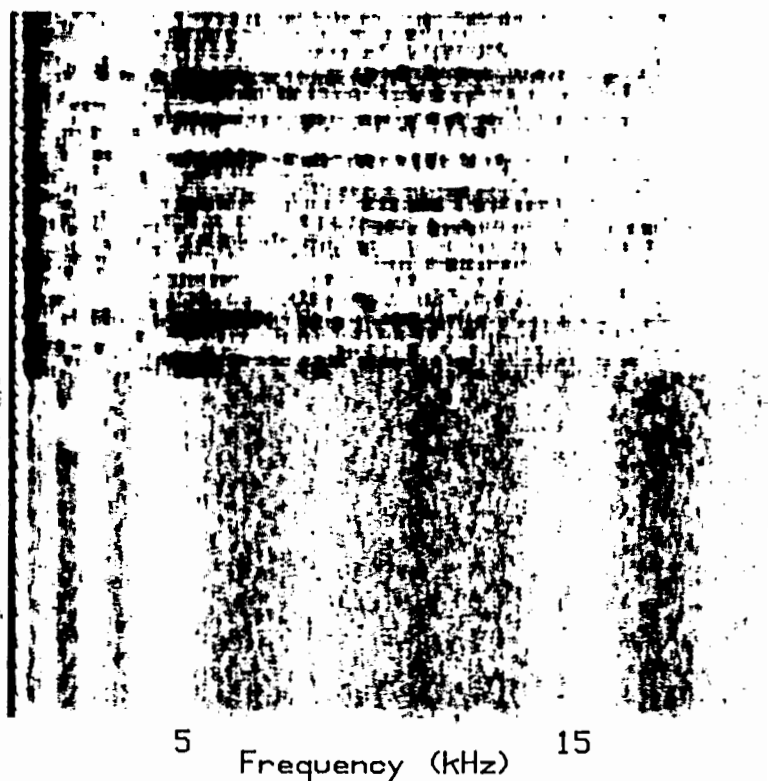
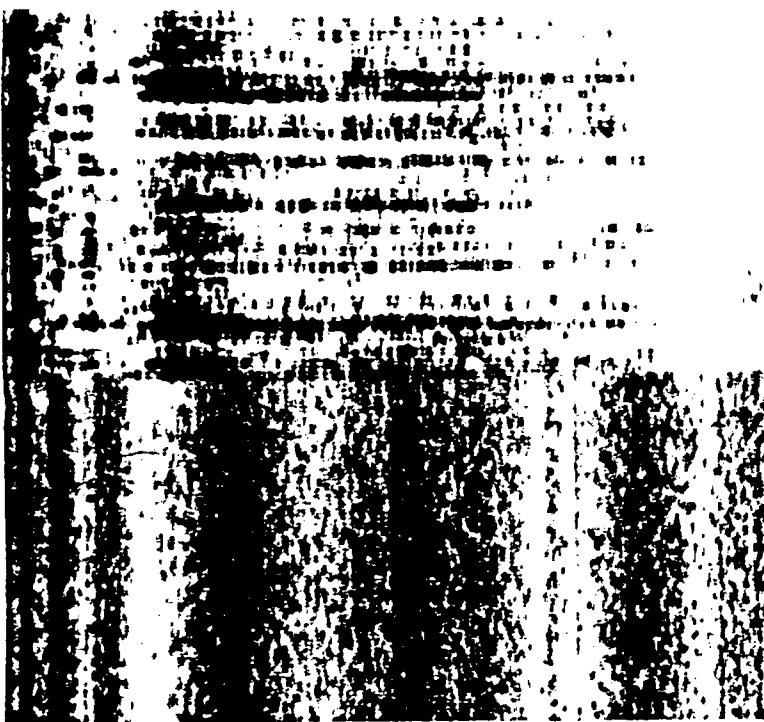


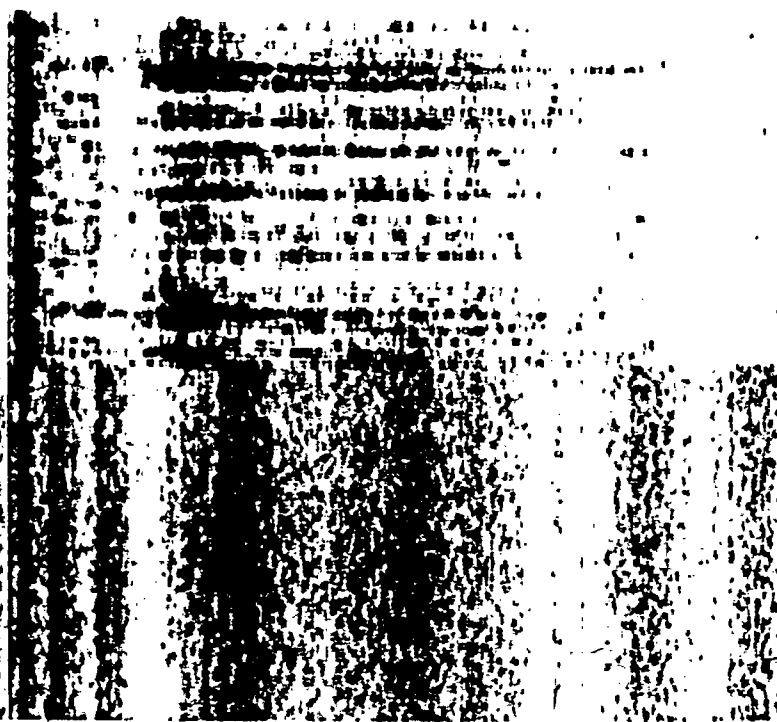
Figure 5.8 - continued

90 DEGREES

100 DEGREES



5 Frequency (kHz) 15



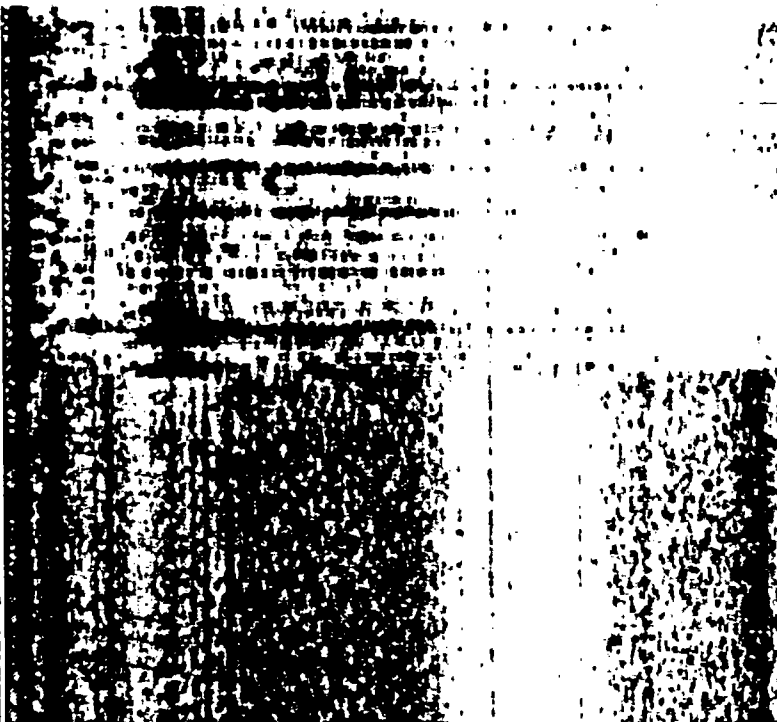
5 Frequency (kHz) 15

110 DEGREES

120 DEGREES



5 Frequency (kHz) 15

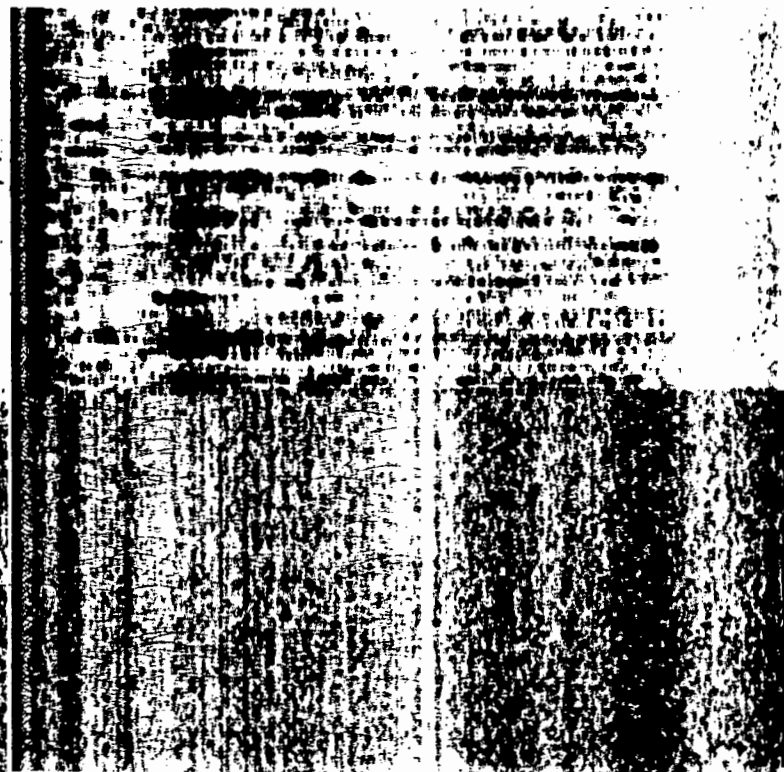
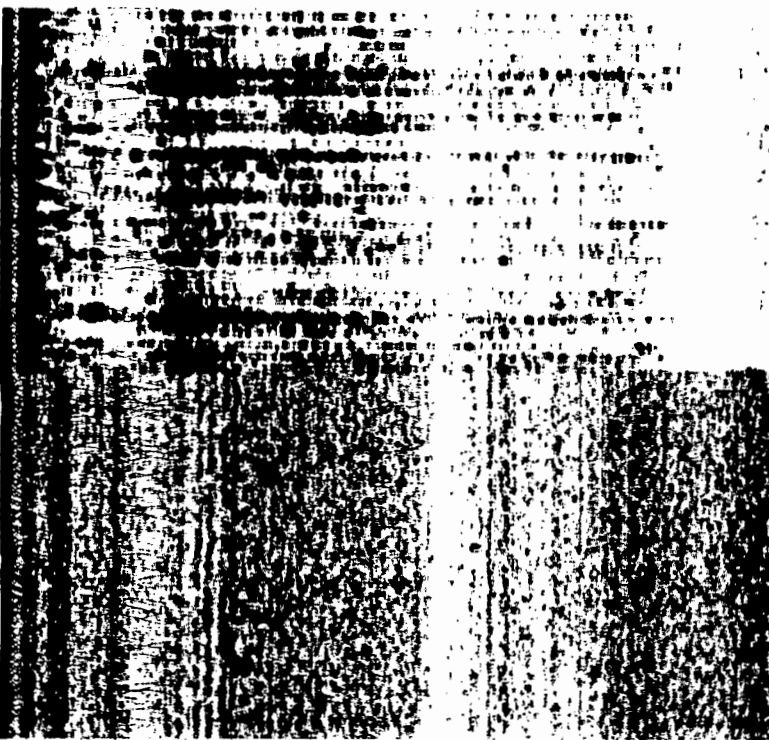


5 Frequency (kHz) 15

Figure 5.8 - continued

130 DEGREES

140 DEGREES



150 DEGREES

160 DEGREES

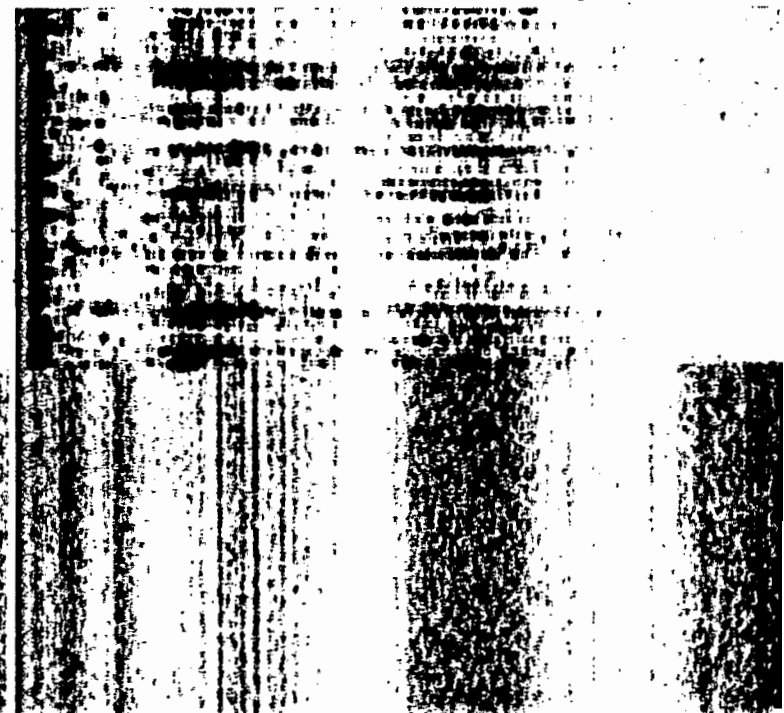
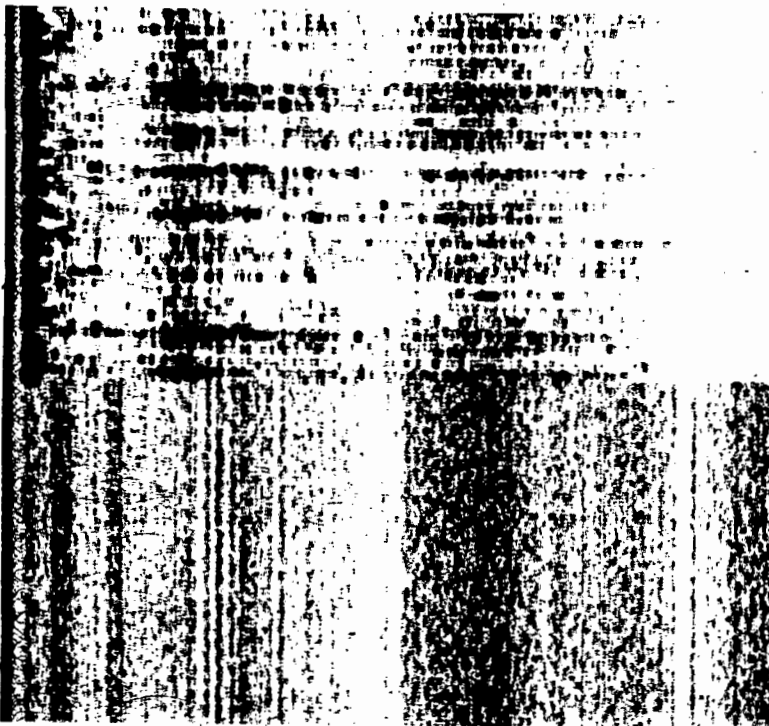
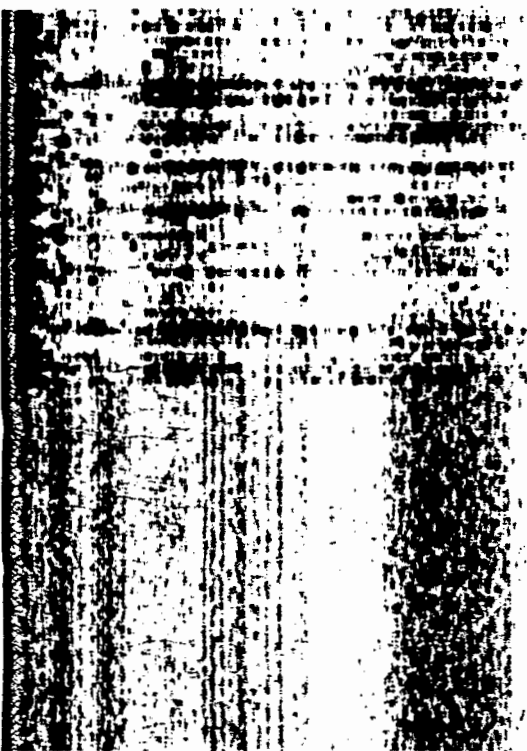


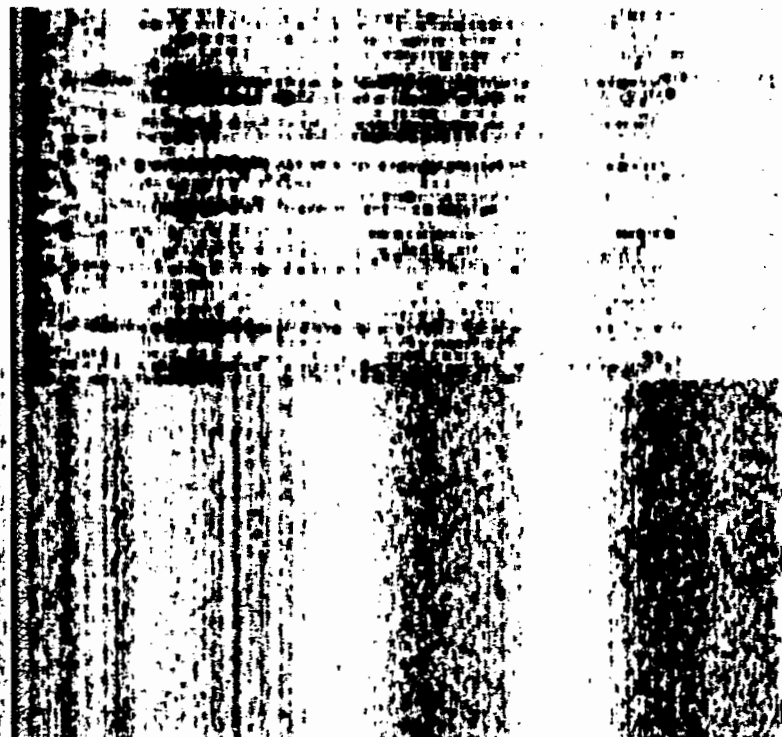
Figure 5.8 - continued

170 DEGREES

180 DEGREES



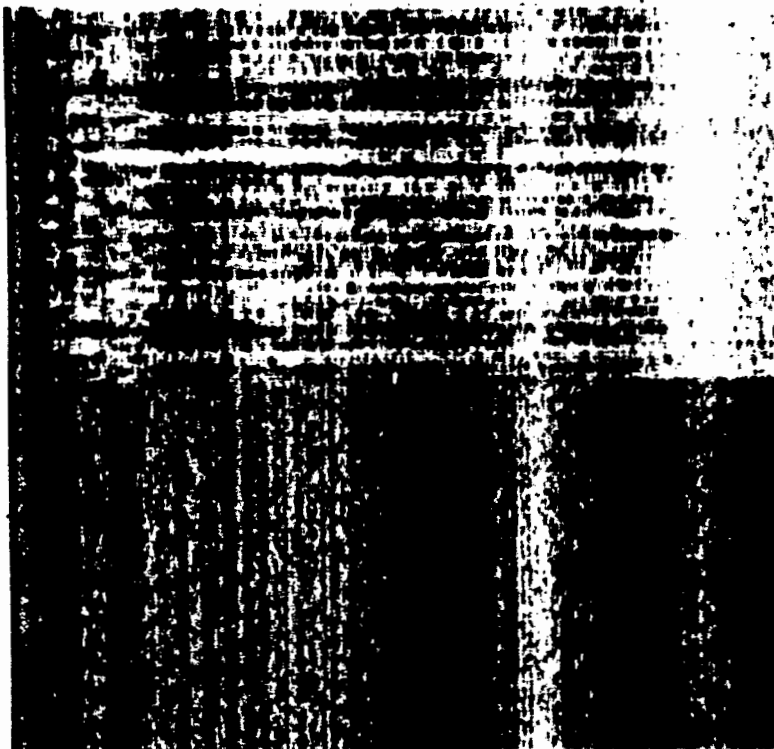
5 Frequency (kHz) 15



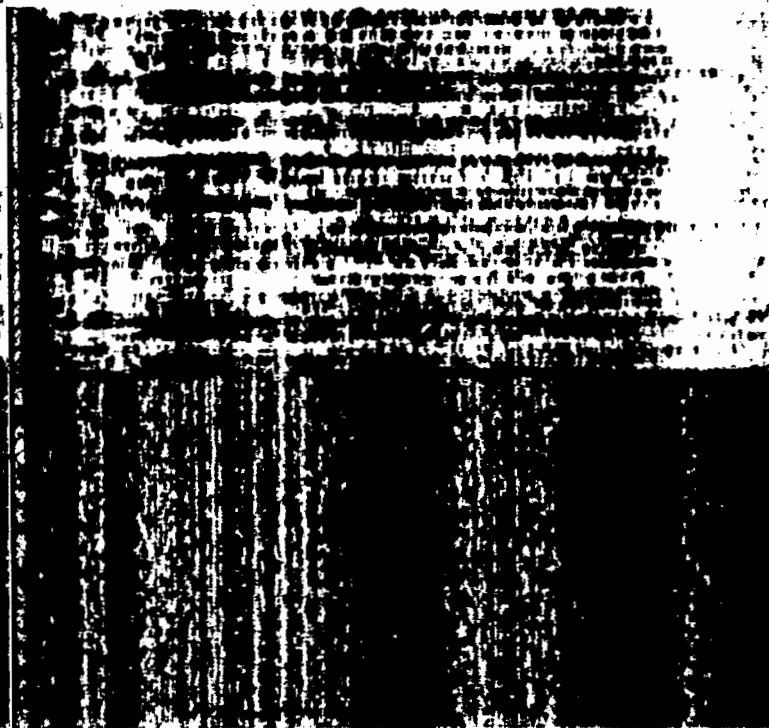
5 Frequency (kHz) 15

190 DEGREES

200 DEGREES



5 Frequency (kHz) 15

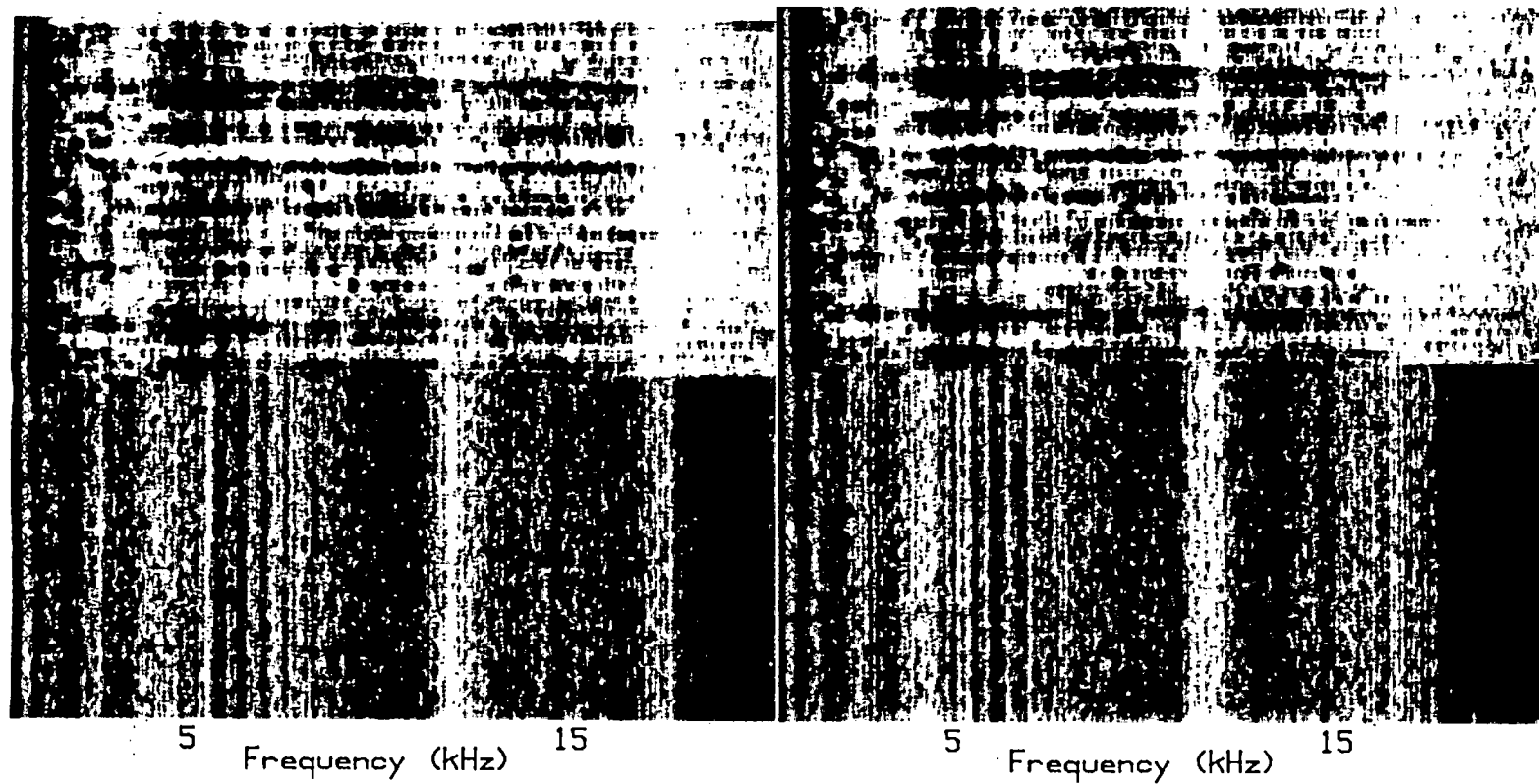


5 Frequency (kHz) 15

Figure 5.8 - continued

210 DEGREES

220 DEGREES



230 DEGREES

240 DEGREES

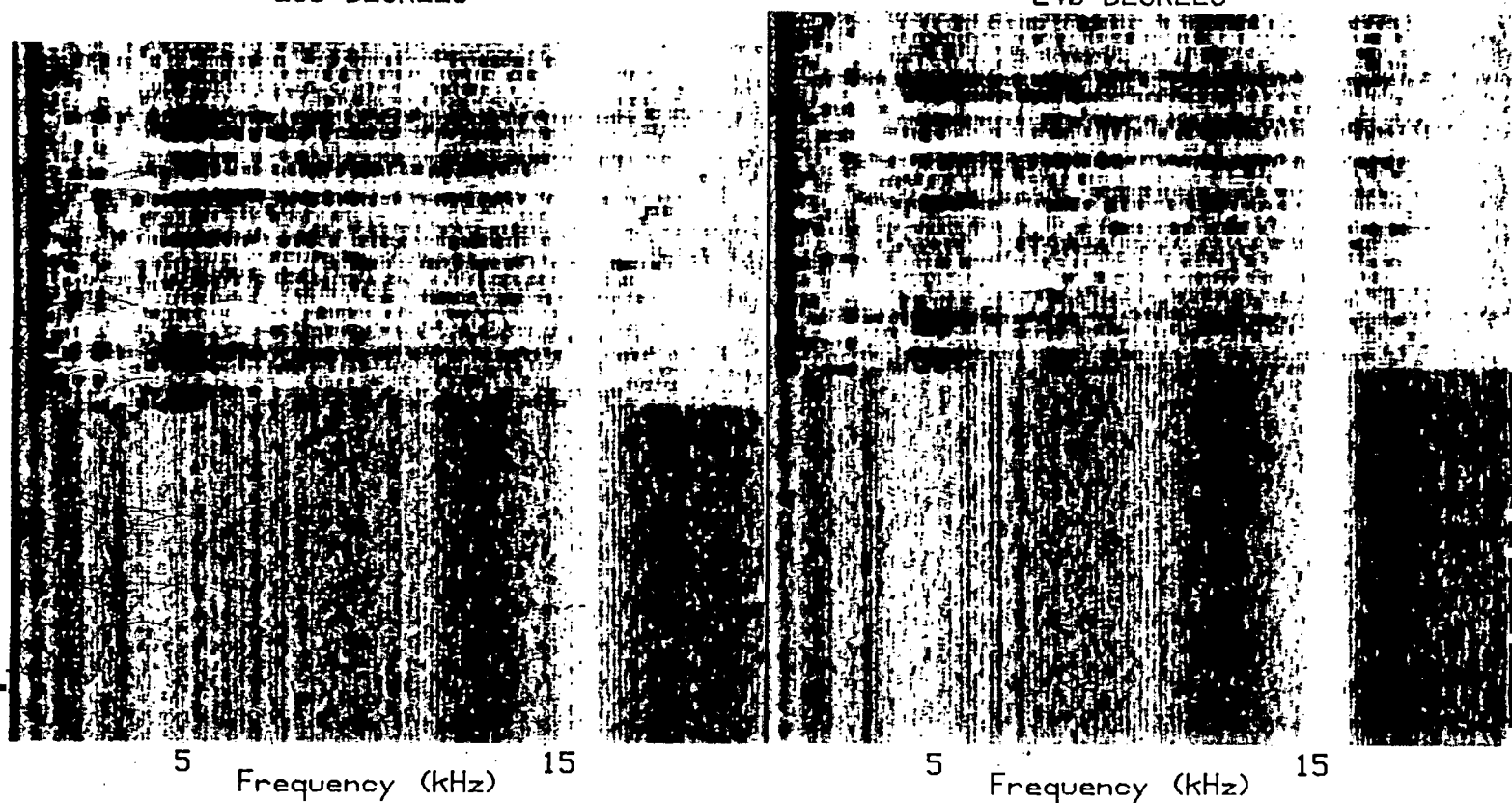
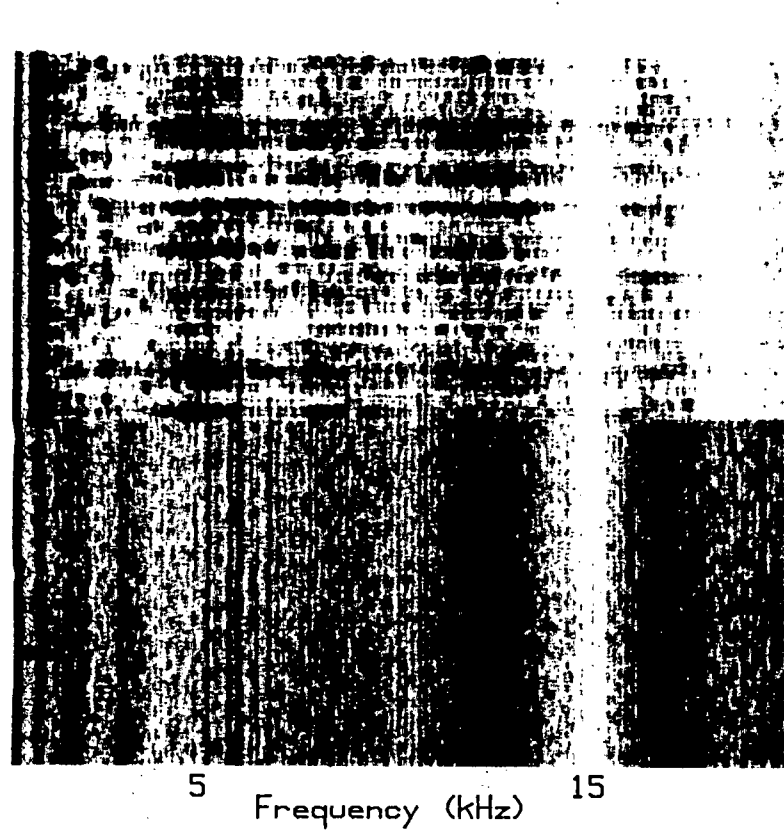


Figure 5.8 - continued

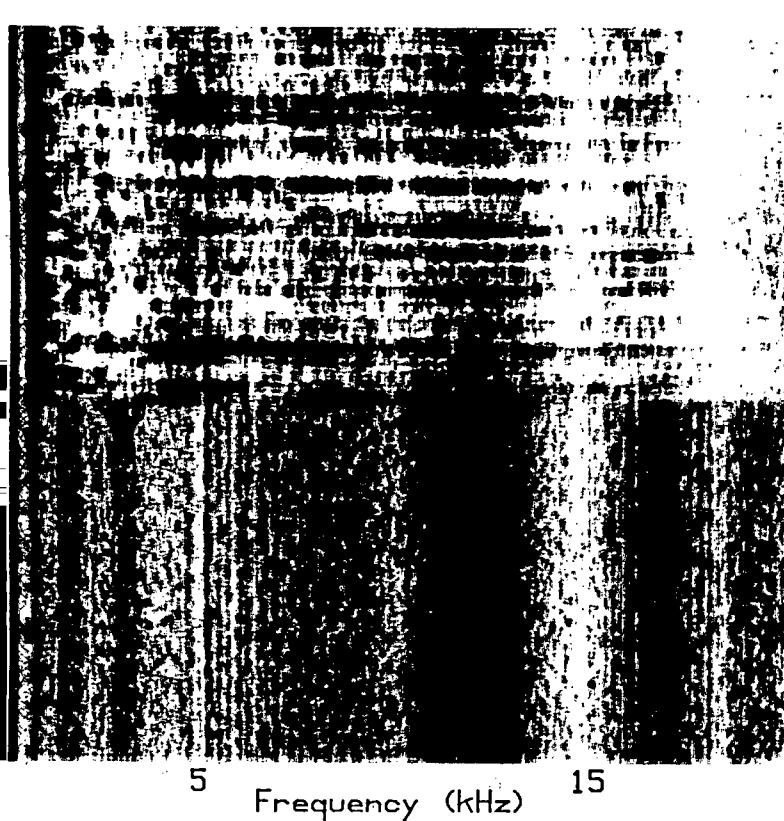
250 DEGREES



260 DEGREES



270 DEGREES



280 DEGREES

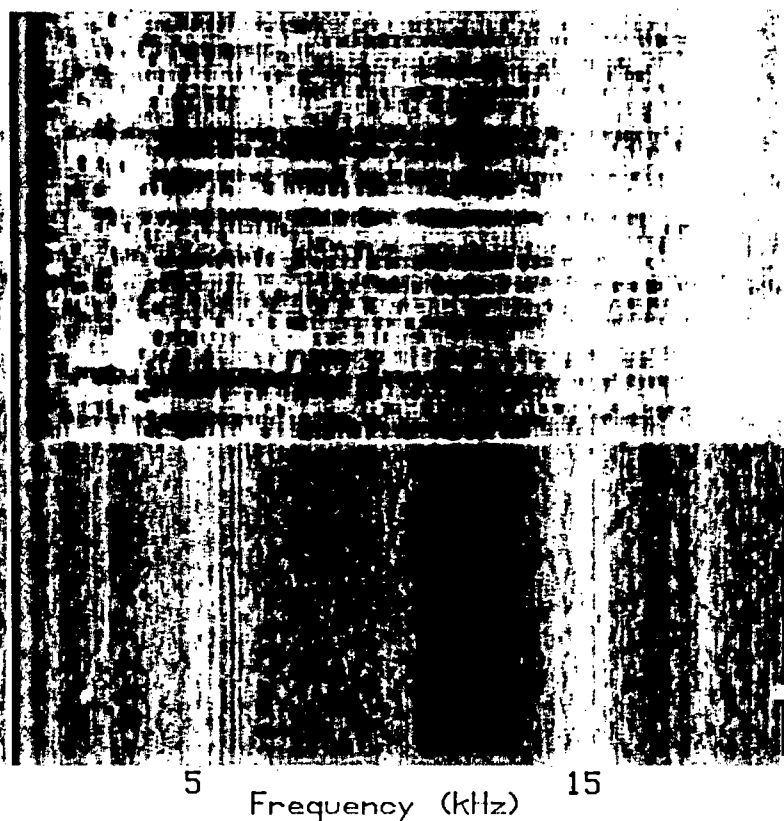


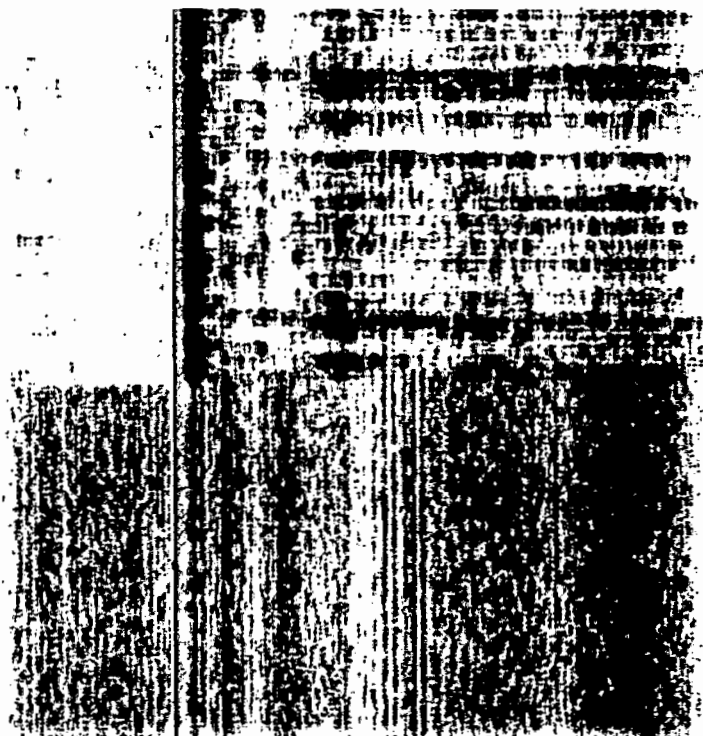
Figure 5.8 - continued

290 DEGREES

300 DEGREES



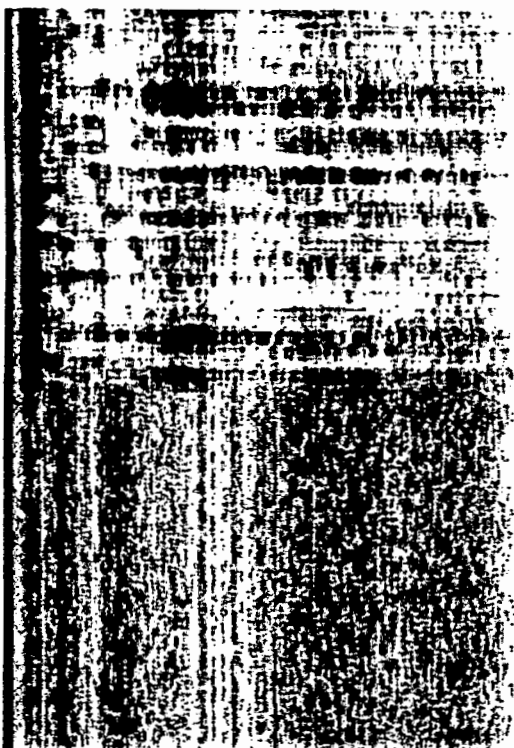
5 Frequency (kHz) 15



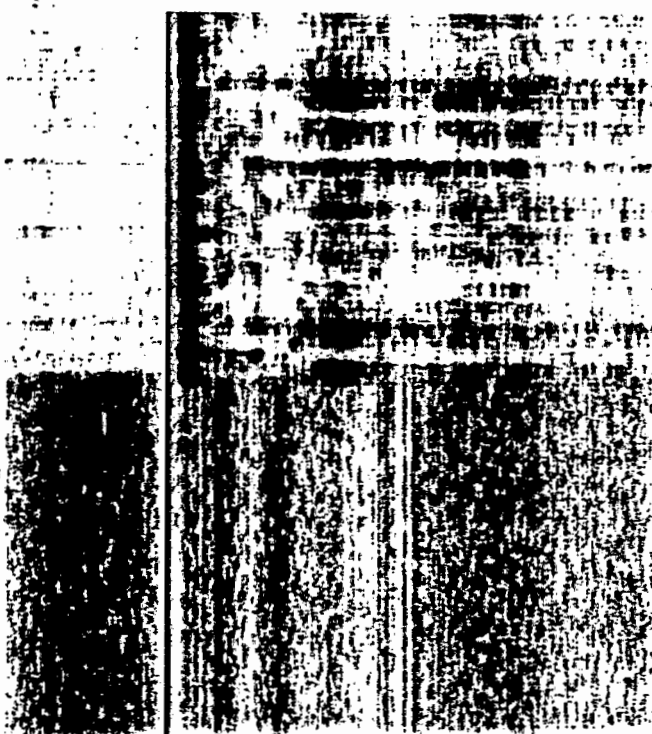
5 Frequency (kHz) 15

310 DEGREES

320 DEGREES



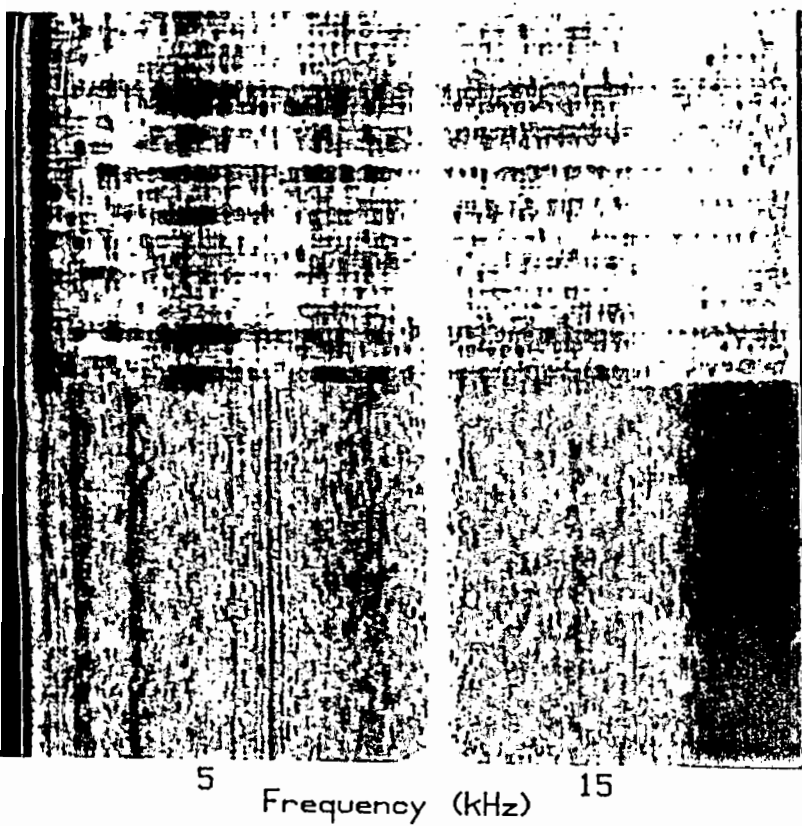
5 Frequency (kHz) 15



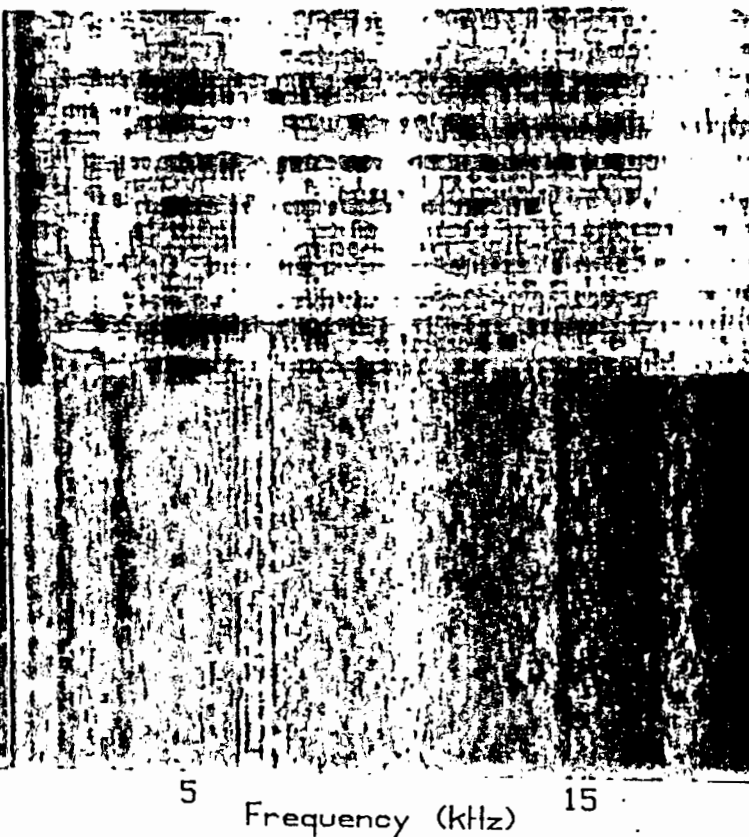
5 Frequency (kHz) 15

Figure 5.8 - continued

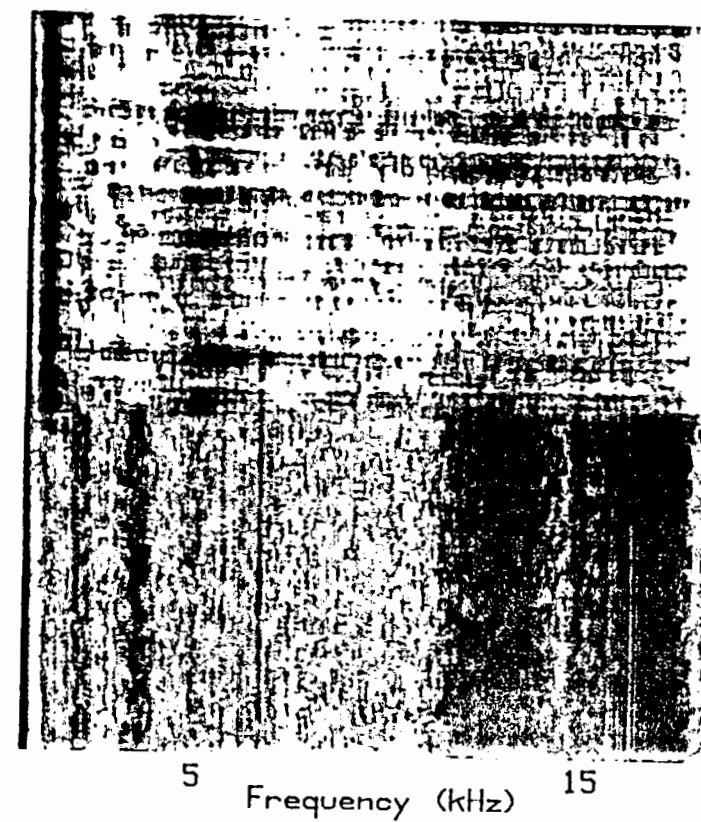
330 DEGREES



340 DEGREES



350 DEGREES



360 DEGREES

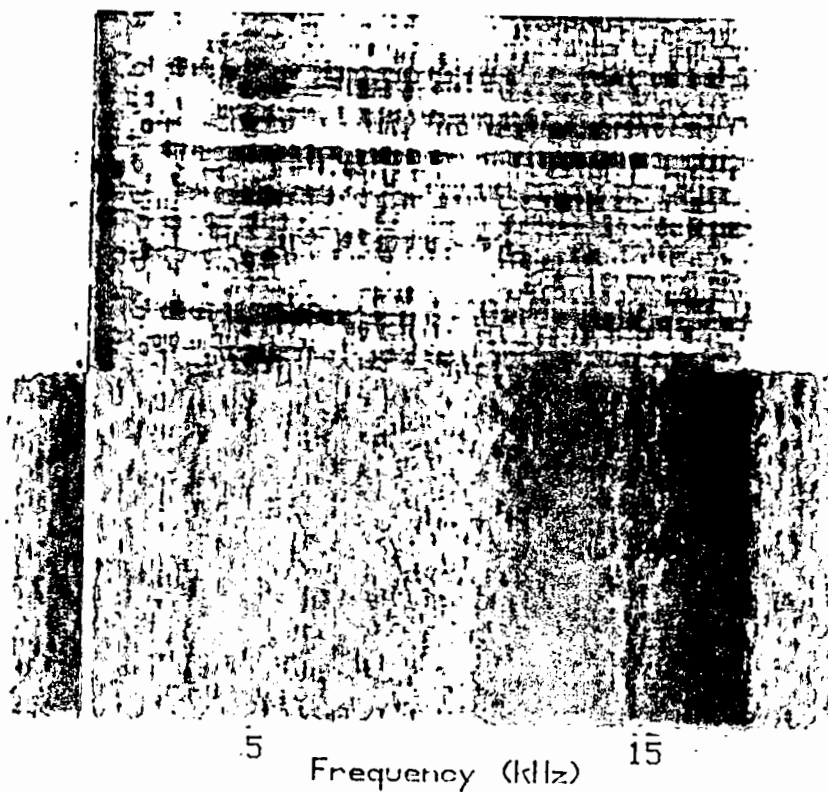


Figure 5.8 - continued

The results obtained by averaging each of these responses, and cross-correlating with the stored pinna magnitude responses to white noise, are shown in figure 5.9.

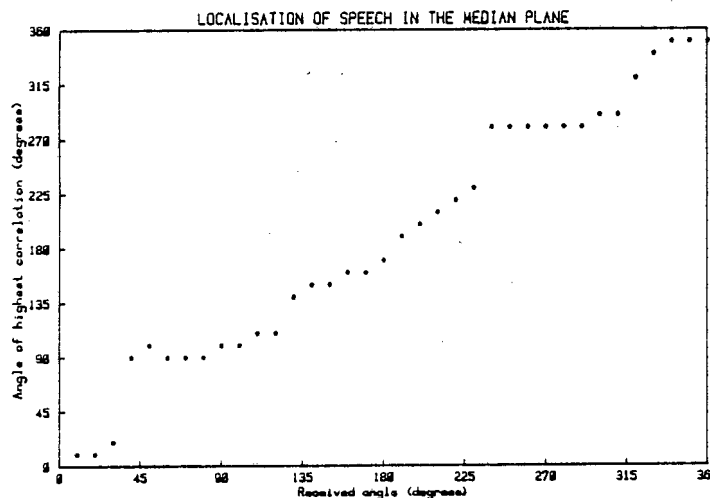


Figure 5.9 - The localisation of a passage of speech. The source was positioned in turn at each of 36 increments, evenly spaced over a 360 degree sector.

5.2.3 Discussion

A visual inspection of the photographic records reveals conspicuous directional features at frequencies above about 5kHz. This is in agreement with the finding that human subjects require spectral components above approximately 7kHz for successful monaural localisation.

It is noteworthy that the directional spectral patterns are only apparent when the complete ensemble of spectra representing a particular direction is viewed; the frequency response of the incident sound obstructs this if only a single spectrum is examined.

The narrow spectral lines evident in the oscillogram records are due to interference caused by multipath echoes. Owing to the length of the recording, it was not possible to gate

6.0 THE DESIGN AND CONSTRUCTION OF AN EXPERIMENTAL ACTIVE SONAR

An experimental active sonar system has been designed, constructed and evaluated in the underwater test facility at the Central Acoustics Laboratory of the University of Cape Town. The sonar uses beamforming by the cross-correlation analysis of received spectra. The main purpose of this experiment has been to verify the simulations of sonar beamforming described in section 4.3.

6.1 System design

The sonar comprises a receiver and a separate transmitter: each uses a PZT ceramic crystal resonant at around 500kHz. The transmitter was inserted into a tube of closed-cell foam: this reduces reverberation by narrowing the transmit beamwidth. An irregular reflecting structure was constructed by surrounding the receive transducer with an aluminium framework to which rolls of 3mm closed-cell foam had been asymmetrically attached. The construction is such that the boresight to the transducer is obstructed. The width of this reflector is 190mm. Therefore, the receiver is 125 wavelengths across at a frequency of 1MHz, the maximum frequency used.

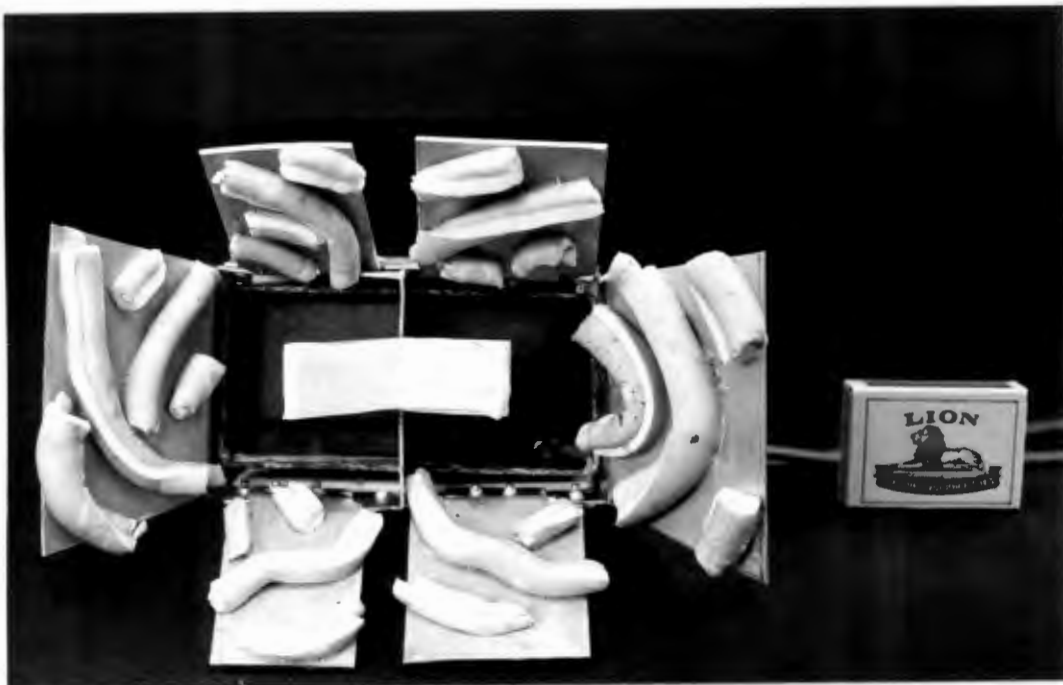


Figure 6.1 - The sonar receiver.

The receiver was suspended from a stepper motor, the drive of which was interfaced to the BCD bus of an HP-85 micro-computer. This allows receiver bearing relative to a fixed position target to be determined remotely. Target returns were captured using a Philips model PM3305 digital storage oscilloscope, sampling at a rate of 2MHz, and then downloaded into the controlling microcomputer for digital analysis.

A wide bandwidth is an essential requirement of this technique of beamforming. Since the PZT crystals used are resonant, having a Q of around 10, widebanding techniques were employed. The bandwidth of the transmit pulse was increased by loading both faces of the transmit crystal. The crystal was backed with lead-packed Ciba-Geigy UREOL 6409A polyurethane resin; while the front-face was loaded using green casting resin ($c=2300$ meters per second) as a quarter wavelength matching transformer (Kossoff, 1966). The receive transducer was also loaded. This was achieved using the matching circuitry at the front-end of the receiver amplifier. The receive crystal was air-backed, using a closed-cell high density polyurethane foam, while the front-face was insulated with a thin layer of Araldite epoxy. Although two crystals were mounted in the receiver, only one was used.

A low-noise wideband receive amplifier, having a gain of approximately 50dB was constructed. Figure 6.2 shows the combined frequency response of the transmitter, receive crystal and low-noise amplifier. A wide usable bandwidth has been achieved: the spectral fluctuations did not hamper the effectiveness of the sonar since the frequency response was equalised in software. The transmit signal used was an 80 volt, 0,6 microsecond pulse.

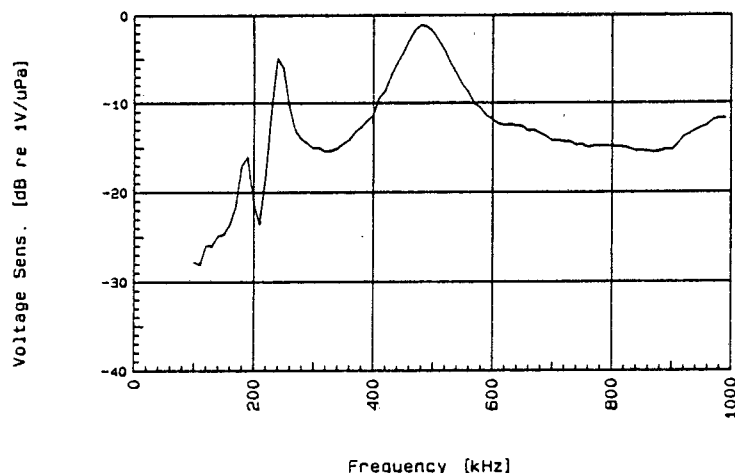


Figure 6.2 - The combined frequency response of the transmitter, receive transducer and receive amplifier.

Multipath interference was avoided by time gating the direct echo. This could be achieved since the time delay between the direct echo and the first reflection was greater than the echo duration of 0,16ms.

6.2 Experimental method

The sonar constructed can be used as a three-dimensional beamforming system. However, owing to the limited storage capacity of the flexible discs used, it was only evaluated over a 40 degree sector in the azimuth plane.

The target used was a ping-pong ball, suspended a distance of one metre from the receiver in the plane of intended operation.



Figure 6.3 - The sonar system in operation.

The receiver was calibrated by recording its output at single step intervals of 0,19 degrees along the sector of scan. The calibration was automated: received waveforms were captured using the digital storage oscilloscope, and then stored on microcomputer disc.

The receiver's Fresnel zone stretches to approximately 38 meters; consequently it was necessary to operate in the near-field. The spectrum modifications imposed on incident signals were therefore range dependent: targets to be localised were required to occupy the same range bin as that used when calibrating the receiver.

The spectra of the calibration signals were computed using a Fast Fourier Transform (FFT) algorithm. Unwanted spectral features due to the frequency responses of system components other than the irregular reflector were represented in the resulting magnitude responses. To remove these features, each individual calibration spectrum was divided by the mean of the calibration spectra.

The transmitter beamwidth was necessarily narrow. It was therefore not possible to simultaneously insonify more than a single target. Consequently, multiple-target situations were obtained by recording the receiver output to each target individually, and then summing the resulting spectra. This procedure is entirely equivalent to the simultaneous insonification of multiple targets. In all tests, the targets used were ping-pong balls.

6.3 Results

Figure 6.4 shows the localisation of a single target. A low level of noise due to reverberation was present: the signal-to-noise ratio was 20dB.

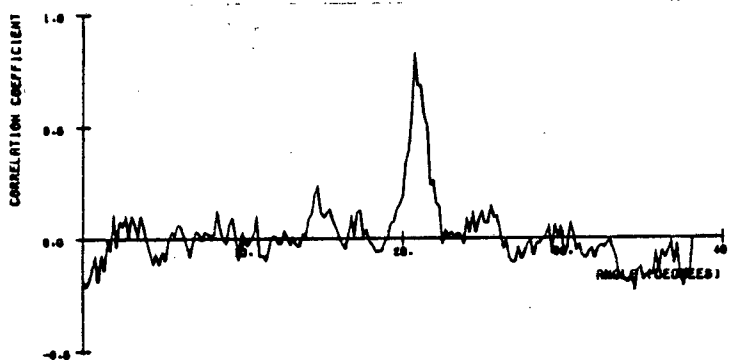


Figure 6.4 - The localisation of a single target at 20,9 degrees.

The localisation of multiple targets of equal strength is illustrated in figure 6.5. Figure 6.5(a) shows the localisation of two simultaneously received targets, while figure 6.5(b) shows the localisation of three simultaneously received targets. In each instance the signal-to-noise ratio was 20dB.

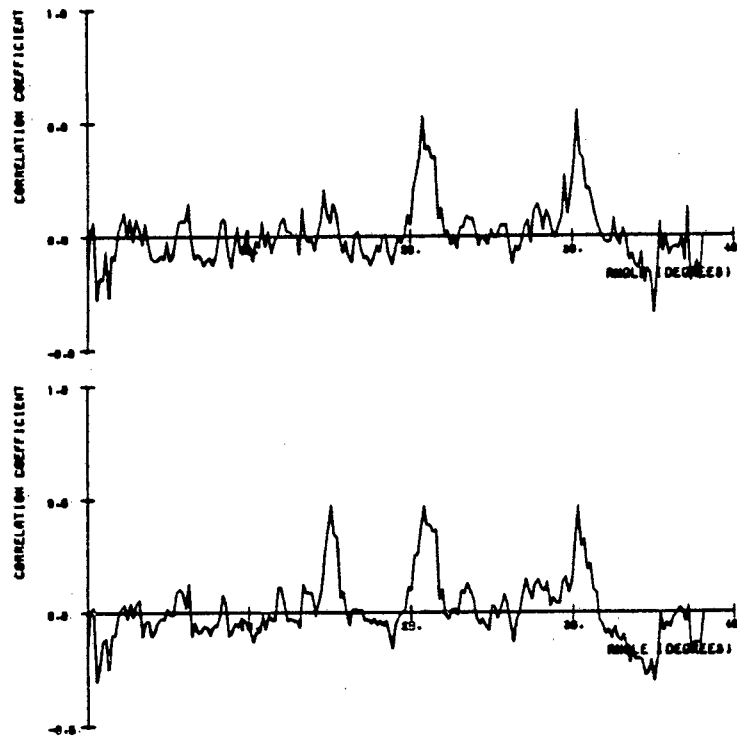


Figure 6.5 - The localisation of multiple targets.
 (a) Targets at 20,9 and 30,2 degrees.
 (b) Targets at 15, 20,9 and 30,2 degrees.

The localisation of two simultaneously received targets of unequal strength is shown in figure 6.6. A strong target at 30,2 degrees and a weak target at 20,9 degrees were present. The weak target strength was 10dB less than that of the strong target, and the weak-signal to noise ratio was 7dB. In figure 6.6(a) only the target at 30,2 degrees has been located. Therefore, the iterative technique developed in section 4.3 was used to remove the contribution of the strong target to the incident spectrum. Figure 6.6(b) shows the result - the target at 20,9 degrees is clearly evident.

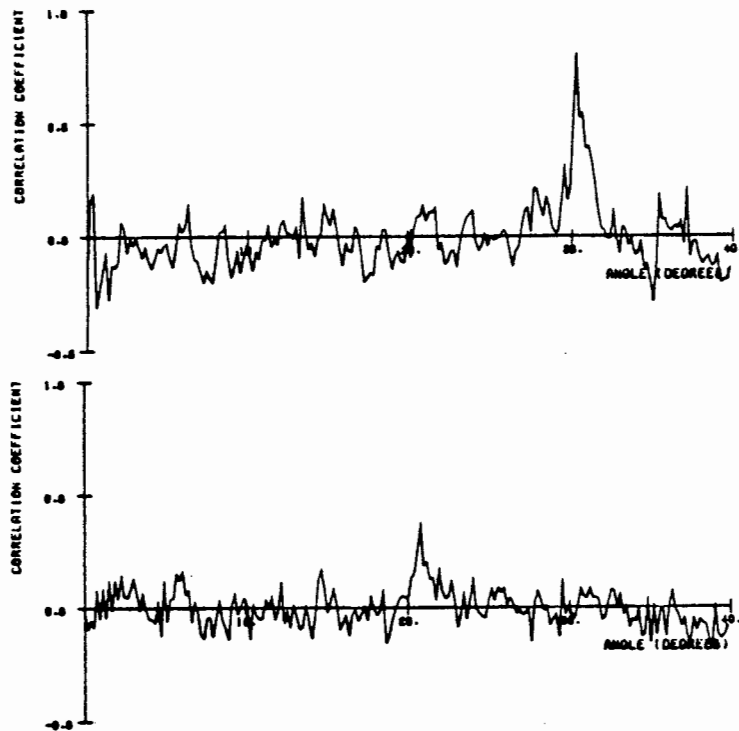


Figure 6.6 - Simultaneously received targets of unequal strength.

Figure 6.7 illustrates the use of the Fourier-t-transform to determine the bearing and range of a target simultaneously.

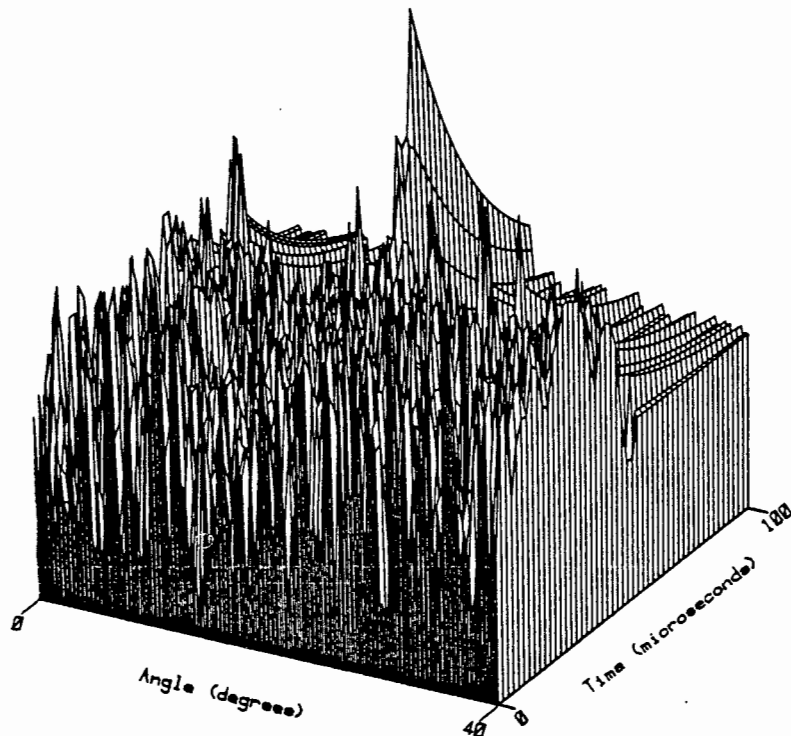


Figure 6.7 - The simultaneous bearing and range determination of a target at 20,9 degrees.

6.4 Discussion

Accurate target localisation was performed by the experimental sonar: the width between which the correlation-coefficient is $1/\sqrt{2}$ of its peak value is comparable to the 0,45 degree angular resolution which would be obtained from a similarly dimensioned conventional system. However, the remarkable feature is that this is achieved using only a single active receiving element. A corresponding three-dimensional phased transducer array requires at least 15625 active elements, as well as the accompanying beamforming and digital processing equipment - an extremely costly proposition.

The proposed sonar is superior to many other alternatives to the phased array in that it is capable of localising multiple simultaneously received target echoes. The localisation of a weak target which was initially masked by a substantially stronger target was also demonstrated.

Target localisation results obtained using the experimental sonar system correspond closely with those obtained in computer simulations. Therefore, the validity of the computer simulations described in section 4.3 is confirmed.

The enormous practical advantages of a sonar based upon the cross-correlation analysis of received spectra strongly suggest that the sonar techniques demonstrated in this section could fulfil many beamforming requirements at a fraction of the present cost.

7.0 CONCLUSION

High resolution sonar systems are both complex and costly. This has led to the development of a novel alternative to the conventional array, inspired by suspected mechanisms of animal sonar.

The groundwork involved a study of animal echolocation. The bats and cetaceans were found to possess highly evolved active sonar systems, while passive localisation in humans was also found to be well developed. It was learned that the angular localisation capability of animal sonar relies to a large degree upon the monaural cue: recognition of the direction dependent spectrum modifications which the reflecting facets of a pinna impose on incident sounds. Therefore, the objective became to develop a beamforming system which uses only a single active element surrounded by an irregular reflecting structure - the analog of a pinna.

A number of realisations of this scheme were evaluated in computer simulations. A technique based upon the cross-correlation analysis of received spectra was demonstrated to be capable of locating sources under diverse conditions. An experiment in which a mannikin human head was required to locate sounds confirmed that this technique closely emulates some of the monaural capabilities of human localisation. Proposed methods of overcoming the crucial difficulty of localising unknown spectra were successfully implemented for two classes of commonly occurring sounds.

An active sonar system based upon the cross-correlation analysis of received spectra was designed and constructed. Its angular resolution is similar to that of a conventional array of comparable dimensions; however, its detection performance was shown to be somewhat inferior. The significant advantage lies in the simplicity of construction and modest digital processing requirement.

Efforts to develop a sonar beamforming system based upon animal echolocation techniques have resulted in a working experimental system. Its operation differs in concept from that of conventional systems: multiple beams are achieved using a fixed single-element system by exploiting directional cues which exist in the frequency domain. Although the detection performance of a system based upon monaural localisation is inferior to that of a comparable conventional array, in some applications it could be more economic to construct a large passive reflecting structure than even a far smaller transducer array. This substantial practical advantage suggests that the proposed system could be a viable and inexpensive alternative to certain sonar applications.

8.0 REFERENCES

- Airapet'yants, E.S. and Konstantinov, A.I., Echolocation in Animals, Keter Press, Jerusalem, 1973.
- Allen, J.B., Cochlear Modelling, IEEE ASSP Magazine, 2, pp3 - 29, January 1985.
- Angell, J.A. and Fite, W., Further Observations on the Monaural Localisation of Sound, The Psychological Review, September 1901.
- Au, W.W.L., Echolocation Signals of the Atlantic Bottlenose Dolphin (*Tursiops truncatis*) in Open Waters, in Animal Sonar Systems, Busnel, R.G. and Fish, J.F. (eds.), Plenum Press, New York, 1980.
- Au, W.W.L. and Snyder, K.J., Long-Range Target Detection in Open Waters by an Echolocating Atlantic Bottlenose Dolphin (*Tursiops Truncatis*), J. Acoust. Soc. Am., 68, pp 1077-1084, 1980.
- Batteau, D.W., The Role of the Pinna in Human Localisation, Proceedings of the Royal Society of London, 168, pp 158-180, 1967.
- Blauert, J., Sound Localisation in the Median Plane, Acustica, 22, pp 205-213, 1969.
- Blauert, J., Spatial Hearing, MIT Press, Cambridge, Massachusetts, 1983.
- Bloom, P.J., Determination of Monaural Sensitivity Changes Due to the Pinna by use of Minimum-Audible-Field Measurements in the Lateral Plane, J. Acoust. Soc. Am., 61, pp 820-828, March 1977.
- Brown, P.E. and Grinell, A.D., Echolocation Ontogeny in Bats, in Animal Sonar Systems, Busnel, R.G. and Fish, J.F. (eds.), Plenum Press, New York, 1980.
- Burdic, W.S., Underwater Acoustic System Analysis, Prentice-Hall, New Jersey, 1984.
- Butler, R.A. and Belendink, K., Spectral Cues Utilised in the Localisation of Sound in the Medial Sagittal Plane, J. Acoust. Soc. Am., 61, pp 1264-1269, May 1977.
- Denbigh, P.N., Private Sonar Notes, University of Cape Town, 1987.
- Ebata, M., Sone, T. and Nimwa, T., On the Perception of the Direction of Echo, J. Acoust. Soc. Am., 44, pp 542-547, 1968.

Evans, W.E., Echolocation by Marine Delphinids and One Species of Fresh-Water Dolphin, J. Acoust. Soc. Am., 54, pp 181-189, 1973.

Fenton, M.B., Adaptiveness and Ecology of Echolocation in Terrestrial (aerial) Systems, in Animal Sonar Systems, Busnel, R.G. and Fish, J.F. (eds.), Plenum Press, New York, 1980.

Freedman, J., Resolution in Radar Systems, Proc. IRE, 39, pp 813-818, July 1951.

Gardner, M.B. and Gardner, R.S., Problem of Localisation in the Median Plane: Effect of Pinna Cavity Occlusion, J. Acoust. Soc. Am., 53, pp 400-408, 1973.

Gardner, M.B., Some Monaural and Binaural Facets of Median Plane Localisation, J. Acoust. Soc. Am., 54, pp 1489-1495, 1973.

Greiner, Y., Non-Stationary Signal Modelling with Application to Bat Echolocation Calls, Acustica, 61, pp 155-165, September 1986.

Griffen, D.R., The Navigation of Bats, Scientific American, pp 52-114, August 1950.

Griffen, D.R., Listening in the Dark, Yale University Press, New Haven, 1958.

Griffen, D.R., More about Bat "Radar", Scientific American, pp 40-44, July 1958.

Griffen, D.R., Echoes of Bats and Men, William Heinemann, Ltd., London, 1960.

Grinell, A.D., The Neurophysiology of Audition in Bats: Resistance to Interference, Journal of Physiology, 167, pp 114-127, 1963a.

Grinell, A.D., The Neurophysiology of Audition in Bats: Directional Localisation and Binaural Interaction. Journal of Physiology, 167, pp 97-113, 1963b.

Grinell, A.D., Neural Processing Mechanisms in Echolocating Bats Correlated with Differences in Emitted Sounds, J. Acoust. Soc. Am., 54, pp 147-156, 1973.

Grinell, A.D. and Grinell, V.S., Neural Correlates of Vertical Localisation in Echolocating Bats, Journal of Physiology, 181, pp 830-851, 1965.

Grinell, A.D. and Schnitzler, H.U., Directional Sensitivity of Echolocation in the Horseshoe Bat, Rhinolophus ferrumequinum, J. Comp. Phys., 116, pp 63-77, 1977.

Guelke, R.W. and Bunn, A.E., Resonance in the Travelling Wave Theory of Hearing, *Acustica*, 48, pp 260-263, 1981.

Haftner, E.R., Dye, R.H. and Gilkey, R.H., Lateralisation of Tonal Signals Which Have Neither Onsets Nor Offsets, *J. Acoust. Soc. Am.*, 65, pp 471-477, February 1979.

Hansz, W., Angular Location, Monopulse and Resolution, *Microwave Journal*, pp 60-65, February 1964.

Hebrank, J. and Wright, D., Are Two Ears Necessary for Localisation of Sound Sources on the Median Plane?, *J. Acoust. Soc. Am.*, 56, pp 935-938, September 1974.

Hebrank, J. and Wright, D., Spectral Cues used in the Localisation of Sound Sources in the Median Plane, *J. Acoust. Soc. Am.*, 56, pp 1829-1835, December 1974.

Hiranaka, Y. and Yamasaki, H., Envelope Representation of Pinna Impulse Responses Relating to Three-Dimensional Localisation of Sound Sources, *J. Acoust. Soc. Am.*, 73, pp 291-295, January 1983.

Keeping, E.S., Introduction to Statistical Inference, D. van Nostrand and Company Inc., New York, 1962.

Kellogg, W.N., Porpoises and Sonar, University of Chicago Press, Chicago, 1961.

Kossoff, G., The Effects of Backing and Matching on the Performance of Piezoelectric Ceramic Transducers, *IEE Trans. on Sonics and Ultrasonics*, 13, pp 20-30, March 1966.

Lawrence, B.D. and Simmons, J.A., Echolocation in Bats: The External Ear and Perception of the Vertical Positions of Targets, *Science*, 218, pp 481-483, 1982.

Livshits, M.S., Correlation Model of the Recognition of Objects by Echolocating Animals, *Biofizika*, 20, pp 920-927, 1975.

Ludloff, A., Radar and Radar Signal Processing, Lecture Notes, Graduate Course, Department of Electrical Engineering, University of Cape Town, 1982.

Mehrgardt, S., and Mellert, V., Transformation Characteristics of the External Human Ear, *J. Acoust. Soc. Am.*, 61, pp 1567-1576, June 1977.

Miller, I. and Freund, J.E., Probability and Statistics for Engineers, Prentice-Hall Inc., New Jersey, 1965.

Murchison, A.E., Detection Range and Range Resolution of Echolocating Bottlenose Porpoise, in *Animal Sonar Systems*, Busnel, R.G., Fish, J.F., (eds.), Plenum Press, New York, 1980.

Nachtigall, P.E., Odontocete Echolocation Performance on Object Size, Shape and Material, in Animal Sonar Systems, Busnel, R.G., Fish, J.F., (eds.), Plenum Press, New York, 1980.

Musicant, A.D. and Bulter, R.A., Influence of Monaural Spectral Cues on Binaural Localisation, J. Acoust. Soc. Am., 77, pp 202-208, January 1985.

Nachtigall, P.E., Murchison, A.E. and Au, W.W.L., Cylinder and Cube Shape Discrimination by an Echolocating Blindfolded Bottlenosed Dolphin, in Animal Sonar Systems, Busnel, R.G. and Fish, J.F. (eds.), Plenum Press, New York, 1980.

Neuweiler, G., How Bats Detect Flying Insects, Physics Today, pp 34-40, 1980a.

Neuweiler, G., Auditory Processing of Echoes: Peripheral Processing, in Animal Sonar Systems, Busnel, R.G. and Fish, J.F. (eds.), Plenum Press, New York, 1980b.

Neuweiler, G., Bruns, V. and Schuller, G., Ears Adapted for the Detection of Motion, and How Echolocating Bats have Exploited the Capacities of the Mammalian Auditory System, J. Acoust. Soc. Am., 68, pp 741-753, 1980.

Novick, A., Echolocation in Bats: A Zoologists View, J. Acoust. Soc. Am., 54, pp 139-146, 1973.

Oppenheim, A.V., Applications of Digital Signal Processing, Prentice-Hall, New Jersey, 1978.

Oppenheim, A.V. and Lim, J.S., The Importance of Phase in Signals, Proc. IEEE, 69, pp 529-541, May 1981.

Penner, R.H. and Kadane, J., Biosonar Detection in Noise, in Animal Sonar Systems, Busnel, R.G. and Fish, J.F. (eds.), Plenum Press, New York, 1980.

Peff, T.C. and Simmons, J.A., Horizontal Angle Resolution in Echolocating Bats, J. Acoust. Soc. Am., 51, pp 2063-2065, 1972.

Pollack, G.D., Organisation and Encoding Features of Single Neurons in the Inferior Colliculus of Bats, in Animal Sonar Systems, Busnel, R.G. and Fish, J.F., (eds.), Plenum Press, New York, 1980.

Popper, A.N., in Cetacean Behavior: Mechanisms and Functions, ed. Henson, L.M., John Wiley and Sons, New York, 1981.

Pye, J.D., Echolocation Signals and Echoes in Air, in Animal Sonar Systems, Busnel, R.G. and Fish, J.F.. (eds.). Plenum Press, New York, 1980.

Pye, J.D., Sonar Signals and System Performance, *Acustica*, 61, pp 166-175, September 1986.

Rayleigh, Lord J.W., Investigations in Optics with Special Reference to the Spectroscope, *Collected Scientific Papers*, 1, pp 261-274, 1879.

Rodgers, C.A.P., Pinna Transformations and Sound Reproduction, *J. Audio Eng. Soc.*, 29, pp 226-234, April 1981.

Runciman, P., A Three Dimensional Imaging Sonar, Masters Dissertation, Electrical Engineering Department, University of Cape Town, 1986.

Sales, G. and Pye, D., *Ultrasonic Communication by Animals*, Chapman and Hall, London, 1974.

Sayers, B.M. and Cherry E.C., Mechanism of Binaural Fusion in the Hearing of Speech, *J. Acoust. Soc. Am.*, 29, pp 973-987, September 1957.

Shaw, E.A.G., Transformation of Sound Pressure Level from the Free Field to the Ear Drum in the Horizontal Plane, *J. Acoust. Soc. Am.*, 56, pp 1848-1861, December 1974.

Shaw, E.A.G., External Ear Response and Sound Localisation, in *Localisation of Sound: Theory and Applications*, R.W. Gatehouse (ed.), Amphora Press, Connecticut, 1979.

Shimozawa, T., Suga, N., Hender, P. and Schuetze, S., Directional Sensitivity of Echolocation System in Bats Producing Frequency-Modulated Signals, *Journal of Experimental Biology*, 60, pp 53-69, 1974.

Schnitzler, H.U. and Henson, O.W., Performance of Airborne Animal Sonar Systems. 1: Microchiroptera, in *Animal Sonar Systems*, Busnel, R.G. and Fish, J.F. (eds.), Plenum Press, New York, 1980.

Schroeder, M.R., Models of Hearing, *Proceedings of the IEEE*, 63, pp 1332-1350, 1975.

Schwartz, M., *Information, Transmission, Modulation and Noise*, McGraw-Hill, USA, 1970.

Simmons, J.A., The Sonar Sight of Bats, *Psychology Today*, pp 50-57, November 1968.

Simmons, J.A., The Resolution of Target Range by Echolocating Bats, *J. Acoust. Soc. Am.*, 54, pp 157-172, 1973.

Simmons, J.A., Response of the Doppler Echolocation System in the Bat, *Rhinolophus ferrumequinum*, *J. Acoust. Soc. Am.*, 56, pp 672-682, 1974.

Simmons, J.A., The Processing of Sonar Echoes by Bats, in Animal Sonar Systems, Busnel, R.G. and Fish, J.F. (eds.), Plenum Press, New York, 1980.

Simmons, J.A., Howell, D.J. and Suga, N., Information Content of Bat Sonar Echoes, American Scientist, 63, pp 204-215, 1975.

Simmons, J.A., Kick, S.A., Lawrence, B.D., Hale, C., Bard, C. and Escudie, B., Acuity of Horizontal Angle Discrimination by the Echolocating Bat, Eptesicus fuscus, J. Comp. Physiol., 153, pp 321-330, 1983.

Simmons, J.A., Lavender, W.A. and Lavender, B.A., Target Structure and Echo Spectral Discrimination by Echolocating Bats, Science, 186, pp 1130-1132, 1974.

Skolnik, M.I., Introduction to Radar Systems, McGraw-Hill, Tokyo, 1982.

Sokolnikoff, I.S. and Redheffer, R.M., Mathematics of Physics and Modern Engineering, McGraw-Hill Inc., Tokyo, 1966.

Steinberg, D.I., Computational Matrix Algebra, McGraw-Hill Inc., New York, 1974.

Stevens, S.A. and Waskofsky, F. Sound and Hearing, Time Life International, Amsterdam, 1966.

Suga, N., Analysis of Frequency-Modulated Sounds by Auditory Neurones of Echolocating Bats, Journal of Physiology, 179, pp 26-53, 1965.

Suga, N. and O'Neill, W.E., Mechanisms of Echolocation in Bats - Comments on the Neuroethnology of the Biosonar System of "CF-FM" Bats, TINS, August, 1978.

Suga, N. and Schlegel, P., Coding and Processing in the Auditory Systems of FM-Signal Producing Bats, J. Acoust. Soc. Am., 54, pp 174-190, 1973.

Terhardt, E., Fourier Transformation of Time Signals: A Conceptual Revision, Acustica, 57, pp 242-256, 1985.

Urick, Principles of Underwater Sound, McGraw-Hill, USA, 1983.

Watkins, A.J., Psychoanalytical Aspects of Synthesized Vertical Cues, J. Acoust. Soc. Am., 63, pp 1152-1165, April 1978.

Watkins, W.A., Click Sounds from Animals at Sea, in Animal Sonar Systems, Busnel, R.G. and Fish, J.F. (eds.), Plenum Press, New York, 1980.

Wood, F.G. and Evans, W.E., Adaptiveness and Ecology of Echolocation in Toothed Whales, in Animal Sonar Systems, Busnel, R.G. and Fish, J.F. (eds.), Plenum Press, New York, 1980.

Wright, D., Hebrank, J.H. and Wilson, B., Pinna Reflections as Cues for Localisation, J. Acoust. Soc. Am., 56, pp 957-962, September 1974.

Zwicker, E., and Terhardt, E., Analytical Expression for Critical-Band Rate and Critical Bandwidth as a Function of Frequency, J. Acoust. Soc. Am., 68, pp 1523-1525, November 1980.

APPENDIX A
COMPUTER PROGRAMS USED IN BEAMFORMING SIMULATIONS

A.1: Beamforming by the solution of simultaneous equations

- | | | |
|-------|---|-----|
| A.1.1 | PROGRAM BATPLOT3S - simulates a receiver surrounded by an irregular reflector, and predetermines spectrum modifications imposed by the reflector. | A-2 |
| A.1.2 | PROGRAM TARGET3S - simulates target echoes, and locates targets by solving a set of linear equations. | A-4 |
| A.1.3 | PROGRAM MATCONDITION - determines the condition numbers of a coefficient matrix. | A-9 |

A.2: Beamforming by the deconvolution processing of received sounds

- | | | |
|-------|---|------|
| A.2.1 | PROGRAM IMPRESP2 - plots six impulse responses of a simulated receiver. | A-11 |
| A.2.2 | PROGRAM PINNIMP2 - calculates the spectral amplitude and phase modifications required to approximate the inverse filter of the impulse responses of a simulated receiver. | A-15 |
| A.2.3 | PROGRAM DETECT2 - locates a source by passing a receiver output through each of six inverse filters. | A-22 |

A.3: Beamforming by the cross-correlation analysis of received spectra

- | | | |
|-------|---|------|
| A.3.1 | PROGRAM FREQ2 - simulates a receiver surrounded by an irregular reflector, and predetermines spectrum modifications imposed by the reflector. | A-31 |
| A.3.2 | PROGRAM CORLATE2B - simulates target echoes and ambient noise, and cross-correlates the received spectrum with each stored spectrum. Strong target echoes are subtracted out from the incident signal to locate weaker targets. | A-34 |

A.4: Simultaneous angle and range determination

- | | | |
|-------|---|------|
| A.4.1 | PROGRAM CALIBRATE - simulates a receiver surrounded by an irregular reflector, and predetermines spectrum modifications imposed by the reflector. | A-39 |
| A.4.2 | PROGRAM FINDRANGE - simultaneously determines the bearing and range of a target. | A-41 |

HO*PAT1-83(1).BATPLOT3S

```

1      C      *****PROGRAM BATPLOT3S*****
2      C      *
3      C      * THIS PROGRAM CALCULATES THE OUTPUT VALUES OF A 2-DIM ARRAY
4      C      * FOR 31 DIFFERENT FREQUENCY BANDS, EACH OF CONSTANT FRACT-
5      C      * IONAL BANDWIDTH OVER THE RANGE 25 TO 100 KHZ.
6      C      *
7      C      * OUTPUT VALUES ARE CALCULATED IN 3 DEGREE INCREMENTS OVER
8      C      * THE RANGE 0 TO 90 DEGREES.
9      C      *
10     C      * THE ARRAY CONTAINS 200 POINTS.THE CO-ORDINATES OF EACH
11     C      * ARE RANDOMLY ASSIGNED.
12     C      *
13     C      * A TIME DELAY OF BETWEEN 0 AND 29 MICROSECONDS (CORRESPONDING
14     C      * TO A DISTANCE OF 10 CM) IS ASSIGNED TO EACH ARRAY POINT.
15     C      *
16     C      * THE FREQUENCY OUTPUTS ARE STORED IN "MATRIX."
17     C      * THE DISTANCES BETWEEN ARRAY ELEMENTS ARE STORED
18     C      * IN "ARRAY."
19     C      *
20     C      *****
21
22     C      --- ALL PROGRAM VARIABLES ARE INITIALISED.
23
24     REAL ARRAY(200,2) , MATRIX(31) , CFREQ(31) , PI ,
25     + HFREQ , LFREQ , VALA , VALB , ANG , ANGL ,
26     + Q , XAX , YAX , KAY , SUM , TIME(200)
27
28     INTEGER LOOP1 , LOOP2 , LOOP3 , ISEED , I
29
30     C      --- THE RANDOM GENERATOR SEED IS ASSIGNED.
31
32     ISEED = 1
33
34     C      --- THE VALUE OF PI IS INITIALISED.
35
36     PI=3.141592654
37
38     C      --- THERE ARE 31 "CONSTANT-Q" FILTERS, EACH OF Q = 23
39
40     Q = 23.
41
42     C      --- THE ARRAY CO-ORDINATES ARE RANDOMLY ASSIGNED.
43     C      --- THE MAXIMUM CO-ORDINATE SIZE IS 0.018 METRES.
44
45     DO 10 LOOP1 = 1,200
46
47         DO 20 LOOP2 = 1,2
48             ARRAY(LOOP1,LOOP2) = URAND(ISEED) * .018
49             CONTINUE
50         CONTINUE
51
52     C      --- A TIME DELAY EQUIVALENT TO 10 CM IS ASSIGNED TO EACH POINT---
53     C      --- THE RANDOM NUMBER GENERATOR SEED IS ASSIGNED.
54
55     ISEED = 2
56
57     DO 15 LOOP1 = 1,200
58         TIME(LOOP1) = URAND(ISEED) * 0.166667
59     CONTINUE
60
61

```

```

62 C      --- EACH ANGLE IS TREATED IN DO LOOP 30      ---
63
64      DO 30 LOOP1 = 1,31
65      ANG = ( (FLOAT(LOOP1)-1.) * 3.) * PI/180.
66
67 C      --- EACH FREQUENCY IS TREATED IN DO LOOP 30      ---
68
69      LFREQ = 25000.
70
71      DO 40 LOOP2 = 1,31
72
73      HFREQ = LFREQ * ( (2.*Q+1.) / (2.*Q-1.) )
74      CFREQ(LOOP2) = (HFREQ + LFREQ) / 2.
75      LFREQ = HFREQ
76      KAY = 2. * PI * CFREQ(LOOP2) / 344.
77      XAX = 0.
78      YAX = 0.
79
80 C      --- EACH ARRAY ELEMENT IS TREATED IN DO LOOP 50      ---
81
82      DO 50 LOOP3 = 1,200
83
84      VALA = SQRT (ARRAY(LOOP3,1)**2. + ARRAY(LOOP3,2)**2.)
85
86      IF (ARRAY(LOOP3,1).EQ.0.) THEN
87      VALB = PI / 2.
88      GO TO 250
89      END IF
90
91      VALB = ANG + ATAN(ARRAY(LOOP3,2) / ARRAY(LOOP3,1))
92 250      ANGL = KAY * ( VALA * SIN(VALB) + TIME(LOOP3) )
93      XAX = XAX + COS(ANGL)
94      YAX = YAX + SIN(ANGL)
95 50      CONTINUE
96
97      SUM = SQRT (XAX**2. + YAX**2.)
98      MATRIX(LOOP2) = SUM
99 40      CONTINUE
100
101 C      --- THE OUTPUTS FOR EACH FREQUENCY AT EACH ANGLE ARE      ---
102 C      --- WRITTEN INTO DATA FILE "BATPLOT3S" VIA THE      ---
103 C      --- @USE 17,BATPLOT3S COMMAND.      ---
104
105      WRITE (17) (MATRIX(I) , I = 1,31)
106
107 C      --- THE FREQUENCY OUTPUTS ARE PRINTED.      ---
108
109      ANG = ANG * 180./PI
110
111      WRITE (*,201) ANG
112 201      FORMAT(/1X,'THE FREQUENCY OUTPUTS FROM 25KHZ TO 100KHZ'
113 +      ' FOR AN INCOMING PULSE AT ',F4.1,' DEGREES ARE :')
114
115      WRITE (*,300) (MATRIX(I) , I = 1,31)
116 300      FORMAT (1X , 10F12.4)
117 30      CONTINUE
118      STOP
119      INCLUDE UCT*ASCII.URAND
120      END

```

RT,S PAT1-83.TARGET3S

)*PAT1-83(1).TARGET3S

```

1      C      *****PROGRAM TARGET3S*****
2      C      *
3      C      * THIS PROGRAM READS THE ARRAY OUTPUT VALUES STORED IN FILE
4      C      * "BATPLOT3S." THESE VALUES ARE THEN USED AS THE COEFFICIENTS
5      C      * FOR A SERIES OF LINEAR EQUATIONS DESIGNED TO OBTAIN THE
6      C      * DIRECTIONS OF APPROACH OF A NUMBER OF TARGET ECHOES.
7      C      *
8      C      * THE TARGETS CAN BE POSITIONED AT ANY ANGLE BETWEEN
9      C      * 0 AND 90 DEGREES.
10     C      *
11     C      * THESE SIMULTANEOUS EQUATIONS ARE SOLVED BY A GAUSS-JORDAN
12     C      * REDUCTION TECHNIQUE CONTAINED IN THE UNIVAC MATH. PACK
13     C      * LIBRARY OF ROUTINES.
14     C      *
15     C      * THE SOLUTION VECTOR CONTAINS THE DIRECTIONAL INTENSITY OF
16     C      * THE INCOMING WAVEFRONT WHICH IS THEN PLOTTED.
17     C      *
18     C      *****
19
20     CHARACTER*60 MESSAG
21
22     REAL ARRAY(200,2) , MATRIX(31,32) , HORAX(31) , SUM(31) ,
23     + DIRECT(200) , POWER(20) , V(2) , CFREQ(31) , DIR ,
24     + HFREQ , LFREQ , VALA , VALB , ANG , ANGL , PI , XAX , YAX ,
25     + KAY , SUMM , POW , Q , XINC , XPAGE , XNUM , XP ,
26     + YPAGE , YNUM , YP , TIME(200)
27
28     INTEGER LOOP1 , LOOP2 , LOOP3 , NUM , ISEED , I , JC(31) , J
29
30     C      --- THE RANDOM GENERATOR SEED IS ASSIGNED.      ---
31
32     ISEED = 1
33
34     C      --- THE VALUE OF PI IS INITIALISED.      ---
35
36     PI=3.141592654
37
38     C      --- THERE ARE 31 "CONSTANT-Q" FILTERS, EACH OF Q = 23      ---
39
40     Q = 23.
41
42     C      --- THE ARRAY CO-ORDINATES ARE RANDOMLY ASSIGNED.      ---
43     C      --- THE MAXIMUM CO-ORDINATE SIZE IS 0.018 METRES.      --
44
45     DO 10 LOOP1 = 1,200
46
47         DO 20 LOOP2 = 1,2
48             ARRAY(LOOP1,LOOP2) = URAND(ISEED) * .018
49         20 CONTINUE
50     10 CONTINUE
51
52     C      --- A TIME DELAY EQUIVALENT TO 10CM IS ASSIGNED TO EACH POINT ---
53     C      --- THE RANDOM NUMBER GENERATOR SEED IS ASSIGNED.      ---
54
55     ISEED = 2
56
57     DO 15 LOOP1 = 1 , 20
58         TIME(LOOP1) = URAND(ISEED) * 0.166667
59     15 CONTINUE
60
61     C      --- THE NUMBER OF TARGETS IS GIVEN BY "NUM."      ---

```


NUM = 2

```

62
63
64
65 C    --- THE ARRAY OUTPUT VALUES ARE READ FROM FILE "BATPLOT3S"    ---
66 C    --- INTO ARRAY "MATRIX."    ---
67
68      DO 30 LOOP1 = 1,31
69      READ(17) SUM
70
71          DO 40 LOOP2 = 1,31
72          MATRIX(LOOP2,LOOP1) = SUM(LOOP2)
73      40      CONTINUE
74
75      30      CONTINUE
76
77 C    --- ARRAY "SUM" IS INITIALISED TO ZERO. ARRAY "SUM" NOW    ---
78 C    --- ACCUMULATES THE SUMS OF THE INCOMING TARGET ECHOES AT    ---
79 C    --- EACH OF 31 FREQUENCIES USED.    ---
80
81      DO 50 LOOP1 = 1,31
82      50      SUM(LOOP1) = 0.
83
84 C    --- THE INCOMING ECHO DIRECTION IS GIVEN BY "DIR" WHILST THE    ---
85 C    --- RELATIVE STRENGTH OF THE INCOMING ECHO IS DENOTED "POW."    ---
86
87 C    --- THE PINNA OUTPUT FOR EACH TARGET ECHO IS CALCULATED.    ---
88 C    --- THE SUM OF THESE OUTPUTS IS STORED IN ARRAY "SUM."    ---
89
90      DO 60 LOOP1 = 1 , NUM
91      READ (*,101) DIR , POW
92      101      FORMAT ( )
93
94      DIRECT(LOOP1) = DIR
95      POWER(LOOP1) = POW
96
97      ANG = DIR * PI/180.
98
99 C    --- EACH FREQUENCY IS TREATED IN DO LOOP 30    ---
100
101      LFREQ = 25000.
102
103      DO 70 LOOP2 = 1,31
104
105          HFREQ = LFREQ * ( (2.*Q+1.) / (2.*Q-1.) )
106          CFREQ(LOOP2) = (HFREQ + LFREQ) / 2.
107          LFREQ = HFREQ
108          KAY = 2. * PI * CFREQ(LOOP2) / 344.
109          XAX = 0.
110          YAX = 0.
111
112 C    --- EACH ARRAY ELEMENT IS TREATED IN DO LOOP 50    ---
113
114      DO 80 LOOP3 = 1,200
115
116          VALA = SQRT (ARRAY(LOOP3,1)**2. + ARRAY(LOOP3,2)**2.)
117
118          IF (ARRAY(LOOP3,1).EQ.0.) THEN
119              VALB = PI / 2.
120              GO TO 250
121          END IF
122
123          VALB = ANG + ATAN(ARRAY(LOOP3,2) / ARRAY(LOOP3,1))

```

```

24      250      ANGL = KAY * ( VALA * SIN(VALB) + TIME(LOOP3) )
25      XAX = XAX + COS(ANGL)
26      YAX = YAX + SIN(ANGL)
27      80      CONTINUE
28
29      SUMM = SQRT (XAX**2. + YAX**2.)
30      SUM(LOOP2) = SUM(LOOP2) + SUMM * POW
31      70      CONTINUE
32      60      CONTINUE
33
34
35
36      C      --- THE CONTENTS OF ARRAY "SUM" ARE READ INTO THE 32ND
37      C      --- COLUMN OF MATRIX "MATRIX." THE SYSTEM OF EQUATIONS IS
38      C      --- THEN SOLVED.
39
40      DO 90 LOOP1 = 1,31
41      90      MATRIX(LOOP1,32) = SUM(LOOP1)
42
43      V(1) = 4.
44      CALL GJR(MATRIX,32,31,31,32,$880,JC,V)
45
46      C      --- THE ABSCISSAE CO-ORDINATES ARE STORED IN ARRAY "HORAX."
47
48      DO 100 LOOP1 = 1,31
49      100      HORAX(LOOP1) = (LOOP1-1) * 3.
50
51      WRITE (*,102)
52      102      FORMAT (///1X,'RECEIVED ECHO INTENSITY FROM EACH DIRECTION IS: '//
53
54      WRITE (*,103) ( MATRIX(J,32) , IFIX(HORAX(J)) , J = 1,31 )
55      103      FORMAT ( /1X , 10 (F5.2 , I3 , 3X ))
56
57
58
59      C      *** PLOTS TO FIT ON A4 SIZE SHEET ***
60      C      *** X-AXIS TO BE 25 CMS LONG ***
61      C      *** Y-AXIS TO BE 16 CMS LONG ***
62
63      C      --- OPEN PLOTTING FILE ---
64      CALL PLOTS(0, 0, 0)
65
66      C      --- SET PAGE SIZE (ONLY NECESSARY FOR GDP) ---
67      CALL PAGESIZ(32.0, 22.0)
68
69      C      ---CHANGE TO INK PENS---
70      MESSAG='PLS LOAD P1-BK/I P2-RD/I'
71      CALL OPMES(24,MESSAG)
72
73      CALL NEWPEN(1)
74
75      C      --- DRAW A-4 SIZE PAGE ---
76      CALL PLOT(1.0, 1.0, -3)
77      CALL PLOT(0.0, 20.9, 2)
78      CALL PLOT(29.7, 20.9, 2)
79      CALL PLOT(29.7, 0.0, 2)
80      CALL PLOT(0.0, 0.0, 2)
81
82      C      --- ESTABLISH NEW ORIGIN ---
83      CALL PLOT(4.5, 4.5, -3)
84
85      C      --- DRAW THE AXES ---

```

```

186      CALL PLOT(23.0, 0.0, 2)
187      CALL PLOT(0.0, 0.0, 3)
188      CALL PLOT(0.0, 12.0, 2)
189
190      C      ---THE GRAPH IS TITLED---
191      MESSAG='DIRECTIONS OF TARGET ECHOES'
192      CALL SYMBOL(2.3,13.2,.5,MESSAG,0.,39)
193
194
195      C      --- MARK OFF THE AXES ---
196      C      --- X-AXIS HAS 9 DIVISIONS OF 10 DEGREES EACH ---
197      XINC=23./9.
198      XPAGE = 0.0
199      DO 110 I = 1,9
200          XPAGE = XPAGE + XINC
201          CALL SYMBOL(XPAGE, 0.0, 0.5, 13, 0.0, -1)
202          XNUM = FLOAT(I) * 10.0
203          XP = XPAGE - 0.5
204          CALL NUMBER(XP, -0.6, 0.2, XNUM, 0.0, 1)
205      110  CONTINUE
206
207      C      ---THE 'X' AXIS IS LABELLED---
208      MESSAG='ANGLE (DEGREES)'
209      CALL SYMBOL(18.6,-1.5,.3,MESSAG,0.,15)
210
211      C      --- Y-AXIS HAS 5 DIVISIONS OF 0.2, FROM 0 TO 1.
212      YPAGE = -2.4
213      DO 120 I = 1, 6
214          YPAGE = YPAGE + 2.4
215          YNUM = FLOAT(-1 + I) * 0.2
216          CALL SYMBOL(0.0, YPAGE, 0.5, 13, 90.0, -1)
217          YP = YPAGE - 0.16
218          CALL NUMBER(-1.4, YP, 0.2, YNUM, 0.0, 2)
219      120  CONTINUE
220
221      C      ---THE 'Y' AXIS IS LABELLED---
222      MESSAG='INTENSITY'
223      CALL SYMBOL (-2.3,8.6,.3,MESSAG,90.,23)
224
225      DO 140 I=1,NUM
226          DIR = DIRECT(I) * 23./90.
227          POW = POWER(I)*12.
228          CALL SYMBOL (DIR,POW,.2,4,0.,-1)
229      140  CONTINUE
230
231      CALL NEWPEN(2)
232
233      C      --- PLOT THE GRAPHS ---
234      CALL PLOT(0.0, 0.0, 3)
235      DO 130 I = 1, 31
236          XPAGE = (HORAX(I) * 23.0) / 90.0
237          YPAGE = MATRIX(I,32) * 12.
238          CALL PLOT(XPAGE, YPAGE, 2)
239      130  CONTINUE
240
241      MESSAG='TARGET3S'
242      CALL PAGNAM(MESSAG)
243
244      C      --- CLOSE OFF PLOT ---
245      CALL PLOT(0.0,0.0,999)
246
247      GO TO 900

```

```
248
249      880  WRITE (*,104) JC(1),V(1)
250      104  FORMAT (1X,'ERROR RETURN CONDITION ',I3,F8.2)
251
252      900  STOP
253          INCLUDE UCT*ASCII.URAND
254          END
```

T,S PAT2-82.MATCONDITION

O*PAT2-82(1).MATCONDITION

```

1      C      *****PROGRAM MATCONDITION*****
2      C      *
3      C      * THIS PROGRAM CALCULATES CONDITION NUMBERS FOR AN ARRAY. *
4      C      * THE DETERMINANT OF "BATPLOT4D" IS ALSO CALCULATED. *
5      C      *
6      C      * "RCON" IS THE CONDITION NUMBER OBTAINED BY TAKING THE *
7      C      * ROW SUM NORM. *
8      C      *
9      C      * "CCON" IS THE CONDITION NUMBER OBTAINED BY TAKING THE *
10     C      * COLUMN SUM NORM. *
11     C      *
12     C      *****
13
14     DIMENSION A(31,31),B(31),JC(31),V(2)
15     Z=31.
16
17     C      --- THE ARRAY OUTPUTS ARE READ FROM FILE "BATPLOT4D" ---
18     C      --- INTO ARRAY "A." ---
19
20         DO 10 I=1,31
21         READ (17) B
22
23             DO 20 J=1,31
24             A(J,I)=B(J)
25     20      CONTINUE
26
27     10      CONTINUE
28
29     C      --- THE ROW SUM NORM AND THE COLUMN SUM NORM OF ARRAY ---
30     C      --- "A" ARE CALCULATED. ---
31
32     ROSUM=0.
33     COSUM=0.
34
35         DO 30 I=1,31
36         RSUM=0.
37         CSUM=0.
38
39             DO 40 J=1,31
40             RSUM=RSUM+A(J,I)
41             CSUM=CSUM+A(I,J)
42     40      CONTINUE
43
44             IF(RSUM.GE.ROSUM)ROSUM=RSUM
45             IF(CSUM.GE.COSUM)COSUM=CSUM
46     30      CONTINUE
47
48     C      --- THE INVERSE OF "A" IS CALCULATED VIA A GAUSS- ---
49     C      --- JORDAN REDUCTION TECHNIQUE CONTAINED IN THE MATH- ---
50     C      --- PACK LIBRARY OF ROUTINES. ---
51
52     V(1)=3.
53     CALL GJR(A,31,31,31,31,$880,JC,V)
54
55     C      --- THE ROW AND COLUMN SUM NORMS ARE NOW CALCULATED. ---
56
57     VROSUM=0.
58     VCOSUM=0.
59
60         DO 50 I=1,31
61         VRSUM=0.

```

```

62          VCSUM=0.
63
64          DO 60 J=1,31
65              VRSUM=VRSUM+A(J,I)
66              VCSUM=VCSUM+A(I,J)
67          60      CONTINUE
68
69              IF(VRSUM.GE.VROSUM)VROSUM=VRSUM
70              IF(VCSUM.GE.VCOSUM)VCOSUM=VCSUM
71          50      CONTINUE
72
73      C      ---THE CONDITION NUMBERS ARE CALCULATED.      ---
74
75          RCON=ROSUM*VROSUM
76          ZRCON=ZCON/Z
77          Z2RCON=ZRCON/Z
78
79          CCON=CONSUM*VCOSUM
80          ZCCON=CCON/Z
81          Z4DCON=ZCCON/Z
82
83      C      --- THE MATRIX DETERMINANT IS CALCULATED      ---
84
85          DTERM = V(1) * EXP(V(2))
86
87          WRITE(*,99) DTERM
88          99      FORMAT('1THE DETERMINANT OF "BATPLOT4D" IS: '/1X,E10.2)
89
90          WRITE(*,100)RCON,ZRCON,Z2RCON,CCON,ZCCON,Z4DCON
91          100      FORMAT(//1X,'ROW SUM CONDITION NUMBER: '/1X,F9.2,
92          + //1X,'(ROW SUM CONDITION NUMBER)/(DIMENSION): '/1X,F9.2,
93          + //1X,'(ROW SUM CONDITION NUMBER)/(DIMENSION)**2: '/1X,F9.2,
94          + ////1X,'COLUMN SUM CONDITION NUMBER: '/1X,F9.2,
95          + //1X,'(COL SUM CONDITION NUMBER)/(DIMENSION): '/1X,F9.2,
96          + //1X,'(COL SUM CONDITION NUMBER)/(DIMENSION)**2: '/1X,F9.2////////)
97
98          GO TO 1000
99          880      WRITE(*,104)JC(1)
100          104      FORMAT('ERROR RETURN CONDITION ',I3)
101          1000      STOP
102          END

```

T,S PAT.BINAURAL2

```

C *****PROGRAM IMPRESP2*****
C *
C * This program is used to plot the impulse response of a *
C * simulated pinna at each of six angles *
C *
C * The pinna is simulated by a number of line reflectors *
C *
C * By P. A. Tollman *
C * 14 June 1985 *
C *
C *****

```

```

REAL BIG, PINNIMP(2048)

```

```

INTEGER LOOP1

```

```

C ---Set up graph axes and scaling ---

```

```

CALL SETUP

```

```

C --- Step through each direction ---

```

```

DO 10 LOOP1 = 1, 6

```

```

C --- Calculate pinna impulse response ---

```

```

CALL PINNA_IMP (LOOP1, PINNIMP, BIG)

```

```

C --- Plot impulse response ---

```

```

CALL DRAW (LOOP1, PINNIMP, BIG)
10 CONTINUE

```

```

CALL FINITT (0,0)

```

```

STOP

```

```

END

```

```

C *****SUBROUTINE PINNA_IMP*****

```

```

C --- This subroutine calculates the impulse response of a ---
C --- two dimensional simulated pinna for a specific ---
C --- direction of incidence ---

```

```

SUBROUTINE PINNA_IMP (LOOP1, PINNIMP, BIG)

```

```

REAL PI, C, PINNIMP(2048), LENGTH, TIME, SAMPLE
+ ANGLE, DIRECTION, BIG

```

```

INTEGER LOOP1, LOOP2, LOOP3, SEED

```

```

PARAMETER ( PI = 3.141592654 )
PARAMETER ( C = 344. )

```

```

C --- A number of line reflectors are used to simulate the ---
C --- pinna. Dimensions give a maximum impulse response ---
C --- length of 350 micro-seconds ---

```

DIRECTION = FLOAT (LOOP1-1) *18. * PI / 180.

C --- Initialise PINNIMP ---

DO 5 LOOP2 = 1 , 2048

PINNIMP(LOOP2) = 0.

5 CONTINUE

C --- Calculate output for each reflector in turn ---

C --- ANGLE = orientation of reflector

C --- LENGTH = dimension of reflector

C --- TIME = time delay prior to adding reflector outputs

DO 10 LOOP2 = 1 , 15

C --- Initialise SEED ---

SEED = LOOP2*1000 + 3

ANGLE = RAN(SEED) * PI - PI/2.

LENGTH = RAN(SEED) * .2

TIME = RAN(SEED) * 350E-6 + 100E-6

C --- Sample is the length of one sample (5 microseconds) ---

C --- LENGTH*SIN(ANGLE-DIRECTION)/C is the length of the ---

C --- reflected pulse. ---

C --- COS(ANGLE-DIRECTION)/SIN(ANGLE-DIRECTION) is the ---

C --- amplitude of the reflected pulse, while 100E-6/TIME ---

C --- is the 1/r falloff ---

DO 20 LOOP3 = 1 , 2048

SAMPLE = FLOAT(LOOP3) * 5E-6

IF (SAMPLE .LT. TIME) THEN

PINNIMP(LOOP3) = PINNIMP(LOOP3) + 0.

ELSE IF (SAMPLE .GE. TIME .AND. SAMPLE .LT.

+ TIME + ABS (LENGTH*SIN(ANGLE-DIRECTION)/C)) THEN

PINNIMP(LOOP3) = PINNIMP(LOOP3) + 100E-6/TIME*

+ ABS ((COS(ANGLE-DIRECTION)/SIN(ANGLE-DIRECTION)))

ELSE IF (SAMPLE .GT.

+ TIME + ABS (LENGTH*SIN(ANGLE-DIRECTION)/C)) THEN

PINNIMP(LOOP3) = PINNIMP(LOOP3) + 0.

END IF

20 CONTINUE

10 CONTINUE

C --- Calculate largest value for auto-scaling ---

BIG = 0.

DO 30 LOOP2 = 1,2048

IF(PINNIMP(LOOP2) .GE. BIG) BIG=PINNIMP(LOOP2)

30 CONTINUE

RETURN

END

C *****SUBROUTINE SETUP*****

SUBROUTINE SETUP

C --- This subroutine sets up the graphing package, the ---
C --- scaling and the axes ---

INTEGER NDEV

CHARACTER*6 PORT

C --- Graph axes are drawn ---

PORT = '_TTC4:'

NDEV = 2

CALL GRAFIC (NDEV , PORT)

C --- Size and position of axes are set ---

CALL POSN (1 , 50 , 950 , 30 , 700)

C --- Axes are drawn and tic'ed ---

CALL DRWAXES (0., 0., 10.24, 2., 0., 0., 6., 1., 1)

C --- Axes are drawn and numbered ---

CALL AXNUM (1 , 1 , 1 , 1 , 1 , 1 , 1)

C --- Graph is titled ---

CALL POSLAB (1 , 12)

CALL CARWRT ('PINNA OUTPUT')

C --- Axes are titled ---

CALL ALPSIZ (2.)

CALL TCURS (420 , 30)

CALL CARWRT ('TIME (MS)')

CALL RROTAT (90.)

CALL TCURS (20 , 300)

CALL CARWRT ('DIRECTION')

CALL RROTAT (0.)

RETURN

END

C *****SUBROUTINE DRAW*****

C --- This subroutine graphs the impulse response of a ---
C --- filter output ---

SUBROUTINE DRAW (LOOP1 , PINNIMP , BIG)

REAL PINNIMP(2048) , X_VAL , Y_VAL , SCALE

```
INTEGER LOOP1 , LOOP2
```

```
C      --- Implement auto-scaling ---
```

```
IF (LOOP1 .EQ. 1) SCALE = BIG
```

```
C      --- Plot the graph ---
```

```
DO 10 LOOP2 = 1 , 2048
```

```
Y_VAL = PINNIMP (LOOP2) / (SCALE * 3.) + FLOAT (LOOP1)
```

```
X_VAL = FLOAT (LOOP2) * 10.24 / 2048.
```

```
CALL GRAPH ( LOOP1 , X_VAL , Y_VAL , 0 , 1 )
```

```
10      CONTINUE
```

```
RETURN
```

```
END
```

A-15

```

C *****PROGRAM PINNIMP2*****
C *
C * This program calculates amplitude and phase
C * correction factors for a specific pinna.
C * These are calculated at chosen angular increments
C * of incidence across 40 frequency bands.
C *
C * These correction factors are such that, if
C * applied to an incident impulse from the direction
C * for which they have been calculated, the output
C * once the filter outputs are summed will also be
C * an impulse.
C *
C * By: P. A. Tollman
C * 3 June 1985
C *
C *****

COMPLEX CFACT(40)

REAL WINDOW(501) , FILTER_IMP(2048,40) , PINNIMP(2048)

INTEGER LOOP1

C --- A windowing function of coefficients for the filters ---
C --- is calculated ---

CALL KATSER (WINDOW)

C --- Open data file into which correction factors are ---
C --- to be written --

OPEN (UNIT = 25 , STATUS = 'NEW' , FILE = 'PHCHANGE')

C --- Increment angles of impulse incidence ---

DO 10 LOOP1 = 1 , 6

C --- Calculate pinna impulse response for incremented ---
C --- directions ---

CALL PINNA_IMP (LOOP1 , PINNIMP)

C --- Filter impulse responses are calculated, and windowed ---

CALL FILTER (WINDOW , FILTER_IMP)

C --- Convolve with filters to find positions of first ---
C --- peaks ---

CALL CONVOLVE (FILTER_IMP , PINNIMP , CFACT)

C --- Store positions and amplitudes of first peaks as ---
C --- correction factors ---

CALL STORE (CFACT)

10 CONTINUE

C --- Close data file ---

```

CLOSE (UNIT = 25)

A-16

STOP
END

C *****SUBROUTINE KAISER*****

SUBROUTINE KAISER (WINDOW)

C --- This subroutine calculates 450 KAISER window ---
C --- coefficients to window the truncated impulse ---
C --- response ---

REAL WINDOW (501) , ARG , N , E , DE , SQDE , EO

INTEGER LOOP1 , LOOP2

PARAMETER (PI = 3.141592654)
PARAMETER (THRESH = 1.E-08)

DO 10 LOOP1 = 1 , 501

N = FLOAT (LOOP1 - 1)

ARG = PI * SQRT (1. - N*N / 25.E4)

E = 1.

DE = 1.

C --- The BESSEL summation is continued until it is within ---
C --- 1.E-08 of its final value ---

DO 20 LOOP2 = 1 , 1000

DE = DE * ARG / FLOAT (LOOP2)

SQDE = DE * DE

E = E + SQDE

IF (THRESH .GT. SQDE) GO TO 30

20 CONTINUE

30 IF (LOOP1 .EQ. 1) EO = E

WINDOW (LOOP1) = E / EO

10 CONTINUE

RETURN

END

C *****SUBROUTINE FILTER*****

C --- This subroutine calculates the impulse response of a ---
C --- bank of finite impulse response filters, centred at ---
C --- frequencies "CENTRE_F" ---

SUBROUTINE FILTER (WINDOW , FILTER_IMP)

```
REAL CENTRE_F , N , FILTER_IMP (2048 ,40) , PI , WINDOW(501)
```

```
INTEGER LOOP1 , LOOP2
```

```
PARAMETER ( PI = 3.141592654 )
```

```
C      --- Each filter is calculated in turn ---
```

```
DO 10 LOOP1 = 1 , 40
```

```
  CENTRE_F = ( FLOAT(LLOOP1)/2. - .25 ) * 1000.
```

```
C      --- Initialise FILTER_IMP ---
```

```
DO 15 LOOP2 = 1 , 2048
```

```
  FILTER_IMP(LLOOP2 , LLOOP1) = 0.
```

```
15    CONTINUE
```

```
C      --- The filter impulse response is calculated, ---
```

```
C      --- and multiplied by the windowing coefficients ---
```

```
  FILTER_IMP(501 , LLOOP1) = 0.005
```

```
DO 20 LOOP2 = 1 , 501
```

```
  N = FLOAT (LLOOP2)
```

```
  FILTER_IMP (501+LLOOP2 , LLOOP1) = (2./(N*PI))
```

```
+    * COS(N*2*PI*CENTRE_F/200.E3) * SIN (N*PI/400.)
```

```
  FILTER_IMP(501 + LLOOP2,LLOOP1) =
```

```
+    FILTER_IMP(501+LLOOP2 , LLOOP1) * WINDOW(LLOOP2)
```

```
  FILTER_IMP(501-LLOOP2,LLOOP1)=FILTER_IMP(501+LLOOP2,LLOOP1)
```

```
20    CONTINUE
```

```
10    CONTINUE
```

```
RETURN
```

```
END
```

```
C      *****SUBROUTINE PINNA_IMP*****
```

```
C      --- This subroutine calculates the impulse response of a ---
```

```
C      --- two dimensional simulated pinna for each direction. ---
```

```
C      --- of incidence in turn ---
```

```
SUBROUTINE PINNA_IMP (LLOOP1 , PINNIMP)
```

```
REAL PI , C , PINNIMP(2048) , LENGTH , TIME , SAMPLE
```

```
+  ANGLE , DIRECTION
```

```
INTEGER LOOP1 , LOOP2 , LOOP3 , SEED
```

```
PARAMETER ( PI = 3.141592654 )
```

```
PARAMETER ( C = 344. )
```

```
C      --- A number of line reflectors are used to simulate the ---
```

```
C      --- pinna. Dimensions give a maximum impulse response ---
```

```
C      --- length of 350 micro-seconds ---
```

```
DIRECTION = ( FLOAT (LOOP1-1) *18.) *PI / 180.
```

```
C --- Initialise PINNIMP ---
```

```
DO 5 LOOP2 = 1 , 2048
```

```
PINNIMP(LOOP2) = 0.
```

```
5 CONTINUE
```

```
C --- Calculate output for each reflector in turn ---
```

```
C --- ANGLE = orientation of reflector
```

```
C --- LENGTH = dimension of reflector
```

```
C --- TIME = time delay prior to adding reflector outputs
```

```
DO 10 LOOP2 = 1 , 15
```

```
C --- Initialise SEED ---
```

```
SEED = LOOP2*I000 + 3
```

```
ANGLE = RAN(SEED) * PI - PI/2.
```

```
LENGTH = RAN(SEED) * .2
```

```
TIME = RAN(SEED) * 350E-6 + 100E-6
```

```
C --- SAMPLE is the length of one sample (5 microseconds) ---
```

```
C --- LENGTH*SIN(ANGLE-DIRECTION)/C is the length of the ---
```

```
C --- reflected pulse. ---
```

```
C --- (COS(ANGLE-DIRECTION)/SIN(ANGLE-DIRECTION)) is the ---
```

```
C --- pulse height, while 100E-6/TIME is the 1/r falloff ---
```

```
DO 20 LOOP3 = 1 , 2048
```

```
SAMPLE = FLOAT(LOOP3) * 5E-6
```

```
IF (SAMPLE .LT. TIME) THEN
```

```
PINNIMP(LOOP3) = PINNIMP(LOOP3) + 0.
```

```
ELSE IF (SAMPLE.GE.TIME .AND. SAMPLE .LT.
```

```
+ TIME + ABS ( LENGTH*SIN(ANGLE-DIRECTION)/C ) ) THEN
```

```
+ PINNIMP(LOOP3) = PINNIMP(LOOP3) + 100E-6/TIME*
```

```
+ ABS ( (COS(ANGLE-DIRECTION)/SIN(ANGLE-DIRECTION)) )
```

```
ELSE IF (SAMPLE .GT.
```

```
+ TIME + ABS ( LENGTH*SIN(ANGLE-DIRECTION)/C ) ) THEN
```

```
PINNIMP(LOOP3) = PINNIMP(LOOP3) + 0.
```

```
END IF
```

```
20 CONTINUE
```

```
10 CONTINUE
```

```
RETURN
```

```
END
```

```
C *****SUBROUTINE CONVOLVE*****
```

```
C --- This subroutine convolves the pinna impulse response ---
```

```

C      --- With that of the filters. The convolution ---
C      --- is performed using the FFT approach. For a ---
C      --- description of this approach, see page 202 of "THE ---
C      --- FAST FOURIER TRANSFORM" by E. O. Brigham ---

```

```

SUBROUTINE CONVOLVE(FILTER_IMP , PINNIMP , CFACT)

```

```

COMPLEX AFILT(2048 , 40) , APINNIMP(2048) , AVECT(2048) ,
+ CFACT(40)

```

```

REAL FILTER_IMP(2048 , 40) , PINNIMP(2048) , AMPL

```

```

INTEGER LOOP1 , LOOP2 , M , IWK(12)

```

```

C      ---The FFTC fourier transform routine of the IMSL set ---
C      --- of library routines is used. In the routine: ---
C      --- A--- = complex vector of length N = M**2
C      --- M = exponent to which 2 is raised
C      --- IWK = complex vector of length M+1

```

```

C      --- Transfer data into complex arrays ---

```

```

DO 10 LOOP1 = 1 , 40
DO 20 LOOP2 = 1 , 2048

```

```

IF (LOOP1 .EQ. 1) THEN
APINNIMP(LOOP2) = CMPLX ( PINNIMP(LOOP2) , 0.)
END IF

```

```

AFILT(LOOP2,LOOP1) = CMPLX(FILTER_IMP(LOOP2,LOOP1)
+ , 0.)

```

```

20 CONTINUE
10 CONTINUE

```

```

C      --- Transform pinna impulse response into the frequency domain ---

```

```

M = 11
CALL FFT2C (APINNIMP , M , IWK)

```

```

C      --- Transform filter impulse response into freq domain ---

```

```

DO 30 LOOP1 = 1 , 40
DO 40 LOOP2 = 1 , 2048
AVECT(LOOP2) = AFILT(LOOP2 , LOOP1)
40 CONTINUE

```

```

CALL FFT2C(AVECT , M , IWK)

```

```

C      --- Multiply the frequency response of the sound with ---
C      --- that of the filter ---

```

```

DO 50 LOOP2 = 1 , 2048
AFILT(LOOP2,LOOP1) = AVECT(LOOP2) * APINNIMP(LOOP2)
50 CONTINUE
30 CONTINUE

```

```

C      --- To perform the inverse FFT, do an FFT on a scaled ---
C      --- version of the complex conjugate ---

```

```

DO 60 LOOP1 = 1 , 40

```

```

DO 70 LOOP2 = 1 , 2048
  AVECT(L00P2) = CONJG(AFILT(L00P2,L00P1)) / 2048.
CONTINUE

```

70

```
CALL FFT2C(AVECT , M , IWK)
```

```

C    --- Store the convolved filter output in matrix ---
C    --- FILTER_IMP.---

```

```

DO 80 LOOP2 = 1 , 2048
  FILTER_IMP(L00P2,L00P1) = REAL(AVECT(L00P2))
CONTINUE

```

80

```

C    --- The position and amplitude of the highest peak ---
C    --- of each filter impulse response is determined ---

```

```
AMPL = 0.
```

```

DO 90 LOOP2 = 1 , 2048
  IF (FILTER_IMP(L00P2,L00P1) .GE. AMPL) THEN
    PH_POS = FLOAT (LOOP2)
    AMPL = FILTER_IMP(L00P2 , L00P1)
  END IF

```

```
CFACT(L00P1) = CMPLX (PH_POS , AMPL)
```

```
90    CONTINUE
```

```
60    CONTINUE
```

```
RETURN
```

```
END
```

```
C    *****SUBROUTINE STORE*****
```

```

C    --- This subroutine stores the relative phases and ---
C    --- amplitudes of the filter outputs ---

```

```
SUBROUTINE STORE (CFACT)
```

```
COMPLEX CFACT(40)
```

```
REAL PH_POS(40) , AMPL(40) , MINPHASE , REFERENCE
```

```
INTEGER LOOP1
```

```

C    --- Absolute phase and amplitude is converted into ---
C    --- relative amplitude and phase relative to the ---
C    --- centre of the filter impulse response ---

```

```
MINPHASE = 501.
```

```
REFERENCE = AIMAG(CFACT(1))
```

```
DO 10 LOOP1 = 1 , 40
```

```
PH_POS(L00P1) = REAL(CFACT(L00P1)) - MINPHASE
```

```
AMPL(L00P1) = REFERENCE / AIMAG(CFACT(L00P1))
```

```
CFACT(L00P1) = CMPLX (PH_POS(L00P1) , AMPL(L00P1))
```

```
WRITE (25 , *) CFACT(L00P1)
```

```
10    CONTINUE
```


RETURN
END

```

C *****PROGRAM DETECT2*****
C *
C * This program is used to detect the location of a sound *
C * source. The sound strikes the pinna, the output of *
C * which is passed through a bank of 40 finite impulse *
C * response filters. Pre-calculated direction dependent *
C * phase and amplitude correction factors are applied to *
C * these filtered outputs, which are then summed, and the *
C * composite wave plotted. *
C *
C * The pinna is simulated by a number of line reflectors *
C * *
C * Inspection of such plots for a number of sets of *
C * correction factors yields the location of the sound *
C * source. *
C *
C * By P. A. Tollman *
C * 4 June 1985 *
C *
C *****
REAL SOUND(2048) , DIRECTION , WINDOW(501) , SIGNAL_OUT(2048)
+ , FILTER_IMP(2048,40) , ENERGY(40) , BIG , PINNIMP(2048)

INTEGER LOOP1

C --- Obtain inputted information ---
CALL INPUT (SOUND , DIRECTION)

C --- Calculate pinna impulse response ---
CALL PINNA_IMP (DIRECTION , PINNIMP)

C --- Calculate coefficients of windowing function ---
CALL KAISER (WINDOW)

C --- Calculate filter impulse responses, and window each ---
CALL FILTER (WINDOW , FILTER_IMP)

C --- Convolve each filter impulse response with the pinna ---
C --- impulse response ---
CALL SOUND_CONV (FILTER_IMP , PINNIMP , ENERGY)

C --- Convolve with the target sound ---
CALL SOUND_CONV (FILTER_IMP , SOUND , ENERGY)

C ---Set up graph axes and scaling ---
CALL SETUP

C --- Open the file containing the correction factors ---
OPEN (UNIT=25 , STATUS='OLD' , FILE='PHCHANGE')

C --- Step through sets of correction factors ---

```

```
DO 10 LOOP1 = 1 , 6
```

```
C --- Apply correction factors to impulse response ---
```

```
CALL CORRECTION (FILTER_IMP , SIGNAL_OUT , ENERGY , BIG)
```

```
C --- Plot summed output ---
```

```
CALL DRAW (LOOP1 , SIGNAL_OUT , BIG)
```

```
10 CONTINUE
```

```
CLOSE (UNIT=25)
```

```
CALL FINITT (0,0)
```

```
STOP
```

```
END
```

```
C *****SUBROUTINE INPUT*****
```

```
C
```

```
C --- Inputs impulse direction and target signature ---
```

```
C
```

```
SUBROUTINE INPUT (SOUND , DIRECTION)
```

```
REAL SOUND(2048) , DIRECTION , SUM
```

```
INTEGER LOOP1
```

```
CHARACTER*13 DATFNAME
```

```
C --- Enter direction from which impulse is required ---
```

```
WRITE (6 , 101)
```

```
101 FORMAT (IX , 'Enter impulse response direction (Degrees) : ' )
```

```
ACCEPT * , DIRECTION
```

```
C --- Enter data file name containing target signature ---
```

```
WRITE (6 , 102)
```

```
102 FORMAT (IX , 'Enter file containing target signature:')
```

```
READ (5 , 103) DATFNAME
```

```
103 FORMAT (A13)
```

```
C --- Read data file ---
```

```
OPEN (UNIT=25 , STATUS='OLD' , FILE=DATFNAME)
```

```
READ (25 , *) (SOUND(LOOP2) , LOOP2=1,1024)
```

```
CLOSE (UNIT=25)
```

```
C --- Remove DC ---
```

```
SUM = 0.
```

```
DO 10 LOOP1 = 1 , 64
```

```
SUM = SUM + SOUND(LOOP1)
```

```
10 CONTINUE
```

```
DO 20 LOOP1 = 1 , 1024
```

```

20      SOUND(LOOP1) = SOUND(LOOP1) - (SUM/64)
      CONTINUE

```

```

      RETURN
      END

```

```

C      *****SUBROUTINE PINNA_IMP*****

```

```

C      --- This subroutine calculates the impulse response of a ---
C      --- two dimensional simulated pinna for a specific ---
C      --- direction of incidence ---

```

```

      SUBROUTINE PINNA_IMP (DIRECTION , PINNIMP)

```

```

      REAL PI , C , PINNIMP(2048) , LENGTH , TIME , SAMPLE
      *   ANGLE , DIRECTION

```

```

      INTEGER LOOP1 , LOOP2 , LOOP3 , SEED

```

```

      PARAMETER ( PI = 3.141592654 )

```

```

      PARAMETER ( C = 344. )

```

```

C      --- A number of line reflectors are used to simulate the ---
C      --- pinna. Dimensions give a maximum impulse response ---
C      --- length of 350 micro-seconds ---

```

```

      DIRECTION = DIRECTION * PI / 180.

```

```

C      --- Initialise PINNIMP ---

```

```

      DO 5 LOOP2 = 1 , 2048

```

```

      PINNIMP(LOOP2) = 0.

```

```

5      CONTINUE

```

```

C      --- Calculate output for each reflector in turn ---

```

```

C      --- ANGLE = orientation of reflector

```

```

C      --- LENGTH = dimension of reflector

```

```

C      --- TIME = time delay prior to adding reflector outputs

```

```

      DO 10 LOOP2 = 1 , 15

```

```

C      --- Initialise SEED ---

```

```

      SEED = LOOP2*1000 + 3

```

```

      ANGLE = RAN(SEED) * PI - PI/2.

```

```

      LENGTH = RAN(SEED) * .2

```

```

      TIME = RAN(SEED) * 350E-6 + 100E-6

```

```

C      --- Sample is the length of one sample (5 microseconds) ---

```

```

C      --- LENGTH*SIN(ANGLE-DIRECTION)/C is the length of the ---

```

```

C      --- reflected pulse. ---

```

```

C      --- COS(ANGLE-DIRECTION)/SIN(ANGLE-DIRECTION) is the ---

```

```

C      --- amplitude of the reflected pulse, while 100E-6/TIME ---

```

```

C      --- is the 1/r falloff ---

```

```

      DO 20 LOOP3 = 1 , 2048

```

```
SAMPLE = FLOAT(LOOP3) * 5E-6
```

```
IF (SAMPLE .LT. TIME) THEN
PINNIMP(LOOP3) = PINNIMP(LOOP3) + 0.
ELSE IF(SAMPLE.GE.TIME .AND. SAMPLE .LT.
+ TIME + ABS ( LENGTH*SIN(ANGLE-DIRECTION)/C ) ) THEN
PINNIMP(LOOP3) = PINNIMP(LOOP3) + 100E-6/TIME*
+ ABS ( (COS(ANGLE-DIRECTION)/SIN(ANGLE-DIRECTION)))
ELSE IF (SAMPLE .GT.
+ TIME + ABS ( LENGTH*SIN(ANGLE-DIRECTION)/C ) ) THEN
PINNIMP(LOOP3) = PINNIMP(LOOP3) + 0.
END IF
```

```
20      CONTINUE
10      CONTINUE
```

```
RETURN
END
```

```
C *****SUBROUTINE KAISER*****
```

```
SUBROUTINE KAISER (WINDOW)
```

```
C --- This subroutine calculates 501 KAISER window ---
C --- coefficients to window the truncated impulse ---
C --- response ---
```

```
REAL WINDOW (501) , ARG , N , E , DE , SQDE , EO
```

```
INTEGER LOOP1 , LOOP2
```

```
PARAMETER (PI = 3.141592654)
PARAMETER (THRESH = 1.E-08)
```

```
DO 10 LOOP1 = 1 , 501
N = FLOAT (LOOP1 - 1)
ARG = PI * SQRT (1. - N*N / 25.E4)
```

```
E = 1.
DE = 1.
```

```
C --- The BESSEL summation is continued until it is within ---
C --- 1.E-08 of its final value ---
```

```
DO 20 LOOP2 = 1 , 1000
DE = DE * ARG / FLOAT(LOOP2)
SQDE = DE * DE
E = E + SQDE
```

```
IF (THRESH .GT. SQDE) GO TO 30
```

```
20      CONTINUE
```

```
30      IF (LOOP1 .EQ. 1) EO = E
WINDOW(LOOP1) = E / EO
```

10 CONTINUE

RETURN
END

C *****SUBROUTINE FILTER*****

C --- This subroutine calculates the impulse response of a ---
C --- bank of finite impulse response filters, centred at ---
C --- frequencies "CENTRE_F" ---

SUBROUTINE FILTER (WINDOW , FILTER_IMP)

REAL CENTRE_F , N , FILTER_IMP (2048 ,40) , PI , WINDOW(501)

INTEGER LOOP1 , LOOP2

PARAMETER (PI = 3.141592654)

C --- Each filter is calculated in turn ---

DO 10 LOOP1 = 1 , 40
CENTRE_F = (FLOAT (LOOP1)/2. - .25) * 1000.

C --- The filter impulse response is calculated, ---
C --- and multiplied by the windowing coefficients ---

FILTER_IMP(501 , LOOP1) = 0.005

DO 20 LOOP2 = 1 , 501

N = FLOAT (LOOP2)

FILTER_IMP (501+LOOP2 , LOOP1) = (2./ (N*PI))
* COS(N*2*PI*CENTRE_F/200.E3) * SIN (N*PI/400.)

FILTER_IMP(501 + LOOP2,LOOP1) =

FILTER_IMP(501+LOOP2 , LOOP1) * WINDOW (LOOP2)
FILTER_IMP(501-LOOP2,LOOP1)=FILTER_IMP(501+LOOP2,LOOP1)

20 CONTINUE

10 CONTINUE

RETURN
END

C *****SUBROUTINE SOUND_CONV*****

C --- This subroutine convolves a sequence with 40 FIR filter ---
C --- impulse responses. The convolution ---
C --- is performed using the FFT approach. For a ---
C --- description of this approach, see page 202 of "THE ---
C --- FAST FOURIER TRANSFORM" by E. O. Brigham ---

```
SUBROUTINE SOUND_CONV(FILTER_IMP , SOUND , ENERGY)
```

```
COMPLEX AFILT(2048 , 40) , ASOUND(2048) , AVECT(2048)
```

```
REAL FILTER_IMP(2048 , 40) , SOUND(2048) , ENERGY(40)
```

```
INTEGER LOOP1 , LOOP2 , M , IWK(12)
```

```
C      ---The FFTC fourier transform routine of the IMSL set ---
C      --- of library routines is used. In the routine:      ---
C      --- A--- = complex vector of length N = M**2
C      --- M = exponent to which 2 is raised
C      --- IWK = complex vector of length M+1
C      --- Transfer data into complex arrays ---
```

```
DO 10 LOOP1 = 1 , 40
```

```
DO 20 LOOP2 = 1 , 2048
```

```
IF (LOOP1 .EQ. 1) THEN
```

```
ASOUND(LOOP2) = CMPLX ( SOUND(LOOP2) , 0.)
```

```
END IF
```

```
AFILT(LOOP2,LOOP1) = CMPLX(FILTER_IMP(LOOP2,LOOP1)
+ , 0.)
```

```
20 CONTINUE
```

```
10 CONTINUE
```

```
C      --- Transform time sequence ---
```

```
M = 11
```

```
CALL FFT2C (ASOUND , M , IWK)
```

```
C      --- Transform filter impulse response into freq domain ---
```

```
DO 30 LOOP1 = 1 , 40
```

```
DO 40 LOOP2 = 1 , 2048
```

```
AVECT(LOOP2) = AFILT(LOOP2 , LOOP1)
```

```
40 CONTINUE
```

```
CALL FFT2C(AVECT , M , IWK)
```

```
C      --- Multiply the frequency response of the sound with ---
```

```
C      --- that of the filter ---
```

```
DO 50 LOOP2 = 1 , 2048
```

```
AFILT(LOOP2,LOOP1) = ASOUND(LOOP2) * AVECT(LOOP2)
```

```
50 CONTINUE
```

```
30 CONTINUE
```

```
C      --- To perform the inverse FFT, do an FFT on a scaled ---
```

```
C      --- version of the complex conjugate ---
```

```
DO 60 LOOP1 = 1 , 40
```

```
DO 70 LOOP2 = 1 , 2048
```

```
AVECT(LOOP2) = CONJG(AFILT(LOOP2,LOOP1)) / 2048.
```

```
70 CONTINUE
```

```
CALL FFT2C(AVECT , M , IWK)
```

```

C      --- Store the convolved filter output in matrix ---
C      --- FILTER_IMP. At the same time, calculate the ---
C      --- energy out of each filter ---

```

```

ENERGY(LOOP1) = 0.

```

```

      DO 80 LOOP2 = 1 , 2048
      FILTER_IMP(LOOP2,LOOP1) = REAL(AVECT(LOOP2))
      ENERGY(LOOP1) = ENERGY(LOOP1) +
+      FILTER_IMP(LOOP2,LOOP1)*FILTER_IMP(LOOP2,LOOP1)
80    CONTINUE
60    CONTINUE

```

```

RETURN
END

```

```

C      *****SUBROUTINE SETUP*****

```

```

SUBROUTINE SETUP

```

```

C      --- This subroutine sets up the graphing package, the ---
C      --- scaling and the axes ---

```

```

INTEGER NDEV

```

```

CHARACTER*6 PORT

```

```

C      --- Graph axes are drawn ---

```

```

PORT = '_TTC4:'
NDEV = 2

```

```

CALL GRAFIC (NDEV , PORT)

```

```

C      --- Size and position of axes are set ---

```

```

CALL POSN (1 , 50 , 950 , 30 , 700)

```

```

C      --- Axes are drawn and ticked ---

```

```

CALL DRWAXES (0., 0., 10.24, 2., 0., 0., 6., 1., 1)

```

```

C      --- Axes are drawn and numbered ---

```

```

CALL AXNUM (1 , 1 , 1 , 1 , 1 , 1 , 1)

```

```

C      --- Graph is titled ---

```

```

CALL POSLAB (1 , 12)
CALL CARWRT ( 'PINNA OUTPUT')

```

```

C      --- Axes are titled ---

```

```

CALL ALPSIZ (2.)
CALL TCURS (420 , 30)
CALL CARWRT ('TIME (MS)')

```



```

CALL RROTAT (90.)
CALL TCURS (20 , 300)
CALL CARWRT ('DIRECTION')
CALL RROTAT (0.)

```

```

RETURN
END

```

```

C *****SUBROUTINE CORRECTION*****
C --- This subroutine applies angular correction factors to ---
C --- the spectral components obtained at the filter outputs ---
C --- and then sums these outputs ---

SUBROUTINE CORRECTION (FILTER_IMP , SIGNAL_OUT , ENERGY , BIG)

COMPLEX FACTOR(40)

REAL FILTER_IMP(2048,40) , SIGNAL_OUT(2048) , FILTER_OUT(2048,40)
+ , ENERGY(40) , NUM , DENOM , MAG , BIG

INTEGER ISHIFT , LOOP1 , LOOP2

C --- Read correction factors from data file ---

READ (25 , *) ( FACTOR(LOOP1) , LOOP1 = 1 , 40 )

C --- Calculate what the absolute magnitude of the correction ---
C --- factor for the lowest frequency filter should be ---

NUM = 0.
DENOM = 0.

DO 10 LOOP1 = 1 , 40
  NUM = NUM + ENERGY(LOOP1)
  DENOM = DENOM + ENERGY(LOOP1)
+ * AIMAG (FACTOR(LOOP1)) * AIMAG (FACTOR(LOOP1))
10 CONTINUE

MAG = SQRT (NUM / DENOM)

C --- Shift and multiply each filter output by the ---
C --- appropriate correction factor ---

DO 20 LOOP1 = 1 , 40
  ISHIFT = IFIX (REAL (FACTOR(LOOP1)))

  DO 30 LOOP2 = 1 , 2048

    IF (LOOP2+ISHIFT.LE.2048 .AND. LOOP2+ISHIFT.GE.1) THEN
      FILTER_OUT(LOOP2,LOOP1) = FILTER_IMP(LOOP2+ISHIFT,LOOP1)
+ * AIMAG (FACTOR(LOOP1)) * MAG
    ELSE
      FILTER_OUT(LOOP2,LOOP1) = 0.
    END IF

  30 CONTINUE
20 CONTINUE

```

```

C      --- Now sum the corrected filter outputs. Use the peak of ---
C      --- summed output for auto-scaling in the plotting routine ---

```

```

      BIG = 0.

```

```

      DO 40 LOOP1 = 1 , 2048
        SIGNAL_OUT(LOOP1) = 0.

```

```

      DO 50 LOOP2 = 1 , 40
        SIGNAL_OUT(LOOP1) = SIGNAL_OUT(LOOP1) +
+      FILTER_OUT(LOOP1 , LOOP2)
50      CONTINUE

```

```

      IF(SIGNAL_OUT(LOOP1) .GE. BIG) BIG = SIGNAL_OUT(LOOP1)
40      CONTINUE

```

```

      RETURN
      END

```

```

C      *****SUBROUTINE DRAW*****

```

```

C      --- This subroutine graphes the impulse response of a ---
C      --- filter output ---

```

```

      SUBROUTINE DRAW (LOOP1 , SIGNAL_OUT , BIG)

```

```

      REAL SIGNAL_OUT(2048) , X_VAL , Y_VAL , SCALE

```

```

      INTEGER LOOP1 , LOOP2

```

```

C      --- Implement auto-scaling ---

```

```

      IF (LOOP1 .EQ. 1) SCALE = BIG

```

```

C      --- Plot the graph ---

```

```

      DO 10 LOOP2 = 1 , 2048

```

```

        Y_VAL = SIGNAL_OUT(LOOP2)/(SCALE*3.) + FLOAT (LOOP1)

```

```

        X_VAL = FLOAT (LOOP2) * 10.24 / 2048.

```

```

        CALL GRAPH ( LOOP1 , X_VAL , Y_VAL , 0 , 1 )

```

```

10      CONTINUE

```

```

      RETURN
      END

```

O*PAT2-83(1).FREQ2

```

1      C      *****PROGRAM FREQ2*****
2      C      *
3      C      * THIS PROGRAM CALCULATES THE OUTPUT VALUES OF A 2-DIM ARRAY
4      C      * FOR 100 DIFFERENT FREQUENCY BANDS, EACH OF CONSTANT FRACT-
5      C      * IONAL BANDWIDTH OVER THE RANGE 25 TO 100 KHZ.
6      C      *
7      C      * OUTPUT VALUES ARE CALCULATED IN 0,5 DEGREE INCREMENTS OVER
8      C      * THE RANGE 0 TO 90 DEGREES.
9      C      *
10     C      * THE ARRAY CONTAINS 1000 POINTS.THE CO-ORDINATES OF EACH
11     C      * ARE RANDOMLY ASSIGNED.
12     C      *
13     C      * A TIME DELAY OF BETWEEN 0 AND 2,9 MILLISECONDS (CORRESPONDING*
14     C      * TO A DISTANCE OF 1 M) IS ASSIGNED TO EACH ARRAY POINT.
15     C      *
16     C      * THE PROCEDURE IS REPEATED 5 TIMES, FOR THE SAME ARRAY BUT
17     C      * WITH 5 DIFFERENTLY ASSIGNED TIME DELAYS (ANALOGOUS TO
18     C      * 5 DIFFERENT HYDROPHONE POSITIONS.
19     C      *
20     C      * THE FREQUENCY OUTPUTS ARE STORED IN "MATRIX."
21     C      * THE DISTANCES BETWEEN ARRAY ELEMENTS ARE STORED
22     C      * IN "ARRAY."
23     C      *
24     C      *****
25
26     C      --- ALL PROGRAM VARIABLES ARE INITIALISED.      ---
27
28     REAL ARRAY(1000,2) , MATRIX(400) , CFREQ(400) , PI ,
29     + HFREQ , LFREQ , VALA(1000) , VALB(1000) , ANG , ANGL ,
30     + Q , XAX , YAX , KAY , SUM , TIME(1000) , ANG(1000)
31     + , SARR , LTIME
32
33     INTEGER LOOP0 , LOOP1 , LOOP2 , LOOP3 , ISEED , I
34     + , NPT , NHYD , NFIL
35
36     READ (* , 101) Q , NPT , SARR , NHYD , LTIME , NFIL
37 101  FORMAT()
38
39
40     C      --- THE RANDOM GENERATOR SEED IS ASSIGNED.      ---
41
42     ISEED = 1
43
44     C      --- THE VALUE OF PI IS INITIALISED.      ---
45
46     PI=3.141592654
47
48
49     C      --- THE ARRAY CO-ORDINATES ARE RANDOMLY ASSIGNED.      ---
50
51     DO 10 LOOP1 = 1,NPT
52
53         DO 20 LOOP2 = 1,2
54             ARRAY(LOOP1,LOOP2) = URAND(ISEED) * SARR
55 20     CONTINUE
56
57         VALA(LOOP1)=SQRT (ARRAY(LOOP1,1)*ARRAY(LOOP1,1) +
58     + ARRAY(LOOP1,2)*ARRAY(LOOP1,2) )
59
60         ANG(LOOP1) = ATAN( ARRAY(LOOP1,2) / ARRAY(LOOP1,1) )
61

```

```

62
63      10      CONTINUE
64
65      C      --- THE OUTPUT FOR DIFFERENT SETS OF TIME DELAYS ARE CALCULATED -
66
67      DO 12 LOOP0 = 1,NHYD
68
69      C      --- A TIME DELAY EQUIVALENT TO 1 M IS ASSIGNED TO EACH POINT---
70      C      --- THE RANDOM NUMBER GENERATOR SEED IS ASSIGNED.          ---
71
72      ISEED = LOOP0 + 1
73
74      DO 15 LOOP1 = 1,NPT
75      TIME(LOOP1) = URAND(ISEED) * LTIME
76
77      C      --- DISTANCE TO EACH POINT CALCULATED ---
78      15      CONTINUE
79
80
81      C      --- EACH ANGLE IS TREATED IN DO LOOP 30          ---
82
83      DO 30 LOOP1 = 1,181
84      ANG = ( (FLOAT(LOOP1)-1.) * .5) * PI/180.
85
86      DO 35 LOOP2 = 1,NPT
87
88      IF (ARRAY(LOOP3,1) .EQ. 0.) THEN
89      VALB(LOOP2) = 0.
90      ELSE
91      VALB(LOOP2) = SIN(ANG + ANGC(LOOP2))
92      END IF
93
94      35      CONTINUE
95
96
97      C      --- EACH FREQUENCY IS TREATED IN DO LOOP 30          ---
98
99      LFREQ = 25000.
100
101      DO 40 LOOP2 = 1,NFIL
102
103      HFREQ = LFREQ * ( (2.*Q+1.) / (2.*Q-1.) )
104      CFREQ(LOOP2) = (HFREQ + LFREQ) / 2.
105      LFREQ = HFREQ
106      KAY = 2. * PI * CFREQ(LOOP2) / 344.
107      XAX = 0.
108      YAX = 0.
109
110      C      --- EACH ARRAY ELEMENT IS TREATED IN DO LOOP 50          ---
111
112      DO 50 LOOP3 = 1,NPT
113
114
115      ANGL = KAY*(VALA(LOOP3)*VALB(LOOP3)+TIME(LOOP3))
116      XAX = XAX + COS(ANGL)
117      YAX = YAX + SIN(ANGL)
118      50      CONTINUE
119
120      SUM = SQRT (XAX*XAX + YAX*YAX)
121      MATRIX(LOOP2) = SUM
122      40      CONTINUE
123

```

```
124 C --- THE OUTPUTS FOR EACH FREQUENCY AT EACH ANGLE ARE ---
125 C --- WRITTEN INTO DATA FILE "FREQ2" VIA THE ---
126 C --- @USE 17,FREQ2 COMMAND. ---
127
128 WRITE (17) (MATRIX(I) , I = 1,NFIL)
129
130 30 CONTINUE
131 12 CONTINUE
132 STOP
133 INCLUDE UCT*ASCII.URAND
134 END
```

IO*PAT2-83(1).CORLATE2B

```

1      C      *****PROGRAM CORLATE2B*****
2      C      *
3      C      * THIS PROGRAM READS THE ARRAY OUTPUT VALUES STORED IN FILE
4      C      * "FREQLD."
5      C      *
6      C      * TARGET ECHOES OF UNKNOWN DIRECTION ARE CORRELATED WITH THESE
7      C      * VALUES TO DETERMINE THE POSITION OF THE TARGET IN
8      C      * QUESTION.
9      C      *
10     C      * THE TARGETS CAN BE POSITIONED AT ANY ANGLE BETWEEN 0 AND
11     C      * 90 DEGREES.
12     C      *
13     C      * CURVES OF CORRELATION COEFFICIENT VERSUS ANGLE ARE PLOTTED.
14     C      *
15     C      *****
16
17     CHARACTER*60 MESSAG
18
19     REAL ARRAY(1000,2) , MATRIX(200) , HORAX(181) , SUM(200) ,
20     + DIRECT(20) , POWER(20) , CFREQ(200) , DIR , SUMM , YSQ ,
21     + HFREQ , LFREQ , VALA , VALB , ANG , ANGL , PI , XAX , YAX ,
22     + KAY , POW , Q , XINC , XPAGE , XNUM , XP , XSQ ,
23     + YPAGE , YNUM , YP , TIME(1000) , CORLAT(181) , XMEAN ,
24     + YMEAN , XYSUM , NUMER(181) , FACTOR(181) , BIG , FCTOR
25
26     INTEGER LOOP0 , LOOP1 , LOOP2 , LOOP3 , NUM , ISEED , ANGLE
27
28     C      --- THE RANDOM GENERATOR SEED IS ASSIGNED.      ---
29
30     ISEED = 1
31
32     C      --- THE VALUE OF PI IS INITIALISED.      ---
33
34     PI=3.141592654
35
36     C      --- THERE ARE 200 "CONSTANT-Q" FILTERS, EACH OF Q = 144      ---
37
38     Q = 144.
39
40     C      --- THE ARRAY CO-ORDINATES ARE RANDOMLY ASSIGNED.      ---
41     C      --- THE MAXIMUM CO-ORDINATE SIZE IS 0.05 METRES.      ---
42
43     DO 10 LOOP1 = 1,1000
44
45         DO 20 LOOP2 = 1,2
46             ARRAY(LOOP1,LOOP2) = URAND(ISEED) * .05
47             20 CONTINUE
48             10 CONTINUE
49
50     C      --- A TIME DELAY EQUIVALENT TO 16 CM IS ASSIGNED TO EACH POINT ---
51     C      --- THE RANDOM NUMBER GENERATOR SEED IS ASSIGNED.      ---
52
53     ISEED = 2
54
55     DO 25 LOOP1 = 1 , 1000
56         TIME(LOOP1) = URAND(ISEED) * .16
57         25 CONTINUE
58
59     C      --- THE NUMBER OF TARGETS IS GIVEN BY "NUM."      ---
60
61     NUM = 3

```

```

62
63
64 C      --- ARRAY "SUM" IS INITIALISED TO ZERO. ARRAY "SUM" NOW      ---
65 C      --- ACCUMULATES THE SUMS OF THE INCOMING TARGET ECHOES AT      ---
66 C      --- EACH OF 200 FREQUENCIES USED.                             ---
67
68      DO 30 LOOP1 = 1,200
69 30      SUM(LOOP1) = 0.
70
71 C      --- THE INCOMING ECHO DIRECTION IS GIVEN BY "DIR" WHILST THE  ---
72 C      --- RELATIVE STRENGTH OF THE INCOMING ECHO IS DENOTED "POW."  ---
73
74 C      --- THE PINNA OUTPUT FOR EACH TARGET ECHO IS CALCULATED.      ---
75 C      --- THE SUM OF THESE OUTPUTS IS STORED IN ARRAY "SUM."        ---
76
77      DO 40 LOOP1 = 1 , NUM
78      READ (*,101) DIR , POW
79 101     FORMAT ( )
80
81      DIRECT(LOOP1) = DIR
82      POWER(LOOP1) = POW
83
84      ANG = DIR * PI/180.
85
86 C      --- EACH FREQUENCY IS TREATED IN DO LOOP 30                  ---
87
88      LFREQ = 25000.
89
90      DO 50 LOOP2 = 1,200
91
92      HFREQ = LFREQ * ( (2.*Q+1.) / (2.*Q-1.) )
93      CFREQ(LOOP2) = (HFREQ + LFREQ) / 2.
94      LFREQ = HFREQ
95      KAY = 2. * PI * CFREQ(LOOP2) / 344.
96      XAX = 0.
97      YAX = 0.
98
99 C      --- EACH ARRAY ELEMENT IS TREATED IN DO LOOP 50            ---
100
101      DO 60 LOOP3 = 1,1000
102
103      VALA = SQRT (ARRAY(LOOP3,1)**2. + ARRAY(LOOP3,2)**2.)
104
105      IF (ARRAY(LOOP3,1).EQ.0.) THEN
106      VALB = PI / 2.
107      GO TO 250
108      END IF
109
110      VALB = ANG + ATAN(ARRAY(LOOP3,2) / ARRAY(LOOP3,1))
111 250      ANGL = KAY * ( VALA * SIN(VALB) + TIME(LOOP3) )
112      XAX = XAX + COS(ANGL)
113      YAX = YAX + SIN(ANGL)
114 60      CONTINUE
115
116      SUMM = SQRT (XAX**2. + YAX**2.)
117      SUM(LOOP2) = SUM(LOOP2) + (SUMM*POW) , * (SUMM*POW)
118 50      CONTINUE
119 40      CONTINUE
120
121 C      --- INTRODUCE AMBIENT NOISE ---
122
123      REWIND 17

```

```

124
125      DO 61 LOOP1 = 1 , 181
126      READ (17) (MATRIX(I) , I = 1 , 200)
127
128          DO 63 LOOP2 = 1 , 200
129          MATRIX(LOOP2) = MATRIX(LOOP2)*MATRIX(LOOP2)
130          SUM(LOOP2) = SUM(LOOP2) + MATRIX(LOOP2)*0.00005499
131      63      CONTINUE
132      61      CONTINUE
133
134      C      --- OPEN PLOTTING FILE ---
135      CALL PLOTS(0, 0, 0)
136
137      DO 65 LOOP0 = 1 , 7
138
139      REWIND 17
140
141          DO 70 LOOP1 = 1,181
142          XMEAN = 0.
143          YMEAN = 0.
144          XYSUM = 0.
145          XSQ = 0.
146          YSQ = 0.
147
148          READ (17) ( MATRIX(I) , I = 1,200 )
149
150              DO 80 LOOP2 = 1,200
151              MATRIX(LOOP2) = MATRIX(LOOP2)*MATRIX(LOOP2)
152              XMEAN = XMEAN + SUM(LOOP2)
153              YMEAN = YMEAN + MATRIX(LOOP2)
154              XYSUM = XYSUM + SUM(LOOP2) * MATRIX(LOOP2)
155              XSQ = XSQ + SUM(LOOP2) ** 2
156              YSQ = YSQ + MATRIX(LOOP2) ** 2
157      80          CONTINUE
158
159          XMEAN = XMEAN / 200.
160          YMEAN = YMEAN / 200.
161          NUMER(LOOP1) = XYSUM - 200. * XMEAN * YMEAN
162          FACTOR(LOOP1) = YSQ - 200. * (YMEAN ** 2)
163          DENOM = SQRT((XSQ-200.*XMEAN**2) * FACTOR(LOOP1))
164          CORLAT(LOOP1) = NUMER(LOOP1) / DENOM
165          HORAX(LOOP1) = (FLOAT(LOOP1) - 1.) / 2.
166      70      CONTINUE
167
168      C      *** PLOTS TO FIT ON A4 SIZE SHEET ***
169      C      *** X-AXIS TO BE 25 CMS LONG      ***
170      C      *** Y-AXIS TO BE 16 CMS LONG      ***
171
172      IF (LOOP0 .NE. 1) CALL NEWPAG
173
174      C      --- SET PAGE SIZE (ONLY NECESSARY FOR GDP) ---
175      CALL PAGESIZ(32.0, 22.0)
176
177      C      ---CHANGE TO INK PENS---
178      MESSAG='PLS LOAD P1-BK/I P2-RD/I'
179      CALL OPMES(24,MESSAG)
180
181      C      --- DRAW A-4 SIZE PAGE ---
182      CALL NEWPEN(1)
183      CALL PLOT(1.0, 1.0, -3)
184      CALL PLOT(0.0, 20.9, 2)
185      CALL PLOT(29.7, 20.9, 2)

```



```

186      CALL PLOT(29.7, 0.0, 2)
187      CALL PLOT(0.0, 0.0, 2)
188
189      C      --- ESTABLISH NEW ORIGIN ---
190      CALL PLOT(4.5, 9.0, -3)
191
192      C      --- DRAW THE AXES ---
193      CALL PLOT(23.0, 0.0, 2)
194      CALL PLOT(0.0, -8.0, 3)
195      CALL PLOT(0.0, 8.0, 2)
196
197      C      ---THE GRAPH IS TITLED---
198      MESSAG='CORRELATION COEFFICIENT VS ANGLE'
199      CALL SYMBOL(2.3,8.7,.5,MESSAG,0.,32)
200
201      C      --- MARK OFF THE AXES ---
202      C      --- X-AXIS HAS 9 DIVISIONS OF 10 DEGREES EACH ---
203      XINC=23./9.
204      XPAGE = 0.0
205      DO 90 LOOP1 = 1 , 9
206          XPAGE = XPAGE + XINC
207          CALL SYMBOL(XPAGE, 0.0, 0.5, 13, 0.0, -1)
208          XNUM = FLOAT(LOOP1) * 10.0
209          XP = XPAGE - 0.5
210          CALL NUMBER(XP, -0.6, 0.2, XNUM, 0.0, 1)
211      90 CONTINUE
212
213      C      ---THE 'X' AXIS IS LABELLED---
214      MESSAG='ANGLE (DEGREES)'
215      CALL SYMBOL(20.,-1.5,.3,MESSAG,0.,15)
216
217      C      --- Y-AXIS HAS 8 DIVISIONS OF 0.25, FROM -1 TO +1
218      YPAGE = -10.0
219      DO 100 LOOP1 = 1 , 9
220          YPAGE = YPAGE + 2.0
221          YNUM = FLOAT ( -5 + LOOP1 ) / 4.0
222          CALL SYMBOL(0.0, YPAGE, 0.5, 13, 90.0, -1)
223          YP = YPAGE - 0.16
224          CALL NUMBER(-1.4, YP, 0.2, YNUM, 0.0, 2)
225      100 CONTINUE
226      C      ---THE 'Y' AXIS IS LABELLED---
227      MESSAG='CORRELATION COEFFICIENT'
228      CALL SYMBOL(-2.3,1.3,.3,MESSAG,90.,23)
229
230      CCC      DO 110 LOOP1 = 1,NUM
231      CCC          DIR = DIRECT(LOOP1) * 23./90.
232      CCC          POW = POWER(LOOP1) * 8.
233      CCC          CALL SYMBOL (DIR,POW,.2,4,0.,-1)
234      CCC110 CONTINUE
235
236      C      --- PLOT THE GRAPH ---
237      CALL NEWPEN(2)
238      CALL PLOT(0.0, 0.0, 3)
239      DO 120 LOOP1 = 1 , 181
240          XPAGE = ( HORAX (LOOP1) * 23.0 ) / 90.0
241          YPAGE = CORLAT(LOOP1) * 8.0
242          CALL PLOT(XPAGE, YPAGE, 2)
243      120 CONTINUE
244
245      MESSAG='CORLATE2B'
246      CALL PAGNAM(MESSAG)
247

```

```

248
249      WRITE( * , 3 )
250 3      FORMAT(///,1X,'THE CORRELATION COEFFICIENTS IN 0.1 DEGREE'
251      + ' INCREMENTS FROM 0 TO 90 DEGREES ARE:')
252
253 C      THE CORRELATION COEFFICIENT AT EACH ANGLE IS
254 C      PRINTED.
255
256          DO 130 LOOP1 = 1 , 181 , 10
257          WRITE( *,102 )(CORLAT(J),HORAX(J),J=LOOP1,LOOP1+9)
258 102      FORMAT ( /1X , 10 (F5.2 , 1X , F4.1 , 3X) )
259
260 130      CONTINUE
261
262      BIG = 0.
263
264          DO 140 LOOP1 = 1 , 181
265          IF (CORLAT(LOOP1) .GE. BIG) THEN
266              ANGLE = LOOP1
267              BIG = CORLAT(LOOP1)
268          END IF
269 140      CONTINUE
270
271      IF (LOOP0 .EQ. 3) ANGLE = 21
272      IF (LOOP0 .EQ. 4) ANGLE = 67
273      IF (LOOP0 .EQ. 5) ANGLE = 21
274      IF (LOOP0 .EQ. 6) ANGLE = 67
275      REWIND 17
276
277          DO 150 LOOP1 = 1 , ANGLE
278          READ (17) (MATRIX(I) , I = 1 , 200)
279 150      CONTINUE
280
281      FCTOR = NUMER(ANGLE) / FACTOR(ANGLE)
282
283          DO 160 LOOP1 = 1,200
284          MATRIX(LOOP1) = MATRIX(LOOP1)*MATRIX(LOOP1)
285          SUM(LOOP1) = SUM(LOOP1) - MATRIX(LOOP1) * FCTOR
286 160      CONTINUE
287
288 65      CONTINUE
289
290 C      --- CLOSE OFF PLOT ---
291      CALL PLOT(0.0, 0.0, 999)
292
293      STOP
294      INCLUDE UCT*ASCII.URAND
295      END

```

```

100 *****PROGRAM CALIBRATE*****
110 *
120 * Calculates final FTT of impulse response of receiver
130 * at 1 degree angular increments between 0 and 90
140 * degrees. These are stored for reference by program
150 * FINDRANGE.
160 *
170 * By: P. A. Tollman
180 * 4 October 1986
190 *
200 *****
210 *
220     REAL DIR,DECAY,RESP(150),RTM,FRESP(100)
230     INTEGER L1,L2
240
250 *--- Initialise FTT exponential decay factor. ---
260 *--- RTM=exponential response time ---
270     RTM=40.E-6
280     DECAY=1./RTM
290
300 *--- Calculate for each direction in turn ---
310     DO 10 L1=1,90
320         DIR=FLOAT(L1)
330
340 *--- Calculate receiver impulse response ---
350         CALL IRESP(DIR,RESP)
360
370 *--- Calculate final FTT of pinna impulse response ---
380         CALL FTT(RESP,DECAY,FRESP)
390
400 *---Store FTT ---
410         WRITE(11,*)(FRESP(L2),L2=1,100)
411 10     CONTINUE
420
430     STOP
440     INCLUDE UCT*ASCII.URAND
450     END
460
470
480
490
500
510     SUBROUTINE IRESP(DIR,RESP)
520 *--- Subroutine simulates a receiver with 500 reflectors ---
530 *--- of varying lengths and orientations. The highest ---
540 *--- frequency is 50 kHz, the receiver is 50 ---
550 *--- wavelengths across at this frequency. The impulse ---
560 *--- response time is therefore 1 milliseconds. The ---
570 *--- sampling frequency is 1.5xNyquist rate, ie 150kHz ---
580
590     REAL DIR,RESP(150),ANGLE,LENGTH,TIME
600     INTEGER L1,L2,SEED
610     PARAMETER (PI=3.141592654)
620
630     DIR=DIR*PI/180.
640
650 *---Initialise response ---
660     DO 10 L1=1,150
670         RESP(L1)=0.
680 10     CONTINUE
690
700 *--- For each reflector, ANGLE=orientation ---

```

```

710 *--- LENGTH=length in seconds ---
720 *--- TIME=delay before adding outputs ---
730 *--- Initialise seed ---
740 SEED=12363
750 DO 20 L1=1,1000
760 ANGLE=URAND(SEED)*PI - PI/2.
770 LENGTH=URAND(SEED)*6.67E-6
780 TIME=URAND(SEED)*SIN((URAND(SEED)*PI/2.)+DIR)*1.E-3
790
800 *--- SAMPLE=length of 1 sample ---
810 *--- COS(ANGLE-DIR)/SIN(ANGLE-DIR)=ampl of reflected ---
820 *--- pulse ---
830 *--- LENGTH*SIN(ANGLE-DIR)=length of reflected pulse ---
840 DO 30 L2=1,150
850 SAMPLE=FLOAT(L2)/150.E3
860 IF(SAMPLE.GE.TIME .AND.
870 & SAMPLE.LT.TIME+ABS(LENGTH*SIN(ANGLE-DIR))) THEN
880 RESP(L2)=RESP(L2)+ABS((COS(ANGLE-DIR))/(SIN(ANGLE-DIR)))
890 END IF
900 30 CONTINUE
910 20 CONTINUE
920
930 RETURN
940 END
950
960
970
980
990 SUBROUTINE FTT(RESP,DECAY,FRESP)
1000 *--- Calculates final FTT of impulse response ---
1010
1020 REAL DECAY,RESP(150),FRESP(100),FREQ,FPHASE(100),FQUAD(100),TM
1030 INTEGER L1,L2
1040 PARAMETER (PI=3.141592654)
1050
1060 *--- Set time between samples ---
1070 TM=1./150.E3
1080
1090 *--- Step through time samples and frequencies ---
1100 DO 10 L1=1,150
1110 DO 20 L2=1,100
1120 IF(L1.EQ.1) THEN
1130 FPHASE(L2)=TM*RESP(1)
1140 FQUAD(L2)=0.
1150 GOTO 20
1160 END IF
1170 FREQ=2.*PI*500.*FLOAT(L2)
1180 FPHASE(L2)=FPHASE(L2)*EXP(-DECAY*TM) +
1190 & TM*RESP(L1)*COS(FREQ*TM*FLOAT(L1))
1200 FQUAD(L2)=FQUAD(L2)*EXP(-DECAY*TM) +
1210 & TM*RESP(L1)*SIN(FREQ*TM*FLOAT(L1))
1220 20 CONTINUE
1230 10 CONTINUE
1240
1250 DO 30 L1=1,100
1260 FRESP(L1)=(SQRT(FPHASE(L1)*FPHASE(L1)+
1270 & FQUAD(L1)*FQUAD(L1)))
1280 30 CONTINUE
1290
1300 RETURN
1310 END

```

```

100 *****PROGRAM FINDRANGE*****
110 *
120 * Program correlates FTT of received sample with
130 * FTT which have been pre-determined in program
140 * CALIBRATE. The correlation is performed as a
150 * function of time
160 *
170 * P. A. Tollman
180 * 4 October 1986
190 *
200 *****
210
220     REAL RESP(200),DIR,DECAY,RTM,FRESP(100)
230
240 *--- Enter direction of sound ---
250     DIR=1
260
270 *--- Enter response time of FTT exponential decay ---
280     RTM=40.E-6
290     DECAY=1./RTM
300
310 *--- Calculate impulse response ---
320     CALL IRESP(DIR,RESP)
330
340 *--- Setup SACLANT parameters ---
350     WRITE(12,*)90,20
360     WRITE(12,*)0,2,0,2
370
380 *--- Calculate FTT of impulse response. From FTT correlate --
390 *--- time samples with predetermined FTT's & store in a ---
400 *--- file for plotting ---
410     CALL FTT(RESP,DECAY,FRESP)
420
430     STOP
440     INCLUDE UCT*ASCII.URAND
450     END
460
470
480
490
500     SUBROUTINE IRESP(DIR,RESP)
510 *--- Subroutine simulates a receiver with 500 reflectors ---
520 *--- of varying lengths and orientations. The highest ---
530 *--- frequency is 50 kHz, the receiver is 50 ---
540 *--- wavelengths across at this frequency. The impulse ---
550 *--- response time is therefore 1 milliseconds. The ---
560 *--- sampling frequency is 1.5xNyquist rate, ie 150kHz ---
570
580     REAL DIR,RESP(200),ANGLE,LENGTH,TIME
590     INTEGER L1,L2,SEED
600     PARAMETER (PI=3.141592654)
610
620     DIR=DIR*PI/180.
630
640 *---Initialise response ---
650     DO 10 L1=1,200
660         RESP(L1)=0.
670 10    CONTINUE
680
690 *--- For each reflector, ANGLE=orientation ---
700 *--- LENGTH=length in seconds ---
710 *--- TIME=delay before adding outputs ---

```

```

720 *--- Initialise seed ---
730     SEED=12363
740     DO 20 L1=1,1000
750     ANGLE=URAND(SEED)*PI - PI/2.
760     LENGTH=URAND(SEED)*6.67E-6
770     TIME=URAND(SEED)*SIN((URAND(SEED)*PI/2.)+DIR)*1.E-3
780
790 *--- SAMPLE=length of 1 sample ---
800 *--- COS(ANGLE-DIR)/SIN(ANGLE-DIR)=ampl of reflected ---
810 *--- pulse ---
820 *--- LENGTH*SIN(ANGLE-DIR)=length of reflected pulse ---
830     DO 30 L2=1,200
840     SAMPLE=FLOAT(L2)/150.E3
850     IF(SAMPLE.GE.TIME .AND.
860     &     SAMPLE.LT.TIME+ABS(LENGTH*SIN(ANGLE-DIR))) THEN
870     RESP(L2)=RESP(L2)+ABS((COS(ANGLE-DIR))/(SIN(ANGLE-DIR)))
880     END IF
890 30     CONTINUE
900 20     CONTINUE
910
920     RETURN
930     END
940
950
960
970
980
990
1000     SUBROUTINE FTT(RESP,DECAY,FRESP)
1010 *--- Calculates FTT of impulse response ---
1020
1030     REAL DECAY,RESP(200),FRESP(100),FREQ,FPHASE(100),FQUAD(100),TM
1040     INTEGER L1,L2
1050     PARAMETER (PI=3.141592654)
1060
1070 *--- Set time between samples ---
1080     TM=1./150.E3
1090
1100 *--- Step through time samples and frequencies ---
1110     DO 10 L1=1,200
1120     DO 20 L2=1,100
1130     IF(L1.EQ. 1) THEN
1140     FPHASE(L2)=TM*RESP(1)
1150     FQUAD(L2)=0.
1160     GOTO 20
1170     END IF
1180     FREQ=2.*PI*500.*FLOAT(L2)
1190     FPHASE(L2)=FPHASE(L2)*EXP(-DECAY*TM) +
1200     &     TM*RESP(L1)*COS(FREQ*TM*FLOAT(L1))
1210     FQUAD(L2)=FQUAD(L2)*EXP(-DECAY*TM) +
1220     &     TM*RESP(L1)*SIN(FREQ*TM*FLOAT(L1))
1230 20     CONTINUE
1240
1250     IF(L1.LT.101.OR.FLOAT(L1/5).NE.FLOAT(L1)/5.) GOTO 10
1260     DO 30 L2=1,100
1270     FRESP(L2)=(SQRT(FPHASE(L2)*FPHASE(L2)+
1280     &     FQUAD(L2)*FQUAD(L2)))
1290 30     CONTINUE
1300     CALL CORLAT(FRESP,L1)
1310 10     CONTINUE
1320
1330     RETURN

```

```

1340      END
1350
1360
1370
1380
1390 *--- Subroutine correlates FTT with pre-determined ---
1400 *--- response of receiver ---
1410      SUBROUTINE CORLAT(FRESP,L1)
1420
1430      REAL FRESP(100),CLBRT(100),COEF(90),FE,FMEAN,EMEAN,
1440      &FSQ,ESQ,N,D(90),MEAN(100)
1450      INTEGER L1,L3,L4
1460
1470      REWIND 13
1480      REWIND 11
1490 *--- Divide out mean ---
1500      READ(13,*)(MEAN(L3),L3=1,100)
1510      DO 5 L3=1,100
1520          FRESP(L3)=FRESP(L3)/MEAN(L3)
1530 5      CONTINUE
1540
1550 *--- Correlate with each direction in turn ---
1560      DO 10 L3=1,90
1570          READ(11,*) (CLBRT(L4),L4=1,100)
1580          FE=0.
1590          FMEAN=0.
1600          EMEAN=0.
1610          FSQ=0.
1620          ESQ=0.
1630          DO 20 L4=1,100
1640              CLBRT(L4)=CLBRT(L4)/MEAN(L4)
1650              FE=FE+FRESP(L4)*CLBRT(L4)
1660              FMEAN=FMEAN+FRESP(L4)/100.
1670              EMEAN=EMEAN+CLBRT(L4)/100.
1680              FSQ=FSQ+FRESP(L4)*FRESP(L4)
1690              ESQ=ESQ+CLBRT(L4)*CLBRT(L4)
1700 20      CONTINUE
1710          N=FE-100.*FMEAN*EMEAN
1715          IF(L1.LE.150) THEN
1720              D(L3)=SQRT((FSQ-100.*FMEAN*FMEAN)*(ESQ-100.*EMEAN*EMEAN))
1725          END IF
1730          COEF(L3) = N/D(L3)
1740 10      CONTINUE
1750
1760 *--- Print correlation coefficients ---
1770 CC      WRITE(*,102) (COEF(L3),L3=1,90)
1780 CC102    FORMAT(5(/,1X,18(F4.2,1X))//)
1790
1800      WRITE(12,105)(COEF(L3),L3=1,90)
1810
1820 105      FORMAT(17(5E13.5,/),5E13.5)
1830
1840      RETURN
1850      END

```

APPENDIX B
COMPUTER PROGRAMS USED IN THE LOCALISATION OF SOUNDS BY A
MANNIKIN HUMAN HEAD

B.1	PROGRAM SCP2CH - downloads samples from a Phillips Digital Oscilloscope into an HP-85 microcomputer.	B-2
B.2	PROGRAM UNIVAC - converts numeric data to ASCII strings to be read into a Sperry mainframe computer.	B-4
B.3	PROGRAM IMPRESPONSE - determines the magnitude response of a received sound at each recorded angle.	B-5
B.4	PROGRAM FINDSOUND - cross-correlates a received spectrum with each of 36 predetermined spectra.	B-8
B.5	PROGRAM FFT - determines the magnitude response of an averaged ensemble of spectra.	B-13
B.5	PROGRAM CORPLT - correlates the magnitude response of an ensemble of spectra with the predetermined magnitude responses of the mannikin head.	B-15


```

10 ! *****
20 ! *****PROGRAM SCP2CH*****
30 ! *****
40 !
50 ! "Program to download 128 values from PHILLIPS 'scope"
60 CLEAR
70 BEEP
80 DISP "Input file name:" @ INPUT F$
90 OPTION BASE 1
100 DIM V1(128),V2(128)
110 !
120 ! *** Inititalize 'scope ***
130 CLEAR 7 @ RESET 7
140 CONTROL 7,16 ; 1,10
150 OUTPUT 708 USING "K" ; "SPR"
160 OUTPUT 708 USING "K" ; "USP /"
170 OUTPUT 708 USING "K" ; "TIM 10E-3/8GN 950/END 4096/CNT 1/DAT ALL/DAT ?"
180 !
190 ! **** Implement software trigger
200 T=32 ! Set trigger level
210 F1=0 @ F2=0 @ C1=20 @ C2=20 @ V1(128)=0 @ V2(128)=0
220 !
230 FOR I=1 TO 20
240 ENTER 708 ; V1(I) @ ENTER 708 ; V2(I)
250 ENTER 708 ; D @ ENTER 708 ; D ! Discard alternate samples
260 NEXT I
270 !
280 C1=C1+1 @ C2=C2+1
290 ENTER 708 ; D @ ENTER 708 ; D ! Discard alternate samples
300 IF F1=1 THEN 360
310 IF F1=1 OR ABS (V1(C1-1)-V1(C1-2))>T THEN 360
320 IF V1(128)=0 THEN 350
330 FOR I=1 TO 19 @ V1(I)=V1(109+I) @ NEXT I
340 C1=20 @ V1(128)=0
350 ENTER 708 ; V1(C1) @ GOTO 430
360 IF C1>128 THEN ENTER 708 ; D @ GOTO 420
370 IF F1=1 THEN 400
380 FOR I=1 TO 20 @ V1(I)=V1(C1-21+I) @ NEXT I
390 C1=21 @ F1=1
400 ENTER 708 ; V1(C1)
410 !
420 IF F2=1 THEN 480
430 IF ABS (V2(C2-1)-V2(C2-2))>T THEN 480
440 IF V2(128)=0 THEN 470
450 FOR I=1 TO 19 @ V2(I)=V2(109+I) @ NEXT I
460 C2=20 @ V2(128)=0
470 ENTER 708 ; V2(C2) @ GOTO 280
480 IF C1>128 AND C2>128 THEN 570
490 IF C2>128 THEN ENTER 708 ; D @ GOTO 280
500 IF F2=1 THEN 530
510 FOR I=1 TO 20 @ V2(I)=V2(C2-21+I) @ NEXT I
520 C2=21 @ F2=1
530 ENTER 708 ; V2(C2) @ GOTO 280
540 !
550 ! *** Plot data ***
560 !
570 CLEAR 7 @ RESET 7
580 GRAPH
590 GCLEAR

```

```
600 SCALE 0,128,0,512
610 MOVE 0,0
620 FOR I=1 TO 128
630 PLOT I,V1(I)
640 NEXT I
650 MOVE 0,0
660 FOR I=1 TO 128
670 PLOT I,V2(I)+256
680 NEXT I
690 !
700 ! *** Store data ***
710 PAUSE
720 ON ERROR GOTO 750
730 CREATE F$&"L",1,1024
740 CREATE F$&"R",1,1024
750 OFF ERROR
760 S1=0 @ S2=0
770 FOR I=1 TO 128
780 S1=S1+V1(I) @ S2=S2+V2(I)
790 NEXT I
800 S1=S1/128 @ S2=S2/128
810 FOR I=1 TO 128
820 V1(I)=V1(I)-S1 @ V2(I)=V2(I)-S2
830 NEXT I
840 CRT OFF
850 ASSIGN# 1 TO F$&"L" @ ASSIGN# 2 TO F$&"R"
860 PRINT# 1 ; V1() @ PRINT# 2 ; V2()
870 ASSIGN# 1 TO * @ ASSIGN# 2 TO *
880 CRT ON
890 BEEP
900 END
```

```

10 | *****
20 | *****PROGRAM UNIVAC*****
30 | *****
40 |
50 | *** Converts numeric data to ASCII ***
55 |
60 OPTION BASE 1
70 CLEAR
80 DISP "BEGIN ";TIME
90 DIM D(128),L$(80)
100 F1$="SM" @ C=0 @ ASSIGN# 2 TO "UNIVAC:D701"
110 FOR I=0 TO 35
120 F2$=F1$&VAL$ (I*10)
130 FOR J=1 TO 2
140 IF J=1 THEN F3$=F2$&"L"
150 IF J=2 THEN F3$=F2$&"R"
152 |
153 | *** Read numeric data ***
154 |
160 ASSIGN# 1 TO F3$ @ READ# 1 ; D()@ ASSIGN# 1 TO *
165 |
166 | *** Convert to ASCII ***
167 |
170 FOR K=0 TO 4
180 L$=""
190 FOR L=1 TO 26
200 IF K=4 AND L=25 THEN GOTO 230
210 L$=L$&VAL$ (IP (D(K*26+L)+500))
220 NEXT L
222 |
223 | *** Store ASCII strings ***
224 |
230 C=C+1 @ PRINT# 2,C ; L$
240 NEXT K @ NEXT J @ NEXT I
250 C=C+1 @ PRINT# 2,C ; "@END"
260 ASSIGN# 2 TO *
270 DISP "END ";TIME
280 END

```

```

100 *****PROGRAM IMPRESPONSE*****
110 * This program calculates and plots the *
120 * impulse responses of the mannikin head at *
130 * 10 degree increments over 360 degrees. *
140 * *
150 * P. A. Tollman *
160 * 28 July 1986. *
170 * *
180 *****
190
200 REAL PROBE(128),PRFREQ(100),HEAD(128),HFREQ(100)
210 INTEGER L1,L2
220
230 *---Read free-field response of mic to speaker ---
240 READ (11,*) (PROBE(L1) , L1=1,128)
250
260 *--- Calculate FTT of microphone probe ---
270 CALL FTT (PRFREQ , PROBE)
280
290 *--- Open plotting file ---
300 CALL PLOTS (0,0,0)
310
320 *---Read response of head to loudspeaker for each ---
330 *--- angle in turn ---
340 DO 20 L1=1,36
350 READ (12,*) (HEAD(L2) , L2=1,128)
360
370 *--- Calculate FTT of head response ---
380 CALL FTT (HFREQ , HEAD)
390
400 *--- Divide head response by probe response ---
410 *--- Convert result to dB setting largest value ---
420 *--- as 0 dB ---
430 BIG = -999999999999999.
440 DO 30 L2=1,100
450 HFREQ(L2) = 20*ALOG10(HFREQ(L2)/PRFREQ(L2))
460 IF(HFREQ(L2) .GE. BIG) BIG=HFREQ(L2)
470 30 CONTINUE
480
490 DO 40 L2=1,100
500 HFREQ(L2)=HFREQ(L2)-BIG
510 40 CONTINUE
520
530 *--- Plot impulse response ---
540 CALL GPLOT(HFREQ , L1)
550
560 *--- Store impulse response ---
570 WRITE (13,*) (HFREQ(L2) , L2=1,100)
580
590 20 CONTINUE
600
610 *--- Close off plots ---
620 CALL PLOT (0,0,999)
630
640 STOP
650 END
660
670
680
690
700 *--- Computes the final FTT of a 128 point sample ---
710 SUBROUTINE FTT (FDOM , TDOM)

```

```

720
730 REAL TDOM(128),FDOM(100),FPHASE(100),FQUAD(100),FREQ,TM
740 INTEGER L1,L2
750 PARAMETER (PI = 3.141592654)
760
770 *--- Set time between samples ---
780 TM = 1/50.E3
790
800 *--- Step through frequencies at 200Hz increments ---
810 DO 10 L1=1,100
820 FREQ = 2.*PI*200.*FLOAT(L1)
830 FPHASE(L1) = TDOM(1)*TM
840 FQUAD(L1) = TDOM(1)*TM
850
860 *--- Step through time samples ---
870 DO 20 L2=2,128
880 FPHASE(L1) = FPHASE(L1)+TM*TDOM(L2)*COS(FREQ*TM*FLOAT(L2))
890 FQUAD(L1) = FQUAD(L1)+TM*TDOM(L2)*SIN(FREQ*TM*FLOAT(L2))
900 20 CONTINUE
910 FDOM(L1)=SQRT(FPHASE(L1)*FPHASE(L1)+FQUAD(L1)*FQUAD(L1))
920 10 CONTINUE
930
940 RETURN
950 END
960
970
980
990
1000 *--- Subroutine GPLOT plots frequency response ---
1010 SUBROUTINE GPLOT (HFREQ , L1)
1020
1030 CHARACTER*60 MESSAG
1040 REAL HFREQ(100),XINC,XWR,XNUM,XP,YINC,YWR,YNUM,YP
1050 INTEGER L1,L2,LDEG
1060
1070 *--- Open new page in plot file ---
1080 CALL NEWPAG
1090
1100 *--- Plots to fit on A4 page,X-axis to be 25cm ---
1110 *--- Y-axis to be 16cm. Scale from A4 using FACTOR ---
1120 CALL MAGNFY (.32)
1130
1140 *--- Set page size (only necessary for GDP) ---
1150 CALL PAGESIZ(32.0 , 22.0)
1160
1170 *--- Change to ink pens ---
1180 MESSAG = 'PLS LOAD P1-BK/I4'
1190 CALL OPMES (24 , MESSAG)
1200
1210 *--- Draw A4 page ---
1220 CALL NEWPEN(1)
1230 CALL PLOT(1.0 , 1.0 , -3)
1240 CALL PLOT(0.0 , 20.9 , 2)
1250 CALL PLOT(29.7 , 20.9 , 2)
1260 CALL PLOT(29.7 , 0.0 , 2)
1270 CALL PLOT(0.0 , 0.0 , 2)
1280
1290 *--- Establish new origin ---
1300 CALL PLOT(4.5 , 2.5 , -3)
1310
1320 *--- Draw axes ---
1330 CALL PLOT(23.0 , 0.0 , 2)

```

```

1340      CALL PLOT(0.0 , 0.0 , 3)
1350      CALL PLOT(0.0 , 16.0 , 2)
1360
1370 *--- Mark off axes ---
1380 *--- X-axis 4 divisions of 5kHz each ---
1390      XINC = 23./4.
1400      XWR = 0.
1410      DO 10 L2=1,4
1420      XWR = XWR+XINC
1430      CALL SYMBOL(XWR , 0. , .5 , 13 , 0. , -1)
1440      XNUM = FLOAT(L2)*5.
1450      XP=XWR-.5
1460      CALL NUMBER(XP , -.6 , .25 , XNUM , 0. , 1)
1470 10    CONTINUE
1480
1490 *--- Y-axis has 3 divisions of 20dB each ---
1500      YINC=16./3.
1510      YWR = -16./3.
1520      DO 20 L2=1,4
1530      YWR = YWR+YINC
1540      CALL SYMBOL(0. , YWR , .5 , 13 , 90. , -1)
1550      YNUM = -80.+FLOAT(L2)*20.
1560      YP = YWR-.1
1570      CALL NUMBER(-1.8 , YP , .25 , YNUM , 0. , 2)
1580 20    CONTINUE
1590
1600 *--- Draw labels ---
1610 *--- Title graph ---
1620      MESSAG = 'MAGNITUDE RESPONSE AT      DEGREES'
1630      LDEG = (L1-1)*10
1640      WRITE (MESSAG(23:25) , 111) LDEG
1650 111    FORMAT (I3)
1660      CALL SYMBOL(2.3 , 16.6 , .5 , MESSAG , 0. , 33)
1670
1680 *--- Label X-axis ---
1690      MESSAG = 'FREQUENCY (KHZ)'
1700      CALL SYMBOL(9. , -1.5 , .3 , MESSAG , 0. , 15)
1710
1720 *--- Label Y-axis ---
1730      MESSAG = 'SPECTRAL POWER (DB)'
1740      CALL SYMBOL(-2.4 , 5. , .3 , MESSAG , 90. , 19)
1750
1760 *--- Plot the graph ---
1770      CALL PLOT (0. , 0. , 3)
1780      DO 30 L2=1,100
1790      XP = FLOAT(L2)*23./100.
1800      YP = HFREQ(L2)*16./60.+16.
1810      CALL PLOT (XP , YP , 2)
1820 30    CONTINUE
1830
1840      RETURN
1850      END

```

```

100 *****PROGRAM FINDSOUND*****
110 *
120 * Program attempts to locate a sound at each
130 * of 36 positions. It calculates and plots the
140 * FTT at each position, and correlates this at
150 * intervals along the time axis with the
160 * magnitude responses of the pinna at each
170 * position.
180 *
190 * P. A. Tollman
200 * 15 August 1986
210 *
220 *****
230
240     REAL SOUND(128),PROBE(100),MEAN(100)
250     INTEGER L1,L2,L3,NUM
260
270 *--- Read the power spectrum of the probe tube ---
280 *--- to remove this from the response of the ear ---
290 *--- Also read the mean magnitude response of the --
300 *--- ear to divide through by ---
310     READ(13,*)(PROBE(L1) , L1=1,100)
320     READ(14,*)(MEAN(L1) , L1=1,100)
330
340 *--- Open plotting file ---
350     CALL PLOTS(0,0,0)
360
370 *--- Calculate for each sound in turn ---
380     DO 5 L3=2,2
390     NUM=L3+14
400 *
410 *--- Calculate for each position in turn ---
420     DO 10 L1=1,36
430     READ(NUM,*)(SOUND(L2) , L2=1,128)
440
450 *--- Setup graph and axes ---
460     IF(L1.EQ.14)THEN
470         CALL GSET(L1)
480
490 *--- Calculate FTT. From subroutine FTT, call ---
500 *--- plotting routine and correlation routine ---
510         CALL FTT(SOUND,PROBE,MEAN,L1)
520     END IF
530 10     CONTINUE
540 5     CONTINUE
550
560 *--- Close off plots ---
570     CALL PLOT(0,0,999)
580
590     STOP
600     END
610
620
630
640
650 *--- Subroutine GSET sets up axes ---
660     SUBROUTINE GSET (L1)
670
680     CHARACTER*60 MESSAG
690     REAL XINC,XWR,XNUM,YINC,YWR,YNUM
700     INTEGER L1,L2,LDEG

```

```

720 *--- Open new page in plot file ---
730     CALL NEWPAG
740
750 *--- Plots to fit on A4 page,X-axis to be 25cm ---
760 *--- Y-axis to be 16cm. Scale from A4 using FACTOR ---
770     CALL MAGNFY (.7)
780
790 *--- Set page size (only necessary for GDP) ---
800     CALL PAGESIZ(32.0 , 22.0)
810
820 *--- Change to ink pens ---
830     MESSAG = 'PLS LOAD P1-BK/I3'
840     CALL OPMES (24 , MESSAG)
850
860 *--- Draw A4 page ---
870     CALL NEWPEN(1)
880     CALL PLOT(1.0 , 1.0 , -3)
890     CALL PLOT(0.0 , 20.9 , 2)
900     CALL PLOT(29.7 , 20.9 , 2)
910     CALL PLOT(29.7 , 0.0 , 2)
920     CALL PLOT(0.0 , 0.0 , 2)
930
940 *--- Establish new origin ---
950     CALL PLOT(3. , 3. , -3)
960
970 *--- Draw axes ---
980     CALL PLOT(23.7 , 0.0 , 2)
990     CALL PLOT(23.7 , 14.9 , 2)
1000    CALL PLOT(0.0 , 14.9 , 2)
1010    CALL PLOT(0.0 , 0.0 , 2)
1020
1030 *--- Mark off axes ---
1040 *--- X-axis 4 divisions of 0.64ms each ---
1050     XINC = 23.7/4.
1060     XWR = 0.
1070     DO 10 L2=1,4
1080         XWR = XWR+XINC
1090         CALL SYMBOL(XWR , 0. , .5 , 13 , 0. , -1)
1100         XNUM = FLOAT(L2)*.64
1110         XP=XWR-.5
1120         CALL NUMBER(XP , -.6 , .3 , XNUM , 0. , 2)
1130 10     CONTINUE
1140
1150 *--- Y-axis has 4 divisions of 5kHz each ---
1160     YINC=14.9/4.
1170     YWR = -14.9/4.
1180     DO 20 L2=1,5
1190         YWR = YWR+YINC
1200         CALL SYMBOL(0. , YWR , .5 , 13 , 90. , -1)
1210         YNUM = 25.-FLOAT(L2)*5.
1220         YP = YWR+.5
1230         CALL NUMBER(-.6 , YP , .3 , YNUM , -90. , 1)
1240 20     CONTINUE
1250
1260 *--- Draw labels ---
1270 *--- Title graph ---
1280     MESSAG = 'FTT FOR SOUND AT      DEGREES'
1290     LDEG = (L1-1)*10
1300     WRITE (MESSAG(18:20) , 111) LDEG
1310 111    FORMAT (I3)

```



```

1340 *--- Label X-axis ---
1350     MESSAG = 'TIME (MS)'
1360     CALL SYMBOL(10.4 , -1.5 , .35 , MESSAG , 0. , 15)
1370
1380 *--- Label Y-axis ---
1390     MESSAG = 'FREQUENCY (KHZ)'
1400     CALL SYMBOL(-1.5 , 10.02 , .35 , MESSAG , -90. , 19)
1410
1420 *--- Label top of X-axis ---
1430     MESSAG = 'AMPLITUDE (DB)'
1440     CALL SYMBOL(9.1 , 15.1 , .4 , MESSAG , 0. , 14)
1450
1460     RETURN
1470     END
1480
1490
1500
1510
1520
1530 *--- Subroutine calculates FTT ---
1540     SUBROUTINE FTT(TDOM,PROBE,MEAN,L1)
1550
1560     REAL TDOM(128),FDOM(100),FPHASE(100),FQUAD(100),FREQ,TM
1570     &,BIG,ENERGY,PREV,ENGINC,PROBE(100),MEAN(100)
1580     INTEGER L1,L2,L3
1590     PARAMETER (PI=3.141592654)
1600
1610 *--- Set time between samples ---
1620 *--- Initialise energy increment to 0 ---
1630     TM = 1./50.E3
1640     PREV=0.
1650
1660 *--- Step through time samples ---
1670     DO 10 L2=1,128
1680 *--- Step through frequencies ---
1690     DO 20 L3=1,100
1700         IF(L2 .EQ. 1) THEN
1710             FPHASE(L3)=TM*TDOM(1)
1720             FQUAD(L3)=0.
1730             GOTO 20
1740         END IF
1750         FREQ = 2.*PI*200.*FLOAT(L3)
1760         FPHASE(L3)=FPHASE(L3)+TM*TDOM(L2)*COS(FREQ*TM*FLOAT(L2))
1770         FQUAD(L3)=FQUAD(L3)+TM*TDOM(L2)*SIN(FREQ*TM*FLOAT(L2))
1780 20     CONTINUE
1790
1800 *--- Calculate, plot and correlate every 4th FTT ---
1810     IF(FLOAT(L2/4) .EQ. FLOAT(L2)/4.) THEN
1820         BIG = -999999999999999999.
1830         ENERGY = 0.
1840         DO 30 L3=1,100
1850             FDOM(L3)=SQRT(FPHASE(L3)*FPHASE(L3)+FQUAD(L3)*FQUAD(L3))
1860             ENERGY = ENERGY+FDOM(L3)*FDOM(L3)
1870             FDOM(L3)=20.*ALOG10(FDOM(L3))-MEAN(L3)-PROBE(L3)
1880             IF(FDOM(L3) .GE. BIG) BIG=FDOM(L3)
1890 30     CONTINUE
1900     ENGINC = 20.*ALOG10(ENERGY-PREV)
1910     PREV = ENERGY
1920     DO 40 L3=1,100
1930         FDOM(L3)=FDOM(L3)-BIG
1940 40     CONTINUE

```

```

1960          CALL CORLAT(FDOM,ENGINC,MEAN,L1,L2)
1970          END IF
1980 10      CONTINUE
1990
2000          RETURN
2010          END
2020
2030
2040
2050
2060
2070 *--- Subroutine plots graph ---
2080          SUBROUTINE GPLOT(FDOM,L2)
2090
2100          REAL FDOM(100),INC,XP,YP
2110          INTEGER L1,L2
2120
2130 *--- Set position of each plot ---
2140          INC = FLOAT(L2)*23.7/128.
2150
2160 *--- Plot the graph ---
2170          XP = INC+FDOM(1)/15.
2180          CALL PLOT(XP , 14.9 , 3)
2190          DO 10 L1=2,100
2200             XP = INC+FDOM(L1)/15.
2210             YP = 14.9-FLOAT(L1)*14.9/100.
2220             CALL PLOT(XP , YP , 2)
2230 10      CONTINUE
2240
2250          RETURN
2260          END
2270
2280
2290
2300
2310 *--- Subroutine correlates FTT with magnitude ---
2320 *--- response of ear ---
2330          SUBROUTINE CORLAT(FDOM,ENGINC,MEAN,L1,L2)
2340
2350          CHARACTER*60 MESSAG
2360          REAL FDOM(100),EAR(100),COEF(36),FE,FMEAN,EMEAN,
2370          &FSQ,ESQ,N,D,ENGINC,MEAN(100)
2380          INTEGER L1,L2,L3,L4,LDEG,NUM
2390
2400          REWIND 12
2410 *--- Check for start of a new sound or a new direction ---
2420          IF (L2 .EQ. 4) THEN
2430             IF (L1 .EQ. 1) THEN
2440                MESSAG = 'CORRELATION COEFFICIENTS FOR NEXT SOUND'
2450                WRITE(*,104) MESSAG
2460 104      FORMAT('1','*****')
2470          & /1X,A39/'*****')
2480             END IF
2490             MESSAG='CORRELATION COEFFICIENT FOR SOUND AT      DEGREES'
2500             LDEG = (L1-1)*10
2510             WRITE (MESSAG(38:40) , 111) LDEG
2520 111      FORMAT(I3)
2530             WRITE (*,101) MESSAG
2540 101      FORMAT (//////,1X,'*****',A48,'*****')
2550             END IF
2560
2570 *--- Correlate with each direction in turn ---

```

```

2580      DO 10 L3=1,36
2590      READ(12,*) (EAR(L4),L4=1,100)
2600      FE=0.
2610      FMEAN=0.
2620      EMEAN=0.
2630      FSQ=0.
2640      ESQ=0.
2650          DO 20 L4=1,100
2660              EAR(L4) = EAR(L4)-MEAN(L4)
2670              FE=FE+FDOM(L4)*EAR(L4)
2680              FMEAN=FMEAN+FDOM(L4)/100.
2690              EMEAN=EMEAN+EAR(L4)/100.
2700              FSQ=FSQ+FDOM(L4)*FDOM(L4)
2710              ESQ=ESQ+EAR(L4)*EAR(L4)
2720 20      CONTINUE
2730      N=FE-100.*FMEAN*EMEAN
2740      D=SQRT((FSQ-100.*FMEAN*FMEAN)*(ESQ-100.*EMEAN*EMEAN))
2750      COEF(L3) = N/D
2760 10      CONTINUE
2770
2780 *--- Print energy increment from previous FTT ---
2790      MESSAG = 'ENERGY INCREMENT IS'
2800      WRITE(*,103)MESSAG,ENGINC
2810 103      FORMAT(/,1X,A19,F9.2)
2820
2830 *--- Print correlation coefficients ---
2840      WRITE(*,102) (COEF(L3),L3=1,36)
2850 102      FORMAT(1X,18(F4.2,1X),/,1X,18(F4.2,1X))
2860
2870 *--- Write correlation coefficients to file for ---
2880 *--- plotting by SACLANT routine ---
2890      NUM = 20+((L1+5)/6)
2900      IF (L2 .EQ.4)THEN
2910          WRITE(NUM,*)36,28
2920          WRITE(NUM,*)1,36,1,25
2930      END IF
2940
2950      IF(L2 .GT. 16)THEN
2960          WRITE(NUM,105)(COEF(L3),L3=1,36)
2970 105      FORMAT(5(6E13.5,/),6E13.5)
2980      END IF
2990
3000      RETURN
3010      END

```

```

10 ! *****
20 ! *****PROGRAM FFT*****
30 ! *****
40 !
50 ! *** Calculates magnitude response of a 128 sample sequence ***
60 ! *** Adapted from software distributed by Hewlett-Packard ***
70 !
80 OPTION BASE 1
90 DIM R(64),I(64),N(128)
100 F=1 @ N=128 @ N2=N/2 @ P1=7 @ J=0
110 GOSUB 180
120 STOP
130 END
140 J=0
150 !
160 ! *** Read time sequence ***
170 !
180 CLEAR @ BEEP
190 DISP "Enter file name: ";@ INPUT N$
200 ASSIGN# 1 TO N$
210 READ# 1 ; N( )
220 ASSIGN# 1 TO *
230 !
240 ! *** Calculate quadrature and in-phase components ***
250 !
260 FOR I=1 TO 128 STEP 2
270 R((I+1)/2)=N(I)
280 I((I+1)/2)=N(I+1)
290 NEXT I
300 GOSUB 490
310 B=0
320 !
330 ! Calculate magnitude response ***
340 !
350 FOR I=1 TO 32
360 R(I)=20*LGT (SQR (R(I)*R(I)+I(I)*I(I)))
370 IF R(I)>B THEN B=R(I)
380 NEXT I
390 !
400 ! *** Plot response ***
410 !
420 GRAPH @ GCLEAR @ FRAME
430 SCALE 1,32,0,1.1
440 AXES 16,1.1
450 FOR I=1 TO 32
460 DRAW I,R(I)/B
470 NEXT I
480 PRINT @ PRINT @ RETURN
490 B=N2
500 RAD
510 K=0
520 FOR J=1 TO N2-1
530 I=2
540 IF K<N2/I THEN 560
550 K=K-N2/I @ I=I+I @ GOTO 540
560 K=K+N2/I
570 IF K<= J THEN 590
580 A=R(J+1) @ R(J+1)=R(K+1) @ R(K+1)=A @ A=I(J+1) @ I(J+1)=I(K+1) @ I(K+1)=A
590 NEXT J
600 G=.5 @ P2=1

```

```

630 P2=(1-2*(I=1))*SQR ((1+P2)/2)
640 FOR R=1 TO G
650 FOR J=R TO N2 STEP G+G
660 I(K)=J+G @ A=C*R(K)+E*I(K) @ B=E*R(K)-C*I(K) @ R(K)=R(J)
-A @ I(K)=I(J)+B @ R(J)=R(J)+A @ I(J)=I(J)-B
670 NEXT J
680 A=E*P2+C*Q @ C=C*P2-E*Q @ E=A
690 NEXT R
700 NEXT I
710 A=PI/N2 @ P2=COS(A) @ Q=F*SIN(A) @ A=R(1) @ R(1)=A+I(1) @ I(1)=A-I(1)
720 R(1)=R(1)/2 @ I(1)=I(1)/2
730 C=F @ E=0
740 FOR J=2 TO N2/2
750 A=E*P2+C*Q @ C=C*P2-E*Q @ E=A @ K=N2-J+2 @ A=R(J)+R(K)
760 B=(I(J)+I(K))*C-(R(J)-R(K))*E @ U=I(J)-I(K)
770 V=(I(J)+I(K))*E+(R(J)-R(K))*C
780 R(J)=(A+B)/2 @ I(J)=(U-V)/2 @ R(K)=(A-B)/2 @ I(K)=-((U+V)/2)
790 NEXT J
800 I(N2/2+1)=-I(N2/2+1)
810 IF F=-1 THEN 510
820 FOR J=1 TO N2
830 R(J)=R(J)/N2 @ I(J)=I(J)/N2
840 NEXT J
850 RETURN

```

```

10 ! *****
20 ! *****PROGRAM CORPLT*****
30 ! *****
40 !
50 ! *** Program correlates a received speech signal with ***
60 ! *** predetermined spectra from 36 directions ***
70 !
80 CLEAR
90 DISP "A PROGRAM IS CURRENTLY RUNNING" @ DISP
100 DISP "Do not tamper with this machine until the message: 'PROGRAM END' appears on the screen"
110 OPTION BASE 1
120 DIM M(100),N(100),S(100),C(36)
130 FOR I1=1 TO 36
140 !
150 ! *** Read speech spectrum ***
160 ASSIGN# 1 TO "S"&VAL$(I1*10)
170 READ# 1 ; S()
180 ASSIGN# 1 TO *
190 !
200 ! *** Read mean of predetermined spectra ***
210 ASSIGN# 1 TO "MEAN"
220 READ# 1 ; M()
230 ASSIGN# 1 TO *
240 FOR I=30 TO 100
250 S(I)=S(I)/M(I)
260 NEXT I
270 !
280 ! ***Read predetermined spectra***
290 FOR I=1 TO 36
300 ASSIGN# 1 TO "N"&VAL$(I*10)
310 READ# 1 ; N()
320 ASSIGN# 1 TO *
330 FOR J=30 TO 100
340 N(J)=N(J)/M(J)
350 NEXT J
360 !
370 ! ***Obtain correlation coefficient ***
380 P=0 @ S1=0 @ S2=0 @ X2=0 @ Y2=0
390 FOR J=30 TO 100
400 P=P+S(J)*N(J)
410 X2=X2+S(J)*S(J)
420 Y2=Y2+N(J)*N(J)
430 S1=S1+S(J)
440 S2=S2+N(J)
450 NEXT J
460 C(I)=(P-S1*S2/71)/SQR ((X2-S1*S1/71)*(Y2-S2*S2/71))
470 NEXT I
480 ! ***Plot response of head***
490 IF I1#1 THEN GOTO 730
500 PLOTTER IS 705
510 GCLEAR
520 LOCATE 15,135,10,90
530 FRAME @ SCALE 0,360,360,0
540 LAXES -45,-45,0,360
550 ! ***Number Y axis***
560 DEG @ LDIR 270 @ LORG 6
570 FOR I=1 TO 7
580 F=(I-1)*60 @ PLOT 0,F @ PLOT 3.3,F @ PEN UP
590 MOVE -3.3 F @ LABEL VAL$(F)

```

```
620 MOVE 180,378
630 LORG 6
640 LABEL "Received angle (degrees)"
650 MOVE 180,-3.6 @ LORG 4 @ CSIZE 3.75
660 LABEL "Correlation coefficient"
670 MOVE -14,180 @ LORG 6
680 DEG @ LDIR 270 @ CSIZE 3.5
690 LABEL "Angle (degrees)"
700 MOVE 365,180
710 LORG 4 @ CSIZE 4
720 LABEL "CORRELATION COEFFICIENT VS ANGLE"
730 FOR I=1 TO 36 @ C(I)=C(I)*20+I1*10 @ NEXT I
740 FOR I=1 TO 36
750 PLOT C(I),I*10
760 NEXT I
770 PEN UP
780 NEXT I1
790 PEN UP
800 DISP "PROGRAM END"
810 END
```

APPENDIX C TRANSDUCER EQUIVALENT CIRCUIT AND RECEIVER DESIGN

A piezo-ceramic transducer can be modelled using the following equivalent circuit:

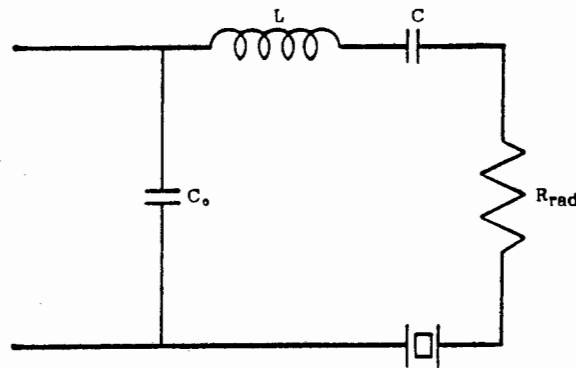


Figure C.1 - Transducer equivalent circuit.

Values of the circuit elements are determined from the transducer circle diagram: a plot of susceptance versus conductance at frequencies around resonance.

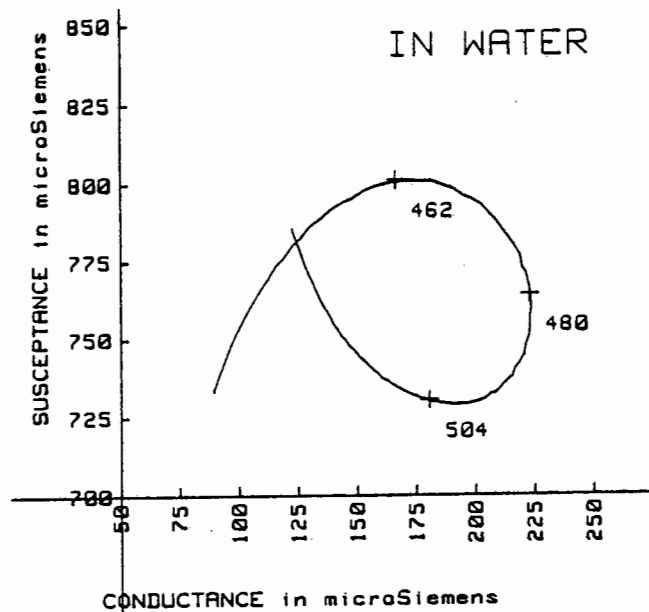


Figure C.2 - Circle diagram of PZT crystals used in the experimental sonar.

The frequency at resonance is 480kHz. The susceptance at this frequency is 760 microsiemens, consequently the shunt capacitance is 250pF. The radiation resistance is the reciprocal of the conductance at resonance: 4,55k . The inductance is determined using the bandwidth of 42kHz indicated on the diagram:

$$B/W = R/(2\pi L) \quad (C.1)$$

$$\text{Hence, } L = 4,55/(2.\pi.42) = 17,2\text{mH} \quad (C.2)$$

The series capacitance is determined using the expression for resonant frequency:

$$\omega_0^2 = 1/LC \quad (C.3)$$

$$\text{Hence, } C = 1/((2.\pi.480000)^2.17,2\text{E-3}) = 6,3\text{pF} \quad (C.4)$$

A shunt inductance was used to match the output impedance of the transducer to the input impedance of the receiver by cancelling out the clamp capacitance at resonance. Hence:

$$L = 1/((2.\pi.480000)^2.250\text{E-12}) = 0,44\text{mH} \quad (C.5)$$

The receiver is a modified version of a wideband amplifier designed by Runciman (1986).

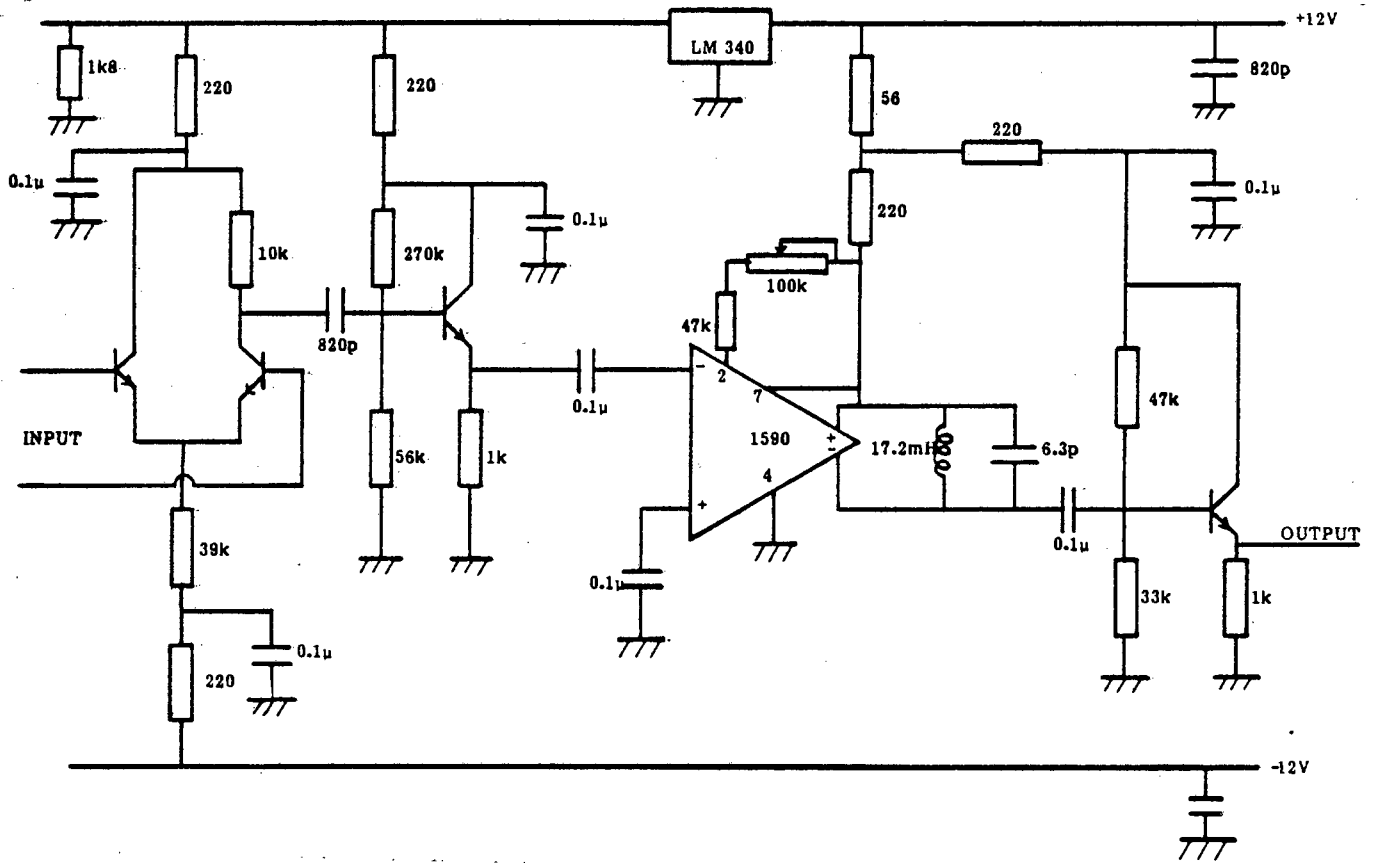


Figure C.3 - Receiver circuit diagram.

APPENDIX D
COMPUTER PROGRAMS USED BY THE ACTIVE SONAR

D.1	PROGRAM CAL312 - steps sonar receiver through 0,19 degree increments, and stores ASCII formatted target echoes on flexible disc.	D-2
D.2	PROGRAM SETSONAR - calculates the magnitude responses of recorded echoes.	D-4
D.3	PROGRAM RUNSONAR - cross-correlates received spectra with predetermined magnitude responses.	D-6
D.4	PROGRAM SUBSONAR - locates weaker masked targets by removing the contributions of stronger targets to incident spectra.	D-10
D.5	PROGRAM SETRANGE - determines the magnitude responses of recorded echoes using the FTT.	D-15
D.6	PROGRAM RANGESONAR - simultaneously determines the bearing and range of a target.	D-17

```

10 | *****
20 | *****PROGRAM CAL312*****
30 | *****
40 |
50 | ***Program to download 312 values from PHILLIPS 'scope***
60 | ***at each of 210 angular positions***
70 |
80 CLEAR
90 OPTION BASE 1
100 SHORT V1(312)
110 DIM L$(80)
120 ASSIGN# 1 TO "PING2"
130 FOR I1=1 TO 210
140 |
150 | *** Step sonar receiver***
160 CONTROL 3,2 ; 16
170 WAIT 500
180 CONTROL 3,2 ; 0
190 WAIT 2000
200 CLEAR 7 @ RESET 7
210 CONTROL 7,16 ; 1,10
220 OUTPUT 708 USING "K" ; "SPR"
230 OUTPUT 708 USING "K" ; "USP /"
240 OUTPUT 708 USING "K" ; "TIM 10E-3/BGN 950/END 4096/CNT 1/DAT ALL/DAT ?"
250 |
260 | **** Implement software trigger
270 T=16 ! Set trigger level
280 F1=0 @ C1=10 @ V1(312)=0
290 |
300 FOR I=1 TO 10
310 ENTER 708 ; V1(I)
320 NEXT I
330 |
340 C1=C1+1
350 IF F1=1 OR ABS (V1(C1-1)-V1(C1-2))>T THEN 400
360 IF V1(312)=0 THEN 390
370 FOR I=1 TO 9 @ V1(I)=V1(303+I) @ NEXT I
380 C1=10 @ V1(312)=0
390 ENTER 708 ; V1(C1) @ GOTO 460
400 IF C1>312 THEN ENTER 708 ; D0 GOTO 470
410 IF F1=1 THEN 440
420 FOR I=1 TO 10 @ V1(I)=V1(C1-11+I) @ NEXT I
430 C1=11 @ F1=1
440 ENTER 708 ; V1(C1)
450 |
460 GOTO 340
470 IF C1>312 THEN 510
480 |
490 | ***Plot data***
500 |
510 CLEAR 7 @ RESET 7
520 GRAPH
530 GCLEAR
540 SCALE 0,312,0,256
550 MOVE 0,0
560 FOR I=1 TO 312
570 PLOT I,V1(I)
580 NEXT I
590 | IF I1/10=INT (I1/10) THEN PRINT I1 @ COPY
600 |
610 | ***Store data in strings for transferral to Sperry mainframe***
620 |

```

```
630 CRT OFF
640 FOR J=1 TO 12
650 L$=""
660 FOR K=1 TO 26
670 L$=L$&VAL$ (V1((J-1)*26+K)+256)
680 NEXT K
690 ! DISP L$
700 PRINT# 1,(I1-1)*12+J ; L$
710 NEXT J
720 CRT ON
730 NEXT I1
740 ASSIGN# 1 TO *
750 BEEP
760 END
```

```

100 *****PROGRAM SETSONAR*****
110 *
120 * Calculates final FTT of impulse response of receiver
130 * at .19 degree angular increments between 0 and 40
140 * degrees. These are stored for reference by program
150 * RUNSONAR.
160 *
170 * By: P. A. Tollman
180 * 7 January 1987
190 *
200 *****
210 *
220     REAL RESP(312),FRESP(200)
230     INTEGER L1,L2
240
250 *--- Calculate for each direction in turn ---
260     DO 10 L1=1,210
270         READ(11,*)(RESP(L2),L2=1,312)
280
290 *--- Calculate final FTT of receiver impulse response ---
300     CALL FTT(RESP,FRESP)
310
320 *---Store FTT ---
330     WRITE(12,101)(FRESP(L2),L2=1,200)
340 101     FORMAT(39(5E13.5,/),5E13.5)
350 10     CONTINUE
360
370     STOP
380     END
390
400
410
420
430     SUBROUTINE FTT(RESP,FRESP)
440 *--- Calculates final FTT of impulse response ---
450
460     REAL RESP(312),FRESP(200),FREQ,FPHASE(200),FQUAD(200),TM
470     INTEGER L1,L2
480     PARAMETER (PI=3.141592654)
490
500 *--- Set time between samples ---
510     TM=1./2.E6
520
530 *--- Step through time samples and frequencies ---
540     DO 10 L1=1,312
550         DO 20 L2=1,200
560             IF(L1 .EQ. 1)THEN
570                 FPHASE(L2)=TM*RESP(1)
580                 FQUAD(L2)=0.
590                 GOTO 20
600             END IF
610             FREQ=2.*PI*5000.*FLOAT(L2)
620             FPHASE(L2) = FPHASE(L2)+
630             &             TM*RESP(L1)*COS(FREQ*TM*FLOAT(L1))
640             FQUAD(L2) = FQUAD(L2)+
650             &             TM*RESP(L1)*SIN(FREQ*TM*FLOAT(L1))
660 20     CONTINUE
670 10     CONTINUE
680
690     DO 30 L1=1,200
700     FRESP(L1)=(SQRT(FPHASE(L1)*FPHASE(L1)+
710     &             FQUAD(L1)*FQUAD(L1)))

```

720 30	CONTINUE
730	
740	RETURN
750	END

```

100 *****PROGRAM RUNSONAR*****
110 *
120 * Program attempts to locate a sound.
130 * It calculates the FFT and correlates this
140 * at 0.19 degree increments with stored
150 * spectra.
160 *
170 * P. A. Tollman
180 * 8 January 1987
190 *
200 *****
210
220 REAL SOUND1(312),SOUND2(312),SOUND3(312),MEAN(200),FDM(200)
230 INTEGER L1,L2,L3,N1,N2,N3
240
250 *--- Read the mean magnitude response of the ---
260 *--- ear to divide through by ---
270 READ(14,*)(MEAN(L1) , L1=1,200)
280
290 *--- Open plotting file ---
300 CALL PLOTS(0,0,0)
310
320 N1=80
330 N2=160
340 N3=110
350
360 *--- Calculate for each position in required ---
370 DO 10 L2=1,N1
380 READ(11,*)(SOUND1(L3) , L3=1,312)
390 10 CONTINUE
400
410 REWIND 11
420 DO 20 L2=1,N2
430 READ(11,*)(SOUND2(L3) , L3=1,312)
440 20 CONTINUE
450
460 REWIND 11
470 DO 30 L2=1,N3
480 READ(11,*)(SOUND3(L3) , L3=1,312)
490 30 CONTINUE
500
510 *--- Combine to form multiple targets ---
520 DO 40 L2=1,312
530 SOUND1(L2)=SOUND1(L2)*1.+SOUND2(L2)*1.+SOUND3(L2)*1.
540 40 CONTINUE
550
560 *--- Setup graph and axes ---
570 CALL GSET(L1)
580
590 *--- Calculate FTT. From subroutine FTT, call ---
600 *--- plotting routine and correlation routine ---
610 CALL FTT(SOUND1,MEAN,FDM)
620
630 *--- Close off plots ---
640 CALL PLOT(0,0,999)
650
660 STOP
670 END
680
690
700
710

```



```

720 *--- Subroutine GSET sets up axes ---
730     SUBROUTINE GSET (L1)
740
750     CHARACTER*60 MESSAG
760     REAL XINC,XWR,XNUM,YINC,YWR,YNUM
770     INTEGER L1,L2,LDEG
780
790 *--- Open new page in plot file ---
800     CALL NEWPAG
810
820 *--- Plots to fit on A4 page,X-axis to be 25cm ---
830 *--- Y-axis to be 16cm. Scale from A4 using FACTOR ---
840     CALL MAGNFY (.707)
850
860 *--- Set page size (only necessary for GDP) ---
870     CALL PAGSIZ(32.0 , 22.0)
880
890 *--- Change to ink pens ---
900     MESSAG = 'PLS LOAD P1-BK/I3'
910     CALL OPMES (24 , MESSAG)
920
930 *--- Draw A4 page ---
940     CALL NEWPEN(1)
950     CALL PLOT(1.0 , 1.0 , -3)
960     CALL PLOT(0.0 , 20.9 , 2)
970     CALL PLOT(29.7 , 20.9 , 2)
980     CALL PLOT(29.7 , 0.0 , 2)
990     CALL PLOT(0.0 , 0.0 , 2)
1000
1010 *--- Establish new origin ---
1020     CALL PLOT(4.5 , 9. , -3)
1030
1040 *--- Draw axes ---
1050     CALL PLOT(23.0 , 0.0 , 2)
1060     CALL PLOT(0.0 , -8.0 , 3)
1070     CALL PLOT(0.0 , 8.0 , 2)
1080
1090 *--- Mark off axes ---
1100 *--- X-axis 4 divisions of 10deg each ---
1110     XINC = 23./4.
1120     XWR = 0.
1130     DO 10 L2=1,4
1140         XWR = XWR+XINC
1150         CALL SYMBOL(XWR , 0. , .5 , 13 , 0. , -1)
1160         XNUM = FLOAT(L2)*10.
1170         XP=XWR-.3
1180         CALL NUMBER(XP , -.6 , .25 , XNUM , 0. , 0)
1190 10     CONTINUE
1200
1210 *--- Y-axis has 4 divisions of .5 each ---
1220     YINC=4.
1230     YWR = -12.
1240     DO 20 L2=1,5
1250         YWR = YWR+YINC
1260         CALL SYMBOL(0. , YWR , .5 , 13 , 90. , -1)
1270         YNUM = FLOAT(-3+L2)/2.
1280         YP = YWR-.2
1290         CALL NUMBER(-1.4 , YP , .25 , YNUM , 0. , 1)
1300 20     CONTINUE
1310
1320 *--- Draw labels ---
1330 *--- Title graph ---

```

```

1340      MESSAG = 'CORRELATION COEFFICIENT VS ANGLE'
1350      CALL SYMBOL(3.6 , 8.7 , .5 , MESSAG , 0. , 32)
1360
1370 *--- Label X-axis ---
1380      MESSAG = 'ANGLE (DEGREES)'
1390      CALL SYMBOL(18.5 , -1.5 , .3 , MESSAG , 0. , 15)
1400
1410 *--- Label Y-axis ---
1420      MESSAG = 'CORRELATION COEFFICIENT'
1430      CALL SYMBOL(-2.3 , 1.3 , .3 , MESSAG , 90. , 23)
1440
1450      RETURN
1460      END
1470
1480
1490
1500
1510
1520 *--- Subroutine calculates FTT ---
1530      SUBROUTINE FTT(TDOM,MEAN,FDOM)
1540
1550      REAL TDOM(312),FDOM(200),FPHASE(200),FQUAD(200),FREQ,TM
1560      &,MEAN(200)
1570      INTEGER L1,L2,L3
1580      PARAMETER (PI=3.141592654)
1590
1600 *--- Set time between samples ---
1610 *--- Initialise energy increment to 0 ---
1620      TM = 1./2.E6
1630
1640 *--- Step through time samples ---
1650      DO 10 L2=1,312
1660 *--- Step through frequencies ---
1670      DO 20 L3=1,200
1680          IF(L2 .EQ. 1) THEN
1690              FPHASE(L3)=TM*TDOM(1)
1700              FQUAD(L3)=0.
1710              GOTO 20
1720          END IF
1730          FREQ = 2.*PI*5000.*FLOAT(L3)
1740          FPHASE(L3)=FPHASE(L3)+TM*TDOM(L2)*COS(FREQ*TM*FLOAT(L2))
1750          FQUAD(L3)=FQUAD(L3)+TM*TDOM(L2)*SIN(FREQ*TM*FLOAT(L2))
1760 20      CONTINUE
1770 10      CONTINUE
1780
1790          DO 30 L3=1,200
1800              FDOM(L3)=SQRT(FPHASE(L3)*FPHASE(L3)+FQUAD(L3)*FQUAD(L3))
1810 30      CONTINUE
1820
1830      DO 60 L3=1,200
1840          FDOM(L3)=FDOM(L3)/MEAN(L3)
1850 60      CONTINUE
1860
1870      CALL CORLAT(FDOM,MEAN)
1880
1890      RETURN
1900      END
1910
1920
1930
1940
1950

```

```

1960 *--- Subroutine plots graph ---
1970     SUBROUTINE GPLOT(COEF)
1980
1990     REAL COEF(210),XP,YP
2000     INTEGER L1
2010
2020 *--- Plot the graph ---
2030     CALL PLOT (0. , 0. , 3)
2040     DO 10 L1=1,210
2050         XP=FLOAT(L1-1)*23./210.
2060         YP=COEF(L1)*8.
2070         CALL PLOT(XP , YP , 2)
2080 10     CONTINUE
2090
2100     RETURN
2110     END
2120
2130
2140
2150
2160 *--- Subroutine correlates FFT with magnitude ---
2170 *--- response of ear ---
2180     SUBROUTINE CORLAT(FDOM,MEAN)
2190
2200     CHARACTER*60 MESSAG
2210     REAL FDOM(200),PREDET(200),COEF(210),FE,FMEAN,EMEAN,
2220     &FSQ,ESQ,N,D,MEAN(200)
2230     INTEGER L3,L4
2240
2250     REWIND 12.
2260
2270 *--- Correlate with each direction in turn ---
2280     DO 10 L3=1,210
2290         READ(12,*) (PREDET(L4),L4=1,200)
2300         FE=0.
2310         FMEAN=0.
2320         EMEAN=0.
2330         FSQ=0.
2340         ESQ=0.
2350         DO 20 L4=1,200
2360             PREDET(L4) = PREDET(L4)/MEAN(L4)
2370             FE=FE+FDOM(L4)*PREDET(L4)
2380             FMEAN=FMEAN+FDOM(L4)/200.
2390             EMEAN=EMEAN+PREDET(L4)/200.
2400             FSQ=FSQ+FDOM(L4)*FDOM(L4)
2410             ESQ=ESQ+PREDET(L4)*PREDET(L4)
2420 20     CONTINUE
2430         N=FE-200.*FMEAN*EMEAN
2440         D=SQRT((FSQ-200.*FMEAN*FMEAN)*(ESQ-200.*EMEAN*EMEAN))
2450         COEF(L3) = N/D
2460 10     CONTINUE
2470
2480 *--- Plot the graph ---
2490     CALL GPLOT(COEF)
2500
2510 *--- Print correlation coefficients ---
2520     WRITE(*,102) (COEF(L3),L3=1,210)
2530 102    FORMAT(1X,18(F4.2,1X),/,1X,18(F4.2,1X))
2540
2550
2560     RETURN
2570     END

```

```

100 *****PROGRAM SUBSONAR*****
110 *
120 * Program attempts to locate a sound.
130 * It calculates the FFT and correlates this
140 * at 0.19 degree increments with stored
150 * spectra. Weak targets are located by
160 * removing the spectrum contribution of
170 * stronger targets.
180 *
190 * P. A. Tollman
200 * 8 January 1987
210 *
220 *****
230
240 REAL SOUND1(312),SOUND2(312),SOUND3(312),MEAN(200),FDM(200)
250 INTEGER L1,L2,L3
260
270 *--- Read the mean magnitude response of the --
280 *--- ear to divide through by ---
290 READ(14,*)(MEAN(L1) , L1=1,200)
300
310 *--- Open plotting file ---
320 CALL PLOTS(0,0,0)
330
340 N1=160
350 N2=160
360 N3=110
370
380 *--- Calculate for each position in required ---
390 DO 10 L2=1,N1
400 READ(11,*)(SOUND1(L3) , L3=1,312)
410 10 CONTINUE
420
430 REWIND 11
440 DO 20 L2=1,N2
450 READ(11,*)(SOUND2(L3) , L3=1,312)
460 20 CONTINUE
470
480 REWIND 11
490 DO 30 L2=1,N3
500 READ(11,*)(SOUND3(L3) , L3=1,312)
510 30 CONTINUE
520
530 *--- Combine to form multiple targets ---
540 DO 40 L2=1,312
550 SOUND1(L2)=SOUND1(L2)*.5+SOUND2(L2)*.5+SOUND3(L2)*.30
560 40 CONTINUE
570
580 *--- Calculate FTT. From subroutine FTT, call ---
590 *--- plotting routine and correlation routine ---
600 CALL FTT(SOUND1,MEAN,FDM)
610
620 *--- Close off plots ---
630 CALL PLOT(0,0,999)
640
650 STOP
660 END
670
680
690
700
710 *--- Subroutine GSET sets up axes ---

```

```

720 SUBROUTINE GSET (L1)
730
740 CHARACTER*60 MESSAG
750 REAL XINC,XWR,XNUM,YINC,YWR,YNUM
760 INTEGER L1,L2,LDEG
770
780 *--- Open new page in plot file ---
790 CALL NEWPAG
800
810 *--- Plots to fit on A4 page,X-axis to be 25cm ---
820 *--- Y-axis to be 16cm. Scale from A4 using FACTOR ---
830 CALL MAGNFY (.707)
840
850 *--- Set page size (only necessary for GDP) ---
860 CALL PAGESIZ(32.0 , 22.0)
870
880 *--- Change to ink pens ---
890 MESSAG = 'PLS LOAD P1-BK/I3'
900 CALL OPMES (24 , MESSAG)
910
920 *--- Draw A4 page ---
930 CALL NEWPEN(1)
940 CALL PLOT(1.0 , 1.0 , -3)
950 CALL PLOT(0.0 , 20.9 , 2)
960 CALL PLOT(29.7 , 20.9 , 2)
970 CALL PLOT(29.7 , 0.0 , 2)
980 CALL PLOT(0.0 , 0.0 , 2)
990
1000 *--- Establish new origin ---
1010 CALL PLOT(4.5 , 9. , -3)
1020
1030 *--- Draw axes ---
1040 CALL PLOT(23.0 , 0.0 , 2)
1050 CALL PLOT(0.0 , -8.0 , 3)
1060 CALL PLOT(0.0 , 8.0 , 2)
1070
1080 *--- Mark off axes ---
1090 *--- X-axis 4 divisions of 10deg each ---
1100 XINC = 23./4.
1110 XWR = 0.
1120 DO 10 L2=1,4
1130 XWR = XWR+XINC
1140 CALL SYMBOL(XWR , 0. , .5 , 13 , 0. , -1)
1150 XNUM = FLOAT(L2)*10.
1160 XP=XWR-.3
1170 CALL NUMBER(XP , -.6 , .25 , XNUM , 0. , 0)
1180 10 CONTINUE
1190
1200 *--- Y-axis has 4 divisions of .5 each ---
1210 YINC=4.
1220 YWR = -12.
1230 DO 20 L2=1,5
1240 YWR = YWR+YINC
1250 CALL SYMBOL(0. , YWR , .5 , 13 , 90. , -1)
1260 YNUM = FLOAT(-3+L2)/2.
1270 YP = YWR-.2
1280 CALL NUMBER(-1.4 , YP , .25 , YNUM , 0. , 1)
1290 20 CONTINUE
1300
1310 *--- Draw labels ---
1320 *--- Title graph ---
1330 MESSAG = 'CORRELATION COEFFICIENT VS ANGLE'

```

```

1340      CALL SYMBOL(3.6 , 8.7 , .5 , MESSAG , 0. , 32)
1350
1360 *--- Label X-axis ---
1370      MESSAG = 'ANGLE (DEGREES)'
1380      CALL SYMBOL(18.5 , -1.5 , .3 , MESSAG , 0. , 15)
1390
1400 *--- Label Y-axis ---
1410      MESSAG = 'CORRELATION COEFFICIENT'
1420      CALL SYMBOL(-2.3 , 1.3 , .3 , MESSAG , 90. , 23)
1430
1440      RETURN
1450      END
1460
1470
1480
1490
1500
1510 *--- Subroutine calculates FTT ---
1520      SUBROUTINE FTT(TDOM,MEAN,FDOM)
1530
1540      REAL TDOM(312),FDOM(200),FPHASE(200),FQUAD(200),FREQ,TM
1550      &,MEAN(200)
1560      INTEGER L1,L2,L3
1570      PARAMETER (PI=3.141592654)
1580
1590 *--- Set time between samples ---
1600 *--- Initialise energy increment to 0 ---
1610      TM = 1./2.E6
1620
1630 *--- Step through time samples ---
1640      DO 10 L2=1,312
1650 *--- Step through frequencies ---
1660      DO 20 L3=1,200
1670          IF(L2 .EQ. 1) THEN
1680              FPHASE(L3)=TM*TDOM(1)
1690              FQUAD(L3)=0.
1700              GOTO 20
1710          END IF
1720          FREQ = 2.*PI*5000.*FLOAT(L3)
1730          FPHASE(L3)=FPHASE(L3)+TM*TDOM(L2)*COS(FREQ*TM*FLOAT(L2))
1740          FQUAD(L3)=FQUAD(L3)+TM*TDOM(L2)*SIN(FREQ*TM*FLOAT(L2))
1750 20      CONTINUE
1760 10      CONTINUE
1770
1780          DO 30 L3=1,200
1790              FDOM(L3)=SQRT(FPHASE(L3)*FPHASE(L3)+FQUAD(L3)*FQUAD(L3))
1800 30      CONTINUE
1810
1820      DO 60 L3=1,200
1830          FDOM(L3)=FDOM(L3)/MEAN(L3)
1840 60      CONTINUE
1850
1860      CALL CORLAT(FDOM,MEAN)
1870
1880      RETURN
1890      END
1900
1910
1920
1930
1940
1950 *--- Subroutine plots graph ---

```

```

1960      SUBROUTINE GPLOT(COEF)
1970
1980      REAL COEF(210),XP,YP
1990      INTEGER L1
2000
2010 *--- Plot the graph ---
2020      CALL PLOT (0. , 0. , 3)
2030      DO 10 L1=1,210
2040      XP=FLOAT(L1-1)*23./210.
2050      YP=COEF(L1)*8.
2060      CALL PLOT(XP , YP , 2)
2070 10      CONTINUE
2080
2090      RETURN
2100      END
2110
2120
2130
2140
2150 *--- Subroutine correlates FTT with magnitude ---
2160 *--- response of ear ---
2170      SUBROUTINE CORLAT(FDOM,MEAN)
2180
2190      CHARACTER*60 MESSAG
2200      REAL FDOM(200),PREDET(200),COEF(210),FE,FMEAN,EMEAN,
2210      &FSQ,ESQ,N,D,MEAN(200),NUM,DEN,K
2220      INTEGER L3,L4
2230
2240      DO 5 L0=1,10
2250      REWIND 12
2260
2270 *--- Correlate with each direction in turn ---
2280      DO 10 L3=1,210
2290      READ(12,*) (PREDET(L4),L4=1,200)
2300      FE=0.
2310      FMEAN=0.
2320      EMEAN=0.
2330      FSQ=0.
2340      ESQ=0.
2350      DO 20 L4=1,200
2360      PREDET(L4) = PREDET(L4)/MEAN(L4)
2370      FE=FE+FDOM(L4)*PREDET(L4)
2380      FMEAN=FMEAN+FDOM(L4)/200.
2390      EMEAN=EMEAN+PREDET(L4)/200.
2400      FSQ=FSQ+FDOM(L4)*FDOM(L4)
2410      ESQ=ESQ+PREDET(L4)*PREDET(L4)
2420
2430      IF(FLOAT((L0+2)/3).EQ.FLOAT(L0+2)/3..AND.L3.EQ.160)THEN
2440      NUM=FSQ-200.*FMEAN*FMEAN
2450      DEN=ESQ-200.*EMEAN*EMEAN
2460      END IF
2470
2480      IF(FLOAT((L0+1)/3).EQ.FLOAT(L0+1)/3..AND.L3.EQ.161)THEN
2490      NUM=FSQ-200.*FMEAN*FMEAN
2500      DEN=ESQ-200.*EMEAN*EMEAN
2510      END IF
2520
2530      IF(FLOAT((L0)/3).EQ.FLOAT(L0)/3..AND.L3.EQ.162)THEN
2540      NUM=FSQ-200.*FMEAN*FMEAN
2550      DEN=ESQ-200.*EMEAN*EMEAN
2560      END IF
2570

```

```

2580 20      CONTINUE
2590      N=FE-200.*FMEAN*EMEAN
2600      D=SQRT((FSQ-200.*FMEAN*FMEAN)*(ESQ-200.*EMEAN*EMEAN))
2610      COEF(L3) = N/D
2620 10      CONTINUE
2630
2640 *--- Setup graph and axes ---
2650      CALL GSET(L1)
2660
2670 *--- Plot the graph ---
2680      CALL GPLOT(COEF)
2690
2700 *--- Print correlation coefficients ---
2710      WRITE (*,*)NUM,DEN,K
2720      WRITE(*,102) (COEF(L3),L3=1,210)
2730 102      FORMAT(1X,/,18(F4.2,1X),/,1X,18(F4.2,1X))
2740
2750 *--- Remove contribution to spectrum ---
2760      IF(FLOAT((L0+2)/3).EQ.FLOAT(L0+2)/3.)THEN
2770      K=COEF(160)*NUM/DEN
2780      REWIND 12
2790      DO 30 L3=1,160
2800      READ(12,*)(PREDET(L4),L4=1,200)
2810 30      CONTINUE
2820      END IF
2830
2840      IF(FLOAT((L0+1)/3).EQ.FLOAT(L0+1)/3.)THEN
2850      K=COEF(161)*NUM/DEN
2860      REWIND 12
2870      DO 35 L3=1,161
2880      READ(12,*)(PREDET(L4),L4=1,200)
2890 35      CONTINUE
2900      END IF
2910
2920      IF(FLOAT((L0)/3).EQ.FLOAT(L0)/3.)THEN
2930      K=COEF(162)*NUM/DEN
2940      REWIND 12
2950      DO 37 L3=1,162
2960      READ(12,*)(PREDET(L4),L4=1,200)
2970 37      CONTINUE
2980      END IF
2990
3000      DO 40 L3=1,200
3010      FDOM(L3)=FDOM(L3)-K*PREDET(L3)/MEAN(L3)
3020 40      CONTINUE
3030 5      CONTINUE
3040
3050
3060      RETURN
3070      END

```



```

100 *****PROGRAM SETRANGE*****
110 *
120 * Calculates final FTT of impulse response of receiver *
130 * at .19 degree angular increments between 0 and 40 *
140 * degrees. These are stored for reference by program *
150 * RANGESONAR. *
160 * *
170 * By: P. A. Tollman *
180 * 7 January 1987 *
190 * *
200 *****
210 *
220     REAL RESP(312),FRESP(200)
230     INTEGER L1,L2
240
250 *--- Calculate for each direction in turn ---
260     DO 10 L1=1,210
270         READ(11,*)(RESP(L2),L2=1,312)
280
290 *--- Calculate final FTT of receiver impulse response ---
300     CALL FTT(RESP,FRESP)
310
320 *---Store FTT ---
330     WRITE(12,101)(FRESP(L2),L2=1,200)
340 101     FORMAT(39(5E13.5,/),5E13.5)
350 10     CONTINUE
360
370     STOP
380     END
390
400
410
420
430     SUBROUTINE FTT(RESP,FRESP)
440 *--- Calculates final FTT of impulse response ---
450
460     REAL RESP(312),FRESP(200),FREQ,FPHASE(200),FQUAD(200),TM
470     INTEGER L1,L2
480     PARAMETER (PI=3.141592654)
490
500 *--- Set time between samples ---
510     TM=1./2.E6
520     A=39270.
530
540 *--- Step through time samples and frequencies ---
550     DO 10 L1=1,312
560         DO 20 L2=1,200
570             IF(L1 .EQ. 1)THEN
580                 FPHASE(L2)=TM*RESP(1)
590                 FQUAD(L2)=0.
600                 GOTO 20
610             END IF
620             FREQ=2.*PI*5000.*FLOAT(L2)
630             FPHASE(L2) = FPHASE(L2)*EXP(-A*TM)+
640             &             TM*RESP(L1)*COS(FREQ*TM*FLOAT(L1))
650             FQUAD(L2) = FQUAD(L2)*EXP(-A*TM)+
660             &             TM*RESP(L1)*SIN(FREQ*TM*FLOAT(L1))
670 20     CONTINUE
680 10     CONTINUE
690
700     DO 30 L1=1,200
710         FRESP(L1)=(SQRT(FPHASE(L1))*FPHASE(L1)+

```

```
720      &      FQUAD(L1)*FQUAD(L1))  
730 30      CONTINUE  
740  
750      RETURN  
760      END
```

```

100 *****PROGRAM RANGESONAR***
110 *
120 * Program attempts to locate a sound.
130 * It calculates the FFT and correlates this
140 * at 0.19 degree increments with stored
150 * spectra.
160 *
170 * P. A. Tollman
180 * 8 January 1987
190 *
200 *****
210
220     REAL SOUND1(400),MEAN(200),FDM(200)
230     INTEGER L1,L2,L3
240
250 *--- Read the mean magnitude response of the --
260 *--- ear to divide through by ---
270     READ(14,*)(MEAN(L1) , L1=1,200)
280
290     DO 5 L1=1,400
300     SOUND1(L1)=0.
310 5    CONTINUE
320
330     N1=110
340
350 *--- Calculate for each position in required ---
360     DO 10 L2=1,N1
370     READ(11,*)(SOUND1(L3) , L3=1,312)
380 10    CONTINUE
390
400
410
420 *--- Calculate FTT. From subroutine FTT, call ---
430 *--- plotting routine and correlation routine ---
440     CALL FTT(SOUND1,MEAN,FDM)
450
460     STOP
470     END
480
490
500
510
520
530
540 *--- Subroutine calculates FTT ---
550     SUBROUTINE FTT(TDOM,MEAN,FDM)
560
570     REAL TDOM(400),FDM(200),FPHASE(200),FQUAD(200),FREQ,TM
580     &,MEAN(200),FS(200)
590     INTEGER L1,L2,L3
600     PARAMETER (PI=3.141592654)
610
620 *--- Set time between samples ---
630 *--- Initialise energy increment to 0 ---
640     TM = 1./2.E6
650     A=39270
660
670 *--- Step through time samples ---
680     DO 10 L2=1,400
690 *--- Step through frequencies ---
700     DO 20 L3=1,200
710         IF(L2 .EQ. 1) THEN

```

```

720      FPHASE(L3)=TM*TDOM(1)
730      FQUAD(L3)=0.
740      GOTO 20
750      END IF
760      FREQ = 2.*PI*5000.*FLOAT(L3)
770      FPHASE(L3)=FPHASE(L3)*EXP(-A*TM)
780      FPHASE(L3)=FPHASE(L3)+TM*TDOM(L2)*COS(FREQ*TM*FLOAT(L2))
790      FQUAD(L3)=FQUAD(L3)*EXP(-A*TM)
800      FQUAD(L3)=FQUAD(L3)+TM*TDOM(L2)*SIN(FREQ*TM*FLOAT(L2))
810 20    CONTINUE
820      IF (L2.GT.200.AND.FLOAT(L2)/4..EQ.FLOAT(L2/4)) THEN
830
840          DO 30 L3=1,200
850              FDOM(L3)=SQRT(FPHASE(L3)*FPHASE(L3)+FQUAD(L3)*FQUAD(L3))
860 30      CONTINUE
870
880
890          DO 60 L3=1,200
900              FDOM(L3)=FDOM(L3)/MEAN(L3)
910 60      CONTINUE
920
930          CALL CORLAT(FDOM,MEAN,L2)
940      END IF
950
960 10    CONTINUE
970
980
990      RETURN
1000     END
1010
1020
1030
1040
1050
1060
1070
1080 *--- Subroutine correlates FTT with magnitude ---
1090 *--- response of ear ---
1100     SUBROUTINE CORLAT(FDOM,MEAN,L2)
1110
1120     CHARACTER*60 MESSAG
1130     REAL FDOM(200),PREDET(200),COEF(210),FE,FMEAN,EMEAN,
1140     &FSQ,ESQ,N(210),D(210),MEAN(200)
1150     INTEGER L3,L4
1160
1170     REWIND 12
1180
1190 *--- Correlate with each direction in turn ---
1200     DO 10 L3=1,210
1210         READ(12,*) (PREDET(L4),L4=1,200)
1220         FE=0.
1230         FMEAN=0.
1240         EMEAN=0.
1250         FSQ=0.
1260         ESQ=0.
1270         DO 20 L4=1,200
1280             PREDET(L4) = PREDET(L4)/MEAN(L4)
1290             FE=FE+FDOM(L4)*PREDET(L4)
1300             FMEAN=FMEAN+FDOM(L4)/200.
1310             EMEAN=EMEAN+PREDET(L4)/200.
1320             FSQ=FSQ+FDOM(L4)*FDOM(L4)
1330             ESQ=ESQ+PREDET(L4)*PREDET(L4)

```

```

1340 20      CONTINUE
1350      N(L3)=FE-200.*FMEAN*EMEAN
1360      IF(L2.LE.312)THEN
1370      D(L3)=SQRT((FSQ-200.*FMEAN*FMEAN)*(ESQ-200.*EMEAN*EMEAN))
1380      END IF
1390      COEF(L3) = N(L3)/D(L3)
1400 10      CONTINUE
1410
1420
1430 *--- Print correlation coefficients ---
1440 CCC      WRITE(*,102) (COEF(L3),L3=1,210)
1450 CCC102    FORMAT(1X,18(F4.2,1X),/,1X,18(F4.2,1X))
1460
1470 *--- Write correlation coefficients to file for ---
1480 *--- plotting by SACLANT routine ---
1490      NUM=21
1500      IF (L2 .EQ.204)THEN
1510      WRITE(NUM,*)210,50
1520      WRITE(NUM,*)0,1,0,1
1530      END IF
1540
1550      WRITE(NUM,105)(COEF(L3),L3=1,210)
1560 105      FORMAT(41(5E13.5,/),5E13.5)
1570
1580      RETURN
1590      END

```

APPENDIX E
PUBLISHED PAPERS

- | | | |
|-----|--|------|
| E.1 | Denbigh, P.N. and Tollman, P.A. Beamforming by the cross-correlation analysis of received spectra, in Adaptive Methods in Underwater Acoustics, Urban, H.G. (ed), NATO ASI Series C, D. Reidel, Dordrecht, 1985. | E-2 |
| E.2 | Tollman, P.A. Beamforming based upon animal echolocation techniques, Proceedings of First SA Congress on Acoustics, CSIR, Pretoria, October, 1985. | E-10 |

BEAMFORMING BY THE CROSS-CORRELATION
ANALYSIS OF RECEIVED SPECTRA

P.N. Denbigh and P.A. Tollman

Central Acoustics Laboratory, Department of
Electrical and Electronic Engineering,
University of Cape Town, Rondebosch 7700, R.S.A.

ABSTRACT. The effect of placing an irregular reflecting surface around a receiver is to modify the spectrum of an incoming acoustic signal. The direction of the signal source may be found by correlating the output signal spectrum with the known spectral responses of the receiving system for all angles.

1. INTRODUCTION

The simplest beam steering technique is to place a small receiver at the focal point of a large reflector and to mechanically rotate the whole assembly. The mechanically scanned radar antenna is an example of this. The sonar equivalent is a rotating transducer array in which the individual transducers are connected in parallel to give a single output. However, mechanical scanning is generally undesirable in sonar, because there are physical constraints on rotation and because the low propagation velocity of sound places very severe limits on the scan speed. In order to avoid mechanical scanning it is necessary to have a multi-element array in which the output of each element undergoes some pre-processing and then enters a beamformer. To achieve N angular resolution cells there must be N transducer elements and an N input beamformer. In spite of recent advances in digital processing such a system is generally very complex and costly if N is large. This paper describes a beamforming system which uses a single receiver surrounded by a passive reflector and yet which achieves multiple beams without resorting to mechanical scanning. The technique is an extension of one suggested mechanism of monaural localization (1)

2. DESCRIPTION OF TECHNIQUE

Whereas the typical radar antenna uses a transmitter/receiver at the focal point of a regular parabolic reflector, the proposed system uses a receiver set at an arbitrary position close to a highly irregular reflecting surface. The analogous surface in an animal system would be the pinna. The interaction of an incoming signal with the many facets of the reflecting surface causes a complex interference phenomenon which modifies the spectrum of the received signal. The spectrum modification is unique for each direction and can be predetermined and stored in memory. The basic principle of the proposed sonar system is to determine the correlation coefficient between the received signal spectrum and each of the many stored spectra, there being a stored spectrum for every possible direction. A large correlation coefficient indicates a target in that direction. The technique is applicable to passive listening. It is also applicable to each range resolution cell of an active sonar when a broadband pulse is transmitted and frequency analysis is undertaken in each range bin. If pulses of a large time bandwidth product are used this could be done after pulse compression. The technique has been evaluated in one dimension only using computer simulation. The irregular reflector and receiver has been replaced by a two-dimensional array of randomly spaced receivers lying in the plane of intended operation (Fig. 1).

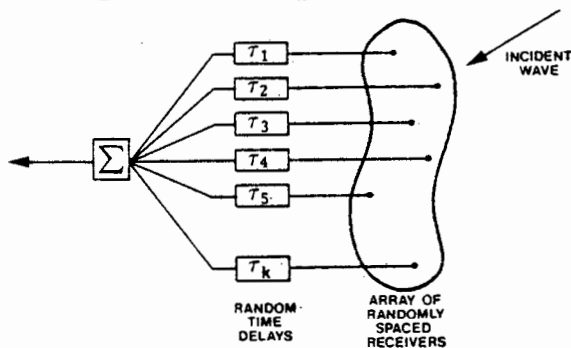


Fig. 1. Model of receiving system.

The outputs of the receivers are passed through a set of random time delays and then summed to give a single output. This procedure gives an interference effect which is closely equivalent to that obtained using a single receiver surrounded by an irregular reflector. The random time delays may be thought of as analogous to the propagation delays between facets on the reflector and the single collection point. The spectral response of the array is calculated for 181 equally spaced angles between 0° and 180° and for 200 equally spaced frequencies between 25 kHz and 100 kHz. An example of the amplitude spectra at different angles is shown in Fig. 2, which is for an array of 200 randomly spaced receivers contained within a square 10.5λ by 10.5λ , where λ is the wavelength at the highest frequency of 100 kHz.

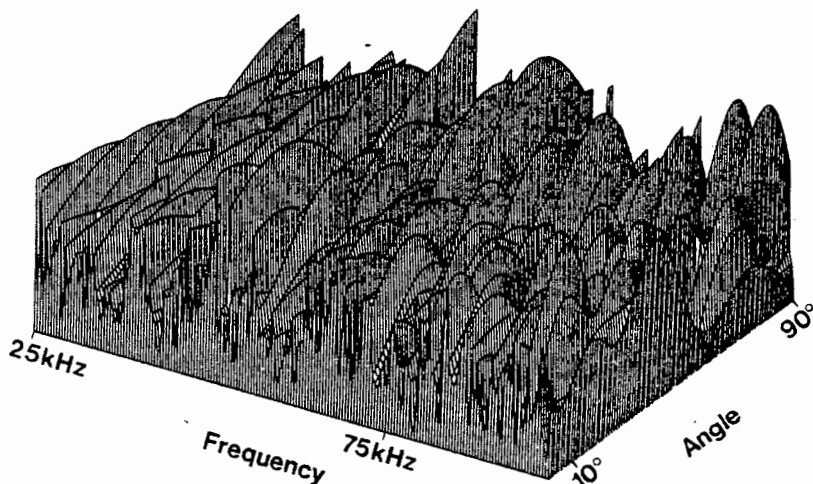


Fig. 2. Amplitude response of receiving system as a function of frequency and angle of incidence

For larger arrays the fluctuations become more rapid with both angle and frequency and are difficult to appreciate on a single plot such as that in Fig. 2.

3. COMPUTER SIMULATIONS

3.1 Single sound source of known spectrum.

The first simulation to demonstrate the technique uses a large number of paralleled receivers contained within a square 15λ by 15λ , where λ is the wavelength at the highest frequency of 100 kHz. A single sound source with a uniform spectrum is introduced at an angle of 50° . The interaction with the array causes the spectrum to be modified to become as shown in Fig.3(a).

Fig. 4(a) shows the correlation coefficient as a function of angle when the spectral points corresponding to Fig. 3(a) are correlated with the stored spectra for 181 angles between 0° and 90° . The correlation coefficient is seen to have a clear maximum at the correct source angle of 50° . The angles between which the correlation coefficient is $1/\sqrt{2}$ of its maximum value is 3.8° . This corresponds closely with the $1/15$ radian resolution expected from a conventional beamformer using a 15 wavelength uniform aperture. It is noted that Fig. 4(a) unfortunately suffers from a noiselike background which would mask any additional weak signal sources. This background arises because, even though the stored spectra for the various angles are very different, there are only a finite number of independent frequency samples within the spectrum to test the hypothesis of zero correlation. The number of independent frequency samples in the simulation is somewhat fewer than the 200 frequency points calculated. However, considering a random sample of size

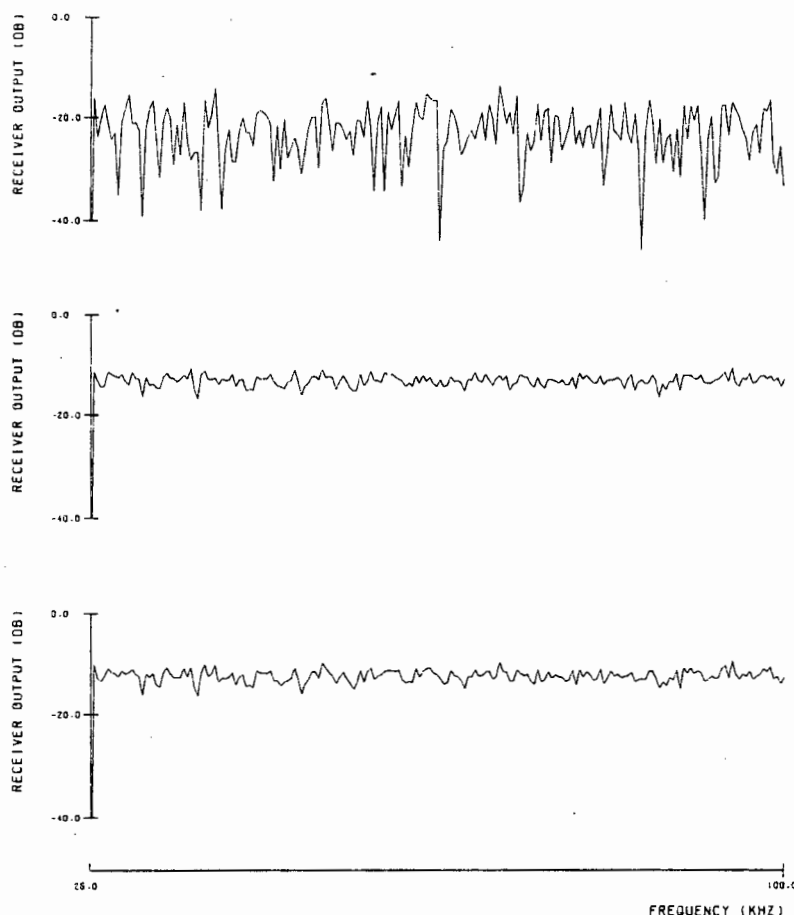


Fig. 3. Spectrum of output signal (a) source alone
(b) noise alone (c) source plus noise; $S/N = -8$ dB.

200 as an example, statistical analysis can be applied to show that the hypothesis of zero correlation at the 0.1% level of confidence can only be rejected if the measured correlation coefficient exceeds 0.217. (2). Significant correlation coefficients may be expected at angles which are devoid of signal sources; hence the noise-like background. However, as will be shown in Sec. 3.3, there are ways in which the consequent masking of weak signal sources may sometimes be overcome.

The next part of the simulation examines localization performance when noise is present. In order to simulate ambient noise the wanted signal source of unity amplitude is accompanied by 181 weak signal sources, each of an amplitude 0.03 at all 181 angular cells used in the simulation. Fig. 3(b) shows the received spectrum resulting from this noise alone. Fig. 3(c) shows the received spectrum when the received noise is added to the received signal, and corresponds to a signal-to-noise ratio of -8 dB. It will be noted that, because of the low signal-to-noise ratio, the resultant spectrum

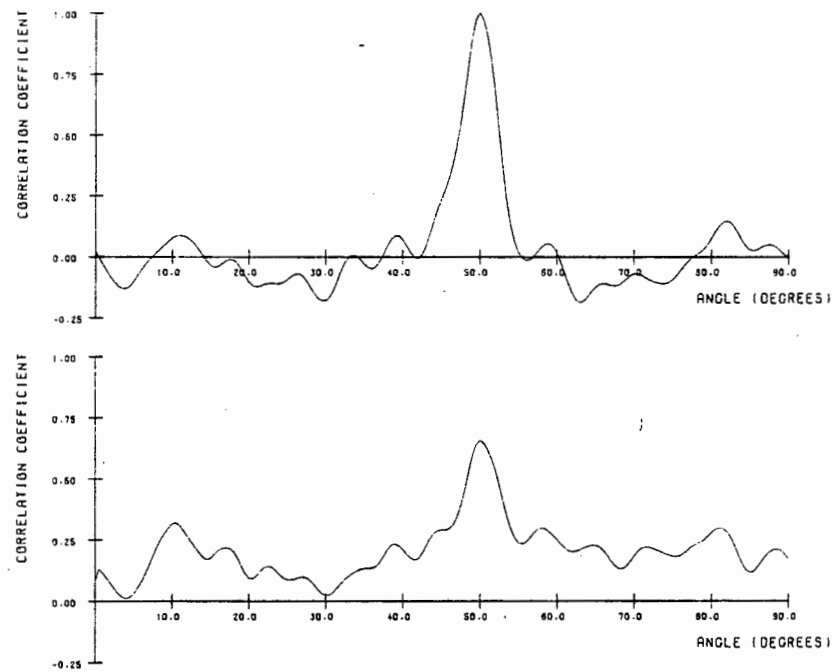


Fig. 4. Correlation coefficient v. angle for a single source at 50° (a) no noise (b) $S/N = -8$ dB.

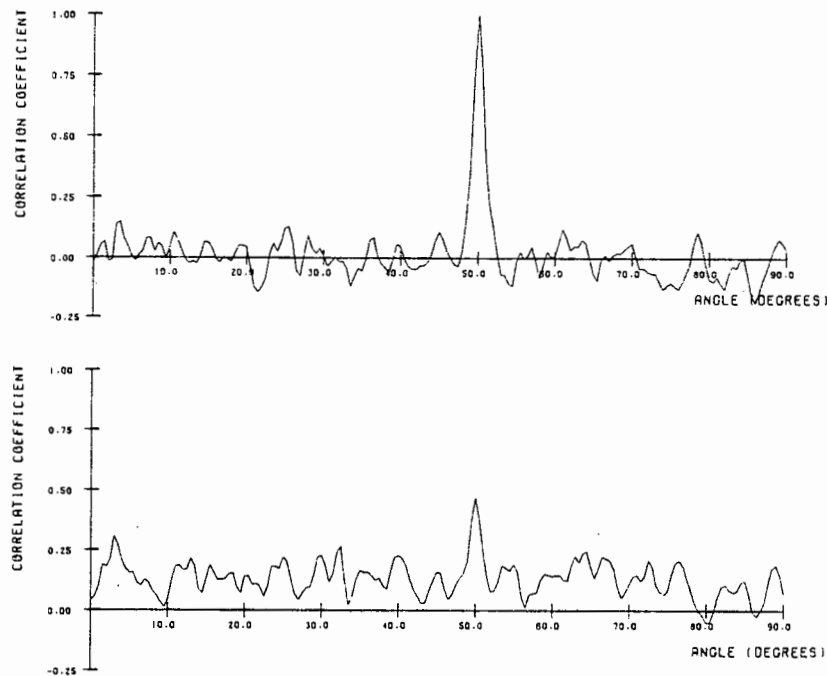


Fig. 5. Results for larger array (a) no noise (b) $S/N = -15$ dB.

resembles that of the noise more closely than that of the signal source. The vertical axes of Fig. 3 are shown on a decibel scale in order to accommodate a wide dynamic range of spectral densities but direct power spectra are used in the evaluation of correlation coefficients in order to achieve a linearity if multiple signal sources are present. Fig. 4(b) shows the correlation coefficient as a function of angle when the spectral points corresponding to Fig. 3(c) are correlated with the stored spectra. A comparison with Fig. 4(a) shows that the correlation peak is reduced because of the ambient noise but is still large enough to reveal the signal source clearly. Similar simulations are shown in Fig. 5 for receivers contained in a larger array, 50λ by 50λ . Fig. 5(a) is for a signal source at an angle of 50° and no noise. Fig. 5(b) is for the same signal source surrounded by noise sources, such that the signal-to-noise ratio is -15 dB. A comparison with Fig. 4 shows that the larger array gives an improved angular resolution and enables detection at a lower signal-to-noise ratio.

3.2 Single sound source of unknown spectrum

Monaural localization by means of spectral cues is generally assumed to require a priori information about the sound source spectrum. However, particularly when the array dimensions are large, the spectral modification due to the array structure can be so substantial and so characteristic of a particular angle that monaural localization is quite feasible even when the sound source spectrum is non-uniform and unknown. The results of Fig. 6 are

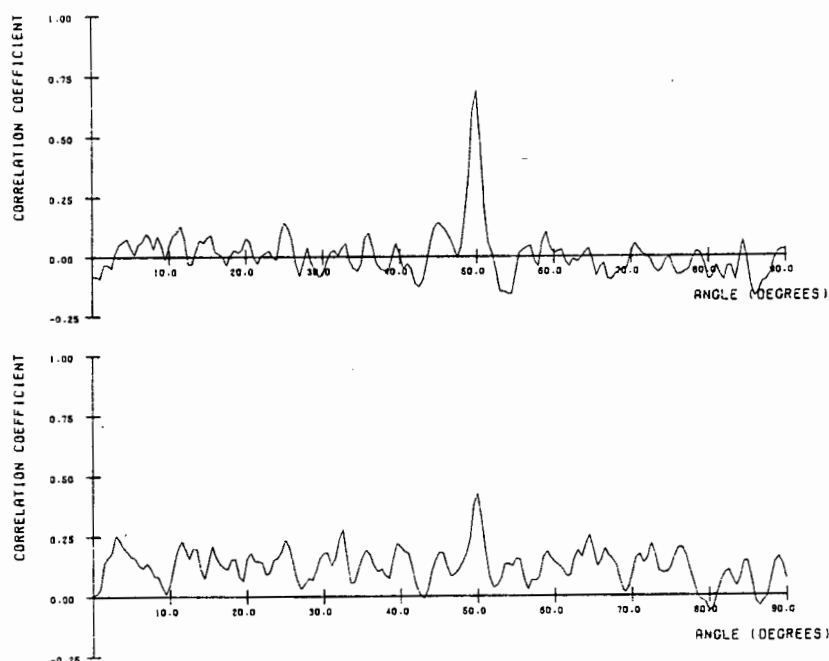


Fig. 6. Results for source of unknown sound spectrum
(a) no noise (b) $S/N = -12$ dB.

similar to those of Fig. 5 but apply to an incoming signal whose spectrum has been modified. The non-uniform signal spectrum in this simulation is arbitrarily taken to have the raised cosine envelope $1 + \cos k\omega$ where k is chosen to give 10 peaks and 10 nulls between 25 kHz and 100 kHz. The spectrum resulting from interaction of this signal with the receiver structure is correlated with stored spectra derived on the basis of a uniform incoming signal spectrum. Fig. 6(a) shows the result when there is no noise. The correlation peak is very distinct, though reduced relative to that of Fig. 5(a). Fig. 6(b) corresponds to a signal-to-noise ratio of -12 dB and gives a result which is only slightly degraded compared with the case of a uniform spectrum shown in Fig. 5(b).

3.3 Multiple sound sources

The final simulation demonstrates how the technique may be extended to perform well with multiple sources, even when some of the sources are so weak that they are masked by the noiselike fluctuations of the correlation coefficient. For the following extended technique to be effective, however, there is this time a requirement that the sound source spectra be known. Uniform sound source spectra are assumed. The simulation uses a source of unity amplitude at an angle of 10° , a source of amplitude 0.9 at an angle of 33° , and a source of amplitude 0.05 at an angle of 52° . In order to simulate ambient noise 181 additional weak sources, each of amplitude 0.013, are spread uniformly over 90° . The array is taken to be 100λ by 100λ . Fig. 7(a) shows the correlation coefficient as a function of angle when the spectrum of the received signal is correlated with the stored spectra from the 181 angular cells. The two strong targets are clearly present. The weak target is lost in the background. As before, this background arises because only a finite number of frequency samples are available to test the hypothesis of zero correlation. However, the correlation peak due to the weak signal can be made to increase, causing it to rise out of the background, if the stronger sources are first removed. This can be achieved because the degree of correlation at a correlation peak can be used to derive the extent by which that source contributes to the measured spectrum. The spectrum contribution due to this source can then be subtracted out from the measured spectrum. When this is done the new resulting spectrum can be correlated with the stored spectra. In our case the first subtraction leads to Fig. 7(b). Now the first source has disappeared and the second source gives a correlation coefficient close to one. The process can be repeated in which the spectra of the second source is subtracted from the remaining spectrum. A third evaluation of the correlation coefficient produces Fig. 7(c). This time the weak source is clearly revealed.

By making use of a second receiving system it is hoped in future work to be able to apply this subtraction technique when the multiple sources have unknown spectra.

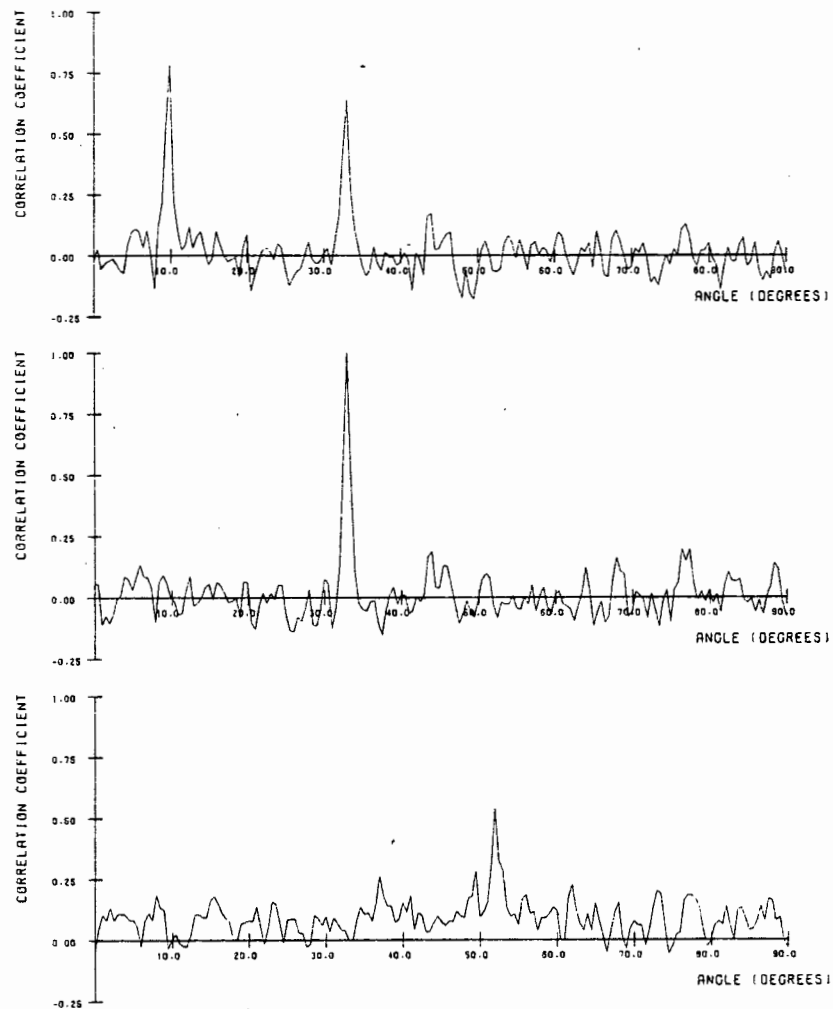


Fig. 7. Extraction of multiple sources (a) first correlation (b) second correlation (c) third correlation.

4. CONCLUSIONS

Computer simulations have indicated that a viable technique of beamforming is to place a receiving element within a large irregularly shaped reflector and to cross-correlate the received signal spectrum with the angle dependent amplitude responses of the receiving system. The great practical advantage is that a very large receiving structure may readily be constructed and that only a single active receiving element is required.

REFERENCES

1. Searle C.L., et al. *Model for auditory localization*. 1976 J. Acoust. Soc. Am., 60, pp 1164,1175.
2. Bendat J.S., Piersol A.G. *Random Data: Analysis and Measurement Procedures*. 1976 Wiley-Interscience.

BEAMFORMING BASED UPON ANIMAL ECHOLOCATION TECHNIQUES

P. A. TOLLMAN

B.Sc. Eng (Natal)

Central Acoustics Laboratory, Department of Electrical and
Electronic Engineering, University of Cape Town
Rondebosch 7700, R.S.A.

ABSTRACT

The external ears of animals cause a spectrum modification of received acoustic signals. The angle dependence of this modification is used to locate signal sources. Analogously, the effect of placing an irregular reflecting surface around a receiver is to modify the spectrum of an incoming signal. Computer simulations indicate that the use of this spectrum modification to locate signals is a viable technique of beamforming.

EKSERP

Die oorskulp van 'n dier beïnvloed die spektrum van 'n akoestiese intreësein. Die feit dat hierdie verandering hoekafhanklik is, word gebruik om die oorsprong van 'n sein te bepaal. Analooë hieraan beïnvloed 'n onreëlmatige weerkaatser rondom 'n ontvanger die spektrum van 'n intreësein. Rekenaar simulasie dui aan dat die gebruik van hierdie spektrumverandering om die oorsprong van 'n sein te bepaal 'n bruikbare tegniek van bundelvorming is.

1. INTRODUCTION

Conventional beamsteering techniques use either mechanical or electronic means to rotate a narrow beam. The radar antenna, in which a small receiver is placed at the focal point of a large rotating reflector, is an example of mechanical beamsteering. Mechanical beamsteering has severe limitations in sonar, however, because the low propagation speed of sound necessitates a very slow scan speed. Electronic techniques of beamsteering, in which the output of each element of a multi-element array is processed separately before entering a beamformer, are therefore preferred. The number of transducer elements in such an array is equal to the number of angular resolution cells required. For a high resolution system, the digital signal processing required is complex and expensive.

This paper describes an alternative beamforming system, in which multiple beams are achieved using a stationary, irregular reflector and a single active element. The techniques evolved from a study of animal echolocation. Animals rely on a multiplicity of signal processing techniques for the aural localisation of sounds. It has been established that some of these rely on the use of only one ear. The beamforming techniques described are models compatible with possible monaural mechanisms of echolocation (1).

2. SIMULATION

Conventional radar antennas use a regular parabolic reflector which sweeps a narrow beam through a scanned sector. In contrast, the proposed beamforming techniques rely on a stationary irregular reflector. The facets of such a reflector cause interference effects which impose spectral modifications on received sounds. This is as a result of the superposition of spectral components which are reflected from these facets. Since the delay between these reflections is a function of angle of incidence, the spectral modifications which a reflector imposes on a received sound can be decoded to determine the location of that sound.

Two techniques of locating signals received by the proposed beamformer have been evaluated in computer simulations. The irregular reflector and receiver were modelled by an array of randomly situated point sources constrained within preselected dimensions. The source outputs were delayed by a set of randomly assigned times and then added. This closely approximates reflections from the facets of a reflector arriving at a single collection point.

The receiver output is frequency analysed by a bank of contiguous bandpass filters (figure 1). The processing of these filter outputs in order to locate sources, has resulted in the development of two techniques. The first is concerned with processing in the frequency domain, whilst the second operates in the time domain.

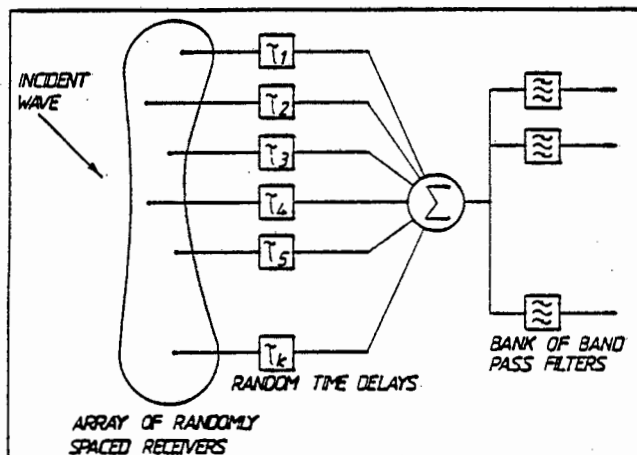


FIG.1: SIMULATED RECEIVING SYSTEM

3. SIGNAL PROCESSING

3.1. Frequency domain processing

The spectral response of a simulated receiver was predetermined by calculating the power at the output of each bandpass filter at closely spaced angular increments. A source could then be located by correlating its spectral response with the predetermined response at each angular increment in turn. A high correlation coefficient indicates source location.

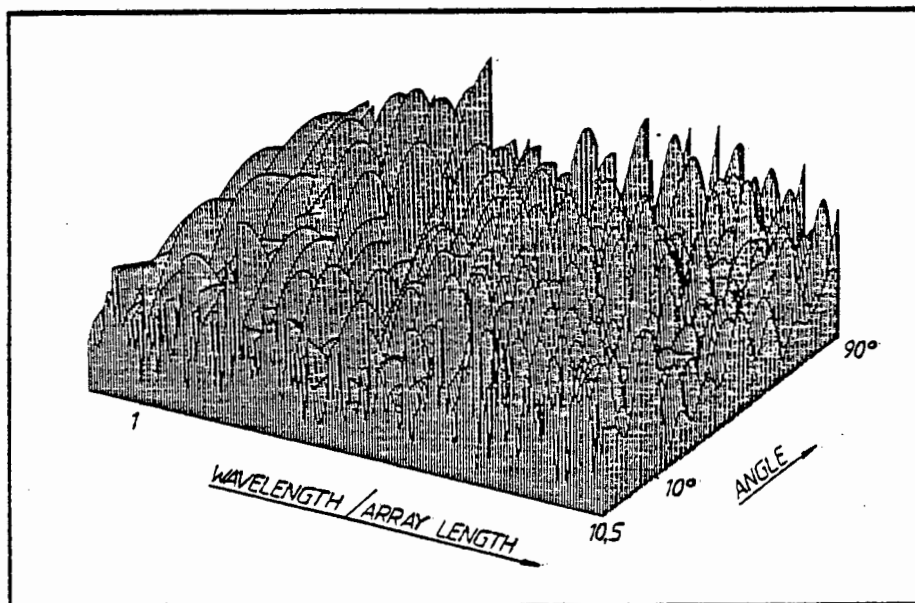


FIG.2. SPECTRAL AMPLITUDE RESPONSE OF RECEIVER SYSTEM AS A FUNCTION OF ANGLE OF INCIDENCE

The spectral response of a simulated array of sources is illustrated in figure 2. The sources were constrained within a square of dimension $10,5\lambda$, where λ is the wavelength of the highest spectral component. For larger arrays, the rate of fluctuation, and hence the disparity between spectra at adjacent angular increments, increases. Such spectral responses are difficult to appreciate on a single plot. However, the array used for the following simulation was 100λ across.

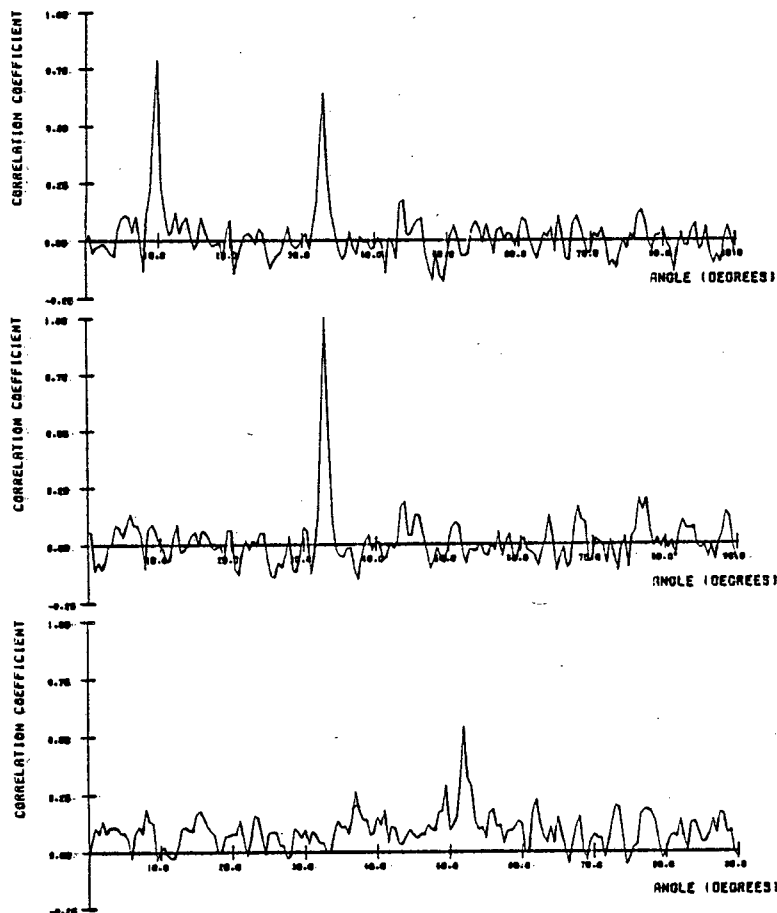


FIG. 3. MULTIPLE TARGET SIMULATION (a) FIRST CORRELATION
(b) SECOND CORRELATION (c) THIRD CORRELATION

Figure 3 is the result of a multiple target simulation. Three targets were located. The first was of amplitude 1 at an angle of 10° . The second was of amplitude 0,9 at an angle of 33° , while the third was of amplitude 0,05 at an angle of 52° . To simulate ambient noise, additional weak "targets" of amplitude 0,013 were introduced at every angular cell of the simulation. A signal-to-noise ratio of -11dB for the weak target was thus achieved. Figure 3(a) shows correlation coefficient as a function of angle when the received spectrum is correlated with the stored spectra. The targets at 10° and 33° are clearly evident. However, the target

at 52° , which is 26dB weaker than the target at 10° , is submerged in noise. An iterative subtraction technique is applied to remove the stronger sources from the received spectrum. This allows the correlation peaks of weak targets to increase above the noise level. First, the contribution of the target at 10° to the original spectrum is subtracted out. The resulting spectrum is again correlated with each of the stored spectra. In figure 3(b), the target at 10° is no longer evident, while the target at 33° has a correlation coefficient close to 1. However, the target at 52° is still submerged in noise. Figure 3(c) is the result of a further iteration aimed at subtracting out the contribution of the target at 33° . The target at 52° is now clearly evident.

This simulation indicates that the cross-correlation of a received signal spectrum with the angle dependant amplitude responses of a large irregular reflector, is a viable technique of beamforming (2). However, the localisation of targets by cross-correlation processing has limitations. When locating multiple sources of unknown spectra, its performance is degraded. The extent of this degradation is a function of the degree of difference between the real source spectra and the estimated spectra used in calculating the correlation coefficients. Furthermore, relatively large reflectors are required to obtain satisfactory angular resolution. In contrast, the pinnae of most mammals capable of localising multiple sources, are of the order of 5 wavelengths across at the highest audible frequency. It appears, therefore, that untapped localisation cues exist.

3.2. Time domain processing

The cross-correlation techniques discussed above are based on measured amplitude spectra. The associated phase spectra are disregarded. Were this phase information to be usefully processed, important additional localisation cues might be obtained. Since in most applications phase is found to play a larger role than amplitude in characterising signals, these phase spectra could play a major role in target localisation (3).

A convenient way of displaying both amplitude and phase information on a single plot, is to display signals in the time domain. Amplitude is represented directly, while phase differences transform into time delays.

In the frequency domain, the receive array was characterised in terms of its spectral response at closely spaced angular increments. In the time domain, the array can be characterised by an impulse response at each

increment. Six impulse responses of a simulated array of sources are shown in figure 4. The array dimension is 3X.

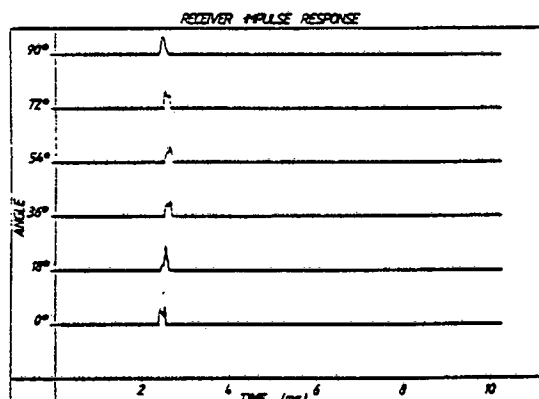


FIG. 4. IMPULSE RESPONSES OF RECEIVER

Were there separate inverse filters for each possible direction, a comparison of their outputs could locate a signal source in the following manner. If the signal were to originate from an inverse filter direction, the filter output would be a replica of the original signal. This is because the filter would deconvolve the signal from the impulse response of the receiver. However, if the signal originated from any other direction, the filter output would be the receiver output convolved with the response of a filter which does not deconvolve the original signal. A comparison of the inverse filter outputs for all possible directions would therefore only yield a deconvolved signal at the filter output representing the correct direction.

Consider the requirements of the inverse filter in the frequency domain. At each frequency, it is necessary to insert a certain amplitude and phase modification. This is achieved by altering the amplitude and phase responses of a bank of ideal and contiguous filters, each with a constant amplitude and a linear phase response.

Figure 5 illustrates the deconvolution of an impulse from each of the six preselected directions. In figure 5(a), the sets of amplitude ratios and phase shifts representing the inverse filter for each direction in turn, were applied to the impulse response at 0°. Only the 0° inverse filter successfully deconvolved the impulse response. In figure 5(b), the same inverse filters were applied to the impulse response at 18°. As a result, only the 18° inverse filter deconvolved the impulse response. Figures 5(c) to 5(f) illustrate the inverse filters applied to impulses at angles of 36° through 90°. In each instance, successful deconvolution only occurred when the inverse filter corresponding

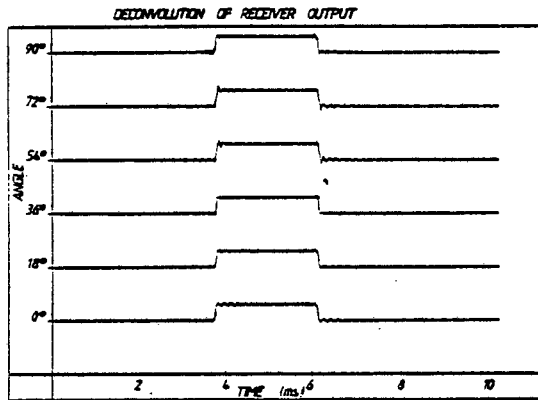


FIG. 6. DECONVOLUTION OF A PULSE AT 36°

To locate an unknown source signature, a method of differentiating a correctly deconvolved signal from a set of outputs which are incorrectly deconvolved, is required. Characteristics of typical sources are used to achieve this. Such sources are usually broadband, and contain sharp wavefronts. When deconvolved correctly these sharp wavefronts are preserved. When deconvolved incorrectly, the wavefronts are smeared to the width of the impulse response. The rising and falling pulse edges of figure 6 illustrate this smearing effect.

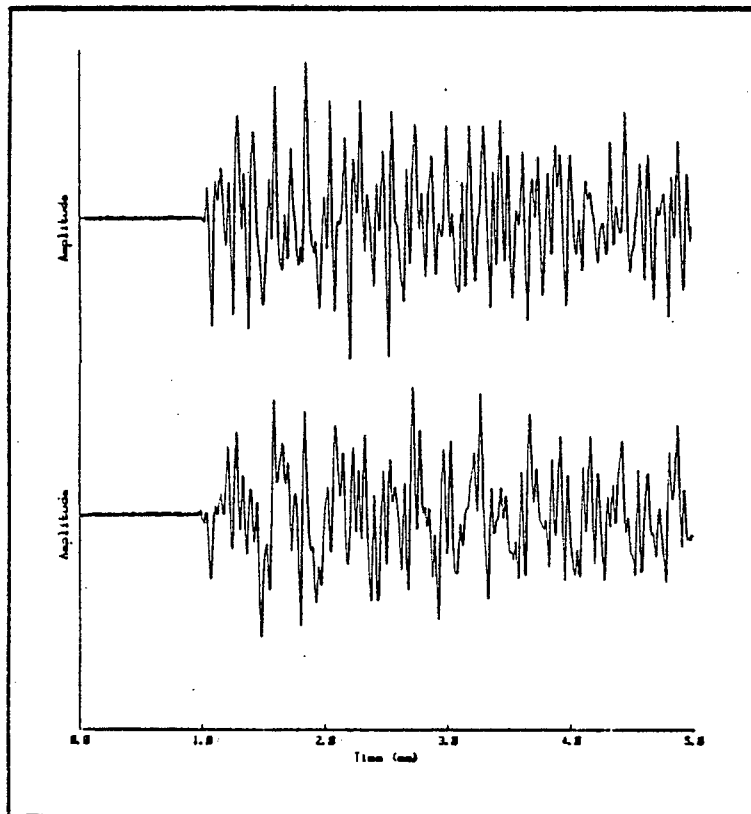


FIG. 7. AN ARBITRARY RECEIVED SIGNAL (a) DECONVOLVED
(b) NOT DECONVOLVED.

An example of a more realistic source is presented in figure 7. Figure 7(a) shows the source when correctly deconvolved. In figure 7(b), the source has not been deconvolved, and consequently the signal onset is more gradual.

By processing the results of real receivers on a computer, it is hoped in future work to use an experimental system to localise sources of unknown signature. The performance of this technique of deconvolution in the presence of noise, and under multiple target conditions, can then be evaluated.

4. CONCLUSION

The evaluation of this technique of sonar beamforming is far from complete. However, results obtained to date do indicate that a single receiving element placed within a very small irregularly shaped reflector can locate targets of unknown spectrum. A great number of practical beamforming applications could be realised using merely an inexpensive and unobtrusive passive reflector and a single active receiving element.

5. ACKNOWLEDGEMENTS

Professor Denbigh has played a substantial role in the development of these techniques.

Much of this work was conducted under the auspices of the Institute for Maritime Technology.

6. REFERENCES

1. Bloom, P.J. Determination of monaural sensitivity changes due to the pinna by use of minimum-audible-field measurements in the lateral vertical plane, 1977, J. Acoust. Soc. Am., 61, pp 820,828.
2. Denbigh, P.N., Tollman, P.A. Beamforming by the cross-correlation analysis of received spectra, Aug. 1984, NATO ASI on adaptive methods in underwater acoustics, Luneberg, Germany.
3. Oppenheim, A.V., LIM, J.S. The importance of phase in signals, 1981, Proc. IEEE, 69, pp 529, 541.